Vrije Universiteit Brussel

FACULTEIT INGENIEURSWETENSCHAPPEN
Vakgroep Industriële Ingenieurswetenschappen

Feasibility and performance assessment of small and medium-sized wind turbines

Table of Contents

Nederlandse samenvatting

Er bestaat een aanzienlijke onzekerheid over de rol die kleine en middelgrote windturbines kunnen spelen voor de productie van duurzame elektriciteit. In dit werk identificeren we de belangrijkste factoren die de haalbaarheid van kleine en middelgrote wind turbines (kortweg KMWTs) beïnvloeden. Daarna lichten we toe hoe de jaarlijkse energieopbrengst van een KMWT efficiënter en betrouwbaarder kan geschat worden. We tonen aan dat deze technologie inderdaad rendabel is, op voorwaarde dat een geschikte turbine wordt geselecteerd, op een winderige site correct wordt geïnstalleerd en de jaarlijkse energieopbrengst zorgvuldig geschat wordt. Deze ogenschijnlijke eenvoudige taken zijn niet triviaal en sommige huidige methodes leiden tot een onbetrouwbare schatting.

Om dit aan te tonen zijn we gestart met het samenstellen van een databank van alle windturbines met een nominaal vermogen tot 100 kW. Een dergelijke databank is nodig om de haalbaarheid van deze wind turbines te onderzoeken, aangezien deze markt nog niet volgroeid is en er een grote spreiding bestaat op de kwaliteit van de verschillende turbines.

Nadien hebben we de jaarlijkse energieopbrengst geschat voor een aantal meetsites in België en Nederland en voor verschillende onafhankelijk geteste KMWTs. Op basis van deze gegevens, tonen we aan wat de beste methode is om de meest geschikte turbine te selecteren en wat de verwachte nauwkeurigheid is van de schatting van de jaarlijkse energieopbrengst.

We hebben vastgesteld dat een bepaalde statistische fout in de huidige methodes om de jaarlijkse energieopbrengst te schatten over het hoofd is gezien. Deze fout wordt veroorzaakt door het verschil in uitmiddelings-tijd waarmee windsnelheden en vermogens worden bemonsterd. Op basis van gemeten windsnelheden en een onafhankelijk gemeten vermogenscurve tonen we aan hoe deze fout geminimaliseerd kan worden.

Onze bevindingen hebben een onmiddellijk praktisch belang. We passen onze methodes toe op een aantal case studies en geven aanbevelingen voor toekomstige KMWT projecten.

English Abstract

There is considerable uncertainty about the role that small and medium wind turbines may play in the production of sustainable electricity. In the present work, we identify the main factors affecting the economic viability of small and medium wind turbines (herafter SMWTs). We then propose a framework for more efficient and reliable predictions of the annual energy production of SMWTs. We demonstrate that these turbines are indeed profitable, provided that an appropriate turbine is selected and that the annual energy production is estimated carefully. These seemingly simple tasks are non-trivial and current practices too often lead to unreliable assessments.

We first assemble a database of wind turbines with a rated power up to 100 kW. Such a database is a necessary tool when assessing the feasibility of a project involving SMWTs, since the market is very immature, with a wide variation in quality between different turbines.

We then calculate the annual energy production (AEP) for a number of measurement sites in Belgium and The Netherlands and for different independently-tested SMWTs. Based on these data and on first principles, we show what the best methods are to select an appropriate turbine and what the expected accuracy is of the AEP estimate.

We have found that a particular statistical error has been overlooked in the current methods to estimate the annual energy production. This error is the possible mismatch of the averaging times with which wind speeds and turbine power outputs are sampled. Using wind speed and power measurements, we show how this error can be minimised.

Our findings have an immediate practical importance. We therefore apply our methods in a number of case studies, and give recommendations for future SMWT projects.

Acknowledgements

When I look back, I feel grateful to the people who helped and supported me during the last few years. Without their help, the accomplishment of this work would never have been possible.

First of all, I would like to express my special appreciation and thanks to my promotors prof. Mark Runacres and prof. Patrick Guillaume. Mark, you have been a tremendous mentor for me. I would like to thank you for encouraging my research and for allowing me to grow as a research scientist. Your advice on both research as well as on my career have been priceless. Patrick, you made all the difference by giving me the opportunity to start my research and by investing time (and of course money) in me.

I would also like to thank the members of the Jury for their interest in the work, the critical reading of the manuscript and the helpful suggestions. I would like to thank prof. Ine Wouters for presiding my jury and prof. Daniel Navarro for his willingness to participate as a foreign Jury member (even in a difficult period). A special thanks also to prof. Tim De Troyer for being the secretary of my jury but foremost for his time and effort during my final year (and of course in the years before). Tim, you really helped me a lot by cracking the necessary Matlab codes, producing the right figures and improving my scientific writing skills.

Furthermore, I would also like to thank my colleagues Arno, Jan, Diego, Guoying and Quentin for their help, especially during the last few years. You all not only helped me a lot by reducing my teaching assignments and setting up yet another measurement campaign but also for the occasional talks and for the nice working atmosphere.

Last but not least I want to thank my family. Words cannot express how grateful I am to my mother, and father for all of the sacrifices that you've made on my behalf. Thanks mom and dad for keeping me on the right track in my teenage years. Without your guidance, I would not even have been able to start an academic career. At the end I would like to express my deepest appreciation to my beloved wife Dorien for her tremendous support

in the final months (and the years before). Thank you for being their for me, for your encouragements and for your unconditional love for me and Elias. Elias, thank you for smiling at me when I was having a hard time, your smile made all the difference.

<div style="text-align: right">

Brussel, 27 March 2015
Jochem Vermeir

</div>

List of publications

During the preparation of this dissertation, our results have lead to the following publications. Most of the results were first published in technical reports.

Technical reports

- Vermeir, J. J., Runacres, M. C. (2015). Rooftop wind resource assessment in Mannheim, Wattwerk Energiekonzepte.

- Vermeir, J. J., Runacres, M. C. (2015). Loss of energy production of a MW wind park due to a high-voltage substation (*Confidential*), Tractebel Engineering (GDF Suez).

- Vermeir, J. J., Runacres, M. C. (2014). Keuze windturbine & schatting jaaropbrengst (*Confidential*), Electrabel (GDF Suez).

- Runacres, M. C., Vermeir, J. J., De Troyer, T. (2014). BIM E11-359: Identificatie sites, opzetten windmetingscampagnes en uitvoering van haalbaarheidsstudies in het Brussels Hoofdstedelijk Gewest, Leefmilieu Brussel. `http://documentatie.leefmilieubrussel.be/documents/RAP_20140331_eindrapport_final.pdf`.

- Runacres, M. C., Vermeir, J. J., De Troyer, T. (2012). Tetra 090192: Gebruik van microwindturbines voor het leveren van hernieuwbare energie aan particulieren en kleine bedrijven, IWT Vlaanderen. `http://www.microwindturbine.be/Vergaderverslagen_files/IWT090192eindrapport.pdf`.

Articles in the proceedings of international conferences

- Vermeir, J. J. , Runacres, M. C., De Troyer, T. (2012). CFD modelling and measurements of the atmospheric boundary layer for mi-

crositing of small wind turbines. In *Proceedings of the European Wind Energy Association Conference*, Copenhagen.

- Vermeir, J. J. , Motte, A., Dominguez, D., Runacres, M. C., De Troyer, T. (2014). Wind prediction in urban environments. In *Proceedings of the European Wind Energy Association Conference*, Barcelona.

Articles in the preprints of international conferences

- Vermeir, J. J. , Runacres, M. C., De Troyer, T. (2013). Improved resource assessment for small wind turbines in rural and urban areas. In *Preprints of the European Wind Energy Association Conference*, Vienna.

List of industrial contracted and research projects

- Windkwaliteit industrieterrein Aarschot (2015), Provincie Vlaams-Brabant.

- Rooftop wind resource assessment in Mannheim (2015), Wattwerk Energiekonzepte.

- Loss of energy production of a MW wind park due to a high-voltage substation (2015), Tractebel Engineering (GDF Suez).

- Keuze windturbine & schatting jaaropbrengst (2014), Electrabel (GDF Suez).

- Identificatie sites, opzetten windmetingscampagnes en uitvoering van haalbaarheidsstudies in het Brussels Hoofdstedelijk Gewest (2014), Leefmilieu Brussel.

- Gebruik van microwindturbines voor het leveren van hernieuwbare energie aan particulieren en kleine bedrijven (2012), IWT Vlaanderen.

List of symbols

Symbol	Unit	Explanation
$C_P(V)$	[-]	power coefficient
$C_{P_{el}}(V)$	[-]	electrical power coefficient derived via the electrical power output of the turbine
F_s	[Hz]	sample frequency of the original data set
$h_\tau(t)$	[1/s]	τ-wide rectangular window
$H_\tau(f)$	[-]	power spectrum of the τ-wide rectangular window
μ_V	[m/s]	mean of the wind speed
N	[-]	number of samples within total measurement time
$P(V)$	[W]	value of the power curve at wind speed V
ρ	[$\mathrm{kg\,m^{-3}}$]	volumetric weight of air
S	[$\mathrm{m^2}$]	wind turbine rotor surface
$S_V(f)$	[$\mathrm{(m/s)^2\,s}$]	wind power spectral density
$\widetilde{S_V(f_k)}$	[$\mathrm{(m/s)^2\,s}$]	DFT estimate of the wind power spectral density
s_τ^2	[$\mathrm{(m/s)^2}$]	variance over a set of τ-averaged wind speed samples
σ_τ^2	[$\mathrm{(m/s)^2}$]	variance of a τ-averaged wind speed sample
$\overline{\sigma_\tau^2}$	[$\mathrm{(m/s)^2}$]	average variance of a τ-averaged wind speed sample
T	[s]	total measurement time
T_s	[s]	sample period of the original data set
τ	[s]	sample period/interval
$V(t)$	[m/s]	wind speed
$\widehat{V}(f_k)$	[m/s]	DFT of the wind speed $V(nT_s)$ at frequency line $f_k = k/T, k = 0, \ldots, N-1$
$\varphi(V)$	[$\mathrm{(m/s)^{-1}}$]	probability density function of the wind speed
Ψ_V^2	[$\mathrm{(m/s)^2}$]	mean square value of the wind speed

List of abbreviations

AEP	Annual Energy Production
BMWT	Building Mounted Wind Turbine
CFD	Computational Fluid Dynamics
DFT	Discrete Fourier Transform
GC	Green Certificates
GPRS	General Packet Radio Service
HAWT	Horizontal Axis Wind Turbine
IEC	International Electrotechnical Commission
IRR	Internal Rate of Return
LCOE	Levelized Cost of Energy
Log	Log Law
LogL	Log Linear Law
LR	Linear Regression
LRE	Linear Regression with Gaussian scatter
MCP	Measure-Correlate-Predict
MEP	Maximum Entropy Principle
NPV	Net Present Value
PDF	Probability Density Function
PL	Power Law
PSD	Power Spectral Density
SISP	Sociétés Immobilières de Service Public
SME	Small and Medium Enterprise
SMWT	Small and Medium Wind Turbine
VAWT	Vertical Axis Wind Turbine
VR	Variance-Ratio

Introduction

This is a dissertation about small and medium-sized wind turbines, with a power typically lower than 100 kW. Such turbines currently occupy only a small fraction of the market. In Belgium in particular, the number of installed small and medium wind turbines is extremely small. Judging from their market share, one may wonder whether these machines deserve a place in the energy mix, or whether investments and research efforts are better directed elsewhere. This question drives the main goal of this dissertation: to investigate under what conditions, if at all, small and medium wind turbines may be a profitable and practically feasible source of sustainable electricity.

In **Chapter 1**, we briefly discuss some basic aspects of wind energy, wind resource assessment, economic assessment and siting studies. We also describe how we categorise small-, medium- and large-scale wind energy. We conclude this chapter with the specific challenges of small and medium wind turbines and present the objectives of this dissertation.

In **Chapter 2**, the factors that affect the feasibility of small and medium wind turbine (SMWT) projects are presented. The essence of a successful wind turbine project is that a good wind turbine is properly installed on a windy terrain. For SMWTs, there are two constraints holding back the economic viability of such projects. Currently the SMWT market is immature. Potential users/investors are therefore likely to select a wind turbine with a sub-optimal efficiency, leading to a low return on investment. Secondly, tools to assess the wind resources or derive the most suitable location to install the turbine are generally prohibitively expensive in relation to the capital cost of the turbine. These assessments are therefore often neglected. The penalty for neglecting a proper resource assessment can be severe, as sites considered for SMWT projects may have unfavourable wind conditions. Moreover, the pattern of wind flow at the typical hub height of these

turbines is generally complex due to the proximity of obstacles. Knowing the local wind resources is therefore critical for a pre-assessment of the economic viability of the project as well as for the selection of the optimal location of the wind turbine on the site. Apart from market and wind conditions, economic factors such as local incentives, the electricity price and the energy consumption of the user(s) will have a critical effect on the viability of a project. As SMWTs are often located close to places where people live or work, the impact of the turbine on the surrounding environment (e.g. shadow flicker and visual impact) and the socio-political acceptance of SMWTs are critical elements in the assessment of the feasibility of a project. All these aspects are introduced in this chapter.

A good prediction of the annual energy production (AEP) is the core of any assessment of an SMWT project. In **Chapter 3** we compare different approaches to estimate the AEP, by applying them to 29 indepently-tested SMWTs and 23 measurement sites. From this analysis, we derive guidelines for end users, policy makers and investors on how to ensure a reliable prediction of the AEP. The most accurate prediction of the AEP is based on hub height wind speed measurements and a reliable power curve of the turbine. For SMWTs, this procedure is often impractical, and less rigorous approaches are frequently used. We show that a turbine's rated power, though a popular way to compare and select a small wind turbine for a given site, is not a satisfactory indicator of the AEP. If only the annual average wind speed at the site is known, the prediction of the AEP based on the Rayleigh distribution (available in IEC test rapports) is a more reliable alternative for rated power. More advanced wind speed distributions such as Weibull or the maximum entropy principle (MEP), can significantly reduce the error on the AEP. The best situation is of course to have wind measurements on site. In this case the data should be used directly rather than through a statistical distribution.

As wind speeds are generally measured over periods of one year or less, they do not represent the average wind conditions over the lifetime of the turbine. We therefore compare three different statistical techniques, so-called measure-correlate-predict (MCP) techniques, to estimate the long-term potential (and thus long-term AEP). Our advice here is to use the variance-ratio method as it provides accurate results and is easy to use. Two approaches to reduce the cost of a measurement campaign are tested: a shorter measurement campaign (1-11 months) and a lower measuring height (smaller mast needed or use of meteorological data). Our analysis

shows that these approaches have a significant impact on the accuracy of the AEP. Guidelines on the proper use of these approaches are formulated.

Even when wind data are available, care should be taken on how to combine the data with the power curve to reliably predict the AEP. A possible mismatch of the averaging time with which the wind speeds and turbine power outputs are sampled causes a systematic error on the prediction of the AEP. A longer averaging interval will decrease the apparent power in the wind: the probability of high and low wind speeds decreases, making the histogram more concentrated around the mean wind speed. When such data are combined with the power curve of a wind turbine, the AEP will be underestimated. Although this fact has been pointed out in the literature, there are to our knowledge no specific instructions on what averaging interval should be used to measure the wind speed and how sensitive the AEP is to this interval. In **Chapter 4**, we develop a theoretical framework to study the variation in averaging time. When using a longer averaging time, the variance over the averaged wind speed samples decreases, but an increase of the variance within each sample is observed. The power curve can then be corrected for this increased variance. As the variance within each sample is not always available (as for example for typical meteorological data), we suggest a procedure to predict this variance. By collecting wind data with a high sample frequency for a short period, the power spectral density of the site can be derived and the variance can be estimated.

In **Chapter 5** and **6**, we illustrate how the methods and techniques from the previous chapters can be applied in practice by assessing the feasibility of SMWTs in rural and urban areas. We first assess the wind potential by using meteorological data supplemented with our own wind speed measurements to create a wind map of Flanders at the typical hub heights for small (15 m) and medium wind turbines (30 m). These data are then correlated with long-term reference data to predict the long-term AEP of four small and medium wind turbines. Next, we provide an economic viability assessment of these turbines, investigate the socio-political acceptance via a market survey and present the legal situation in Flanders. Finally, we present specific case-studies in rural Belgium where we illustrate how numerical simulations can be used for micro-siting and how derating a wind turbine can represent an opportunity for manufacturers to shift the operating conditions to the lower wind regimes that are often present at sites being considered for SMWTs.

In **Chapter 6**, we perform a feasibility study in urban areas, particularly Brussels. In heavily built-up areas the wind flow is more complex than in rural areas. Therefore, we first use an existing analytical approach to create a wind map of Brussels to estimate the above-roof mean wind speed. Using this wind map, we can identify areas with a higher wind potential. To verify the accuracy of our wind map, we validate the predicted wind speed with measured wind data on several locations. As this wind map only indicates the average wind speed, we measure the wind on four of these locations and assess the economic viability of four small and medium wind turbines based on the local incentives for Brussels. Next, we use numerical simulations to identify suitable locations for specific sites in Brussels. In order to generalise these results, we verify if rules of thumb can also be used to pinpoint these locations. Finally, we assess the technical feasibility to ascertain if SMWTs could actually be installed in an urban area such as Brussels.

Finally, the conclusions drawn from this work are presented and future work is discussed in **Chapter 7**.

Chapter 1

Objectives and basic concepts

Abstract—*This chapter briefly introduces some basic concepts on wind turbines, wind resource assessment, and siting studies. It concludes with the objectives and research questions of this dissertation.*

In this chapter we first introduce the basic concepts used in this work (Section 1.1 to 1.9). We then describe the motivation for this research and formulate the basic research objectives (Section 1.10 and 1.11).

1.1   Wind energy basics

The cost of wind energy   Over the past half-century, there has been a tremendous development in sustainable energy technologies. This development has been driven to a large extent by rising or unpredictable fuel prices, environmental concerns (in particular about the effects of global warming) and the public perception of nuclear energy as unsafe.

The goal of any source of sustainable energy is to provide a secure supply of affordable energy, while reducing $CO2$ emissions. (This is sometimes referred to as the energy trilemma). In terms of cost of energy, wind is one of the cheapest sources of sustainable energy, with the exception of hydropower, as shown in Figure 1.1. In terms of reliability, the strong dependence of the energy output of a wind turbine on the wind speed makes wind energy one of the more difficult energy sources to predict. This same dependence is also the reason why relatively small errors in the estimated wind speed can have large effects on the annual energy production, and why careful resource assessment is a prerequisite for any wind energy project, large or small. The effect of wind speed variability on the global energy mix and the various ways in which this effect can be mitigated are beyond the scope of this work. The need for the careful assessment of the wind energy resource, on the other hand, is central to this dissertation.

Power   From basic physics it can be derived that the available wind power P_w, being the amount of kinetic energy flowing through the rotor disk per unit time, can be expressed as

$$P_w = \frac{1}{2}\rho A V^3 \tag{1.1}$$

where ρ is the air density, A the swept area of the rotor disk and V the wind speed. The above equation is derived in wind energy textbooks such as Manwell, McGowan, and Rogers, 2009.

Power coefficient and Betz-Joukowsky limit   Of the available wind power P_w, only a fraction C_P is actually extracted by the rotor. This
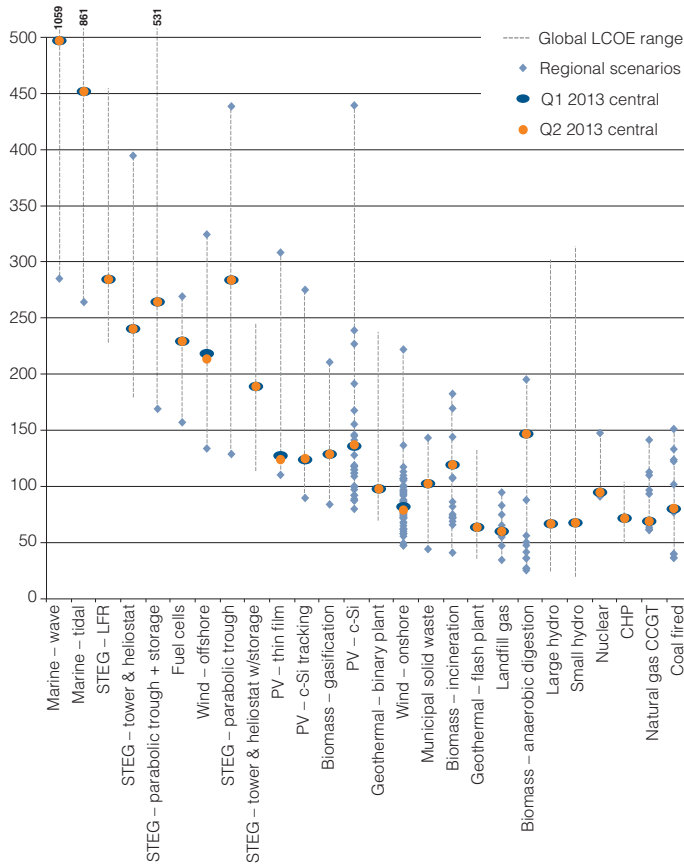
Figure 1.1: Global levelised cost of energy in the first and second quarters of 2013 (USD/MWh). Figure from Salvatore (2013).

fraction is referred to as the power coefficient, and is defined as

$$C_P = \frac{P}{P_w} \tag{1.2}$$

where P is the power extracted from the wind by the rotor. The largest possible value of this fraction for a rotor in open air is $16/27 \approx 59$ %. This limit is known as the Betz-Joukowsky limit (Betz, 1926; Okulov and Kuik, 2012). This limit neglects effects such as drag, tip-loss and wake rotation. Losses in the drivetrain and generator further reduce the power eventually produced in the form of electricity, albeit by a small amount. Modern large wind turbines can reach power coefficients as high as 0.5. This number is

considerably lower for small wind turbines.

Power curve The graph of the power output of a wind turbine as a function of wind speed is called the power curve. The wind speed where the turbine starts to produce electricity is called the cut-in speed. The speed at which the turbine is 'parked' in high winds and no longer produces electricity is called the cut-out speed. When the turbine reaches a certain level referred to as the rated power, wind energy is spilled (either by active pitch or passive stall in the case of a turbine with a fixed angular speed) to reduce the loads on the turbine. The speed at which this happens is referred to as the rated speed. A schematic power curve is shown in Figure 1.2. The constant power beyond rated speed is typical for a pitch-regulated turbine, whereas the power of a stall-regulated turbine rises and falls off again beyond the rated speed[1].
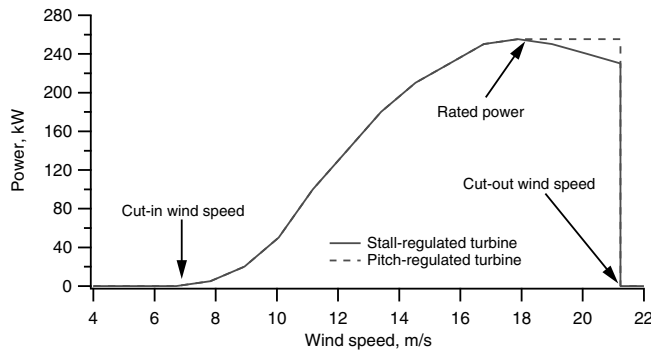
Figure 1.2: Schematic power curve of a wind turbine, giving the power as a function of wind speed. Figure reproduced from Manwell, McGowan, and Rogers (2009).

Using figure 1.2, the electrical power coefficient $C_{P_{el}}(V)$ can be determined. This coefficient is defined by:

$$C_{P_{el}}(V) = \frac{P(V)}{P_w} \tag{1.3}$$

where $P(V)$ is the power curve of the turbine. In contradiction to C_P, $C_{P_{el}}(V)$ takes all the losses in the drivetrain, generator and inverter into account.

---

[1]Some standards use a different definition for the rated power of a (small) wind turbine. These definitions will be discussed in section 3.3

Variability of the wind The main reason why it is so difficult to estimate wind resources is the variability of wind conditions. Wind-speed varies primarily as a function of time, height and location. This is addressed in the following sections.

1.2 Temporal variability of wind conditions

The temporal variation of wind conditions occurs at different time scales: inter-annual, annual, diurnal and short-term (gusts and turbulence). The contribution of these different time-scales to the variability of the wind speed is shown in Figure 1.3. In this figure, a high value corresponds to a significant change in wind speed over the specific time-scale.
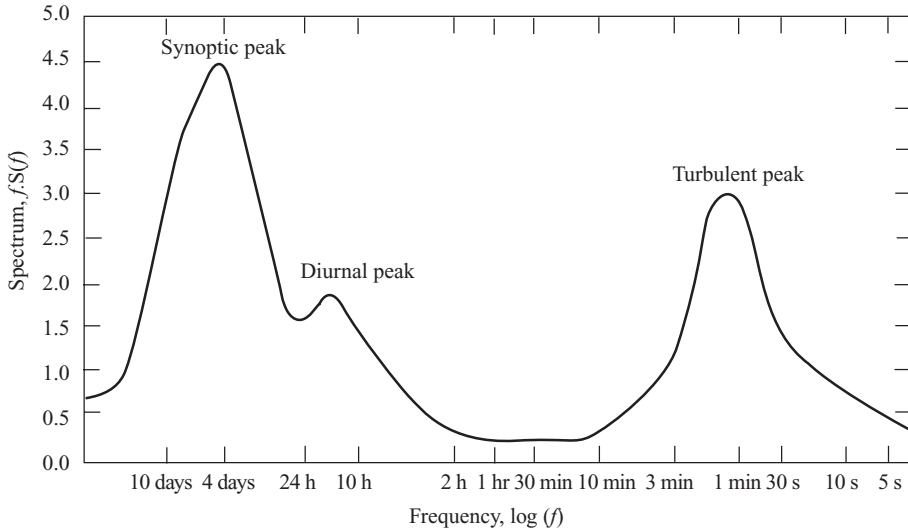
Figure 1.3: Energy spectrum of wind speeds as a function of time scale. From Burton et al., 2001.

Although this graph is site-specific, there are characteristic similarities when comparing different sites. For example, there appears to be a lack of wind speed variation for time-scales of about 10 minutes to 1 hour. These time-scales are often referred to as the spectral gap. This gap separates the graph into two regions with on the left variations on the macro-meteorological level and on the right turbulence and gusts.

As the time-scales at which the wind speeds are measured are not used

consistently (time intervals of 1-minute, 10-minutes or 1 hour are most frequently used for wind energy purposes), it will impact the variations present in the data. As the wind speed is proportional to the cube of the wind speed, this will also affect the energy present in the data. As these data are used to predict the energy production of a wind turbine, using one interval or the other will affect the prediction of the Annual Energy Production (AEP). In Chapter 4, this effect is discussed and we present a procedure on how to minimise the error on the prediction of the AEP.

1.3 Wind shear and terrain roughness

Wind shear describes the variation of wind speed with elevation. The characterisation of wind shear is a rather difficult task as it depends on numerous factors, including wind speed, height, earth's surface, atmospheric stability, and the nature of the terrain. Different approaches exist to represent this wind shear. In this dissertation we only consider neutral stability and thus assume that the characteristics of the vertical wind profile do not vary over time (due to the difference in earth's surface and air temperature). We apply the log law, the linear log law and the power law to extrapolate the wind speed. In this section, we briefly present each law separately. A detailed analysis and comparison will be presented in Chapter 3.

1.3.1 Log law

The log law is based on principles of boundary layer flow and can be described as (Ray, Rogers, and McGowan, 2006):

$$V(z) = \frac{v^*}{\kappa} \ln \left(\frac{z}{z_0} \right) \tag{1.4}$$

with $V(z)$ the wind speed at height z, v^* the friction velocity, κ the von Karman constant (which is typically set to 0.41) and z_0 the roughness height.

The roughness length is a parameter used to characterise shear and is also the height above the ground where the wind speed is theoretically zero. This parameter varies according to the terrain of the site and tables with roughness lengths for each type of vegetation, height and spatial area between buildings are available in the literature (Wieringa, 1992).

The friction velocity v^* is related to the shear stress at the surface and to the density, but is best viewed as a scaling parameter to be determined from wind speed measurements at different heights.

If the wind is measured at two different heights, both the roughness length and the friction velocity can be calculated by applying Eq. (1.4) to the measured wind speeds at both heights:

$$V_1 = V_1(z_1) = \frac{v*}{\kappa} \ln(\frac{z_1}{z_0}) \tag{1.5}$$

$$V_2 = V_2(z_2) = \frac{v*}{\kappa} \ln(\frac{z_2}{z_0}) \tag{1.6}$$

By dividing Eqs. (1.5) and (1.6) we obtain

$$\frac{\ln\left(\frac{z_1}{z_0}\right)}{\ln\left(\frac{z_2}{z_0}\right)} = \frac{V_1}{V_2} \tag{1.7}$$

which can be re-arranged to obtain

$$z_0 = \frac{z_1^{\frac{V_2}{V_2 - V_1}}}{z_2^{\frac{V_1}{V_2 - V_1}}} \tag{1.8}$$

The friction velocity can then be determined with:

$$v* = \frac{\kappa V_1}{\ln\left(\frac{z_1}{z_0}\right)} = \frac{\kappa V_2}{\ln\left(\frac{z_2}{z_0}\right)} \tag{1.9}$$

Eq (1.9) can be used as check to verify whether the two measured wind speeds fit the log law. Computing $v*$ at both heights should lead to the same value. If so, the wind speed can be determined for any reasonable height from Eq. (1.4).

For the built environment, the log law should be modified to account for the high roughness (Plate, 1995). Fitting of the log law with measurements of the wind speed well above the average height of the roughness elements shows a new (virtual) surface level at $d + z_0$ above the earth's surface, where d is the displacement height. The log law for the built environment thus reads:

$$V(z) = \frac{v*}{\kappa} \ln\left(\frac{z - d}{z_0}\right) \tag{1.10}$$

1.3.2   Linear log law

Sometimes, the log law is modified to consider mixing at the earth's surface (Manwell, McGowan, and Rogers, 2009). By applying this mixing, the wind speed below the roughness length is not equal to zero. The wind profile is then described as:

$$V(z) = \frac{v^*}{\kappa} \ln \left(\frac{z + z_0}{z_0} \right) \tag{1.11}$$

This so-called linear log law, i.e. the log law with z_0 in the numerator, is often used in CFD codes for studies of the best on-site location of a turbine (Blocken, Stathopoulos, and Carmeliet, 2007).

1.3.3   Power law

The power law represents a simple model for the vertical wind speed profile (Manwell, McGowan, and Rogers, 2009). Its basic form is:

$$V(z) = V(z_r) \left(\frac{z}{z_r} \right)^{\alpha} \tag{1.12}$$

with α the power law exponent. Early work on this subject showed that under certain conditions α is equal to 1/7, indicating a correspondence between wind profiles and flow over flat plates. In practice, the exponent α is a highly variable quantity (Fox, 2011; Kubik et al., 2013).

1.4   Wind speed variation over terrain—the importance of siting

The wind speed at a given height also depends on the location. Partly this is due to roughness changes over the terrain, but the most direct effect is the wind shading and increase of turbulence caused by obstacles. In particular at the low heights typical for small and medium-sized wind turbines, wind speeds can vary over distances as short as metres.

We will show how numerical simulations can be used to predict this wind shading and avoid installing a wind turbine in the wake of an obstacle or building. This work will be presented in Chapters 5 and 6 and will be carried out using the CFD (computation fluid dynamics) code Open-FOAM. We use RANS (Reynolds Averaged Navier Stokes) simulations in combination with a standard $k - \epsilon$ turbulence model, as it is still by far

the most widely used CFD model (Yoshie et al., 2007; Huang, Li, and Xu, 2007).

Several authors (Blocken, Stathopoulos, and Carmeliet, 2007; Tominaga et al., 2008) have pointed out that validation of the CFD model and the correct implementation of the atmospheric boundary layer is essential for the correct use of these simulations. In the context of our work, we have therefore simulated an atmospheric boundary layer on a flat terrain (to verify if it was implemented correctly) and we validated our CFD model by comparing and reproducing a case from the literature (Blocken, Stathopoulos, and Carmeliet, 2007). This work has been partly presented in Vermeir, Runacres, and De Troyer (2012).

The variation of wind speeds at large meteorological scales is crucial for wind forecasting and thus important when discussing the complementarity of wind in the global energy mix. Since we focus on the (regional and local) conditions that determine the feasibility, large-scale meteorology is not addressed in this dissertation.

1.5   Statistical analysis of the wind resource

1.5.1   Basics

Suppose one has a series of N wind speed observations, V_i, each averaged over the time interval Δt. From these data, the basic statistical properties of the wind speed can be derived: The average wind speed $\overline{V}$ over the total period of data collection is given by:

$$\overline{V} = \frac{1}{N} \sum_{i=1}^{N} V_i \qquad (1.13)$$

The turbulent intensity TI is given by:

$$\mathrm{TI} = \frac{\sigma_V}{\overline{V}} \qquad (1.14)$$

with σ_V the standard deviation of the wind speed.

The average power output of the wind turbine can be written as:

$$\overline{P} = \frac{1}{N} \sum_{i=1}^{N} P(V_i) \qquad (1.15)$$

The values $P(V_i)$ are to be determined either from on-site power measurements or, as is more often the case, from the power curve of the wind turbine being considered for installation.

The AEP can be simply derived from the mean power as the product with the number of hours in a year. With $\overline{P}$ in kW this gives

$$\text{AEP} = 8760 \, \overline{P} \qquad [\text{kWh}] \qquad (1.16)$$

1.5.2 Wind speed distributions

In particular when wind conditions need to be compared between sites, the wind resources can be described by a probability density distribution. Such a distribution then represents the likelihood that a certain wind speed occurs. The benefit of these kinds of distributions is that they can describe the on-site wind conditions in just a few parameters.

When combining the wind speed distribution $\varphi(V)$ of a given site with the power curve $P(V)$ of wind turbine, the mean power $\overline{P}$ is given by

$$\overline{P} = \int_V P(V)\varphi(V) \, \mathrm{d}V \qquad (1.17)$$

with V the wind speed (m/s). The AEP can be derived using Eq. (1.16).

Hereafter, we briefly present two often used statistical distributions. The influence of using these distributions (and other more advanced approaches) to predict the annual production of a turbine are discussed in Section 3.4.

Weibull distribution: The Weibull distribution is the most often used statistical distribution to represent wind speed measurements. Its probability density function (pdf) is defined by:

$$\varphi_{\mathrm{wei}}(V) = \frac{k}{c}\left(\frac{V}{c}\right)^{k-1} \exp\left[-\left(\frac{V}{c}\right)^k\right] \qquad (1.18)$$

The Weibull pdf is determined by two parameters: k, a shape factor, and c, a scale factor. Often k and c are calculated using approximate expressions (see e.g. Manwell, McGowan, and Rogers (2009); Carta, Ramírez, and Velázquez (2009)) as a function of the mean wind speed $\overline{V}$ and the standard deviation σ_V:

$$k = \frac{\sigma_V}{\overline{V}} \qquad (1.19)$$

$$c = \frac{\overline{V}}{\Gamma(1 + \frac{1}{k})} \qquad (1.20)$$

with Γ the gamma function.

Rayleigh distribution: The simplest distribution to represent the on-site wind resources is the Rayleigh distribution as it only requires the knowledge of the mean wind speed $\overline{V}$:

$$\varphi_{\mathrm{ray}}(V) = \frac{\pi}{2}\left(\frac{V}{\overline{V}^2}\right)\exp\left[-\frac{\pi}{4}\left(\frac{V}{\overline{V}}\right)^2\right] \qquad (1.21)$$

It should be noted that the Rayleigh distribution is a special case of the Weibull distribution for which the shape parameter k is equal to 2 (Manwell, McGowan, and Rogers, 2009).

1.5.3 Measure-correlate-predict

For the assessment of wind resources, wind speeds are rarely measured for longer than a year. To predict the annual energy production over the expected lifetime of the turbine (typically 20 years) the measured wind speeds need to be related to the expected wind speeds over the lifetime of the turbine. Therefore, a so-called measure-correlate-predict technique is used in wind resource assessment studies. To apply this statistical technique, the *measured* short-term wind data are *correlated* with long-term data at another site (often a meteorological station). The objective is to correlate the measurement period where the wind speed (and wind direction) are simultaneously measured and find parameters that describe this correlation. These parameters are then applied on the long-term wind data set, to *predict* the long-term wind conditions on the measurement site.

More details about how this technique is applied on measured wind data and what type of error may be expected on the AEP will be presented in section 3.6.

1.6 Wind measurements

For wind energy purposes, the following measurement equipment is used:

- anemometers to measure the wind speed,

- wind vanes to measure the wind direction,

- temperature and pressure sensors to derive the air density.

For each application, the type and amount of instrumentation used varies widely. For example, often measuring the wind speed at one height is not

sufficient. By measuring the wind speed at multiple heights, the vertical wind profile can be estimated (as shown in Eq (1.8)) and the wind data can be extrapolated to hub height. If the wind speed should be sampled with a fine temporal resolution (for turbulence measurements), (ultra)sonic anemometers are used. These anemometers often allow to measure the wind direction as well (when they use multiple pairs of transducers).

In a basic measurement setup, the wind speed and wind direction are measured separately with a cup anemometer and a wind vane. Both are measured with a sample frequency of 1 Hz and per interval of 1 or 10 minutes (IEC, 2006), the mean and standard deviation are registered. For the air temperature and air pressure generally a lower sample frequency is used (at least once a minute), although they are registered at the same interval as the wind speed and direction. By combining the air temperature T and air pressure p, the air density ρ can be derived by (IEC, 2006):

$$\rho = \frac{p}{R_0 T} \tag{1.22}$$

where R_0 is the gas constant of dry air (287 J/(kg K)). All data are saved on a data logger which is connected to the sensors. As these setups are located in remote areas, the data are transmitted via General Packet Radio Service (GPRS). In this dissertation, the results of this kind of wind measurement campaigns will be presented. A basic setup we used in this context, is shown in Figure 1.4.

1.7   Economic measures

In this dissertation, there are three economic measures which will be frequently used: levelized cost of energy (LCOE), payback time and internal rate of return (IRR).

The LCOE is capable of analysing the true economic performance of different wind turbines by neglecting the local incentives and electricity prices. It is defined by the balance between the costs and the energy the turbine produces:

$$\text{LCOE} = \frac{I_0 + \sum_{n=1}^{N} \frac{A_t}{(1+r)^n}}{\sum_{n=1}^{N} \frac{\text{AEP}}{(1+r)^n}} \tag{1.23}$$
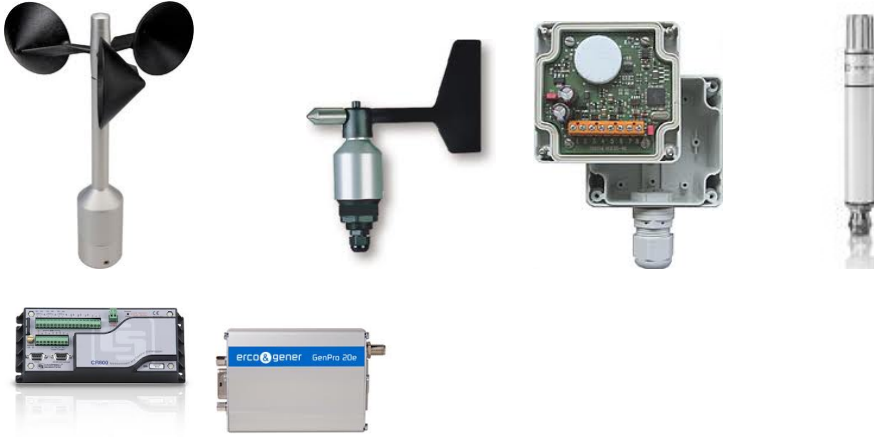
Figure 1.4: Clockwise starting from top left: Thies first class anemometer, Thies compact wind vane, Thies baro transmitter, Genpro 20e GSM/GPRS serial transmitter, Campbell Scientific CR 800 and Thies compact temperature sensor

where I_0 is the initial investment cost, A_t is the maintenance cost in year t, r is the discount rate (typically 3-5 %), AEP is the annual energy production and N is the expected lifetime of the wind turbine in years.

To analyse the economic viability of a small or medium wind energy project for specific regions, areas or countries, the payback time can be used. This measure takes the local incentives, policies and electricity into account to determine the period where break-even is reached. It is defined as the year where the total cash flow (or net present value) of the project equals the investment cost. To determine the payback time, often a distinction is made between a static and dynamic payback time. The static payback time does not take the discount rate into account and is defined as:

$$\text{Static payback time} = \frac{\text{Initial investment}}{\text{Periodic cash flow}} \tag{1.24}$$

The dynamic payback time is calculated using the same procedure, however this method takes the time value of money into account (discount rate).

The internal rate of return (IRR) is determined using the net present value (NPV) as a function of the rate of return. A rate of return for which the NPV is zero is the internal rate of return. It is thus given by:

$$\text{NPV} = \sum_{n=0}^{N} \frac{C_n}{(1+r)^n} = 0 \tag{1.25}$$

where C_n is the cash flow in year n, N the lifetime of the turbine and r the IRR (typically 10-15 %).

1.8   Wind turbine performance assessment

A power curve is essential to assess the performance of a wind turbine. The power curve is derived by the simultaneous measurement of the wind speed and the electrical power during a field test. An example of such a measurement is shown in Figure 1.5 where the wind speed and electrical power of a 5 kW wind turbine is monitored for 2 hours with a measuring interval of 1 minute. More details about these measurements are presented in Section 5.6.
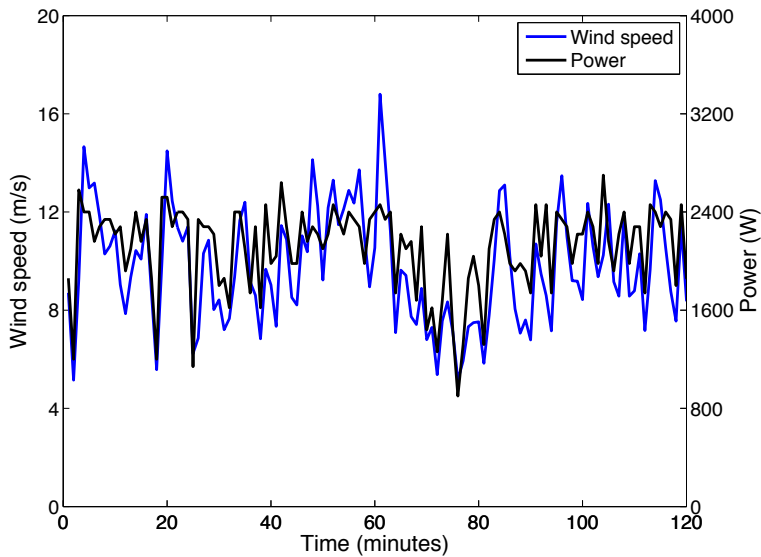
Figure 1.5: Simultaneous measurement of the wind and power of a wind turbine with a rated power 5 kW. More details about these measurements are presented in Section 5.6.

These data can be combined to derive the power curve. In the standards (IEC, 2006) which specify the requirements and the procedure to derive a power curve, the method of bins is used. In this method, bins of 0.5 m/s width are used and the mean value of the wind speed and electrical

power are calculated according to the equations:

$$P_i = \frac{1}{N_i} \sum_{j=1}^{N_i} P_{i,j} \tag{1.26}$$

$$V_i = \frac{1}{N_i} \sum_{j=1}^{N_i} V_{i,j} \tag{1.27}$$

where P_i is the average power output in bin i, $P_{i,j}$ is the power output of sample j in bin i, V_i is the average wind speed in bin i, $V_{i,j}$ is wind speed of sample j in bin i and N_i is the number of bins in the data set. To ensure that the data are representative, each bin should at least contain 30 samples (1-minute samples for small wind turbines and 10-minute samples for large wind turbines).

In the standards (IEC, 2006), the distance between the anemometer and the turbine is specified so as to minimise the interference between the wind turbine rotor whilst maintaining a reasonable correlation between the measured wind data and electrical output of the turbine. Therefore the anemometer should be installed at a distance of 2 to 4 times the rotor diameter of the turbine and at the same height of the hub ($\pm$ 2.5 %). Simultaneously the wind direction is measured to only include the upwind wind speeds (excluding the data where the anemometer is in the wake of the rotor). More details about the specifications (such as the accuracy) of the sensors, measurement procedure and data acquisition can be found in the standards.

1.9 Small and medium-sized wind turbines

1.9.1 Definition

The IEC 61400-2 standard (IEC, 2013) defines a small wind turbine as a 'system of 200 m^2 rotor swept area or less that converts kinetic energy in the wind into electrical energy'. This corresponds to a rotor diameter of 16 m and a typical rated power of about 50 kW.

As the diameter of the largest wind turbines at the time of writing is 164 m (which is more than double the wingspan of an Airbus A380 aeroplane), the cut-off at 16 m is overly restrictive, as a wind turbine with a diameter of 20 m and a rated power of 100 kW is, for all practical purposes, still not large. In this work we have set the upper limit of the turbine sizes we consider by imposing a maximum rated power of 100 kW. We

Figure 1.6: Two wind turbines available on the market as medium wind turbines. Xant-23 (left) by Xant with a rated power of 100 kW and a rotor diameter of 23 m. E3120 (right) by Endurance Wind Power with a rated power of 50 kW and a rotor diameter 19 m.

acknowledge that this is somewhat arbitrary; a value of say 200 kW would have been equally valid. In keeping with what is customary in the industry, we refer to the category above 50 kW, such as for example Xant-23 by Xant or the E3120 by Endurance Wind Power (Figure 1.6), as medium-sized wind turbines. Wind turbines below 10 kW are sometimes referred to as micro wind turbines and rather confusingly this term is also used for turbines with a rated power below 1 kW, used in mainly for marine applications and in telecommunication. In Flanders, the maximum allowed hub height for a wind turbine to qualify as small is 15 m (Van Mechelen and Crevits, 2009).

1.10 The challenge of small and medium wind turbines

Small and medium wind turbines present a number of challenges that set them apart from larger wind turbines.

The market of small and medium wind turbines: Compared to the market of large wind turbines, the market of small wind turbines is extremely immature. To put it bluntly, when one would purchase a small

or medium wind turbine at random, the chances are overwhelming that one would end up with a wind turbine that would not produce a meaningful amount of electricity even in windy conditions. This is a situation which is very different from a mature market. A good example of such a mature market is the car industry, where the difference in quality is much smaller and where a randomly bought new car would be very likely to meet the expectations of the buyer.

Resource assessment for small and medium wind turbines: Due to the relatively low cost of small and medium wind turbines, an assessment of the available wind resources quickly amounts to a sizeable fraction of the total investment cost. A thorough resource assessment is therefore often neglected for small and medium wind turbines (SMWTs). Ironically, one could argue that the need for resource assessment is actually *greater* for SMWTs than for large wind turbines. The low hub height of SMWTs (15 m for a small wind turbine in Flanders, typically 40 m for a medium-sized wind turbine around 100 kW) has two consequences that both point to the necessity of proper resource assessment. First the wind speeds at low hub heights are on average much lower than for large wind turbines (where a hub height of say 85 m would be typical for a 2.5 MW turbine). SMWTs are therefore often installed on sites that have wind speeds that are close to the lower limit of what is economically viable. Resource assessment is therefore imperative, to determine whether the SMWT project is profitable or not. Secondly, the low height implies that the wind turbine often barely protrudes above nearby obstacles such as trees or buildings and that the local wind pattern is strongly influenced by these obstacles. Wind speeds at hub height can therefore vary rapidly over the terrain, and proper siting is a crucial ingredient of the wind resource assessment.

The role of test fields and certification of small and medium wind turbines: The development of test and certification procedures specifically for small and medium wind turbines can help to establish a more mature market. These tests ensure a more reliable operation and allow users/investors to know the performance before it is installed. One of the major issues here is that these tests and certifications procedures are expensive (roughly 100 k€) and time consuming (typically one year). As the market is still relatively small, manufacturers are not able to reach mass production and these costs are often (too) large to bear.

1.11 Objectives and research questions of this work

The broad objective of this dissertation is to investigate under what conditions small and medium wind turbines may be a profitable and practically feasible source of sustainable electricity.

The task of answering this question can be broken up into three parts:

- First, we need to understand the market of SMWTs, to know which turbines are liable to be economically viable if properly installed on a suitable site.

- Second, we investigate how to improve existing resource assessment tools for SMWTs and develop guidelines on how they are correctly used and applied to minimise the error on the prediction of the AEP.

- Finally, we investigate how the most suitable on-site location for the wind turbine can be determined in an affordable manner. The most suitable location is the location where the cost of energy is minimised, while guaranteeing a small impact of the turbine on its surroundings.

Chapter 2

Factors affecting the feasibility of small and medium-sized wind turbines

Abstract—*This chapter introduces the most important parameters and boundary conditions that determine the success (or failure) of a wind turbine installation. The first sections (2.1 to 2.4) elaborate on what determines annual energy production, and illustrate the importance of obtaining a reliable estimate of this AEP. Section 2.5 then links the annual energy production to economic parameters. Sections 2.6 to 2.9 assess the technical, socio-political and legal aspects of turbine installations. This chapter thus sets the scene for the remainder of this dissertation, which is dedicated to providing and illustrating practical guidelines to properly deal with the relevant factors affecting the feasibility of small and medium-sized wind turbines.*

2.1 The choice of the proper wind turbine

The market of small-scale wind energy is immature with huge variations in the efficiency of different turbines (Mertens, 2009). In particular, there is a large number of turbines on the market with an unacceptably low power output (Encraft, 2009). One of the major issues is that SMWTs are not obliged to undergo the same certification procedure as large MW wind turbines (IEC, 2013). Potential users of SMWTs cannot be expected to be experts in the field and therefore the probability of selecting an inappropriate or badly performing wind turbine is too large.

Although this shows a negative note, a significant market growth is seen in the past few years. By the end of 2012 (Gsanger, 2014; Zhang, 2012), a cumulative total of at least 806 000 small wind turbines were installed worldwide, demonstrating a growth of approximately 10 % compared to 2011, when 730 000 units were registered. The most significant growth is concentrated in three countries: China, USA and UK. China is still by far the largest market in terms of installed units with a total number of 570 000 units, representing 70 % of the world market.

A conservative assumption is that an annual growth of 20 % will be seen from 2015 to 2020 (Gsanger, 2014). As the total installed capacity was 678 MW by the end of 2012, this increase in market size will lead to an installed capacity close to 3 GW by 2020.

Currently there are a number of aspects imperative to grow to a more mature market:

- More rigorous standards, incentives and policies;

- Cheaper technology;

- Smaller performance gap compared to large wind turbines.

Feasibility studies, such as the ones performed in the context of this dissertation (Chapters 5 and 6), play a vital role in the evolution towards a more mature market. Dissemination of these studies to the decisive authorities can help to create better (and necessary) incentives and policies and can serve as a base for the development of a (more) rigorous legal framework. As the market evolves, the investment cost of SMWTs will go down. As it is currently still a young market, a significant part of the investment cost is spent on the development or the R&D component of the turbine. In addition, a bigger market size will enable manufacturers to reach mass production and so reducing the total cost of a SMWT. As mentioned above, the

majority of these turbines will still have a low efficiency although a number of good performing turbines are present on the market. Intensive market reviews and the development of standards and certification procedures, such as for example the IEC standards (IEC, 2006), can help to identify these particular turbines. Therefore, we developed a complete database where specifications of all SMWTs were collected, such as,

- rotor diameter D,

- cut-in, V_{in}, and cut-out,V_{out}, wind speed,

- AEP (if a range is given only the annual energy production at 4 m/s is given),

- investment cost,

- on- or off-grid and

- power curve availability.

To our knowledge this is the largest database in the world. In Table 2.1, a typical entry of our database is shown. This database is deliberately not

Name	Manu-facturer	P_{rat} [kW]	D [m]	V_{in} [m/s]	V_{out} [m/s]	AEP [kWh/year]	Cost [€]	Grid	P-curve
Montana	Fortis Energy	5.0	5.0	2	25	2691 [Tested 3.8 m/s]	18508	On-grid	Yes [Certified]

Table 2.1: Typical entry for a turbine in the database.

made publicly available as it is one of the valorisation tools derived from this research. Such a database gives an overview of every segment of the SMWT market and we used it in contract research projects (Vermeir and Runacres, 2014; Vermeir and Runacres, 2015). One of these projects is presented in Chapter 5.

A total of 781 different types of wind turbines were found. The horizontal-axis wind turbines (HAWT), Figure 2.1 top left, dominate the market, with a market segment of 75 %. The two other categories used are vertical-axis wind turbines (VAWT) (which include the Darrieus and H-Type VAWT, shown in Figure 2.1 top middle and top right) and 'other' types (including the Savonius VAWT, shown in Figure 2.1 bottom) with a market segment of respectively 17 % and 8 %. Most of these turbines have

a rated power between 1 and 10 kW (46 %) while still a significant part of the market is concentrated in the micro category with a rated power below 1 kW (30 %). Only 4 % of the SMWT market is concentrated on the medium wind turbine category with a rated power above 50 kW.

Figure 2.1: Database categories: horizontal-axis (top left), vertical-axis (top middle and top right) and 'other' types (bottom) of wind turbines.

2.2   Testing and certification

As mentioned in Section 2.1, manufacturers of SMWTs are not obliged to undergo the same certification procedure as large wind turbines. As these procedures are expensive (sometimes prohibitively so), few SMWTs manufacturers test their turbine before it is launched on the market. The development of specific standards, testing and certification procedures for SMWTs, such as AWEA (AWEA, 2009), RenewableUK (RenewableUK, 2014) and IEC (IEC, 2013), is expected to help promote the better performing wind turbines and can help to establish the growth towards a more mature market. As the current market is not in this stage yet, a reliable and tested power curve (measured by an independent test facility such as for example National Renewable Energy Laboratory (2014)) is a necessary condition for a proper selection of the better performing wind turbines as it ensures an accurate prediction of the energy output of the turbine. Almost

all manufacturers of SMWTs will publish a power curve. The question is if such a power curve (which is not tested) can be used to predict the AEP and determine the economic viability of a project.

A simple example could answer this question. We were contacted by a SME to check the performance of a 200 kW wind turbine, who wanted to buy and install this machine. Via this SME, the manufacturer provided us with 'measured' wind speed and power data of the turbine. We used the IEC standards (IEC, 2006) to derive the power curve. A quick sanity check was performed by calculating the electrical power coefficient and comparing it to the the Betz-Joukowsky limit of 59.3 % (see Chapter 1). This comparison learned that in the wind speed range from 3 to 8 m/s the $C_{P_{el}}$ was close (and over) the Betz-Joukowsky limit as shown in Figure 2.2. An operating turbine is unlikely to reach an electrical power coefficient of more than 0.5 (due to various losses such as the tip loss, drag loss and losses in the drivetrain, generator and inverter).
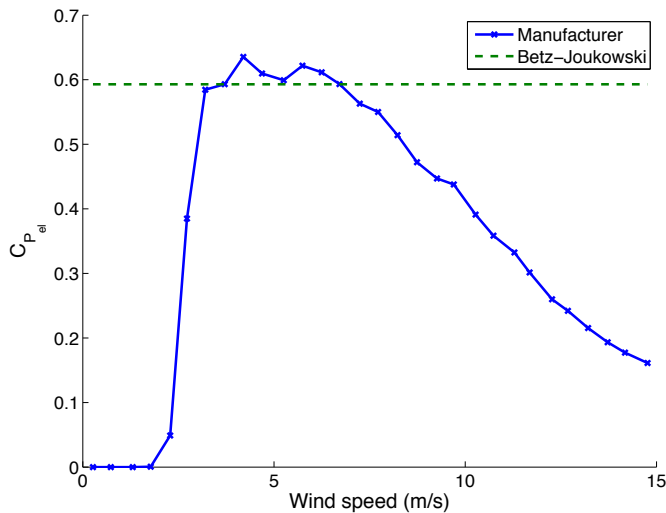
Figure 2.2: Calculated $C_{P_{el}}$ curve according to the measurements of the manufacturer (blue) and the maximum C_P according to the Betz-Joukowsky limit.

This simple example shows that manufacturers tend to overestimate the power of the turbine if it is not independently-measured. Therefore only independently-tested wind turbines should be used in order to ensure an accurate analysis of the economics of a SMWT project. Furthermore, as

these certification procedures include strength and safety tests, these tests ensure a more reliable and safer operation of the turbine.

Using only tested turbines drastically limits the amount of turbines that can be considered for a SMWT project. In the context of this dissertation, a smaller database is made, only including tested wind turbines. As mentioned in Section 2.1, this database is deliberately not made publicly available as it is one of the valorisation tools derived from this research.

2.3 The available wind resource and its assessment

The typical hub height of a SMWT is lower than large wind turbines. At this lower height, the terrain and wind patterns are generally complex. An accurate assessment of the wind resources and the proper derivation of a suitable location to install a wind turbine on the terrain is therefore imperative. One of the major issues for this assessment is that wind resource assessment tools are costly in relation to the investment cost of a SMWT. Typical small wind turbines with a rated power of 3-10 kW cost about 20-50 k€ while a measurement campaign can easily cost 4-7 k€. Certainly for the smaller (cheaper) wind turbines, the cost of a measurement campaign thus represents a significant fraction of the total investment cost of the project. In addition, for SMWT projects the financial yields are often limited even for relatively windy sites. A proper assessment of the wind resources is therefore often neglected although it is one of the essential steps for the accurate prediction of the energy output and so ensuring an accurate economic analysis of the whole project. This represent one of the major challenges for the SMWT industry.

The development of low cost resource assessment tools capable of predicting the wind resources quickly, cheaply and accurately is therefore vital. Wind maps are one of these low-cost tools that can serve as a first estimate of the on-site wind conditions. Such a wind map is created by combining roughness maps and wind data of meteorological stations (Best et al., 2008). It generally gives an indication of the annual average wind speed at a certain height and in Chapter 3 we will offer guidelines on how this average wind speed can be translated to an accurate prediction of the AEP of a turbine. Another advantage of these wind maps is that they are capable of identifying regions with a higher wind potential. In Chapter 6, this methodology is presented and applied to the Brussels Capital Region.

Other examples to reduce the cost of a measurement campaign are to

limit the measurement period or the measurement height. By reducing the measurement period below one year (general recommendation in the literature (Taylor et al., 2004; AWS Scientific Inc., 1997)), one measurement setup can be used on multiple sites over one year and so decrease the cost of one resource assessment study. For medium wind turbines, the typical hub height is in the range of 30-50 m. Using a lower mast height and extrapolating the measured wind data to the hub height can simplify the installation of the mast and reduce the number of man-hours for the installation. Both approaches will inevitably impact the accuracy of the prediction of the AEP. In Chapter 3 we will quantify the typical error on the AEP and offer guidelines on how to keep this error as low as possible.

2.4   Selecting the best spot on a given site

As discussed above, the selection of a good wind turbine (with an independently-tested power curve) and a site with sufficient wind resources are two essential requirements for a successful SMWT project. The proper selection of the most suitable on-site location, generally referred to as *micro-siting* is the third important factor.

In this dissertation, two micro-siting procedures will be applied (and compared) :

- Rules of thumb;

- Numerical simulations using Computational Fluid Dynamics (CFD) software;

A disadvantage specifically of CFD is that it is an additional expense that has to be added to the total cost of the project as CFD still requires an accurate assessment of the on-site wind conditions (by measuring the wind speed). However, these micro-siting studies avoid having to measure at each point on the terrain.

This is particularly important for SMWTs, that present particular challenges compared to large wind turbines:

- SMWT have a lower hub height;

- Regulations generally recommend that the turbine be installed close to a building, to minimise its impact on the landscape.

As a result, the terrains where SMWTs are typically placed are complex, with obstacles that may cause variations of wind speed and turbulent intensity at spatial scales of a few metres or less. The reliable (and cost-effective)

prediction of such variations is not an easy task, but one that is crucial to the success of almost every SMWT installation. As still a significant part of the cost of these studies is related to the modelling of the terrain and obstacles, tools such as Google Earth and Sketchup have significantly reduced the complexity and cost for this part of the study.

We illustrate how CFD can be used to advantage for micro-siting in Chapters 5 and 6.

2.5   Economic parameters

There are different economic parameters that impact the feasibility of a SMWT project:

Investment cost: The total investment cost consists of the costs for the turbine, blades, mast, foundation, grid connection and installation. Although some of these costs are difficult to estimate and are site dependent (especially for medium and large wind turbines where the grid connection and installation cost vary strongly), a typical breakdown of a large (geared) wind turbine is presented in Table 2.2 (Jamieson, 2011).

According to the small wind world report (Gsanger, 2014), the installed cost of a SMWT in the USA averaged €5150 per kW. According to this report, for China, the installed cost is significantly lower with an average of €1550 per kW. It should be noted however that there are questions about the quality of these turbines. During the preparation of this dissertation, we purchased, installed and tested three Chinese small wind turbines (Figure 2.3). For all turbines, we experienced quality issues during the early lifetime of the turbine. Even for the HY5kW wind turbine, which has a similar price as a Western turbine with the same dimensions, problems with the brake and blade pitching mechanism appeared during the first two years (see Chapter 5).

As mentioned in Section 2.1, a significant part of the total cost of the turbine is related to the R&D component or design of the turbine. In a more mature market this cost will decrease and positively impact the feasibility of SMWT projects.

The installed cost per kW of a SMWT obviously scales with the size of the turbine. Using our own database, the total investment cost (Figure 2.4 (left)) and the installed cost per kW (Figure 2.4 (right)) as a function of

Component	Cost [%]	Subcomponent	Cost [%]
Rotor	12	Blades	10
		Hub	1.5
		Rotor Lock	0.5
Nacelle	23	Gearbox	10
		Generator	4
		Brake	1
		Housing	3
		Shaft	2
		Yaw system	1.5
		Bearings	1.5
Electrics and control	10	Pitch system	4
		Inverter and controller	6
Tower	12	Tower	12
Installation and foundation	25	Grid connection	13
		Installation	1
		Transportation	4
		Foundation	7
Operation and maintenance	18	Operation	3
		Maintenance	15

Table 2.2: Typical breakdown of the cost of a geared large wind turbine (Jamieson, 2011).

rated power are derived for each turbine. The average installed cost per kW is about 4 k€ as it combines all markets including USA and China. In Figure 2.4 (right), it can be noticed that the average cost per kW for wind turbines with a rated power below 20 kW is higher than for turbines with a higher rated power. Therefore this figure is rearranged into Figure 2.5, where we distinguish rated powers below 20 kW (left) and rated power equal to or above 20 kW (right). The average cost per kW for rated powers from 20 to 100 kW (2.8 k€/kW) is about half the average cost for rated powers below 20 kW (5.2 k€/kW). In Figure 2.5, a distinction is made between the type of technology of each turbine. This shows that the most complex design (active yawing system and pitch regulated power control) is also the most expensive technology. For other designs, the average cost per kW is more dependent on the manufacturer than on the design choice

Figure 2.3: Wind turbines purchased, installed and tested for this dissertation.

of the turbine.
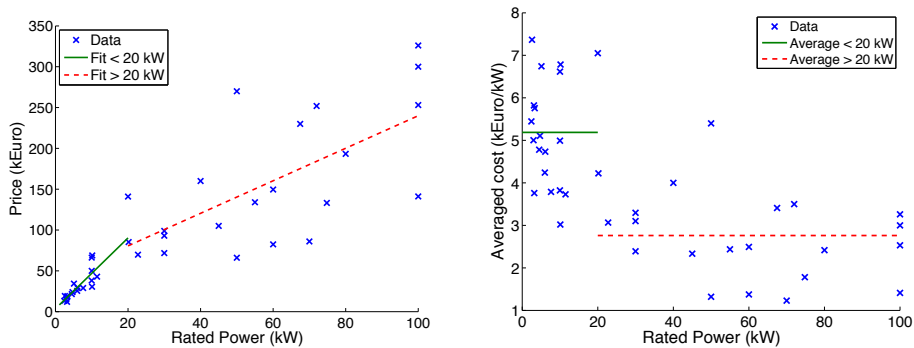
Figure 2.4: The total investment cost (left) and the installed cost per kW (right) as a function of the rated power for each turbine in the database. In the left figure, the data below 20 kW (solid line) and equal to or above 20 kW (dotted line) is fitted. In the right figure, the average installed cost is shown for rated powers below 20 kW (solid line) and equal to or above 20 kW (dotted line).

Incentives: In order for the small and medium wind turbine market to mature, the industry must be driven by support policies. Different supporting mechanisms exist depending on the region (or country). In Belgium, for example, a system of green certificates (GC) applies for renewable energy in general. For wind energy (including small, medium and large wind
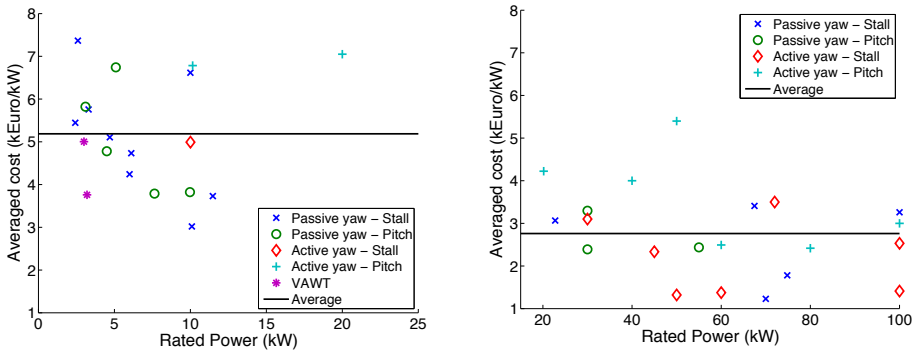
Figure 2.5: The installed cost per kW for wind turbines with a rated power below 20 kW (left) and wind turbines with a rated power between 20 and 100 kW (right). The average cost for each range is indicated on the figure (solid). A distinction is made between the type of technology of each turbine: active or passive-yawing, stall or pitch-regulated and vertical-axis wind turbines.

turbines), one certificate is granted for a certain amount of produced energy. Since January 2013, this amount is set to 1 MWh multiplied by a factor which is region dependent. For Brussels, this factor is more than 1 (see Chapter 6), while for Flanders this value is below one (see Chapter 5). Each certificate has to be sold to the distribution network operators. The price for such a certificate varies although a minimum value of € 97 is guaranteed. Feed-in tariffs are another supporting mechanism frequently used to encourage renewable energy investments. These schemes offer a fixed tariff to renewable system owners for the electricity generated during a fixed contract period, ranging usually between 15 to 20 years. In Table 2.3 the feed-in tariffs are given for the neighbouring countries and leading countries in the industry (Gsanger, 2014; Ragwitz et al., 2012). In the Netherlands, there is no national policy although in specific regions, there is a possibility for a feed-in tariff of 0.03 €/kWh.

Operation and maintenance: When determining the lifecycle cost of a wind turbine, a value that is often used for the cost for operation and maintenance (O&M) is 1-2 % of the investment cost per year (Schallenberg-Rodriguez, 2013). Typically for SMWTs, this cost needs to be determined over the full lifetime rather than spending a fixed cost each year. These types of turbines may not need service or repairs over the first five years, though it is reasonable to expect an expense for operation and maintenance

Region	Size limit [kW]	Feed-in tariff [€/kWh]
France	3	0.077-0.094
Germany	\	0.1013
UK	100	0.207
USA (Hawaii)	20	0.123
USA (Hawaii)	20-100	0.105
USA (Vermont)	15	0.181
USA (Indiana)	5-100	0.130

Table 2.3: Feed-in tariff for neighbouring countries and leading countries in the small-scale wind industry.

of five times 1 to 2 % (thus 5-10 %) of the investment cost after these first year (Sagrillo, 2002).

For direct drive machines, these significant expenses could be to repair or replace generator bearings, yaw bearings or blades. Minor parts like tail bushings, slip rings, brushes or paint are usually wear out until a replacement is necessary (Sagrillo, 2002).

Geared turbines have more moving parts and thus more wear points. Therefore, they will require more cost and more frequent service and repairs. Therefore, Sagrillo (2002) advises to use an O&M cost of 2 % for geared turbines and 1 % for direct drive machines as the direct drive wind turbines are generally more reliable and simple devices. The total predicted cost may seem large to just replace or repair a worn out component, but one should keep in mind that this cost is marginal to the work hours that have to be spent. This service may also need a steeple jack (if the turbine could be repaired on-site) or a crane (when it is repaired at the distributors workshop.

Furthermore, it should be noted that the lifetime of (small) wind turbine is directly proportional to the user's involvement. These types of turbines do need service from time to time and enough money should be allocated in order to reach the nominal 20 year lifetime of the turbine.

Electricity price: The electricity price is a highly variable parameter that directly impacts the cash flow of the investment and it is difficult to predict over the lifetime of the turbine. Although it is generally assumed in feasibility studies that the electricity price will increase with a fixed value each year, the past three years the electricity price in Flanders has rather decreased (see Figure 2.6). This electricity price is also dependent on the

amount of energy locally consumed by the user. Therefore, there is a (large) difference between the electricity price for households and for industry.
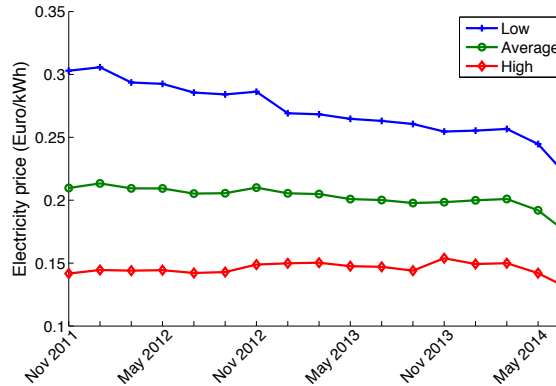
Figure 2.6: Evolution of the electricity price in the past 3 years in Flanders. The price is shown for household with a low (bleu, 600 kWh/year), an average (green curve, 3500 kWh/year) and a high (red curve, 7500 kWh/year) energy consumption (VREG, 2012).

When the current electricity price (at the end of the first semester of 2014) is compared to the neighbouring countries and the leading countries of the SMWT market, it turns out that the electricity price in Flanders is relatively high (European Commission Eurostat, 2014; USA Energy Information Administration, 2014). This is shown in Table 2.4. Differences between these countries exist due to a different distribution of the fuel mix and network costs (quality, age and characteristics of the grid). It should also be pointed out that the electricity price for the industry is less than 50 % of the one for households. This has a direct impact on the return on investment.

It is difficult to determine future electricity prices. Different scenarios exist, but the first prognoses towards 2020 show that electricity price is expected to increase (European commission, 2014). Specifically for the EU, it seems that the prices will then stabilise after 2020 (see Figure 2.7).

Energy consumption: When more energy is produced by the wind turbine than consumed by the user, this energy has to be sold to the grid.

Country	Household [€/kWh]	Industrial [€/kWh]
Belgium	0.233	0.108
Netherlands	0.186	0.097
Germany	0.260	0.128
France	0.139	0.095
UK	0.168	0.114
EU-27	0.189	0.115
USA	0.129	0.072

Table 2.4: Average electricity price for neighbouring countries and the leading countries in the SMWT industry in the first semester of 2014.

Generally the tariff for this selling price is significantly lower than the electricity price. This fact directly impacts the cash flow as a different tariff for this part of the produced energy should be taken into account. Certainly for medium wind turbines and SMEs where a large amount of energy is locally produced and consumed, the balance between both plays a vital role in the return on investment (see Chapter 5).

2.6 Grid connection

For large wind turbines, a significant part of the total investment cost is assigned to the connection to the grid. Jamieson (2011) estimates this cost at 10 % of the total investment cost indicating that it is an important factor of the feasibility of a large wind turbine project. Also for SMWT projects, the grid connection can play an important role in the economic viability of a project.

For SMWTs, both on- and off-grid installations are used. Wether or not the turbine is connected to the grid does not only affect the efficiency of the turbine but also has an impact on the total cost of the project. These off-grid installations are often coupled with batteries, which require additional maintenance (replacement within the lifetime of the turbine is usually necessary) and an additional DC/DC converter. In addition, when the battery is fully loaded and there is no load connected, the turbine dumps the produced energy into a resistor for dissipation or brakes (when the wind conditions are sufficient to allow the turbine to produce electricity), leading to a lower (useful) AEP.

For larger rated power ranges, the connection to the grid is usually
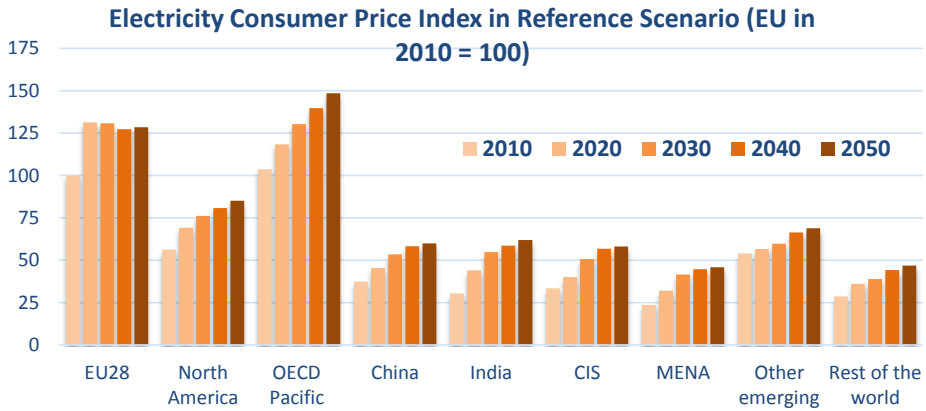
Figure 2.7: One of the scenarios for the future electricity in the EU and the rest of the world. All scenarios predict an increase in the electricity price (European commission, 2014).

more complex and costly. For example in Belgium and for turbines with a peak power above 10 kW, a specific energy meter and grid study is required (VREG, 2014b). This energy meter only allows overproduced energy (when more energy is produced than consumed by the user) to be sold to the grid while for smaller rated powers this energy is subtracted from the consumed energy. This has a direct impact on the cash flow as this selling price is a lot lower (0.04 €/kWh) than the purchase price (see Section 2.5, for SMEs this price is 0.108 €/kWh). The additional expenses for the grid study and the lower price for the produced energy will obviously affect the feasibility of the project.

2.7 Impact of small and medium wind turbines

The feasibility of a SMWT installation is directly influenced by its impact on the environment. Different aspects of the impact of a SMWT on the environment will be discussed:

- Shadow flicker;

- Visual impact;

- Noise and vibrations;

- Biodiversity;

2.7.1 Shadow flicker

Wind turbines, including SMWTs, are large structures and can cast long shadows. When the blades of a turbine rotate in sunny conditions, this will cause moving shadows that result in alternating changes in light intensity. This stroboscopic effect is referred to as *shadow flicker* (schematically shown in Figure 2.8).
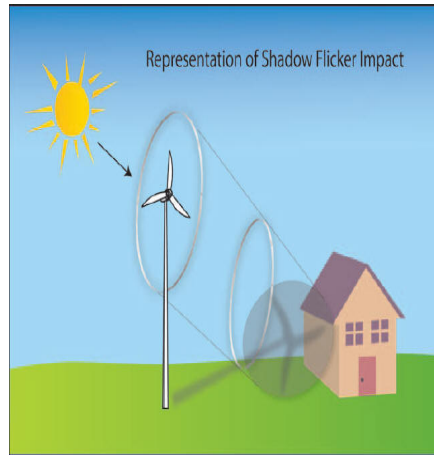
Figure 2.8: Shadow flicker caused by wind turbines (Control Alt Energy LLC, 2014).

The timing, intensity, and location of shadows are influenced by the size and shape of the turbine, landscape features, latitude, weather, and layout of the wind farm if one is dealing with multiple turbines (Rideout, Copes, and Constance, 2010).

Each country or region has his own regulations regarding the maximum times (or periods) that shadow flicker may occur. A frequently found limitation for shadow flicker is 30 hours/year and 30 minutes/day with a clear sky. For large wind turbines, often a 'shadow module' (by Siemens (2009)) is used, which stops the turbine when certain limits are exceeded. Such a system, will not only affect the total investment cost but will also decrease the energy output of the turbine. As for SMWTs, the financial yields are rather limited, using a 'shadow module' can affect the final decision to continue the project or not. Therefore, using such a module should be avoided

for SMWTs at all times by taken the limits on shadow flicker into account during the planning phase of the project.

For SMWTs, in the absence of vegetation between the turbine and the building, the turbine should be installed at a certain distance to limit the time that shadow flicker can occur. From sunset to sunrise, the shadow of a wind turbine is reflected beginning from west and ending to east. As the position of the sunrise and sunset changes during the year, this daily pattern will also change throughout the year. Therefore, a building at a certain distance and orientation of the turbine will only suffer from the turbine's shadow flicker for a specific time and moment during the year (Katsaprakakis, 2012). These specific times and periods can be easily derived using simple mathematics (or software packages such as WindPRO) and draw a zone around the turbine where these effect are above the limits of the applicable regulations.

For Flanders there are specific regulations for SMWTs to avoid having to conduct such a study (Van Mechelen and Crevits, 2009). The regulations draw a zone of twice the total height of the turbine (hub height plus rotor diameter) in order to ensure that the limit of 30 hours/year is not exceeded. As small wind turbines are sometimes installed on top of a building, the building height should be added to the total height of the turbine.

More details about the methodology to asses the shadow flicker can be found in Chapter 6.

2.7.2 Visual impact

Of all the effects on the environmental impact caused by wind turbines, the visual impact on the environment is the most difficult to assess (Hau, 2006) as it is a subjective issue. While some people find wind turbines pleasant to look at or think that it symbolises clean energy, other people believe wind turbines harm the aesthetics of landscapes and/or historical sites.

There are three key elements that determine the visual impact (Engstrom and Pershagen, 1980) of a wind turbine:

- The type of landscape: The visual impact in open landscapes differs markedly from that in more closed-in areas (with trees or buildings).

- The size of the wind turbine: Turbines with a smaller hub height are usually more masked easily in the landscape.

- Psychological factors: What does the observer associate with wind turbines?

In contrast to large wind turbines where urban areas or residential areas are usually avoided, such areas are common operating areas for small and medium wind turbines (as regulations advise to install them preferably in these areas). On the one hand, this is an advantage as they are better integrated in the area as the hub height will be not much higher than the obstacles or buildings already present in the environment. One the other hand more people will visually notice the turbine.

There are possibilities to reduce the visual impact by changing the colour and contrast of the turbine (Bernd, 2005):

- White or light grey coloured blades will allow the blades to better integrate in the skyline (although this can again increase the dead rate of birds);

- The mast can be made green at the base and then gradually changed to grey at the top to reduce the contrast level.

More and more wind turbine manufacturers (especially large and medium wind turbines) take these considerations into account as they can play a significant role in their evaluation process.

2.7.3 Noise and vibrations

The sound produced by a wind turbine has two main sources: mechanical or aerodynamic. The mechanical noise is caused by the relative movement of the rotating components and their interaction with each other, resulting in vibrations. Examples are the bearings of the rotor shaft, yaw-movement, the generator, the gearbox (for geared turbines) or auxiliary equipment (e.g. hydraulics) (Manwell, McGowan, and Rogers, 2009). These mechanical vibrations are transmitted through the nacelle and the mast and that may act as a loudspeaker.

Vibrations are particularly relevant when placing a wind turbine on the roof of a building. These vibrations are transmitted through the structure of the building and can excite building elements (windows, floors, ceilings), potentially affecting the structural integrity of the element and/or resulting in additional noise radiation inside the building.

A second source of the sound production is the aerodynamic noise of a wind turbine. This is caused by the interaction of the air flow and turbine blades and is directly transmitted as a pure sound wave through the air. During the last decades extensive research has been carried out in the field of the aerodynamic design of the wind turbine blades. As a results,

the aerodynamic noise emissions from the modern wind turbines have decreased with about 10 % compared to the wind turbines in the early eighties (Katsaprakakis, 2012).

Although little information about the noise nuisance and actual noise levels of small and medium wind turbines are available (only tested and certified turbines provide (some) information about the sound level the turbine produces), planning permissions are often contested because of expected noise nuisance. Taylor et al. (2013), investigated the noise levels and perception for twelve small and micro wind turbines in urban areas. They measured the difference in sound pressure level between the background noise and the turbine noise by switching the turbine on and off at 15 m distance and a wind speed of 7 m/s. They compared the frequency spectra associated with the data and noticed that for the frequencies below 100 Hz, the increased sound level of the turbine was marginal compared to the background noise. For higher frequency ranges, switching on the turbine lead to a significant increase (up to 20 dB(A)) in the total sound pressure level although the background noise was smaller in these ranges. For all frequencies, the overall sound pressure level at 15 m from the turbine (and switched on) was below 50 dB(A).

A survey showed that the most commonly perceived noises are 'swooshing' and 'humming' and this confirms the increased measured noise levels for the higher frequencies. The results of the survey showed that persons with a more negative attitude towards wind energy perceive more noise from a wind turbine close to their home. This study indicates that it is more a question of convincing the authorities than worrying about the potential noise nuisance.

2.7.4 Biodiversity

The impact on biodiversity is an important element in the feasibility of a wind turbine project and should be studied in the planning phase of the turbine. These studies should then consider the effect of the turbine on the wildlife, birds and bats.

A wind turbine affects the birds and bats in one of the following ways (Katsaprakakis, 2012):

- direct fatalities due to electrical shock or collision with the spinning blades;

- the installation of wind parks in important areas for birds, such as the prey and procreation areas;

- loss or disturbance of habitats in proximity of turbines;

- the installation of wind parks in migration corridors.

Several studies are present in the literature on the impact of large wind turbines on birds (Huppop et al., 2006; Kikuchi, 2008). These studies conclude that wind turbines can constitute a serious danger for birds as strong air streams (typical operating areas of wind turbines) are used as passages especially by migratory birds. On the other hand, other studies (Ligue pour la Protection des oiseaux, 2014) indicate that only 0 to 2 birds are hit by a blade each year, which is a lot lower than the fatalities of several other human activities (as for example one billion birds get killed annually as a result of collision with vehicles (Katsaprakakis, 2012)). Specifically for bats, fatalities due to blade collision are less as they have their echolocation system to allocate the turbine. For bats, fatalities are mainly caused by internal bleeding due to sudden pressure variation in the stream tube of the turbine (Eurobats, 2012; Eurobats, 2006).

Other adverse effects on wildlife, except birds, are that the required infrastructure works for the installation of a wind park can harm the ecosystem through clearing of vegetation, soil disruption and the potential erosion. These changes can lead to habitat loss and fragmentation for forest-dependent species in case of a wind park planned to be installed in a forested area (Katsaprakakis, 2012).

For small and medium wind turbines, no specific studies are found in the literature. Specific aspects can have an effect on biodiversity studies compared to large wind turbines:

- Small and medium wind turbines are generally located in more urban areas. This significantly reduces the amount of present birds and thus the risks of blade collision or habitat loss;

- The higher rotational frequency for these types of turbines can have two possible effects. On the one hand it can increase the risk of bird collision. On the other hand, this could increase the visibility of the rotor as the rotor than looks more like a solid obstacle instead of single moving blades;

- A lower hub height will reduce the impact on migratory routes for migratory birds traveling on higher altitudes;

Studying these aspects specifically for small and medium wind turbines is beyond the scope of this dissertation. In the feasibility study in Chapter 6

where a brief biodiversity study is presented, the studies for large wind turbines are used as a guideline.

2.8 Socio-political acceptance

For wind turbines in general the most common concerns are about aesthetic and noise factors, or stem from Not-In-My-Backyard (NIMBY) behaviour, where the members of the public oppose the development of wind turbines in their immediate vicinity. For SMWTs the socio-political acceptance is further hampered by the fact that many SMWTs are indeed inefficient, unreliable or too expensive. The selection of a wind turbine without any expert knowledge of the wind turbine market or its installation without careful wind resource assessment or micrositing will inevitably lead to a failed project which is bound to exacerbate the negative perception of SMWTs.

The work presented in this dissertation should aid in changing this perception. We offer guidelines for users, in order to increase the number of successful SMWT projects, and also present the results of two feasibility studies in rural and urban areas (Chapter 5 and 6). These studies show that there is indeed a large potential for SMWTs, if a proper turbine is selected and it is installed correctly. A direct followup of this work has resulted in pilot projects that will be launched in the coming years (2015 and 2016) in Brussels and West-Vlaanderen. Dissemination of these results and the successful pilot projects aim to not only convince potential consumers, but also local stakeholders such as authorities, funding institutions or project developers of the benefits of these projects. This will not only help to increase the acceptance, which is vital for this type of technology, but also the replication of SMWT projects.

2.9 Legal framework

The selection of the proper turbine and the best location can also be affected by the legal framework as the applicable regulations can limit the size of the turbine or the area where it could be installed. These regulations are not uniform within Europe and not even in a small country such as Belgium. Each country or region has his own regulations and therefore each feasibility study is specific for that region. In this section, an overview of the legal framework of Belgium (Van Mechelen and Crevits (2009) for Flanders and Nollet and Di Antonio (2013) for Wallonie), the neighbouring countries (Rumeau et al. (2006) for France, Cace (2013) for the Netherlands and

	Small	Medium
Flanders	z_{Hub} <15 m	P_{rat}<300 kW
Wallonia	P_{rat}<100 kW	100 kW <P_{rat}<1 MW
Netherlands	0.6 kW <P_{rat}<6 kW	6 kW <P_{rat}<1MW
Germany	z_{Hub} <50 m	\
France	12 m <z_{Hub} <50 m	z_{Hub} >50 m
UK (Ruk)	P_{rat}<50 kW	50 kW <P_{rat}<500 kW
	A_{Rot} <200 m^2	200 m^2 <A_{Rot} <1000 m^2
UK (MCS)	P_{rat}<15 kW	15 kW <P_{rat}<100 kW
	z_{Total} <50 m	50 m <z_{Total} <250 m
USA	$P_{\text{rat}}\leq$ 100 kW	\

Table 2.5: Limitations for the sizes and types of turbines for Belgium, its neighbouring countries, United Kingdom and Unites States of America. In this table z_{Hub} represents the hub height, A_{Rot} the swept area, P_{rat} the rated power and z_{Total} the hub height plus the blade length.

Erlass des Innenministerium (2010) for Germany) and two leading countries in the SMWT market (RenewableUK (2011); Microgeneration certification scheme (2011) for the United Kingdom and Asmus et al. (2003) for the United States of America) is presented.

Generally, these legal frameworks set regulations about:

Size of the turbine: While in some countries wind turbines are categorised as micro, small, medium and large, other countries only separate a small and large wind turbine categories. Likewise, there is a large discrepancy in the definitions or limitations for these categories. This makes it hard to derive general rules on how to properly locate or select a turbine on a specific site. While small wind turbines generally have less restrictive rules and so can be sited in more residential areas (residential areas), in some countries they have a rated power up to 100 kW. In Table 2.5, an overview of the categories and category definitions is shown for Belgium, its neighbouring countries, the United Kingdom and the United States of America.

Noise: Usually the regulations set limits on the maximum sound pressure levels observed at the closest building. These sound pressure levels are generally applicable in general and there are no specific rules for wind energy. A different limit is used for residential and for industrial areas.

Some countries also use a different limit for the time of the day. In Table 2.6, an overview is given for Belgium, the Netherlands and Germany to emphasise the differences in limitation, even within one country. As for SMWTs, there is no specific control of the turbine to for example limit the sound nuisance during the night, the turbine should not exceed the lowest value (the night value for that type of area).

	Area	Day [dB(A)]	Evening [dB(A)]	Night [dB(A)]
Flanders	Residential	49	44	39
	Industrial	64	59	59
	Rural	49	44	39
Wallonia	Residential	50	50	40
	Rural	50	50	40
Netherlands	Independent	50	45	40
Germany	Residential	55	50	40
	Industrial	70	70	70

Table 2.6: The maximum allowed sound pressure levels measured at the building closest to the wind turbine for Belgium, Netherlands and Germany.

Permit requirements: The procedure to install SMWTs are less complex than for large wind turbines, as they should have a lower impact on the environment. For specific cases a building permit is not even needed (in France for hub heights below 12 m, for the UK for swept areas less than 3.8 m^2). For other countries, the regulations are quite uniform. For small wind turbines a building permit suffices, while for medium wind turbines often an additional environmental permit is required. For these permits, an impact study is necessary. The difference between small and medium also translates into a different decision-making authority. In general, for small and medium wind turbines this is respectively the municipality and the state or province.

Spatial integration: While large wind turbines are generally located in rural areas, small and medium wind turbines are often sited in more built-up areas. Regulations for the proper spatial integration of the turbine in the area are therefore necessary. These regulations ensure that a certain distance to the neighbouring building or parcel is maintained or limit the

	Height	Distance to neighbouring parcel or building
Flanders	\	$>2 * z_{\text{Total}}$
Wallonia	\	$>z_{\text{Total}}$ and >15 m
Netherlands	<10 m	$>4 * z_{\text{Hub}}$
Germany	<30 m	$>4 * z_{\text{Total}}$
France	\	>3 m and $>r_{rotor}$
UK	\	$>z_{\text{Total}} + 10\%$
UK (BMWT)	$z_{\text{Total}} <15$ m <3m above roof	5 m
USA	Ground surface Dependend	10 foot \

Table 2.7: Regulations on the dimensions and spatial integration of small and medium wind turbines with z_{Total} the total height of the turbine, z_{Hub} the hub height and r_{rotor} the radius of the rotor.

height of the turbine. An overview of the different regulations is shown in Table 2.7. The UK uses separate rules for building mounted wind turbines (BMWT) and stand-alone systems. In the USA, the total allowed height of the turbine is dependent on the total ground surface of the installation site. For example, for a ground surface of one acre (40200 m^2), the total height of the turbine is limited to 150 feet (45.7 m).

Safety: To ensure a safe operation, regulations state that the turbine should be designed according to specific standards. In Belgium, Netherlands and Germany the turbine should be certified according to the IEC standards (IEC, 2013). The UK and USA also allow their own standards, the RenewableUK (2014) and AWEA (2009).

2.10 Conclusions

In this chapter, the factors that affect the feasibility of a SMWT project are discussed. Currently, the SMWT market is a young and immature market. Therefore, the probability to select a badly performing turbine as a non-expert in the field is large. In addition, these turbines are often installed without any basic knowledge of the on-site wind conditions as resource assessment tools are costly in relation to the investment cost of

the turbine. Due to the low hub height of these turbines, the wind patterns are more complex and a proper assessment of these wind conditions is therefore imperative. These factors have lead to failed SMWT projects and have created a negative perception about small-scale wind in general.

The past decade the market size has shown a significant growth. As the market grows to more mature market, the investment cost of these turbines is expected to decrease due to the fact that a significant part is presently assigned to the R&D cost of the turbines. A bigger market size will also enable manufacturers to reach mass production, leading to a further decrease of the total cost of a SMWT. As currently the market is not in this stage, incentives such as the green certificates and feed-in tariffs are imperative for a successful SMWT project.

Together with the development of testing and certification standards for small-scale wind, our work aims to change the negative perception about SMWTs. The guidelines for users/investors and the results of feasibility studies in large areas (such as presented in Chapters 3 to 6 for Flanders and Brussels), can help to convince local stakeholders, authorities and funding institutions of SMWT projects of the benefits of these projects.

Chapter 3

Reliable estimation of the annual energy production of small and medium-sized wind turbines

Abstract—*This chapter provides an in-depth discussion of four techniques that are commonly used (independently or in combination) for the prediction of the annual energy production of a wind turbine. We distinguish between these techniques by the type of available wind resource information: the mean wind speed only (Section 3.3), actual measurements or an approximate statistical distribution (Section 3.4), wind data on site but at a different height (Section 3.5), and/or wind data at a different but nearby site (Section 3.6). We conclude every section with practical recommendations.*

3.1 Introduction

The keys to the successful installation of a SMWT are surprisingly simple (or so it seems): choose a windy terrain, pick the best spot on this terrain, and select the most appropriate turbine. In this chapter we formulate guidelines for the user/investor on how to reliably predict the annual energy production (AEP) of the turbine and the corresponding levelized cost of energy (LCOE).

For a given maintenance cost (which we approximated as 1.5 % of the initial investment cost per annum (Schallenberg-Rodriguez, 2013)) and discount rate (set at 3 %), the levelized cost of energy or LCOE (see Eq. 1.23 on p. 16) is defined by the balance between the cost of the investment and the energy the turbine produces. Since the market of SMWTs is immature, there can be a large discrepancy between the cost of a turbine and its annual energy yield. Therefore, it is also necessary to estimate the LCOE and not only the AEP.

Our main contribution in this chapter is on how to handle the wind conditions for AEP prediction. Weekes and Tomlin (2014b) introduced a framework for low-cost wind resource assessment. They compared a boundary-layer scaling model and a data-based approach to decide whether or not a site is suitable. In this chapter, we extend this approach by assessing the AEP based on both the (measured or predicted) wind conditions and independently-measured power curves.

We validate our guidelines with the prediction of the AEP for 23 different measurement sites in Belgium and the Netherlands (hourly mean wind speeds) and 29 different wind turbines. The annual mean wind speeds at the sites vary from 3.5 m/s to 7.8 m/s; the rated powers of the wind turbines vary from 1 kW to 25 kW.

Most of the guidelines presented in this chapter are valid throughout Western Europe, and probably also beyond, even though they have been formulated based on wind data from Belgium and the Netherlands.

With this diversity in wind speeds, we have a good sample of sites that are on both sides of the tipping point of the economic viability of SMWT projects. These sites are most suited to formulate guidelines on how to reliably estimate the AEP of a wind turbine. However, these guidelines are still valid for regions with higher mean wind speeds (e.g. Scotland, Northwestern Denmark, and Norway) and lower speeds (in-land Southern Europe) (Troen and Petersen, 1989), albeit maybe less critical: at the high-wind zones most turbines will operate near rated power, in low-wind zones no small wind turbines should be installed.

3.2 Basic aspects of AEP prediction

According to the IEC standards (IEC, 2006), the AEP of a turbine should be predicted by combining hub height wind measurements and the detailed power curve of the turbine. For a given site, the mean power of a wind turbine $\overline{P}$ (typically in kW for SMWTs) is given by

$$\overline{P} = \int_V P(V)\varphi(V)\,\mathrm{d}V \tag{3.1}$$

with V the wind speed (m/s), $P(V)$ the power curve (kW), and $\varphi(V)$ the probability density function of the wind. The annual energy production (AEP, in kWh) is then easily found by Eq.(1.16).

In practice, the simplest and most accurate way of applying Eq. (3.1) to an actual wind turbine and site is with the so-called direct use of data (Manwell, McGowan, and Rogers, 2009).

Suppose we have a time series of N wind speed observations V_k and a turbine's power curve, then the mean power as given by Eq. (3.1) can be calculated as:

$$\overline{P} = \frac{1}{N} \sum_{k=1}^{N} P(V_k) \tag{3.2}$$

where $P(V_k)$ is the power for wind speed V_k. The AEP can then be calculated by Eq. (1.16). As the resolution of the power curve data (typically 0.5 m/s) is often smaller than the resolution of the wind speed measurements, we linearly interpolate the power curve where necessary. The approach can then be applied to the database which will be used throughout this chapter. The AEP as obtained through Eq. (3.2) is further used as a reference as it is the best possible estimation of the mean power.

Figure 3.1 shows the AEP for all turbines and sites in the database calculated with the reference approach (direct use of data). The overall trend shows that AEP increases for higher rated power and for higher mean wind speed, as can be expected. Yet some peaks appear, indicating that a turbine with a lower rated power does not necessarily produce less energy than a turbine with a higher rated power. Note e.g. that the turbine with a rated power of 10 kW has a higher energy production than turbines with 12-15 kW for most of the measurement sites.
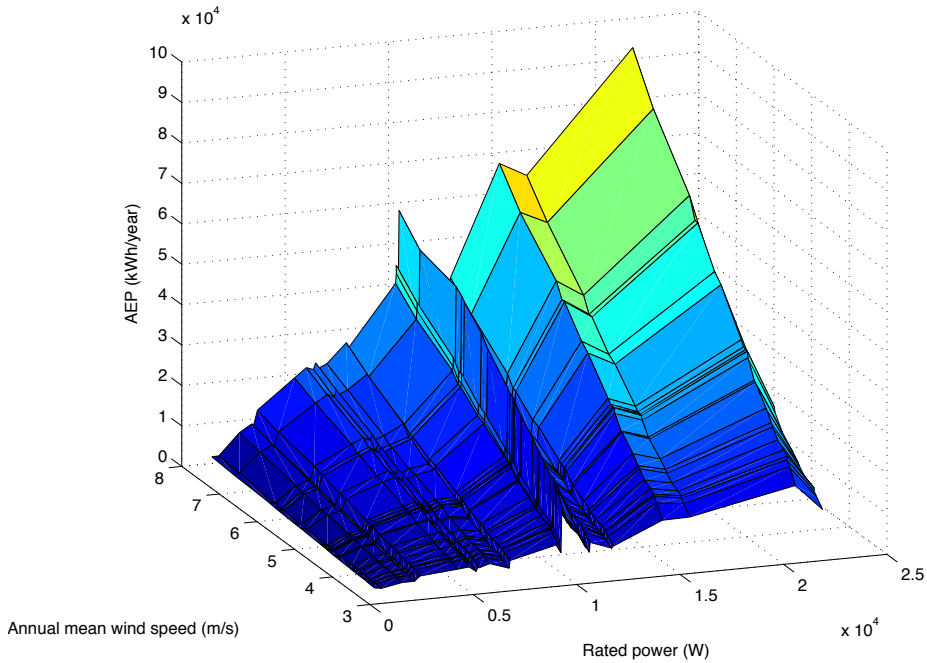
Figure 3.1: Annual energy production for 23 measurement sites and 29 wind turbines. The overall trend shows an increasing AEP for increasing rated power and increasing wind speed. The peaks indicate that those turbines have a higher AEP than neighbouring turbines (with comparable rated powers).

3.3 AEP prediction based on rated power and the average wind speed

Rated power P_{rat} (with rotor diameter as runner-up) is most often used to categorize and name a wind turbine. It is how the turbine is advertised, it is what the potential buyer first learns. Yet no generally accepted definition exists of the rated power of a wind turbine. AWEA (2009) and RenewableUK (2014) state that the rated power is the power at the rated wind speed, 11 m/s. IEC (2006) on the other hand state that rated power is a 'quantity of power assigned, generally by a manufacturer, for a specified operating condition of a component, device or equipment'. Manufacturers of wind turbines tend to choose a higher rated power than according to the AWEA and BWEA standards. Using a higher value for rated power

	Turbine 1	Turbine 2
4 m/s	17.7	24.6
5 m/s	32.1	37.4
6 m/s	46.3	47.2
7 m/s	58.7	53.5
8 m/s	68.5	56.4

Table 3.1: Annual energy production (AEP) in MWh for two different turbines, as listed in publicly-available test reports from independent facilities.

is better for manufacturers as this lowers the investment cost per *installed* kW (Whale, McHenry, and Malla, 2013). Yet, another definition refers to the shape of the power curve of a pitch regulated wind turbine. Above a certain wind speed, the power is held constant by adjusting the blade pitch angle. This constant power is then named as the 'rated power'.

In this section, we first demonstrate the fact that rated power as such is not sufficient to predict the AEP of a turbine. Obviously information about the site of interest should be used to predict the AEP. Therefore we assume that the average wind speed of the site is known and compare three different approaches that use this information with the rated power or the rotor surface of the turbine to predict the AEP. The average wind speed of the site can be estimated from a local wind atlas (Troen and Petersen, 1989), nearby measurement stations or analytical methods to estimate the mean wind speed in a certain region (Millward-Hopkins et al., 2013a; Weekes and Tomlin, 2013). Finally, we give our recommendation and present a viable alternative which can be used if the average wind speed is known.

3.3.1 Why rated power is a bad indicator of AEP

A simple example directly taken from publicly available test reports (National Renewable Energy Laboratory, 2014; Windtest Grevenbroich GmbH, 2014) already makes the case. Two turbines were selected with a different rated power: turbine 1 with a rated power of 15 kW, turbine 2 with only 10 kW. However, the AEP predictions also listed in the same test report tell a different story. Table 3.1 clearly shows that for mean wind speeds up to 6 m/s, turbine 2 produces more power than turbine 1.

We illustrate this for two of our studied sites (named A and B with an annual mean wind speed of resp. 5.6 m/s and 7.3 m/s). The power curves of the turbines are shown in Figure 3.2 (blue curves). The rated power
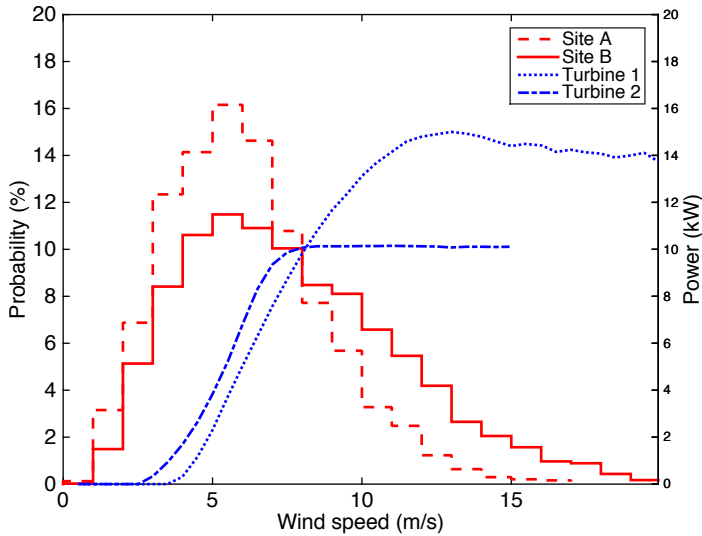
Figure 3.2: Normalised frequency histograms of the wind speed for sites A and B (in red, left ordinate) with an annual mean wind speed of reps. 5.6 m/s and 7.3 m/s, and power curves for turbines 1 and 2 (in blue, right ordinate).

of turbine 1 is clearly higher than the rated power of turbine 2, as is also listed in Table 3.2. (This is the case for both definitions of rated power as described above.) The histograms of the wind speeds of the two studied sites are also plotted in Figure 3.2.

Although the rated power of turbine 1 is approximately 50 % higher, turbine 2 produces about 10 % more energy for site A. This is due to the power curve of turbine 2 being higher than that of turbine 1 for wind speeds below 9 m/s and the high probability for these wind speeds at site A. For site B, turbine 1 produces 11 % more energy. Rated power is clearly not a good indicator of the energy yield of a SMWT on sites with moderate wind.

Whether or not this difference in AEP results in a different LCOE depends on the investment cost of the turbine. In Table 3.3 the LCOE for each turbine and site is shown. The difference in LCOE shows the same kind of trend as for the AEP. Turbine 2 should be selected for site A and turbine 1 should be selected for site B.

	Rated IEC / Producer	Rated AWEA / BWEA	AEP Site A	AEP Site B
Turbine 1	15 kW	14.2 kW	40.8 MWh	62.1 MWh
Turbine 2	10 kW	10.2 kW	45.3 MWh	55.7 MWh

Table 3.2: Comparison of the AEP for two specific wind turbines and sites.

	LCOE Site A	LCOE Site B
Turbine 1	0.207 €/kWh	0.136 €/kWh
Turbine 2	0.192 €/kWh	0.156 €/kWh

Table 3.3: Comparison of the LCOE for two specific wind turbines and sites.

3.3.2 AEP estimation with rated power and a capacity factor

Most methods that use rated power, combine the rated power with some kind of capacity factor C_F to derive the mean power:

$$\overline{P} = P_{\text{rat}}\, C_F \qquad (3.3)$$

Some of these approaches use a fixed capacity factor (Met Office and Entec, 2008), while others adjust the capacity factor to the annual average wind speed at the site of interest (Renewable Energy Research Lab, 2002). We have tested the more general approach with a variable capacity factor (Renewable Energy Research Lab, 2002). The average power is expressed as:

$$\overline{P} = P_{\text{rat}}\, C_F(\overline{V}) \qquad (3.4)$$

where $\overline{V}$ (m/s) is the annual mean wind speed at the installation site. The range in capacity factors are presented in Table 3.4. (Where necessary, we interpolated linearly between the wind speeds.)

In Figure 3.3, the predicted AEP for this approach (further referred to as the capacity factor approach) are compared to the reference method. For each site and each turbine, the normalised difference in predicted AEP is determined. This approach almost always underestimates the AEP. This is due to the fact that the approach, determines a capacity factor (based on the annual average wind speed) for each site and keeps this constant for all turbines. Therefore, the approach does not take into account the

$\overline{V}$ (m/s)	C_F (%)	$\overline{V}$ (m/s)	C_F (%)
3.5	4.2	6.0	23.8
4.0	7.1	6.5	28.3
4.5	10.7	7.0	32.7
5.0	14.8	7.5	36.6
5.5	19.3	8.0	40.3

Table 3.4: Adjusted capacity factor as a function of the annual mean wind speed, from Renewable Energy Research Lab (2002).

difference in performance below rated power of each individual turbine. If the capacity factors were increased, the predictions would improve for some turbines but deteriorate for others.

Figure 3.3: Normalised difference in predicted AEP between the capacity factor and the direct use of data. The black crosses show the individual predictions for all 29 turbines (abscissa) and 23 sites (ordinate). The turbines are ranked according to rated power, from lowest to highest.

3.3.3 AEP estimation based on rotor diameter

Instead of P_{rat}, sometimes the rotor diameter D is used, e.g. as described in OpenEI (2014):

$$\text{AEP} = 1.6 \left(\overline{V}\right)^3 D^2 \tag{3.5}$$

where AEP is expressed in kWh/year. Eq. (3.5) is consistent with assuming an electrical power coefficient $C_{P_{el}}$ of 37.9 % in the standard expression to determine the wind turbine rotor performance (Manwell, McGowan, and Rogers, 2009):

$$P = C_{P_{el}} \frac{1}{2} \rho \frac{\pi D^2}{4} V^3 \tag{3.6}$$

where ρ is the air density.

In Figure 3.4, the results for the rotor surface approach are shown. The error in AEP prediction is again unacceptable. Eq. (3.5) is based on one specific power coefficient. In reality each individual turbine has a specific power coefficient. As this method uses a fixed power coefficient, the estimations will only have a good agreement for some turbines.

Figure 3.4: Normalised difference in predicted AEP between the rotor surface approach and the direct use of data. The black crosses show the individual predictions for all 29 turbines (abscissa) and 23 sites (ordinate). The turbines are ranked according to rated power, from lowest to highest.
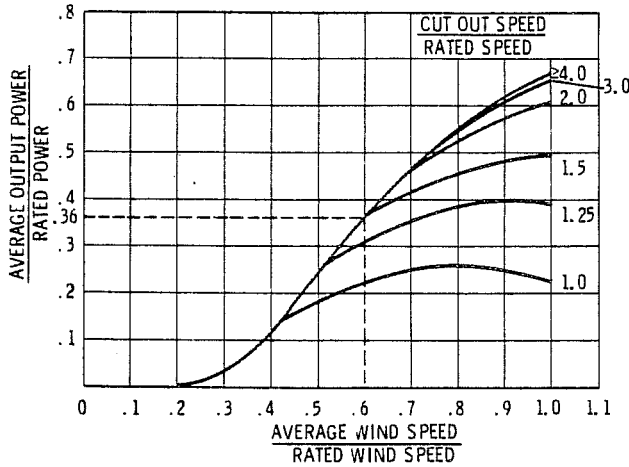
Figure 3.5: Ratio of output power to rated power as a function of the ratio of average wind speed to rated wind speed, with cut-out to rated wind speed as a parameter; reprinted from (Wegley et al., 1980).

3.3.4 Graphical AEP estimation with rated power

Wegley et al. (1980) suggest a graphical method to predict the AEP on a specific site. The approach requires to determine two different ratios:

$$\frac{CO}{RS}, \frac{AA}{RS} \tag{3.7}$$

where CO is the cut-out speed, RS is the rated speed and AA is the annual average wind speed. These two ratios are used in Figure 3.5 to derive:

$$\frac{\overline{P}}{P_{\text{rat}}} \tag{3.8}$$

The AEP can then be calculated by Eq. (1.16). As no generally accepted definition exists of the rated speed and power, the AWEA (2009) and RenewableUK (2014) standards are used and the rated wind speed is fixed at 11 m/s. For none of the turbines in the database, power data were available around the cut-out. Therefore, the CO/RS ratio was set at 2. This is the correct order of magnitude for all turbines and an error for this ratio will only give a small deviation in predicted AEP (as can be seen in Figure 3.5).

In Figure 3.6 the errors on the predicted AEP for this method (further referred to as Wegley) are shown. This approach strongly underestimates

the AEP. The errors are comparable with the capacity factor approach. Here again the same conclusion can be made: using a lower rated speed could improve the accuracy for some turbines but would reduce it for others.
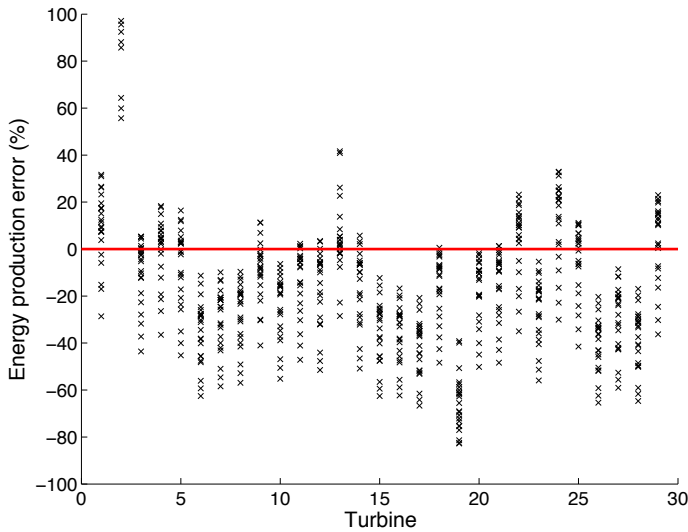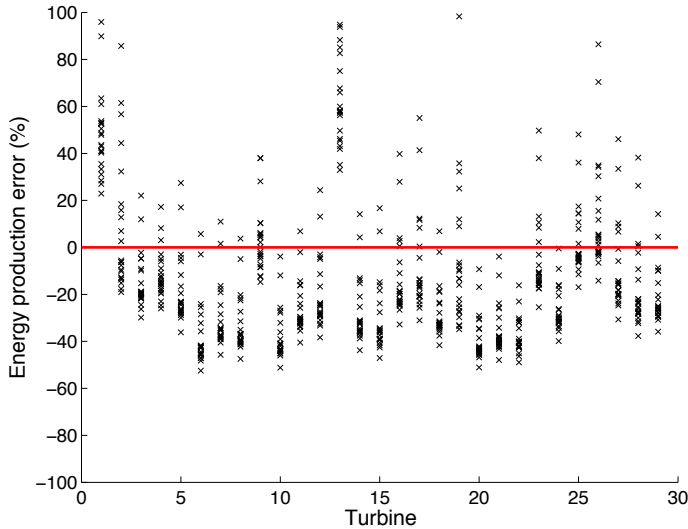

Figure 3.6: Normalised difference in predicted AEP between the Wegley approach and the direct use of data. The black crosses show the individual predictions for all 29 turbines (abscissa) and 23 sites (ordinate). The turbines are ranked according to rated power, from lowest to highest.

3.3.5 AEP estimation based on the IEC test report

All previous methods deviate strongly from the reference method where we use a time series of wind speed measurements as given in Eq. (3.2). Therefore a different approach is recommended. When the wind speed at the site is known, the test reports of the turbines can deliver a viable alternative. In these reports the AEP is determined for an average wind speed of 4, 5, 6, 7, 8, 9, 10 and 11 m/s assuming that the wind speed is Rayleigh-distributed (Ramírez and Carta, 2006). For non-integer values of the annual mean wind speed, the AEP can be linearly interpolated.

In Figure 3.7, this approach (further referred to as the IEC-Rayleigh approach) is compared to the reference method. For each turbine, the AEP is averaged over all measurement sites. This figure shows a good overall

agreement between the direct use of data (Eq. (3.2)) and the IEC-Rayleigh approach.
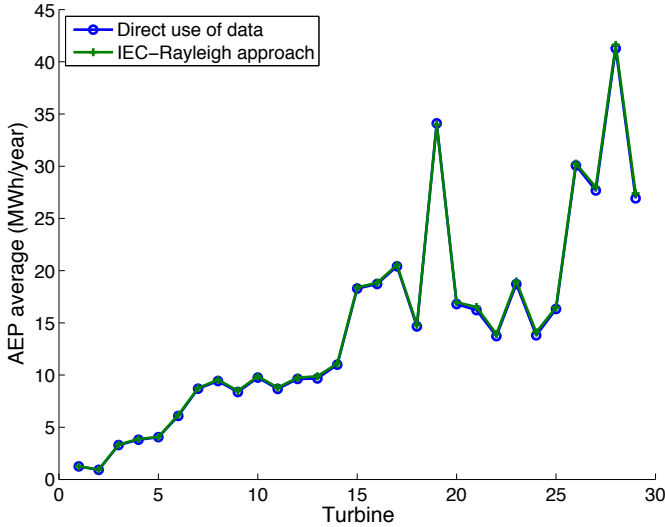
Figure 3.7: AEP (averaged over all 23 sites) as a function of the 29 turbines (which are ranked according to rated power, from lowest to highest).

It should be stressed that these results are averaged over all sites for each turbine. The accuracy of the individual AEP predictions depends on the standard deviation of the measurement site and how it deviates from the standard deviation of the Rayleigh distribution. The Rayleigh distribution implicitly assumes a standard deviation σ_{ray} of $0.523\overline{V}$ (Papoulis, 1991). For a specific site then, when the standard deviation of the wind speed σ_{site} differs from σ_{ray}, also the AEP will differ from the IEC-Rayleigh prediction. When σ_{site} is higher than σ_{ray}, the IEC-Rayleigh approach will underestimate the AEP and vice versa.

This is illustrated in Figure 3.8, where the normalised difference in predicted AEP for two specifically chosen sites is shown for all turbines. For site A, the standard deviation is 15 % lower than σ_{ray}. For site B, the standard deviation is 15 % higher than σ_{ray}. Site A clearly has a negative error for all turbines, which implies an underestimation of the AEP by the IEC-Rayleigh approach. Site B has a positive error for nearly all sites implying that the AEP is overestimated.
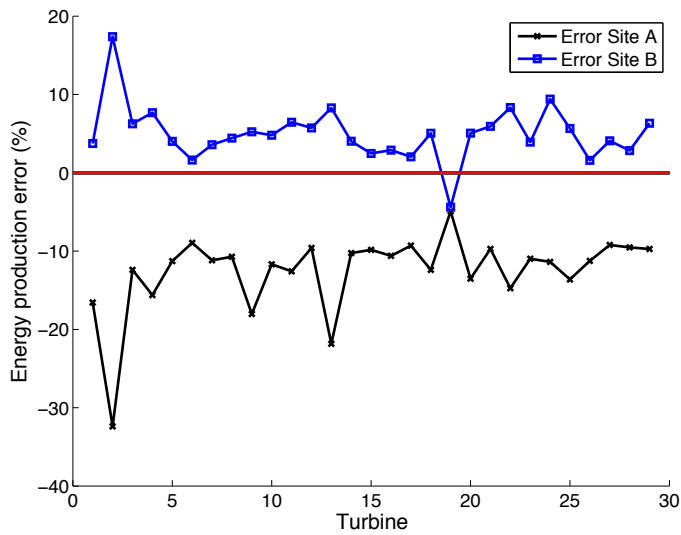
Figure 3.8: Normalised difference in predicted AEP between the IEC-Rayleigh method and the direct use of data. When the standard deviation on the measurement site is higher than σ_{ray}, the IEC-Rayleigh approach will underestimate the AEP (black line with crosses, site A). When the standard deviation is lower, the approach will overestimate the AEP (blue line with squares, site B).
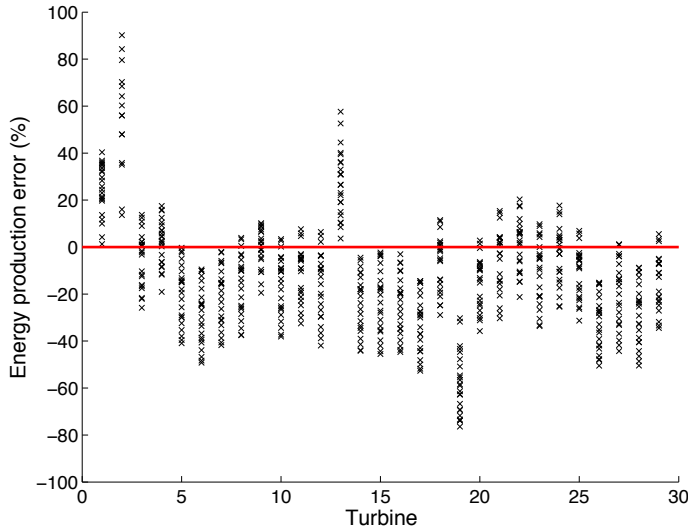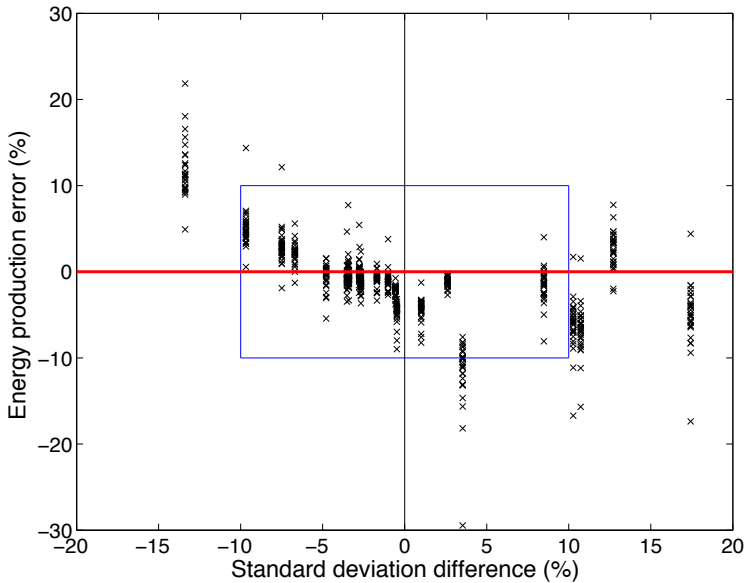
Figure 3.9: Normalised difference in predicted AEP between the IEC-Rayleigh method and the direct use of data. The black crosses show the individual predictions for all 23 sites (abscissa) and 29 turbines (ordinate). The sites are ordered according to the difference in standard deviation measured at the site and the assumed standard deviation of the Rayleigh distribution. The blue box delineates differences of 10 %, both in abscissa and ordinate.

In Figure 3.9, results are summarised for all sites as a function of the difference between σ_{site} and σ_{ray}. Figure 3.9 indicates that the AEP error is less than 10 % if the difference between σ_{site} and σ_{ray} is less than 10 %. This is indicated by the box (blue lines) in the figure. For one specific site, the difference in standard deviation is quite small (+3 %) though the fit between the wind speed data and the Rayleigh wind distribution is poor. For this specific case the error is above 10 % for most of the turbines.

For the measurement sites reviewed in this chapter, the standard deviations are comparable with the Rayleigh distribution. For some specific combinations of turbines and site, the AEP can be misjudged by more than 40 %. If an accurate economic analysis has to be determined in this case, more accurate approaches to predict the AEP should be used. These approaches are more expensive (as they use wind speed measurements), so it will have a negative impact on the LCOE of the project.

3.3.6 Conclusions and recommendations

When only the annual mean wind speed at the site is known, the user should always use the test reports to predict the AEP. For most sites, the error in AEP estimate will be less than 10 %.

A simple factor such as C_F or P_{rat} can never account for the variation in power production as they show one important disadvantage: the wind speed at rated power is invariably much higher than the typical operating conditions of a SMWT. SMWT manufacturers seem to fail in adjusting their turbine to medium-to-low wind speed areas and fix the rated speed to a high value (10-12 m/s). As these wind speeds are rare, a wind turbine with a high rated power will not necessary produce more energy than one with lower rated power. The shape of the power curve below rated speed will ultimately determine the annual energy production of SMWT.

Decreasing the rated power of a turbine, often referred to as 'de-rating', is an opportunity for SMWT manufactures to shift the operating conditions of the turbine to the lower wind regimes. A smaller generator can significantly reduce the total investment cost, as the gearbox, power electronics, main shaft and generator can easily take 40 % of the capital cost of a turbine (Jamieson, 2011). In addition, the lower part load will also affect the efficiency of the generator for the lower more frequent wind speeds. If a proper generator size is chosen, only a marginal decrease of the AEP will be observed. We demonstrate this with a typical example in Chapter 5.

3.4 AEP prediction based on statistical wind speed distributions

Wind speeds are often described by approximate statistical distributions, either because it is convenient to reduce the number of parameters (e.g. in on-line calculator tools) or because only limited on-site wind data are available. Numerous papers have been published in which statistical distributions are suggested for wind energy applications: the Weibull distribution most prominently (Justus et al., 1977; Jowder, 2009; Celik, 2003; Mostafaeipour, 2013), but also log-normal (Carta, Ramírez, and Velázquez, 2009), Rayleigh (Drew, Barlow, and Cockerill, 2013; Zhou et al., 2010; Jowder, 2009), inverse Gaussian (Zhou et al., 2010) and the maximum entropy principle (Carta, Ramírez, and Velázquez, 2009; Chellali et al., 2012; Ramírez and Carta, 2006; Zhou et al., 2010; Akpinar and Kavak Akpinar, 2007; Chang, 2011). When these statistical distributions are combined with

the power curve of a turbine, the AEP can be predicted. But does a good fit of the wind speed data translate into a good prediction of the AEP?

All these methods will yield a particular probability density function $\varphi(V)$ of the wind, which can then be put into Eq. (3.1). We compute Eq. (3.1) according to the IEC standards (IEC, 2006):

$$\overline{P} = \sum_{i=1}^{N_b} [\Phi(V_i) - \Phi(V_{i-1})] \left(\frac{P_i + P_{i-1}}{2} \right) \tag{3.9}$$

where N_b is the number of bins, P_i is the average power in bin i of the power curve (kW), V_i is the average wind speed in bin i of the power curve and $\Phi(V)$ is the cumulative probability distribution function of the wind speed (which can be determined from $\varphi(V)$). The summation is initiated (when i is equal to 1) by setting V_{i-1} equal to $V_i - 0.5$ m/s and P_{i-1} equal to 0.0 kW, as the standards require a power curve to be determined with bin centres at integer multiples of 0.5 m/s and bin widths of 0.5 m/s.

As these statistical distributions are often used to determine the AEP of a turbine, their effect on the accuracy of the AEP predictions is investigated. In this section the Weibull, maximum entropy principle and hybrid methods are reviewed. The accuracy of the Rayleigh distribution is already shown in Section 3.3.5 and will not be repeated in this section.

3.4.1 AEP prediction based on the Weibull distribution

The Weibull distribution was introduced in Section 1.5.2 (Eq.(1.18)). The shape k and scale c parameters can be determined in various ways, from a boundary-layer model and prior information (Weekes and Tomlin, 2014b) or from calculator tools. In this chapter we use the so-called moment method (MM, as described by Eq. 1.20) and the maximum likelihood method (ML, described next) to estimate the parameters directly from the wind measurements at the 23 sites. In this way, we assess the accuracy of the correct Weibull distribution in the prediction of AEP, regardless of any errors that a calculator tool might have in the estimation of k and c.

The maximum likelihood approximation of k is defined by (Carta, Ramírez, and Velázquez, 2009):

$$k = \left(\frac{\sum_{j=1}^{N} V_j^k \ln(V_j)}{\sum_{j=1}^{N} V_j^k} + \frac{1}{N} \sum_{j=1}^{N} \ln(V_j) \right)^{-1} \tag{3.10}$$

with V_j one of the N wind speed measurements in the data set. The shape factor k should be estimated iteratively. The scale factor c is then found

as:

$$c = \left(\frac{1}{N} \sum_{i=1}^{N} (V_i)^k \right)^{\frac{1}{k}} \tag{3.11}$$

Note that the maximum likelihood method requires a full data set to estimate k and c, while only $\overline{V}$ and σ_V are required to construct the Weibull distribution with the moment method.

It can be observed in Figure 3.10 that, compared with the IEC-Rayleigh approach (presented in Section 3.3.5), the Weibull method improves the estimation of the AEP. The error decreases from less than 10 % (in Figure 3.9) to less than 5 %. For one specific site however, the fit between the Weibull distribution and the wind data is insufficient. This site has very poor wind conditions and Weibull overestimates the probability for wind speed below 5 m/s and underestimates the probability for higher wind speeds. For turbines (turbine 1, 2 and 13 in Figure 3.10) with a high cut-in wind speed and large power consumption (negative power) below this cut-in, the AEP is more underestimated than the other turbines. One specific site nearly always overestimates the AEP. This is a site where Weibull significantly overestimates the probability for the wind speeds where most of the power is generated (6-11 m/s).

When the maximum likelihood method is used to estimate the shape and scale parameters, an entire wind speed dataset is needed (as opposed to only $\overline{V}$ and σ_V). Although this method utilizes more information of the measurement site, the accuracy of the predictions decreases. The Weibull distribution nearly always overestimates the AEP. This is shown in Figure 3.14, where the AEP difference from the reference for each site is averaged over all turbines.

3.4.2   AEP prediction based on the Maximum entropy principle

Li and Li (2005) applied the maximum entropy principle to wind speed distributions. The method maximizes the so-called Shannon's entropy subject to the conservation of mass, momentum and energy. The result is a probability density function based on the exponential function:

$$\varphi_{\text{mep}}(V) = V^r \exp \left\{ \alpha_0 - \alpha_1 V - \alpha_2 V^2 - \alpha_3 V^3 \right\} \tag{3.12}$$
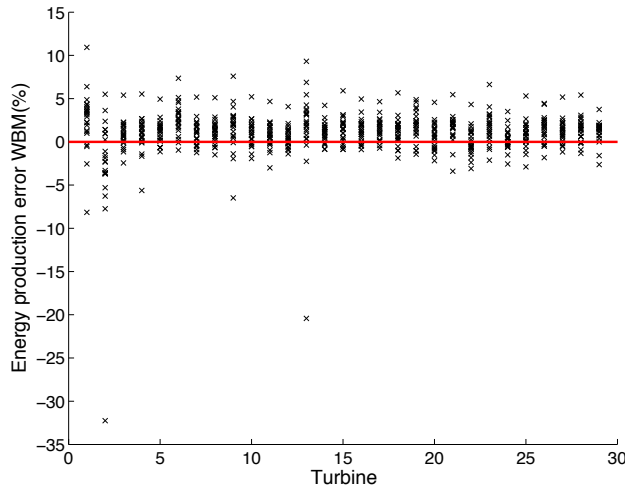
Figure 3.10: Normalised difference in predicted AEP between the Weibull method (with k and c estimated using the moment method) and the direct use of data. The black crosses show the individual predictions for all 29 turbines (abscissa) and 23 sites (ordinate). The turbines are ranked according to rated power, from lowest to highest.

where α_i are unknown Lagrangian multipliers and r is a pre-exponential term. They are determined by:

$$\int_{V_{\min}}^{V_{\max}} V^{r+m} \exp\left(\alpha_0 - \alpha_1 V - \alpha_2 V^2 - \alpha_3 V^3\right) \, \mathrm{d}V = \overline{V^m} \qquad (3.13)$$

where $m = [0, 1, 2, 3]$, and $\overline{V^m}$ represents 1 (imposing that $\overline{V^0} = 1$), the mean of the wind speed ($\overline{V}$), the mean of the squared wind speed ($\overline{V^2}$), and the mean of the cubed wind speed ($\overline{V^3}$), respectively, leading to 4 different equations. The theoretical MEP distribution assumes that $r = 0$; in general r is a non-negative integer. The α_i can be identified iteratively, based on the mean wind speeds (linear, squared, cubed) only.

The behaviour of the MEP distribution is rather unpredictable and until now no specific rule could be derived to determine the optimal pre-exponential term (Chellali et al., 2012). However, the choice of the pre-exponential term has a major impact on the fit between the wind dataset and the distribution. The MEP with a pre-exponential term of 0, e.g., was not capable to fit the data for 8 of the 23 measurement sites we studied. A higher pre-exponential term increased the number of fits but, surprisingly,
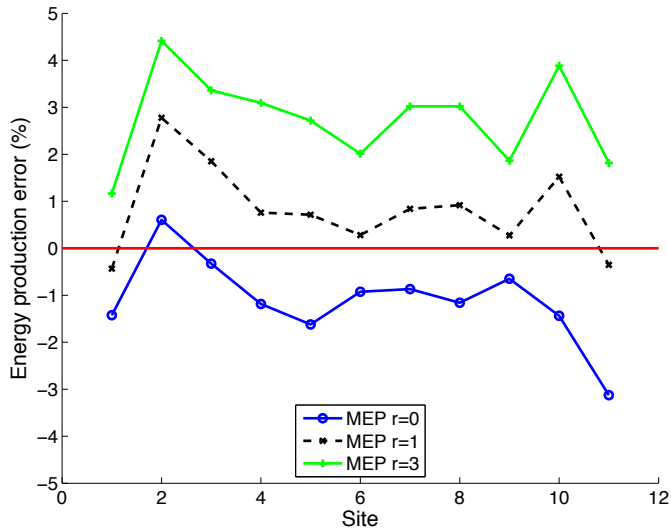
Figure 3.11: Normalised difference in predicted AEP between the MEP with a pre-exponential term of 0, 1, and 3, and the direct use of data. The differences are averaged over all 29 turbines and plotted as a function of 11 sites where a fit could be obtained for three pre-exponential terms. (We only show three pre-exponential terms as the remaining pre-exponential terms show the same trend.)

lowered the accuracy of the AEP prediction.

The effect of varying the pre-exponential term is illustrated in Figure 3.11. The figure shows the normalised difference for each site and for three pre-exponential terms where a fit could be obtained, averaged over all turbines. To not overload the figure, only three pre-exponential terms are shown as they already show the trend of an increasing pre-exponential term. When a valid fit was found, the MEP with a pre-exponential term of 0 provided the best results. A higher pre-exponential term clearly increases the estimation of the AEP and results in an overestimate of the AEP.

It is not always the best fit of the wind speed that provides the best prediction of AEP. In Figure 3.12, it is shown that, for the sites under consideration, the MEP with a pre-exponential term of 4 does not fit the data very well while the pre-exponential term of 0 provides a reasonable fit. For 3 of the 29 turbines, the distribution with a pre-exponential term of 4 gives a better prediction of the AEP. For these specific cases, the overestimation of the probability for low wind speeds is compensated by
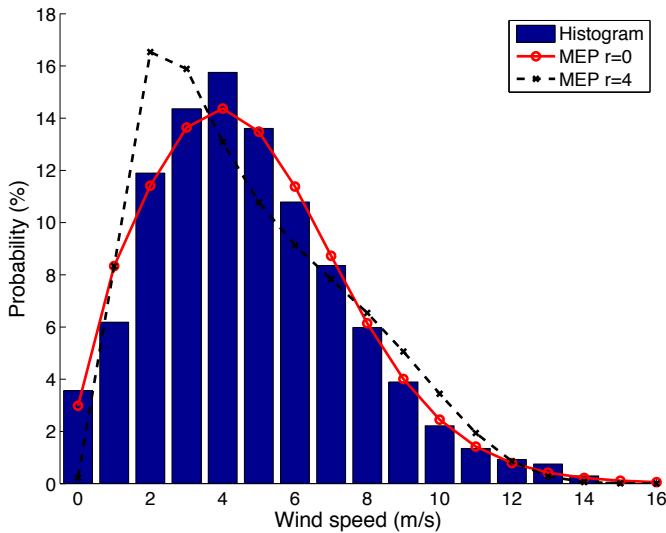
Figure 3.12: Example for one site of the wind speed histogram and the MEP probability density function with a pre-exponential term of 0 and 4.

the underestimation of the probability for higher wind speeds and vice versa. But this compensating effect is coincidental and cannot be relied on.

Figure 3.11 offers only a partial view on the possibilities of the MEP method. On the one hand, it leaves out all sites where no suitable fit was obtained. On the other hand, for every combination of site and turbine, there seems to be at least one pre-exponential choice which yields a good estimate of the AEP.

Figure 3.13 shows just this: if the true AEP would be known (in our case, Eq. (3.2)), how good is the best possible MEP approximation? In this somewhat theoretical case, the MEP method clearly outperforms the Weibull methods. Thus, if future research could discover how to find the best pre-exponential term for a given site and turbine, the MEP surely is a better alternative for the Weibull distribution. To our knowledge, no such method currently exists. Therefore the Weibull distribution remains a better alternative than the MEP.
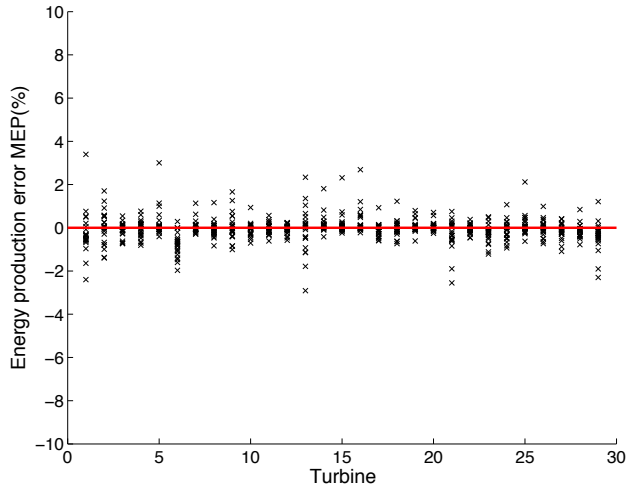
Figure 3.13: Normalised difference in predicted AEP between the MEP method (with the optimal use of the pre-exponential term) and the direct use of data. The black crosses show the individual predictions for all 29 turbines (abscissa) and 23 sites (ordinate). The turbines are ranked according to rated power, from lowest to highest.

3.4.3 Weibull and MEP distributions extended with the hybrid method

Some statistical distributions (e.g. Rayleigh and Weibull) cannot cope with the non-zero probability of very low wind speeds. Although a bad agreement at low wind speeds does not affect the AEP estimation as such, it might also skew the fit at higher wind speeds and thus distort the AEP prediction. To alleviate this problem Takle and Brown (1977) developed the hybrid distribution. This method combines the probability for null wind speeds with any possible wind speed distribution. The hybrid distribution $\varphi_{\mathrm{hyb}}(V)$ is defined as:

$$\varphi_{\mathrm{hyb}}(V) = \varphi_0 \delta(V) + (1 - \varphi_0)\varphi(V) \tag{3.14}$$

where φ_0 is the probability of observing zero wind speeds, $\delta(V)$ is the Dirac delta function and $\varphi(V)$ is the probability density function of the observed non-zero wind wind speeds.

Applying the hybrid method to the Weibull distribution does not significantly change the accuracy of the predictions. It is even so that applying the hybrid distribution to a site with high probability of zero wind doesn't
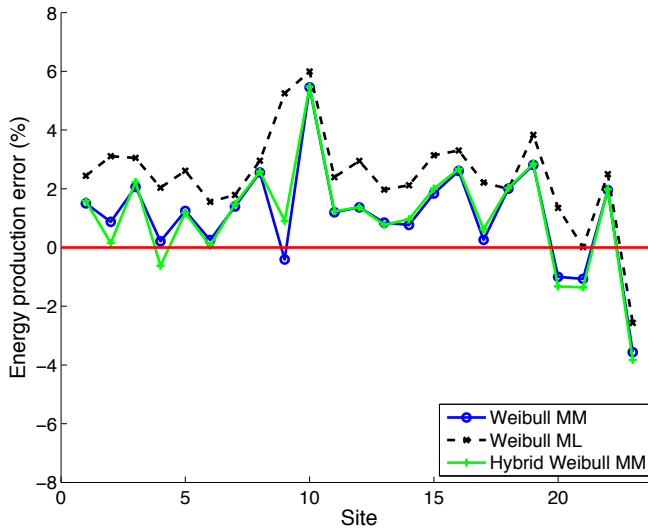
Figure 3.14: Normalised difference in predicted AEP between three different Weibull distributions and the direct use of data. The differences are averaged over all 29 turbines and plotted as a function of the 23 sites.

necessarily decrease the prediction of the AEP. For some of these sites a higher AEP was predicted by the hybrid distribution and the accuracy was decreased (see e.g. site 9).

We also applied the hybrid method to the MEP distributions with pre-exponential terms of 1, 2, 3 and 4. (The MEP method with $r = 0$ already allows a non-zero probability for zero wind speed.) It lowers the estimation of the AEP and as these distributions nearly always overestimate the AEP, the Hybrid method improves the accuracy of the estimations. Roughly it improved the accuracy by up to 2 %.

3.4.4   Conclusions and recommendations

The most commonly used distribution to estimate the AEP is Weibull. It gives a good estimate for most of the sites. Although for some specific cases, unacceptably large errors (up to 30 %) can appear. From Figure 3.13, one could say that the maximum entropy principle is a viable alternative. However until now there is no way to determine *a priori* the appropriate pre-exponential term for each turbine and site. Therefore the Weibull dis-

tribution remains a more reliable option to determine the AEP of a wind turbine. Though we state that whenever wind measurements on-site are available the entire dataset should be used to accurately predict the AEP. If for some reason the data set should be condensed, the data histogram would be a better choice than Weibull. This approach can accurately describe the wind data with just a few more parameters: the probability for each wind speed interval. The loss in accuracy of the AEP prediction is negligible.

3.5 AEP prediction based on the extrapolation from measurements to hub height

In resource assessment studies, the wind speed is often measured below hub height. These measurements then need to be extrapolated to the desired hub height to predict the AEP. There are different approaches present in the literature to model the evolution of wind speed with height, as we described in Section 1.3. As one might expect, the extrapolation to hub height introduces uncertainty on the wind speed. To reduce this uncertainty, a rule of thumb often used in the literature (Measnet, 2009) is the 2/3 rule which implies that the measurement height should be at least 2/3 of the extrapolation height (what is accepted in large wind farm calculations as a 'bankable' extrapolation). Even when this requirement is met, using one approach or the other will result in a different estimation of the extrapolated wind speed. As these wind speeds are then used to estimate the AEP of a wind turbine, this will result in a different estimation of the AEP.

Different authors already discussed these differences in the estimated hub height AEP. Gualtieri and Secci (2014) assessed the performance of two different approaches based on the power law. One approach extrapolated the wind speed time series directly while the other extrapolated the Weibull wind speed distribution. The extrapolation of the wind speed time series from 10 m to 50 m resulted in an overestimation of the mean power of 12 %. Different Weibull based extrapolations were compared where some lead to an underestimation of 16 % and other approaches lead to an overestimation of 20 %, indicating a large discrepancy between the different approaches.

Even when one particular approach is used for the extrapolation, there are different procedures to derive the parameters for the extrapolation resulting in a different estimation of the AEP. Firtin, Guler, and Akdag (2011) measured the wind speed at three different heights and used different pro-

cedures to apply the power law. The wind speed was extrapolated from the lowest height or the middle height and different procedures were used to derive the parameters for the extrapolation. While some procedures tend to accurately predict the wind energy potential, others misjudged the mean power output with nearly 50 %.

Elkinton, Rogers, and McGowan (2006) determined the accuracy of the log and power law, by comparing the extrapolated wind data with actual measured wind data for eleven measurement masts. In order to identify the effects of the terrain, the masts were located in different types of terrains (flat, hills, and forest). The wind data consisted of wind speeds measured at (minimum) three heights and the wind data measured at the lowest height were extrapolated and compared to the actual measured wind conditions. They concluded that there was no significant difference in the performance of the power or log law. It is likely that for some sites, one law better fits the data than for other sites. In complex terrain, none of the tested models was able to accurately predict the wind conditions at the top anemometer. They also noticed that the roughness parameters (such as the roughness length) derived from the measurements deviated from tabulated values found in the literature (Wieringa, 1992).

In this section, different approaches to extrapolate the wind speed to hub height are discussed and their mutual differences are highlighted. First, the measured wind data, used throughout this chapter, will be down-scaled to a lower height using one particular approach and for specific roughness parameters. These parameters are applied to verify the impact of the roughness on the extrapolated wind speed. Then both the measured and the downscaled wind speed are used to extrapolate the wind speed to a specific hub height (taking the 2/3 rule into account) by applying different shear laws. The extrapolated wind speeds are then used to estimate the AEP of the 29 wind turbines in the database. The impact of using one approach or the other to estimate the AEP is studied. Then a typical measurement error is artificially imposed on both the measured and downscaled wind speed and their influence on the AEP is verified.

3.5.1 Uncertainty on the AEP using different shear laws

In this chapter we maintain to use the database of 23 different measurement sites and 29 wind turbines. On the majority of these sites, the measurement height is 10 m (for simplicity we assume all wind speeds are measured at this height as not all specifications of the measurement stations are available). First, we use the log law (presented in Section 1.3, Eq (1.4))

to downscale the wind data from the measurement height to 7.5 m for each site. We repeat this downscaling process two times by applying two roughness lengths z_0. We use one for open terrain (0.1 m) and one for more urban terrain (1 m) to verify the influence of the roughness of the terrain. This procedure leads to two data sets for each site with wind data at two heights. For each of these data sets, we fit a wind shear law (here we use the log law, the linear log law and the power law) and determine the roughness parameters (for the log law, they are obviously identical to the ones imposed in the previous step). For each data set and each shear law, we use these roughness parameters to extrapolate the wind speed to 15 m (thus applying the 2/3 rule). All data sets are then used to predict the AEP of the wind turbines in the database.

We can now for each type of terrain (open and urban) see the impact of using one approach or the other to extrapolate the wind speed. In Figure 3.15, we compare the average AEP (averaged over 29 turbines) of the linear Log Law (LLogL) and power law (PL) to the AEP based on the log law (LogL). Larger differences are observed when the mean AEP of the LogL and the PL are compared to the LogL and LLogL. This could be immediately derived from the equation of the LogL and LLogL (Eqs. 1.4 and 1.11). The wind speed at a certain height for the LogL is equal to the wind speed one roughness length below this height for the LLogL.

As can be derived from Figure 3.15, the difference in AEP is thus dependent on the terrain (or the roughness length). This is also particularly true when the PL and LogL are compared. In rougher terrain, the differences in extrapolated wind speed using one law or the other increase and so increasing the difference in AEP. The difference in AEP is also shown as a function of the average wind speed. This immediately emphasises the importance for small-scale wind as they are generally located in lower wind speed regimes. In a worst case scenario, meaning on a site with poor wind conditions and a rough terrain, using the LogL instead of the PL leads to an average difference in AEP of 8 %.

As the previous figures only show the mean differences, the individual difference on the AEP for each wind turbine and each measurement site are presented in Figure 3.16. Only the results for rough terrain and a comparison between the LogL and PL are presented as these represent the largest differences that would appear within the range of parameters applied in this section. Nearly all estimates of the AEP using the PL are larger than the ones using the LogL especially in low wind speed regimes. The total average is relatively low (6 %) though differences on the AEP
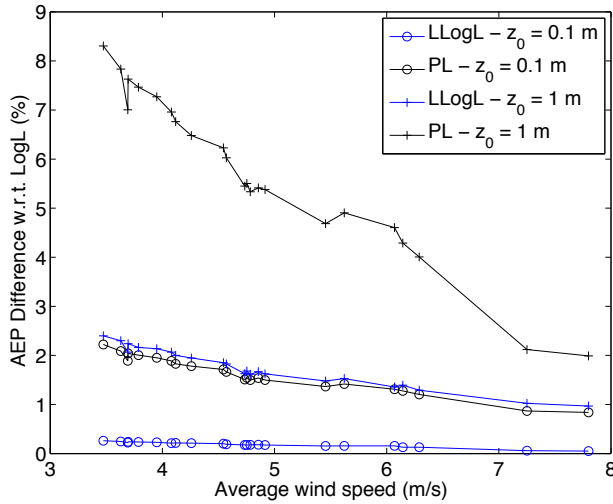
Figure 3.15: Average AEP of the LLogL (blue) and PL (black) law compared to the average AEP based on the Log law as a function of the average wind speed at the site. A roughness length of 0.1 m (circles) and 1 m (plusses) was used for the extrapolation.

above 20 % appear when one shear law is used instead of the other. This indicates that even when the 2/3 rules is met, large errors can occur.

3.5.2 Uncertainty in AEP due to measurement error

For wind energy purposes, the wind speed is generally measured with a cup anemometer. Different standards (IEC, 2006; Measnet, 2009) prescribe what the accuracy of this equipment should be. Even when these standards are met, a typical measurement error is in the order of $\pm$ 0.05 m/s to $\pm$ 0.1 m/s. When these measurement errors occur, an additional uncertainty on the extrapolation of the wind speed will be imposed. In this section, this error is translated to the uncertainty on the estimation of the AEP.

The largest differences in the estimation of the extrapolated wind speed is caused for two specific combinations of measurement errors:

- A positive measurement error on the lower anemometer and a negative error on the upper anemometer. The wind speeds at both anemometers are now closer to each other. This artificially decreases
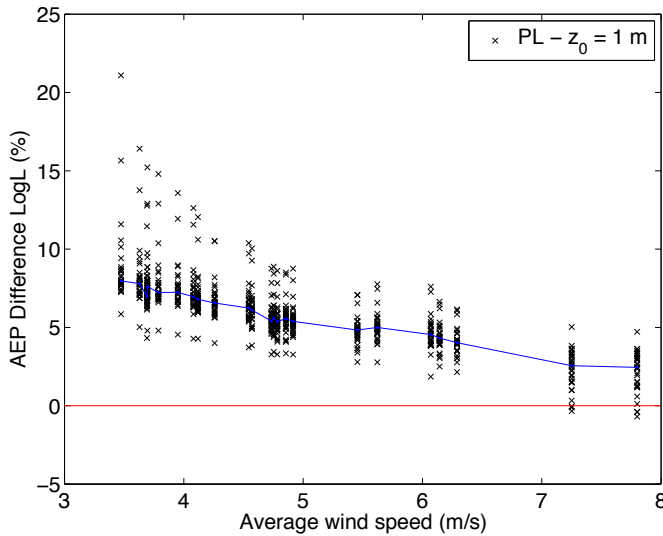
Figure 3.16: AEP difference between the LogL and the PL for each individual wind turbine as a function of the average wind speed for each measurement site. The applied roughness length is 1 m.

the roughness and will result in a higher estimate of the extrapolated wind speed;

- A negative measurement error on the lower anemometer and a positive error on the upper anemometer, resulting in a larger difference between both measured wind speeds. This will increase the roughness parameters and will result in a lower estimate of the extrapolated wind speed.

Instead of comparing the differences between the wind shear laws, we now focus on each wind shear separately. In Figure 3.17, for each wind shear law, the difference in AEP between the lowest and highest extrapolated wind speeds are shown for a rough terrain ($z_0 = 1$m). These differences are shown as a function of the average wind speed at the site. Even when the same shear laws are used and only a measurement error of 0.05 m/s is imposed, the average error on the AEP can go up to nearly 25 %. Clearly, independent of which shear law is used, the error is larger in low wind speed areas. The PL seems to be the most sensitive for these measurement errors. When using the PL in poor wind conditions and rough terrain, in a worst case scenario, these measurement errors can lead to a difference of 85 %

when using them to predict the AEP.
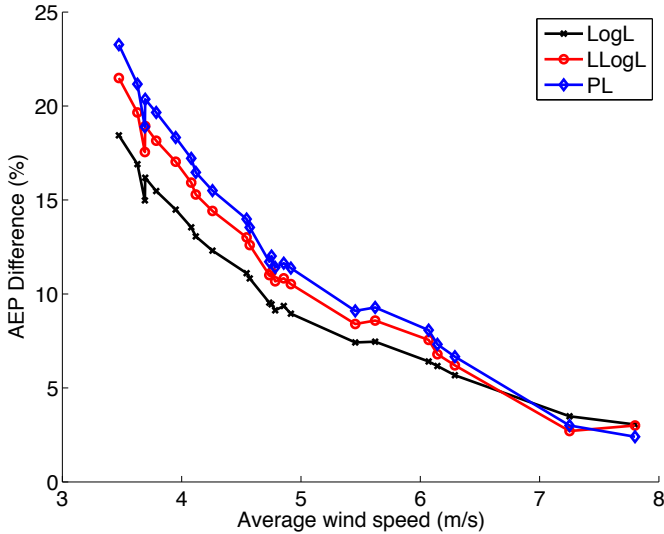
Figure 3.17: AEP difference due to specific combinations of measurement error on the wind speed for each wind shear law as a function of the average wind speed. The AEP difference is determined by estimating the AEP with the lowest and highest extrapolated wind speed. The applied roughness length is 1 m.

3.5.3   Conclusions and recommendations

In the literature, there are three shear laws often used to extrapolate the measured wind speed to hub height. We have discussed these approaches and highlighted their mutual differences. These differences are affected by two main drivers particularly important for SMWT projects: in rougher terrain and in low to medium wind speed regimes, using one shear law or the other will lead to significant differences in the extrapolated wind speed and thus in the prediction of the AEP. These differences are also more pronounced when using the power law instead of the log law or the linear log law. This could also be derived when simply comparing the definitions of these shear laws.

The uncertainty on the wind speed is partly determined by the accuracy of a cup anemometer. Even when using accurate cup anemometers, typical measurement errors are in the order of 0.05 m/s. The error on the measured

wind speed will then affect the extrapolated wind speed and lead to an additional uncertainty on the estimation of the AEP. Even when the 2/3 rule is respected, extrapolation errors on the AEP can be as large as 85 %, when using the power law in rough terrain with poor wind conditions.

Our recommendation is inevitably that extrapolation of the wind speed should be avoided as much as possible. The 2/3 rule is still too mild and lower extrapolation heights will limit the error on the AEP.

Another way of reducing the uncertainty is by using very accurate measurement equipment as typical measurement errors will significantly effect the estimation of the AEP.

3.6 AEP prediction based on Measure-Correlate-Predict

The best way to accurately estimate the AEP of a wind turbine is by measuring the wind conditions for an appropriate period of time. The general recommendation in the literature is that the measurement period should be at least one year to cover the seasonal variations of the measurement site (Taylor et al., 2004; AWS Scientific Inc., 1997). Due to the interannual variability of wind speed, various authors (Landberg et al., 2003; Lackner, Rogers, and Manwell, 2008) have indicated that the wind conditions measured over one year do not fully reflect the average wind conditions over the lifetime of a wind turbine (which is typically 20 years). To avoid measuring over multiple years to ensure an accurate estimate of the average wind conditions, Measure-Correlate-Predict (MCP) approaches are used.

In MCP, (on-site) *measured* short-term wind data are *correlated* with long-term data at another site (often a meteorological station). The objective of this approach is to correlate the measurement period where the wind speed (and wind direction) are simultaneously measured and find parameters that describe this correlation. These parameters are then applied on the long-term wind data set, to *predict* the long-term wind conditions on the measurement site.

Different approaches are present in the literature. For example, Rogers, Rogers, and Manwell (2005) tested four MCP approaches. They compared two one-dimensional and one two-dimensional linear regression approaches and the variance-ratio approach. For each approach, the reference wind data were binned according to the wind direction and for each wind direction the MCP parameters were derived. The goal was to identify the most accurate approach for the studied sites and to derive the most useful

measurement period. They concluded that the variance-ratio provided the most accurate results and that the most useful data length was about 9 months. Only a small improvement in the error was noticed for longer data lengths.

Weekes and Tomlin (2014a) used three approaches to verify what errors could be expected if the measurement period was limited to just 3 months. Therefore they used 11 years of long-term wind data of 22 measurement stations and applied the MCP procedure multiple times for each measurement stations. Each time a concurrent measurement period of 3 months was correlated and repeated by shifting the start of the measurements with one month. By using this procedure, they derived the best period to start the measurements. They concluded that seasons with more variation in wind direction (autumn and spring rather than winter or summer) lead to better estimation of the long-term wind conditions.

A similar study (Lackner, Rogers, and Manwell, 2008) used a Lidar (Light Detection and Ranging) measurement station. The objective was to measure and estimate the long-term wind conditions on two sites in just one year in order to limit the measurement period. They used a so-called round robin approach where the wind speed was measured for 10, 30 and 60 days at one site, then switched the lidar measurement station to the other site and repeat this process for one year. This approach was compared to two more conventional approaches where the wind conditions were continuously measured for 6 months and 1 year. More accurate estimates of the long-term wind conditions were found when using the round robin approach even though the total measurement period was just 6 months. Using just 10 days before switching from one site to the other seemed to give more accurate results than when 30 or 60 days was used, as this procedure captures more of the variability within each period of the season.

In this section, we will compare the accuracy of three approaches and give advice which to use best to assess the long-term wind conditions. In the first part of this section, we will present these approaches. Next, we use long-term data of 23 measurement sites with a measurement period starting from January 2004 and ending in 2013. From each of these long-term data sets, we select a short-term data set of 1 year starting at the first of January 2004. These data are then used to apply the three presented MCP approaches in order to estimate the long-term wind conditions. As the actual measured long-term wind conditions are available, we use the predicted and the measured ones to estimate the AEP of the 29 wind turbines from the database for each MCP approach. This procedure is repeated by

shifting the start of the measurement each time with one month (the second data set than contains one year data from February 2004 to February 2005) creating a sliding window with a width of 1 year. Using this procedure, several short-term data sets are derived for each site and the accuracy of each MCP approach can be determined. In Section 3.6.3, the same procedure is used however, shorter measurement periods are introduced of 1, 2, 3,..., to 11. Finally, conclusions and recommendations concerning MCP are presented in Section 3.6.4.

3.6.1 MCP methods and choices

In this section, we compare the three MCP procedures. They are commonly used for wind energy applications. The first approach uses simple linear regression where the parameters are estimated using a least squares algorithm. The second approach uses the same procedures as the first one but adds residual scatter to the estimated wind speed. The third approach uses a different procedure to determine the parameters for linear regression.

Linear regression: Derrick (1992) was the first to apply linear regression (LR) to characterise the relationship between the target site and the reference site:

$$\widehat{V}_{\mathrm{tar}} = \alpha V_{\mathrm{ref}} + \beta + \epsilon \tag{3.15}$$

where $\widehat{V}_{\mathrm{tar}}$ is the predicted wind speed at the target site (short-term wind measurement site), V_{ref} is the observed wind speed at the reference site (long-term meteorological station), α and β the slope of the linear regression and ϵ an error term which represents the residual scatter. The parameters α and β are determined in a least-squares way for the concurrent measurement period and they are used afterwards to predict the long-term wind conditions on the target site using the long-term data of the reference site. Separate parameters are calculated for data in twelve 30° direction bins defined by the wind direction at the reference site. For this approach, the residual scatter is neglected.

Linear regression with Gaussian scatter: This approach uses the same technique as LR, though the residual scatter is taken into account. If we assume that the residuals are normally distributed about $\widehat{V}_{\mathrm{tar}}$, this scatter will not have a significant effect on the estimated mean wind speed. However, it will have an impact on the shape of the estimated wind

speed distribution and due to the cubic relationship, thus on the estimated power (Weekes and Tomlin, 2014a).

In order to account for the residuals, it is modelled as a Gaussian distribution with a zero-mean $\overline{V}_{\text{tar}}$ (Ellison, Barwick, and Farrant, 2009):

$$\epsilon \sim \mathcal{N}(0, \sigma_{\text{res}}^2) \tag{3.16}$$

where σ_{res} is the standard deviation of the residuals about the estimated wind speed at the target site and derived by (Ellison, Barwick, and Farrant, 2009):

$$\sigma_{\text{res}} = \sqrt{\frac{1}{N-2} \sum_{i=1}^{N} (V_{\text{tar}} - \widehat{V}_{\text{tar}})^2} \tag{3.17}$$

where i represents the ith data point of the measured wind speed V_{tar} and N the total number of observations at the target site. The predicted wind speed is then reconstructed by adding random draws from the Gaussian distribution in equation (3.16). This model is thus a simplification since the underlying joint distribution of V_{tar} and V_{ref} is expected to be joint Weibull rather than joint Gaussian (Romo Perea, Amezcua, and Probst, 2011). This approach will be further referred to as the LRE approach.

Variance-ratio: When using linear regression, the estimated average wind speed at the target site will be close to the actual measured wind speed in the concurrent period. The predicted variance will be less than the measured variance. This can result in a biased prediction of the wind speed distribution and impose an error on the estimated AEP. Therefore the variance-ratio (VR) approach was introduced. This approach involves forcing the variance on the estimated wind speed at the target site to be equal to the measured variance. It uses equation (3.15), but another procedure to determine α and β (Rogers, Rogers, and Manwell, 2005):

$$\alpha = \frac{\sigma_{\text{tar}}}{\sigma_{\text{con}}} \tag{3.18}$$

$$\beta = \overline{V}_{\text{tar}} - \alpha \overline{V}_{\text{con}} \tag{3.19}$$

where σ_{tar} and σ_{con} represent the standard deviation at the candidate and reference site for the concurrent measurement period. Similar to the previous two approaches, these parameters are determined for each 30° wind direction bin. The error term in equation (3.15) is now again neglected.

3.6.2 MCP based on a 1 year measurement period

According to recommendations in the literature, one full year should be measured to cover the seasonal variation of the target site. In this section, we derive a period of one year from each measurement starting from January 2004. To derive multiple one year data sets from each site, we shift the start of the measurement each time with one month creating a sliding window with a width of one year. This implies that for each site, 108 (9 years times 12 months) datasets of one year are selected. For each of these tests, the correlation with the concurrent measurement period of the other sites in the database is verified and the one with the highest correlation is selected as reference station. Once the MCP approach is applied, the long-term AEP of 29 turbines is determined using the predicted long-term wind conditions of the site. These predicted AEPs are then compared to the AEPs calculated using the measured long-term data set of the same site. By using this methodology, the accuracy of each approach can be compared and the expected error on the AEP can be derived.

In Figure 3.18, the estimated mean wind speeds are compared to the measured wind speeds for the three tested approaches. For each measurement site, the predicted mean wind speeds are averaged over the sliding window. When using a full year as measurement period, the mean wind speeds are accurately predicted, to within 1 %. As the LR and LRE approaches are similar (a residual scatter using a zero-mean wind speed is imposed on the LRE approach), the average estimated wind speed are practically equal.

In Figure 3.19, the average AEP error is shown for each measurement site. The 'measured' AEP using the long-term measured data is compared to the predicted AEP using a MCP approach. The results are averaged over all the turbines in the database and over the sliding window. The LR approach seems to underpredict the AEP. When Gaussian scatter is introduced in the linear regression approach, a significant improvement of the estimations is noticed. The performance of this approach and the VR approach are comparable. The mean error is lower than 5 %.

In Figure 3.20, the individual energy production errors are shown for each wind turbine and each measurement site. This figure only shows the results for the VR approach and the errors are averaged over the sliding window. It should be noted that although Figure 3.19 shows a mean error lower than 5 %, large errors up to 20 % are found when applying the MCP
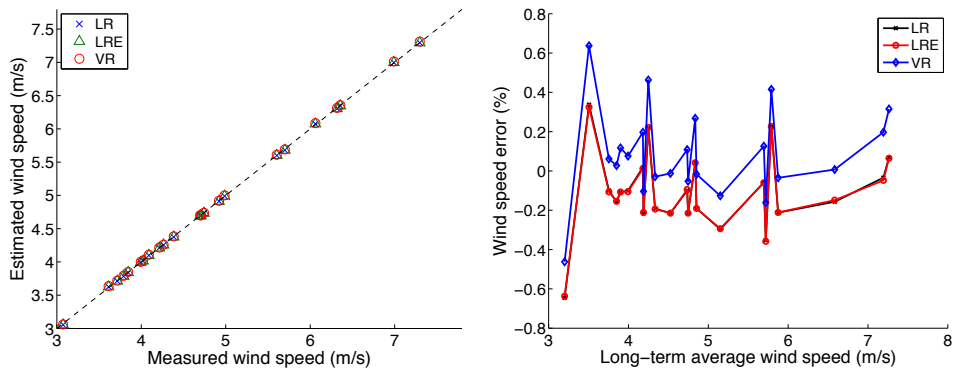
Figure 3.18: Comparison of the predicted and observed wind speed for a measurement period of 12 months. For each site, the predicted wind speeds are averaged over the sliding window. In the right figure, the error between the observed and predicted wind speeds are shown.

approach using 1 year measurements.

To verify if the time to start the measurements has an impact on the accuracy of the AEP predictions, the AEP errors as a function of the start month are shown for the three approaches in Figure 3.21. The AEP errors are averaged over all turbines and measurement sites. The time for the start of the measurements has negligible effect on the accuracy of the estimations if the measurement period is one year.
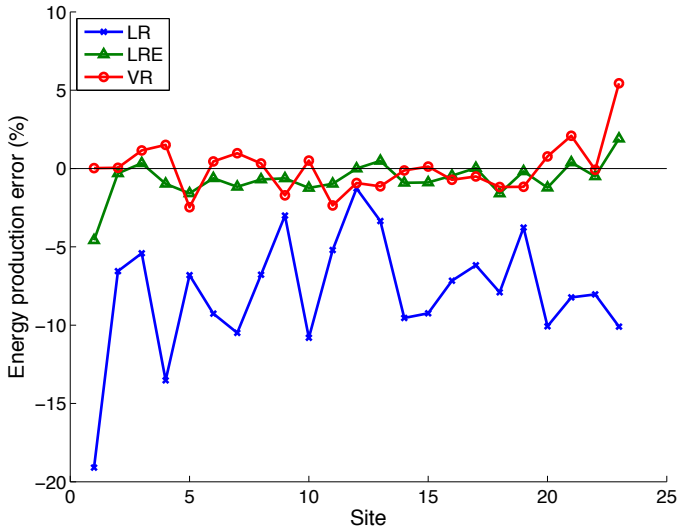
Figure 3.19: AEP error for each measurement site for a measurement period of 12 months. For each site, the AEP error is averaged over all the turbines and the sliding window.
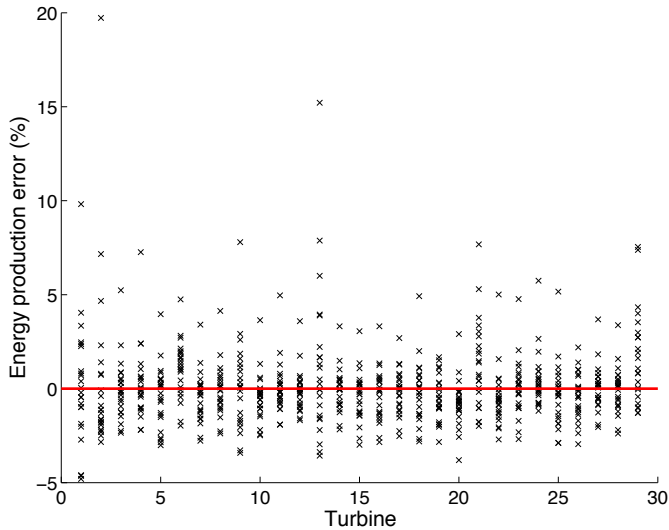
Figure 3.20: AEP error for each measurement site and for each wind turbine using a measurement period of 12 months and the VR approach. The AEPs are averaged over the sliding window.
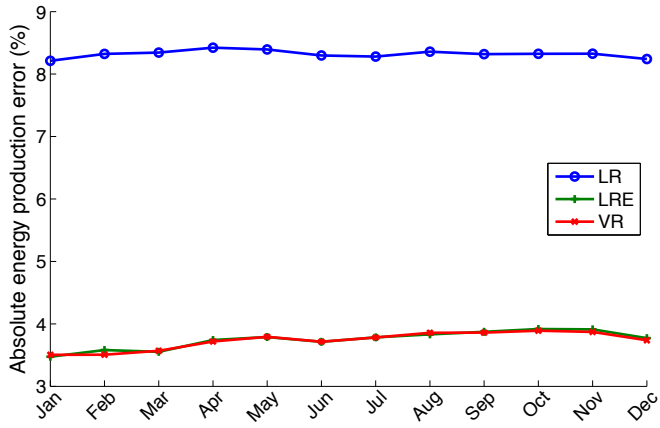
Figure 3.21: Comparison of the absolute energy production error as a function of the start of the measurements. The measurement period is 12 months and the errors are averaged over all turbines and sites.

3.6.3   MCP based on a short measurement period

As shown in Chapter 2, one of the challenges of SMWTs is that wind resource assessment studies are costly in relation to the total investment cost of the turbine. One opportunity to reduce this cost is by reducing the measurement period as more assessment studies can be conducted with one measurement set. Shorter measurement periods will also introduce less accurate long-term predictions of the wind speed and AEP. To investigate this, the procedure presented in the previous sections is repeated with limited measurement periods of 1, 2, 3, 4,... to 11 months.

In Figure 3.22, the observed and estimated mean wind speed are compared for a measurement period of 1 month. The predicted wind speeds are averaged over the tested sliding window for each specific site. Still a good agreement is found between the observed and estimated long-term mean wind speed as the average error is below 3 %.
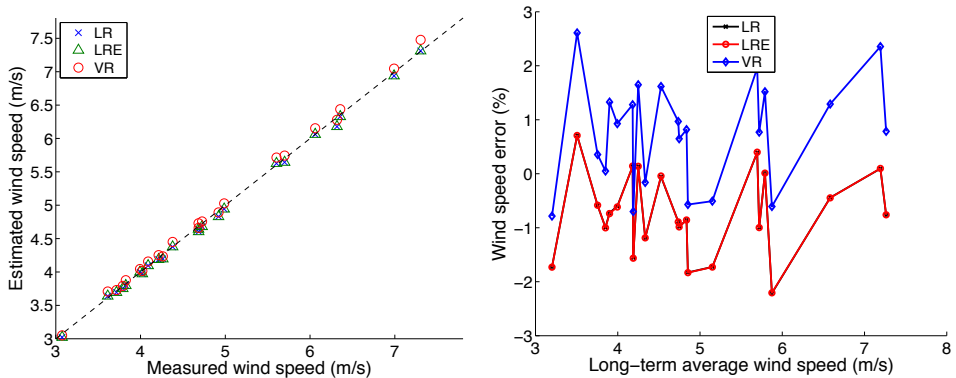
Figure 3.22: Comparison of the predicted and observed wind speed for a measurement period of 1 month. For each site, the predicted wind speeds are averaged over the sliding window. In the right figure, the error between the observed and predicted wind speeds are shown.

In Figure 3.23, the absolute mean error on the AEP is shown as function of the length of the measurement period. Again the performance of both the LRE and VR approach are comparable while the difference between both approaches and the LR approach is smaller for shorter measurement periods. For all approaches, the length of the measurement period has a significant effect on the energy production error. The mean error is reduced by 50 % if the measurement period increases from one month to 12 months. The most explicit decrease is when the measurement period increases from

1 to 3 months. Above 9 months of measurements, the error on the AEP is less dependent on the measurement period and the mean error is below 5 %.
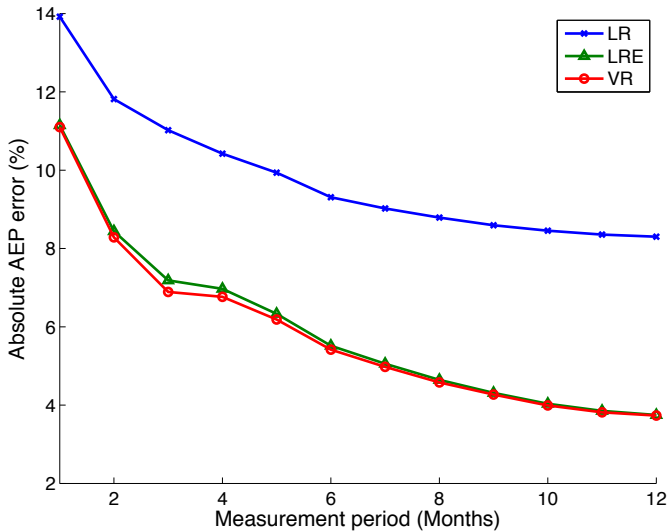
Figure 3.23: The absolute mean error on the estimated AEP as a function of the length of the measurement period.

Similar to a measurement period of 1 year, the best periods to measure the wind conditions are derived. In Figure 3.24, the absolute mean error on the estimated AEP as a function of the start of the measurements is shown for the VR approach. A concurrent measurement period of 1, 3, 6, 9 and 12 months are compared. This figure shows that for shorter measuring periods, the best period to start the measurements is in the months October, December, January or February or in other words the winter months. For short-term measurements above 9 months, the start of the measurements has negligible effect on the estimation of the AEP.

It can be expected that the concurrent measurement period with more variable wind conditions would lead to a better fit between the reference and target site. A similar study, performed by Weekes and Tomlin (2014a), indicated that the best MCP predictions were found in autumn and spring. They concluded that these were the best seasons as they show a greater spread in wind direction and the MCP parameters are determined per sec-
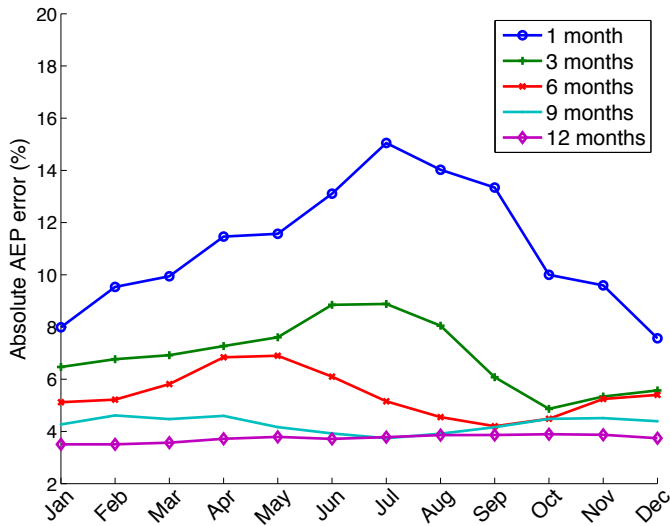
Figure 3.24: The absolute mean error on the estimated wind speed for the variance-ratio approach as function of the start of the measurements. Each curve represent a different length of data used for the concurrent measurement period.

tor. To compare with the conclusions made by Weekes and Tomlin (2014a), we show the spread in wind directions in Figure 3.25 (left) for a measurement period of 3 months. The frequencies per wind direction are averaged over all measurement sites. The months with a higher error (March to August) and a lower error (January, February and September to December) are derived from Figure 3.24 and both are then compared in Figure 3.25. A different wind pattern is found, though the months with the lower error show no better spread over all wind directions contrary to what was found by Weekes and Tomlin (2014a). However, when the average wind speeds are derived per wind direction, a significant difference was found between the months with a high and low error (right Figure 3.25). As the average (and maximum) wind speeds are higher, for each sector a more distributed wind speed can be correlated to the reference data leading to a better fit with the target site. Similar results were found when comparing the months with a low and high error for other measuring periods (e.g. 1 month rather than 3 months).
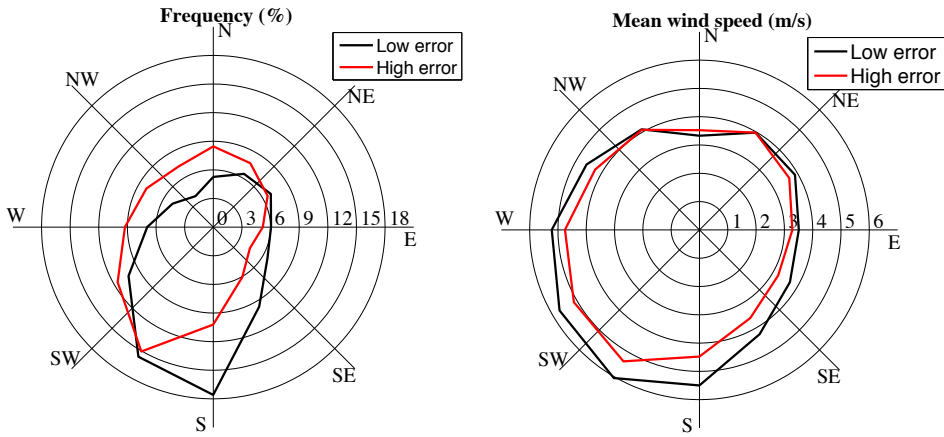
Figure 3.25: Wind roses with the average frequency of occurrence (left) and average wind speed (right) for a measurement period of 3 months, all measurement sites and over the sliding window. The months with a lower error (January, February and September to December) are compared to the months with a higher error (March to August).

3.6.4   Conclusions and recommendations

In this section, three approaches to apply the MCP methodology are compared. The most commonly used approach is linear regression, however from the tested approaches this is the one with the lowest accuracy. The accuracy of both the LRE and VR approach are comparable. For reasons of simplicity our advice is to use the VR approach.

To reduce the measurement periods, a concurrent period between the long-term and short-term data of a full year (which is recommended in the literature) is compared to shorter measurement periods. Even when the concurrent period is just one month, the mean wind speed is well estimated by the three approaches. However, when only one month is used to estimate the long-term AEP of a wind turbine, a mean error of 11 (for LRE and VR) to 14 % (for LR) was found. Even when a full year was used, for specific cases the error on the AEP was 20 % though the mean error was reduced to 4-5 % (for LRE and VR) and to 9 % (for LR). We confirm the recommendations made to measure at least 9 months when possible, in order to have a reliable estimate of the AEP. If shorter measurement periods are used, to reduce the cost of the resource assessment, our tests indicate that it is better to start the measurements in the months October to February. These months seem to have a wider distribution of the wind

speed for all wind directions, leading to a better fit between the candidate and reference site.

3.7   Conclusions

In this chapter, we have reviewed the expected energy output of 29 wind turbines on 23 different measurement sites in Belgium and the Netherlands. This allows us to formulate specific guidelines for the best prediction of the annual energy production (AEP).

A first conclusion is that rated power is not a very good basis to choose a turbine. A turbine with a higher rated power does not necessarily produce more energy than a turbine with a lower rated power.

When only the average wind speed at a site is known, we propose to estimate the AEP with the Rayleigh distribution. We found differences below 10 % as long as the standard deviation at the site did not differ more than 10 % from the one assumed by the Rayleigh distribution (This was the case for 18 of the 23 studied sites).

We found that using the Weibull distribution improved the accuracy in AEP prediction compared with Rayleigh to around 5 % for most sites (for 20 of the 23 sites). For some specific cases however, more complex methods like the MEP method can outperform the Weibull distributions. We can always find one MEP variant that performs better than Weibull. However, the behaviour of this distribution is unpredictable, and until now no specific rule could be derived to determine the best pre-exponential term. We therefore do not suggest to use the MEP method to predict the AEP.

Whenever wind measurements are available, the data should be used directly, i.e. without fitting a statistical distribution to it. Of course the wind data can be binned into a histogram and then used to predict the AEP. This approach gives the best combination of accuracy and ease of use when wind speed measurements are available.

Measure-correlate-predict is a well known technique to estimate the inter annual variations of the on-site wind conditions. According to our validation process, both the linear regression with Gaussian scatter and the variance-ratio approach have similar performance. For simplicity, our advice is to use the variance-ratio approach. Using shorter wind measurement campaigns will reduce the cost of a wind measurement campaign, but it will also significantly increase the error on the AEP. Our recommendation here is to measure at least 9 months if possible. It should be noted, that measuring 3 to 6 months may significantly lower the cost of a resource

assessment campaign. For these periods, the mean error on the AEP can be more than twice as much, however it is better than not measuring at all (or using only the average wind speed). If these shorter measurement periods are used, the measurements should be started in the months October to February.

A frequently used restriction on the vertical extrapolation of the wind speed, advises to measure the wind speed at least 2/3 of the hub height of the turbine. Even when this rule is met, using one approach or another for the extrapolation will create large discrepancies in the estimation of the AEP. When comparing the log and power law, differences up to 20 % were found. Rough terrain, low wind speeds and the inaccuracy of anemometer are factors that negatively affect these differences. Our recommendation here is to avoid extrapolating the wind speed as far as possible. To limit the uncertainty of the estimation, the height difference for the extrapolation should be limited, extrapolations should be conducted in open terrain and accurate anemometers should be used.

Chapter 4

Impact of the averaging times of power curves and wind speeds on the prediction of the annual energy production

Abstract—*This chapter expounds on the choice of the averaging time (i.e. the sampling period) for a wind measurement campaign and its relation to the prediction of the annual energy yield. We point out that neglecting this issue will lead to an erroneous AEP prediction, and provide a theoretical framework to appreciate the effect of the averaging time in terms of turbulence.*

4.1   Problem statement

The power curve of a turbine describes the (electric) power that the turbine produces as a function of wind speed. This curve is typically combined with the wind conditions at an installation site, e.g. a histogram of on-site wind speed measurements, to predict the average energy production. This can be calculated in a number of ways, see e.g. Manwell, McGowan, and Rogers (2009). In any case, an accurate power curve and wind histogram are necessary (but not sufficient) conditions to determine the economic viability of new wind turbine projects.

IEC (2006) describes the standardized procedure to measure the power performance of electricity-producing wind turbines. This standard specifies that wind speed and power measurements should be sampled (and integrated) over 10 minute intervals; for small wind turbines (with a rotor surface smaller than 200 m^2) the interval is 1 minute, as these respond faster to varying wind speeds. The standard further dictates that a test report should provide an estimate of the annual energy production (AEP) by evaluating the turbine for a Rayleigh-distributed wind speed with integer mean speeds between 4 m/s and 11 m/s. No detailed specifications (e.g. with respect to averaging time for our purposes here) are given on how to process actual wind measurements for AEP prediction.

Another part of the standard (IEC 61400 Part 1, on the safety requirements of wind turbine generator systems) does refer to averaging times (in the chapter on the assessment of external conditions), but only in vague terms and related to blade load prediction due to turbulence: "[...], sampling rate and averaging time used to obtain measured data can influence the assessment of turbulence intensity. These effects shall be considered when predicting the turbulence intensity from measured data."

A reasonable approach for resource assessment would be to use the same interval for wind speed measurements as was used for the original power curve measurement. But this is not always done so in practice, e.g. when measurement data of a nearby meteorological station are used. Often hourly wind speed data are used to fit a Weibull distribution, which is then combined with power curve data, for (1 minute averaged) small wind turbines (Celik, 2003; Drew, Barlow, and Cockerill, 2013; Mostafaeipour, 2013) as well as for large ones (Schallenberg-Rodriguez, 2013). Other examples have estimated the AEP of small wind turbines (with 1 minute averaged power curves) using wind speed data with averaging times of 10 minutes (Peacock et al., 2008) and 1 hour (Wang et al., 2008) .

Using different intervals for power curve and wind data does however

affect the prediction of the power output. Say one has one year of wind speed and power output data (sampled at 10 minutes) to construct the power curve. The turbine will have produced a certain amount of electric energy, and that should come out of any (a posteriori) prediction of the AEP based on the same wind data and the power curve. But this is clearly not true when the averaging time of the wind speed changes. With a larger interval (say 1 hour), very high and very low wind speeds will occur less frequently, and the histogram will be more concentrated around the mean; the variance reduces. The issue is that the mean apparent power in the wind decreases for larger intervals. This was pointed out before using 60 days of 1-second-sampled wind speed measurements at the Atlantic Wind Test Site (Brothers, Arthur, and Keller, 1985), and it is easily shown by expressing the mean power in the wind (which is proportional to the mean of the cube of the wind speed) as a function of the mean and the standard deviation of the wind speed:

$$\overline{V^3} \approx (\overline{V})^3 \left[1 + 3 \left(\frac{s_\tau}{\overline{V}} \right)^2 \right] \tag{4.1}$$

with V the wind speed and s_τ^2 the variance over the wind speed samples when an interval of τ is used, and where $\overline{x}$ denotes the time average of x. (See the section 4.3 for an elaboration of the equation.) We conclude that any interval larger than that of the power curve will underestimate the power in the wind (as the variance decreases with increasing τ). One will thus obtain an underbiased estimate of the AEP, even though the same underlying wind conditions and the appropriate power curve are used.

A previous study has found that the available energy in the wind reduced about 5 % when the averaging time was increased from 1 second to 15 minutes (Brothers, Arthur, and Keller, 1985). Other studies that focused on the energy production of actual turbines found similar variations (Carta and Mentado, 2007; Makkawi, Celik, and Muneer, 2009). A recent article studied the effect of varying the averaging time of measurement data to calculate wind turbine power curves (Elliot and Infield, 2014). They also provide recommendations for improved small wind turbine testing and energy yield calculation. But as far as we know, no concrete strategy to cope with inconsistent wind speed and power curve data is available.

From a theoretical point of view, one could construct a different power curve for all of the commonly used averaging times, and then predict the AEP with consistent averaging times. This indeed neutralizes the effect of the averaging time: the power apparently lost in the wind is gained back

in the power curve. Indeed, when variation in the wind is more averaged out because of a large averaging time, then more variation is present within the interval. Stated differently: when the interval is longer, every sampled interval will have a larger variance, while the variance over the sampled speeds will be smaller. There is a shift in variance from over the samples to within every individual sample when the interval increases.

This effect is illustrated in Figure 4.1. We generated a set of uncorrelated Weibull-distributed wind data and corresponding power data (using Eq. 1.3) based on the power coefficient of a real-life 10 kW power curve. We then calculated the power curve according to the IEC standard for three different averaging times: 1, 2, and 5 minutes. Two effects appear. The wind speed histogram becomes more and more concentrated around the mean (which stays obviously the same) since the variance over the samples reduces when τ increases. The effect on the power curve is more subtle. If $C_{P_{el}}$ were constant (i.e. the power is proportional to the cube of the wind speed), then the power curve would grow steeper for increasing averaging times (as the variance within every interval increases). This is effectively what can be observed in Figure 4.1 (right pane) between ca. 3 and 6 m/s, where the effect of varying $C_{P_{el}}$ is small. For higher wind speeds however, $C_{P_{el}}$ drops since the turbine reaches maximum (rated) power of 10 kW at 8 m/s. The result is that the slope of the power curve decreases for increasing averaging times beyond 6 m/s (where the $C_{P_{el}}$ starts to drop). Indeed, when τ increases, and thus the variance within the sampled speeds and power, the average power in the bin will consist of a wider set of sample powers.

One should note that we deliberately excluded the autocorrelated nature of the wind, so as to overemphasize the change in variance when the averaging time changes. In practice, the decrease in variance for increasing averaging time is slower, as we will show later.

Of course, it is impractical for manufacturers to provide different power curves for all (or even a few) possible averaging times. Instead of using an inappropriate sampled power curve however, we suggest to modify the power curve for the change in variance (of the individual samples) for inconsistent averaging times. The right pane of Figure 4.1 and the fact that the variance within the averaging time increases should remind us of the effect of turbulence on the accuracy of the power curve measurement, see e.g. Borg et al. (1986); Hedevang (2014); Lubitz (2014). (A theoretical derivation is presented in section 4.3.3.) It is well known that the power output measurement overestimates the mean power for a given wind speed
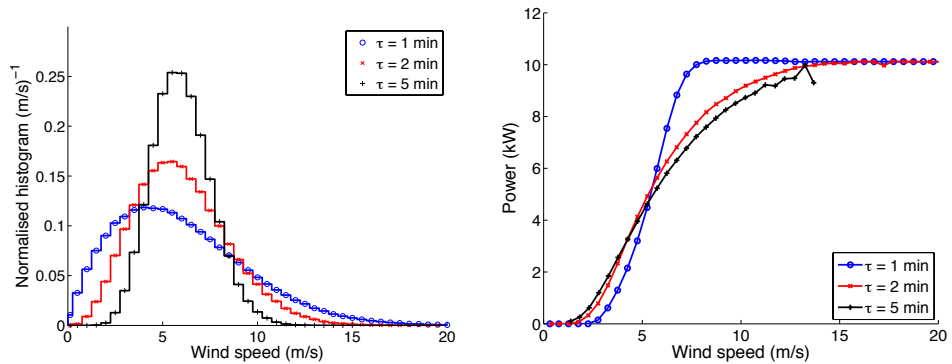
Figure 4.1: Effect of increased averaging times on the wind speed normalised histograms (left) and the power curve (right). The averaging times shown are 1 minute (circles), 2 minutes (crosses) and 5 minutes (pluses). The mean power output (integral of the product of the like curves left and right) is always the same.

bin, and that this overestimation scales with the turbulence intensity. From our analysis, it appears that this is still true for the time intervals in the order of minutes or even hours), where we no longer can speak of turbulence in the strict sense (which is typically reserved to describe stochastic variations faster than say 0.1 Hz).

The question that this chapter addresses then is: can we compensate for differences in averaging time in the same way that we can compensate for turbulence effects?

4.2 Power curve compensation for inconsistent averaging times

We use two sets of wind speed measurements at different locations and a true power curve to demonstrate the inconsistency problem and our proposed solution. In Section 4.2.2 we discuss how the power curve can be compensated in practical applications; in Section 4.2.1 we first illustrate this method using the true variances corresponding to the utilised averaging time.

4.2.1 Compensation of the variance based on detailed measurement data

We have wind measurements at two sites (A and B) sampled at 1 Hz and 4 Hz (F_s is the sample frequency); for a total period of ca. 12 and 10 days respectively. We deliberately selected two sites with distinct wind climates: one with a very low wind speed but with high turbulence, and one with a higher mean but lower turbulence. Site A (a small wind turbine test field located in Belgium) has a mean wind speed of 3.1 m/s (at 15 m height) over the measured period and a high turbulence intensity (32.2 % at 10 minute averaging time). Site B (an off-shore measurement station located in the North Sea) has a decent mean wind speed of 6.7 m/s (at 27 m height) over the period considered, but a markedly lower turbulence intensity (6.9 %, again at 10 minute averaging time), as can be seen in Figure 4.2. Figure 4.3 (left) shows the histograms (which have been normalised so that the area bounded by the graph is 1) of both sites.

These datasets can be re-sampled to any value between the original sample period and the total measurement period, to mimic the effect of varying τ. For every τ we obtain a data set with wind speeds and variances (for every wind speed sample). As expected, the variance (which is the variance within the averaging time) increases for increasing τ. We have tested averaging times between one minute and two hours; in practice one will often have to deal with either 1 minute, 10 minute, or hourly wind speed data.
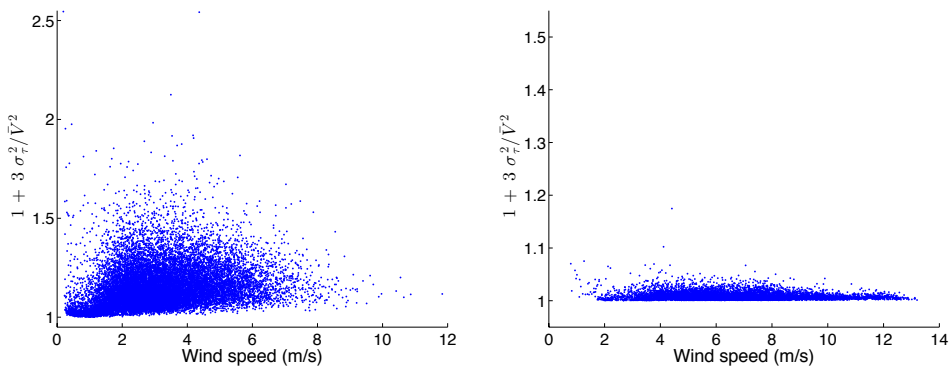
Figure 4.2: Effect of turbulence as a function of wind speed. The turbulence here is given by $1 + 3\sigma_\tau^2/\overline{V}^2$, which is useful to interpret equation 4.21. Site A is left, site B right.

To demonstrate the effect of the averaging time on the mean power, we use the power curve of a 5 kW turbine, see Figure 4.3 (right). This power curve was determined according to the IEC 61400-12-1 standard, with an averaging time of 1 minute, and at a site with a turbulence intensity of ca. 13 %. (The wind speed variances per bin were available.)
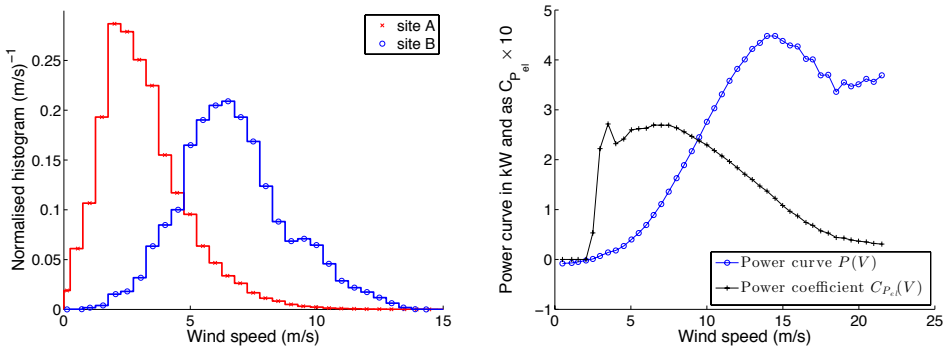
Figure 4.3: The normalised histograms (left) for site A (x) and B (o); and the turbine's power curve (right) in terms of power (blue o) and 10 × the power coefficient (black x) as a function of wind speed.

To have a benchmark, we re-sample the wind speed measurements to 1 minute intervals. This results in a set of wind speed samples (every sample is an average over $60 \times F_s$ values), as well as the corresponding variance within that sample. The power curve is then corrected for the difference in variance between sites A and B and the site where the power curve was determined (hereafter named test site), according to Eq. 4.20, which is derived in section 4.3, following Borg et al. (1986) but in the notation of this dissertation. Since the power curve was originally determined at the test site with 1 minute averages, we will use the mean power calculated with this power curve corrected for the variance at sites A and B *at 1 minute averaging time* as the benchmark estimate.

To investigate the influence of the averaging time, we then re-sampled the data of sites A and B to averaging times τ varying from two minutes to two hours. The mean power is then calculated twice, one time with the original power curve (thus without compensating for the variance), and once with the correction by Eq. 4.20 applied (even though then the averaging time differs between the wind speed and the power curve). The results for
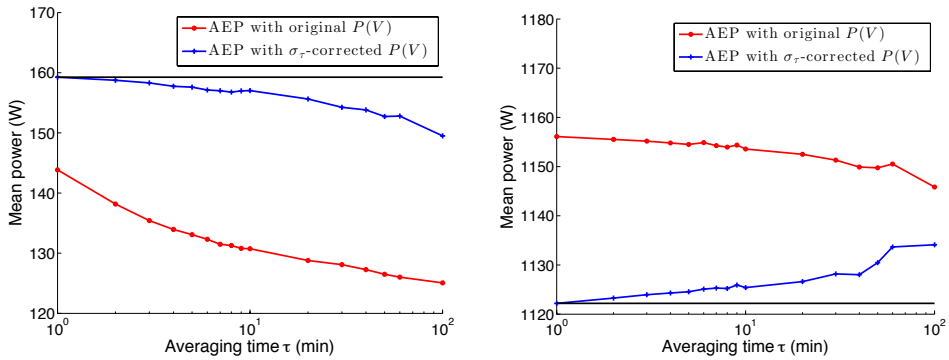
Figure 4.4: Mean-power estimate as a function of the averaging time used. The line with stars shows the estimates with the original power curve (no correction), while the line with pluses shows the estimates with corrected power curve. Site A is left, site B right.

site A and B are printed in Figure 4.4.

As can be expected, when the original power curve is used without correction, the curve is shifted; for a theoretical power curve with a fixed power coefficient, the shift is always upwards when variance of the installation site (in this context site A or B) is lower than that of power curve test site, and downwards when the variance is higher. (For a power curve with a power coefficient that varies with wind speed, the behaviour is more subtle, as is shown in section 4.3.) Also, the slope of the uncorrected curve in Figure 4.4 is negative. This reflects the apparent loss in power when the averaging time increases (and the variance decreases) but the power curve is not compensated. However, when the power curve is corrected with the variance, the downward slope is smaller (site A) or even reversed (site B). It appears that the power-curve compensation for averaging time based on the variance improves the estimate of the mean power, especially for the lower values of τ. Yet the effect is only a matter of a few percent, and the compensation still leaves a residual difference (the line with the pluses still diverges from the horizontal benchmark). The offset in the estimated power between the corrected and uncorrected power curve is much larger (up to almost 20 % for site A with a high turbulence intensity) than the variation over increasing averaging times (i.e. the difference between points along the curves).

4.2.2 A practical alternative: compensation based on short-term measurements

In practice one often has wind speed data available that have been measured with averaging times that are larger than the one used for the derivation of the power curve. In that case, it is impossible to re-sample the data to obtain the variance to compensate the power curve. In this section we therefore discuss an alternative approach, in which the variances are approximated through statistical means, based on the power spectral density (PSD) of the site. It turns out that the change in variance when the averaging time varies is directly related to the power spectral density. More precisely, the average of the variances of all the sampled wind speeds, $\overline{\sigma_\tau^2}$, is a direct function of the PSD:

$$\overline{\sigma_\tau^2} = \lim_{\varepsilon \to 0} \int_\varepsilon^\infty S_V(f) \left[1 - |H_\tau(f)|^2 \right] \, \mathrm{d}f \tag{4.2}$$

where $S_V(f)$ is the PSD and $H_\tau(f)$ the power spectrum of a τ-wide interval. The derivation is shown in section 4.3, where we have combined expressions from Borg et al. (1986) and Bendat and Piersol (1971) to arrive at Eq. 4.2. The power spectral density functions for sites A and B are shown in Figure 4.5.
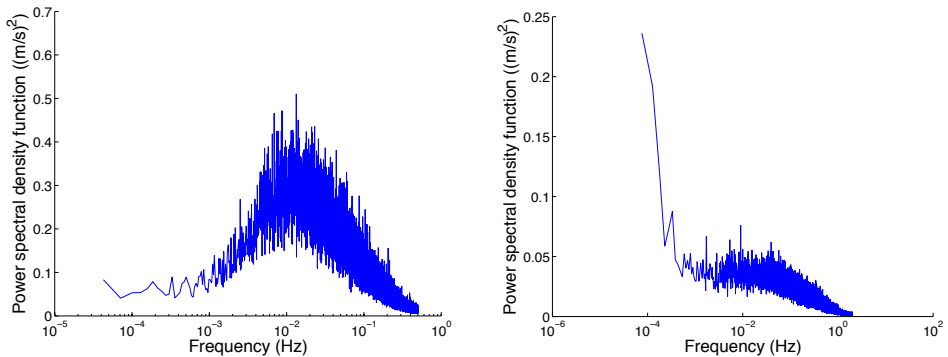
Figure 4.5: The power spectral density function plotted in area-preserving form, that is $f \cdot S_V(f)$, as a function of the frequency in Hz. (The frequency of 1 day is about $1.16\mathrm{e}^{-5}$ Hz; the peak thus reflects the diurnal variations.) Site A is left, site B right.

In general, random data (such as wind speed measurements) are fully described through a probability density function (pdf), a mean square

value, an autocorrelation function and a power spectral density function (PSD) (Bendat and Piersol, 1971). (For stationary data, the autocorrelation function and the PDF are Fourier pairs.) These functions and values are quite easily estimated for a wind speed data set, but especially the PSD requires a sufficiently-high sample frequency to capture the turbulence in the wind.

We therefore propose the following approach. Suppose one has long-term wind speed measurements (but no variances) sampled at an interval that does not correspond to that of the power curve. (Say one has one year of hourly data and a 1 minute power curve.) We suggest to perform an additional short-term measurement campaign of a few (representative) days but at a high sample frequency (say $F_s = 1$ Hz) to calculate the power spectral density of the site. Assuming that this PSD estimate is representative for the entire year (which is reasonable), then use this PSD to calculate the variance corresponding to averaging time of the long-term data (in our example, 1 hour). With this variance, correct the (1 minute) power curve as described before in 4.2.1, to obtain an accurate estimate of the mean power and thus the annual energy production for the site.

In this approach, two assumptions are required that will affect the accuracy. The first assumption has already been referred to: the PSD estimate based on the short measurement campaign should be representative of the true PSD of the site. The second assumption is that the ratio between the variance and the square of the wind speed does not vary with the wind speed. This assumption is often fulfilled in practice, see Borg et al. (1986) and Figure 4.2. With this ratio, we can approximate the variance per wind speed (or per bin) from the average variance that is obtained from equation 4.2:

$$\sigma_\tau^2 = V^2 \left(\frac{\overline{\sigma_\tau^2}}{\overline{V^2}} \right) \tag{4.3}$$

Figure 4.6 illustrates this new approach for the same data sets that were used in section 4.2.1. The PSD was calculated using the wind speed data before re-sampling. It is clear that the approximation of the variance by equations 4.2 and 4.3 can be used to compensate the power curve for inconsistent averaging times, with comparable accuracy as when using the variances directly (as in Section 4.2.1). Still, as before, the effect of the compensation is small (a few percent), certainly smaller than the difference between uncorrected and corrected for turbulence, and there remains a difference between the horizontal benchmark and the corrected AEP pre-
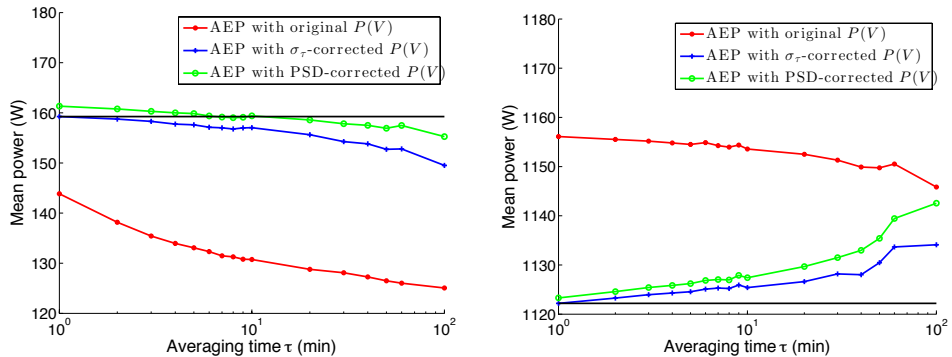
Figure 4.6: Mean power estimate as a function of the averaging time used. The lines with stars and pluses are exactly the same as in Figure 4.4 for easy comparison. The line with circles shows the estimate with the power curve corrected from the power spectral density function. Site A is left, site B right.

diction.

It seems that correcting the power curve for turbulence is always warranted: the AEP prediction decreases (almost monotonically) for increasing averaging time when the power curve is not compensated, even though the wind conditions (and thus the AEP) do not change, only the time over which the samples are averaged. It also seems that basing this correction on a high-sample-frequency measurement campaign of a few days is comparable to using the true (but generally unknown) variances directly (compare circles and pluses in Figure 4.6), which is our main contribution. But it remains unclear whether this correction (using the variances or via the PSD) yields a more accurate AEP estimate, given the residual difference between the prediction and the horizontal benchmark. Yet, it should be noted that the value we used as benchmark (wind and power curve both at 1 minute averaging time) is also uncertain; the true AEP for these data is unknown.

4.3 Theoretical derivation of the power curve compensation

The goal of this section is first to show, when wind speed measurements $V = V(t)$ are averaged over an averaging time of τ, the relation between the variance within every sample, σ_τ^2, and the variance over all the τ-averaged samples, s_τ^2. Next we show how the variance σ_τ^2 can be used to correct

the power curve (as is done for turbulence). We then show how σ_τ^2 can be approximated from the PSD. In this way, this section provides a technical framework to appreciate the effect of averaging time on the turbulence and thus on the AEP prediction.

4.3.1 Introduction: the power spectral density function

The power spectral density function (PSD) describes the power density of a random signal as a function of frequency. Since the power of a signal is given by the mean square value (Bendat and Piersol, 1971),

$$\Psi_V^2 = \lim_{T \to \infty} \frac{1}{T} \int_0^T V^2(t) \, dt \qquad (4.4)$$

the power density can be interpreted as the mean square value of this signal filtered by a narrow passband filter with centre frequency f and bandwidth Δf, divided by Δf:

$$S_V(f) = \lim_{\Delta f \to 0} \frac{\Psi_V^2(f, \Delta f)}{\Delta f} = \lim_{\Delta f \to 0} \frac{1}{\Delta f} \lim_{T \to \infty} \frac{1}{T} \int_0^T V^2(t, f, \Delta f) \, dt \quad (4.5)$$

where $V(t, f, \Delta f)$ denotes the filtered signal and $\Psi_V^2(f, \Delta f)$ its mean square value. Conversely, from the power density, the mean square value can be found as:

$$\Psi_V^2 = \int_0^\infty S_V(f) \, df \qquad (4.6)$$

The variance of a random signal can be obtained as well from the PSD, because it is directly related to the mean square value:

$$\sigma_V^2 = \lim_{T \to \infty} \frac{1}{T} \int_0^T [V(t) - \mu_V]^2 \, dt = \Psi_V^2 - \mu_V^2 \qquad (4.7)$$

with μ_V the mean of $V(t)$. (Note that for zero mean signals, $\Psi_V^2 = \sigma_V^2$, and Eq. 4.6 can be used to calculate σ_V^2.)

In practice, for non-zero mean random signals (as in our case with wind speed), one cannot use Eq. 4.6 directly to calculate the variance. One option is to subtract the mean value from the random signal before calculating the PSD:

$$V_{\text{new}}(t) = V(t) - \mu_V \qquad (4.8)$$

and to work with that. The alternative approach starts by appreciating that a non-zero mean of $V(t)$ will appear in the PSD as a Dirac pulse at

zero frequency (Bendat and Piersol, 1971). (Indeed, the spectral density of a constant signal is a Dirac pulse at zero frequency.) In this case, equation 4.6 needs to be evaluated as:

$$\sigma_V^2 = \lim_{\varepsilon \to 0} \int_\varepsilon^\infty S_V(f)\,\mathrm{d}f \tag{4.9}$$

i.e. by avoiding the Dirac pulse of the mean at zero frequency.

4.3.2 Relation between variance within and over the averaging time

We start from wind speed data measured with a sample frequency of F_s (Hz), where we assume that $F_s >> 1/\tau$ (to ensure that re-sampling from F_s to $1/\tau$ is statistically sound).

When wind measurements are averaged over a period τ and then stored, this corresponds to filtering the signal $V(t)$ with a rectangular window $h_\tau(t)$ (a so-called boxcar function) of width τ:

$$V_\tau(t) = V(t) * h_\tau(t) \tag{4.10}$$

where $h_\tau(t)$ is $1/\tau$ when $-\tau/2 < t < \tau/2$ and 0 elsewhere; $*$ denotes the convolution operation. The PSD of the τ-averaged (filtered) signal is easily found as the product of the original PSD and the square of the filter spectrum $H_\tau(f)$, the well-known sinc-function:

$$H_\tau(f) = \frac{\sin(\pi f \tau)}{\pi f \tau} \tag{4.11}$$

It follows that the variance of the τ-averaged wind speed samples, s_τ^2, and the average variance within every sample, $\overline{\sigma_\tau^2}$, can be calculated as:

$$s_\tau^2 = \lim_{\varepsilon \to 0} \int_\varepsilon^\infty S_V(f)|H_\tau(f)|^2\,\mathrm{d}f, \tag{4.12}$$

$$\overline{\sigma_\tau^2} = \lim_{\varepsilon \to 0} \int_\varepsilon^\infty S_V(f)\left[1 - |H_\tau(f)|^2\right]\,\mathrm{d}f. \tag{4.13}$$

Thus, for increasing τ, the variance of the data set s_τ^2 decreases, as the filter cuts a larger (high-frequency) part of the PSD away. This reflects common sense: when averaging over longer intervals, rare and short (i.e. high-frequency) occurrences of very low and very high wind speeds are lost, and the data have a lower variance.

The variance within the τ-averaged interval however increases. Also this is reasonable: as longer intervals are used, we can expect more variability to be captured within the interval.

4.3.3   Power curve correction for variance

This part reprints the derivation in Borg et al. (1986) for clarity and completeness.

Suppose a true power curve $P(V)$ is measured at a given site, and that a specific part of the measurements is isolated where the wind speed is fairly constant (say, within one bin) with mean value $\overline{V}$ and variance σ_V^2. (This will in practice be done for a given τ of 1 minute or 10 minutes, but this is of no concern for the current derivation.) We define the fluctuations around the mean values as

$$\Delta V(t) = V(t) - \overline{V} \tag{4.14}$$

$$\Delta P(t) = P(t) - \overline{P} \tag{4.15}$$

A Taylor series expansion of the power at wind speed $V(t)$ is:

$$P(\overline{V} + \Delta V(t)) = P(\overline{V}) + \frac{\mathrm{d}P(\overline{V})}{\mathrm{d}V}\Delta V(t) + \frac{\mathrm{d}^2 P(\overline{V})}{\mathrm{d}V^2}\frac{(\Delta V(t))^2}{2} + \mathcal{O}(3) \tag{4.16}$$

where $\mathcal{O}(3)$ refers to the error made by stopping after the second order term; the higher-order terms are usually negligible (Borg et al., 1986).

Rearranging and using primes to denote the derivations, the power is given by

$$P(\overline{V} + \Delta V(t)) = P(\overline{V})\left[1 + \frac{P'(\overline{V})}{P(\overline{V})}\Delta V(t) + \frac{P''(\overline{V})}{P(\overline{V})}\frac{(\Delta V(t))^2}{2}\right] \tag{4.17}$$

so that the mean power reduces to

$$\overline{P(V)} = \overline{P(\overline{V} + \Delta V(t))} = P(\overline{V})\left[1 + 0 + \frac{P''(\overline{V})}{P(\overline{V})}\frac{\sigma_V^2}{2}\right] \tag{4.18}$$

since $\overline{\Delta V(t)} = 0$ per definition (see equation 4.15). Thus, the averaged power measurement is artificially high, and this is proportional to σ_V^2.

Introducing the power coefficient, $C_{P_{el}}(V)$,

$$P(V) = \frac{1}{2}\rho V^3 S C_{P_{el}}(V) \tag{4.19}$$

with ρ the air density and S the rotor surface, and after some calculus, we find that

$$\overline{P(V)} = P(\overline{V})\left[1 + 3\frac{\sigma_V^2}{\overline{V}^2}\left(1 + \overline{V}\frac{C'_{P_{el}}(\overline{V})}{C_{P_{el}}(\overline{V})} + \frac{\overline{V}^2}{6}\frac{C''_{P_{el}}(\overline{V})}{C_{P_{el}}(\overline{V})}\right)\right] \tag{4.20}$$

If $C_{P_{el}}(V)$ were constant, this reduces to

$$\overline{P(V)} = P(\overline{V}) \left[1 + 3\frac{\sigma_V^2}{\overline{V}^2}\right] \tag{4.21}$$

This is too simplified for a good power curve correction. It does however provide some insight in the apparent available power in the wind: divide equation 4.21 by $C_{P_{el}}\rho S/2$, and equation 4.21 boils down to equation 4.1.

In order to evaluate $C_{P_{el}}(V)$ and its first and second derivatives in equation 4.20, we fitted a cubic polynomial through $C_{P_{el}}(V)$. There is no a priori best choice for the order (a second order polynomial was used in Borg et al. (1986)); it depends on the power coefficient of the turbine under study.

Equation 4.20 allows to correct the measured power $\overline{P(t)}$ to the true power $P(\overline{V})$ of the turbine at wind speed $\overline{V}$, provided that the variance σ_V^2 is known. When the wind speed variance at a turbine installation site is known, the power curve can be adapted accordingly to provide a better estimate of the mean power to be expected at the site.

4.3.4 Practical calculation of the variance

For a given wind speed data set of total length T sampled at a frequency of F_s (thus $T_s = 1/F_s$ is the sample period), a raw estimate of the power spectral density function $\widetilde{S_V(f_k)}$ is found as (Bendat and Piersol, 1971):

$$\widetilde{S_V(f_k)} = \frac{2T_s}{N}|\widehat{V}(f_k)|^2 \tag{4.22}$$

where $\widehat{V}(f_k)$ is the discrete Fourier transform of the sampled wind speed $V(nT_s)$ at frequency $f_k = k/T$, with $k = 0, 1, \ldots, N-1$ and N the number of samples ($N = TF_s$).

The variances from equations 4.13 and 4.12 can then be approximated as

$$s_\tau^2 \approx \int_{f_1}^{f_{N/2-1}} \widetilde{S_V(f_k)}|H_\tau(f_k)|^2 \, \mathrm{d}f_k \tag{4.23}$$

$$\overline{\sigma_\tau^2} \approx \int_{f_1}^{f_{N/2-1}} \widetilde{S_V(f_k)} \left[1 - |H_\tau(f_k)|^2\right] \, \mathrm{d}f_k \tag{4.24}$$

where f_1 denotes the second frequency ($k = 0$ is the first), and $f_{N/2-1}$ the Nyquist frequency. We numerically calculated the integral using the

trapezoidal rule. (Note that our equation 4.24 deviates from equation (A.9) in Borg et al. (1986), where the influence of the total measurement time limit was erroneously introduced as a multiplication; it should have been a convolution. The result of this convolution is already in our $\widetilde{S_V(f_k)}$.)

Finally, the variance to calculate the power curve correction according to equation 4.20 is obtained by assuming that the ratio of the variance to the square of the wind speed is constant:

$$\sigma_\tau^2 \approx V^2 \left(\frac{\overline{\sigma_\tau^2}}{\overline{V^2}} \right) \tag{4.25}$$

4.4   Conclusions

In this chapter, we show that an inconsistent averaging time between the wind speed and power curve measurement leads to a systematic error of the mean power prediction. This effect seems to be related to the effect of turbulence. When the averaging time increases, more and more variability of the data is averaged out of the data, the histogram is more concentrated around the mean, and apparently the power available in the wind decreases.

Yet this decrease in variance in the wind corresponds to an increase of the variance of the individual wind speed samples. We have tested whether it is possible to correct the power curve for this higher variance, in the same way as one can correct for a site with a high turbulence level. (Indeed, the variance here should be seen as an extrapolation of the turbulence level, the only difference being that turbulence as such refers to relatively high-frequency variability in the wind. The variance taken into account here represents the variability with shorter periods than the averaging time, which can be as large as one hour.)

We have shown for two sites how the mean power varies as a function of averaging time, and how compensated power curves yield a closer prediction of the turbine output. This approach is also extended towards practical resource assessment campaigns, with comparable accuracy as when the variance data are directly available. When long term low frequency measurements are complemented with a short term campaign at a high sample frequency, one can derive the power spectral density of the wind at the site and use this to predict the variance level at the averaging time of the long term campaign. However, it seems that our correction of the variance as related to the averaging time only partially compensates the AEP prediction. Whether this prediction of AEP is better remains uncertain, as the

true AEP for our wind measurement data and turbine choice is unknown.

Chapter 5

Feasibility of small and medium-sized wind turbines in rural areas

Abstract—*The objective of this chapter is threefold. First, it aims to quantitatively assess the feasibility of small and medium-sized wind turbines in rural areas in Flanders and Wallonia. Second, it illustrates how the methods and techniques from Chapters 2, 3 and 4 are applied in practice. Third, it identifies key handles that ultimately decide whether a project will be feasible and successful or not.*

This chapter provides an assessment of the (economic) wind potential (Sections 5.1 and 5.2), of the socio-political and legal context (Sections 5.3 and 5.4), as well as three detailed case studies (Section 5.5 to 5.7).

We show that under the right conditions, SMWTs are a viable source of sustainable electricity in rural areas in Belgium. More generally we identify the key handles to realise successful SMWT projects in rural areas with moderate wind speeds.

5.1   The wind resources in Flanders

To study the wind potential for small and medium-scale wind energy in rural areas in Flanders and Wallonia, we have assessed the wind resources at 18 different sites. We used meteorological data (purchased from the Belgian Royal Meteorological Institute, RMI) and we performed five wind speed measurement campaigns ourselves at different locations throughout Flanders, to ensure a good geographical spread over the region. In Figure 5.1, all measurement locations are indicated on a map of Flanders. In Figure 5.2, some photographs illustrate three measurements stations from the RMI and one of our own.

Figure 5.1: Measurement sites indicated on a map of Flanders.

All stations are located in rural (or semi-rural) areas where the wind flow is in general little disturbed. The meteorological data are measured at 10 m while our own measurements were performed typically at 15 m (maximum hub height for small wind turbines in Flanders (Van Mechelen and Crevits, 2009)). To estimate the wind potential for small as well as for medium wind turbines, the wind speeds have been extrapolated where necessary using aerodynamic roughness parameters. For the sites where the wind speeds were only measured at one height, the roughness parameters have been estimated based on tables available in the literature (Wieringa, 1992).

Figure 5.2: Three measurement stations of the RMI (Royal Meteorological Institute, 2014): Beitem (top left), Diepenbeek (top right), Zeebrugge (bottom left). Measurement setup of our own measurement station in Wachtebeke (bottom right).

5.1.1 Description of our wind measurement campaigns and the meteo data

The meteorological data, purchased from the RMI, represent the wind speed of the year 2011 at 10 m height. For each measurement site, hourly averaged wind speed and wind direction data were collected. The resolution of the anemometers and wind vanes is not identical for all sites. For Deurne, Kleine-Brogel, Koksijde, Middelkerke, Semmerzake and Zaventem the resolutions of the anemometer and wind vane are respectively 1 m/s and 10°. For the other measurement stations (Beitem, Diepenbeek, Melle, Retie, Sint-Katelijne-Waver, Zeebrugge and Zelzate) the resolution for the anemometer is 0.1 m/s, for the wind vane 1°.

Our own wind measurements have been collected between 2010 and 2014, using different measurement periods. An overview of our measurement campaigns is given in Table 5.1. Our typical measurement set-up consists of a top anemometer installed at 15 m, a wind vane mounted 1.5 to 2.5 m lower (this height is derived from the IEC standards (IEC, 2006) according to the size and shape of the booms to mount both sensors). Usually a second anemometer was installed at 10-12 m, to estimate the roughness characteristics of the terrain. Only for Dilbeek, a single measurement height was used to measure the wind speed and wind direction. The cup anemometer and wind vane were both mounted at 15 m there. For Aarschot, we were asked by the province of Vlaams-Brabant to study the feasibility of small and medium wind turbines. The wind speed was therefore measured at slightly larger heights. The wind speed was measured at 30 and 20 m, the wind direction at 26 m. The equipment was installed on a lattice tower. Due to the structure of the mast, the wind speed is measured at both sides. For all sites, one-minute average wind speed and wind direction data were collected (as we recommended in Chapter 4). The resolution of the anemometers was 0.01 m/s and for the wind vane 0.1°. The accuracy of the used sensors fits the requirements for wind energy purposes (IEC, 2006). We have calibrated all anemometers in the VUB low-speed wind tunnel, which is officially certified for this purpose.

In Table 5.2, all the wind measurements have been gathered, together with the Weibull parameters calculated using the moment method (see Eq. (1.20) and Section 3.4).

To verify how well the data fit the predicted Weibull distribution, we derived the coefficient of determination R^2 for each data set. Only for Kleine-Brogel, the R^2 value is low. This is mainly caused by the fact that

Site	Duration	Period
Aarschot	3 months	July 2014-Oct 2014 (ongoing)
Dilbeek	25 months	Apr. 2010-May 2012
Haacht	3 months	Oct. 2011-Dec. 2011
Ranst	15 months	March 2012-May 2013
Wachtebeke	11 months	Aug. 2012-Jun. 2013

Table 5.1: Measurements periods of our own collected wind data in Flanders.

these data contain lots of zero wind speeds (13 % of the time) and as we mentioned in Section 3.4, the Weibull distribution can not cope with high probability of very low wind speeds.

For the meteorological stations and for Dilbeek, the roughness parameters are estimated using the terrain information and roughness tables (Wieringa, 1992). If no terrain information was available, we used a standard value of 0.15 m, since meteorological stations are generally located in open areas. The meteorological station in Zeebrugge is on a pier in the North Sea and therefore the roughness length is much lower (we used 0.0002 m). For Aarschot, Haacht, Ranst and Wachtebeke, we calculated the roughness length according to the procedure outlined in Section 1.3 (more specifically Eq. (1.8) based on the log law), since we measured at two heights.

The table clearly shows the dominance of the southwest wind direction. Only for Haacht, the dominant wind direction is north, mainly caused by the short measurement period (of just 3 months). These data show that the average wind speed near the coastal regions (Koksijde, Middelkerke, Zeebrugge) is higher than the rest of Flanders as expected. Relatively high values for the average wind speed can be found in other regions in Belgium (Zelzate, Zaventem and Deurne) if we take into account that the wind speeds are measured at just 10 m high.

5.1.2 Flanders' long-term wind potential

To normalise these data (i.e. to compensate for normal variations with respect to the climatological average), we applied the variance ratio MCP procedure (according to our conclusions from Chapter 3). Thirty two meteorological stations from the KNMI are used as a reference site. For each measurement station (in Flanders) and each reference station, the correlation coefficient r for the concurrent measurement period is derived. The

| Site | z_0 | z | $\overline{V}$ | Dominant wind | k | c | R^2 |
	[m]	[m]	[m/s]	direction			
Aarschot	0.16	30	2.8	SW	1.793	3.141	0.9994
Beitem	0.25	10	3.8	SW	1.961	4.271	0.9962
Deurne	0.15	10	3.6	SW	1.917	4.091	0.9953
Diepenbeek	0.1	10	2.9	SW	1.632	3.267	0.9831
Dilbeek	0.25	15	2.6	S	1.403	2.889	0.9572
Haacht	0.36	15	3.0	N	1.472	3.284	0.9844
Kl-Brogel	0.1	10	3.1	SW	1.406	3.383	0.8491
Koksijde	0.15	10	4.7	SW	1.810	5.325	0.9765
Melle	0.25	10	3.4	SW	1.842	3.870	0.9722
Middelkerke	0.15	10	4.9	S	1.961	5.545	0.9899
Ranst	0.04	15	2.8	SW	1.795	3.168	0.9969
Retie	0.1	10	2.7	SW	1.709	2.985	0.9962
Semmerzake	0.15	10	3.3	SW	1.689	3.658	0.9575
St-Kt-Waver	0.15	10	3.2	SW	1.816	3.558	0.9974
Wachtebeke	0.39	15	2.6	S	1.793	2.996	0.9975
Zaventem	0.1	10	3.7	SW	1.723	4.143	0.9879
Zeebrugge	0.0002	10	6.1	SW	2.407	6.848	0.9920
Zelzate	0.5	10	3.5	SW	2.099	3.923	0.9798

Table 5.2: General results of the measurements performed in Flanders.

station with the highest correlation coefficient was selected. The measurement period of the long-term climatological data is from 1 January 1994 to 31 December 2013. These data thus represent the wind speed over a period of the last 20 years.

In Table 5.3, the results are shown. The correlation coefficients range from approximately 0.77 to 0.89, even though the distances between the sites is sometimes over 100 km. Considering the conclusions that have been made in Section 3.6, we emphasise the uncertainty for the average wind speeds for Aarschot and Haacht as the measurement period was limited to just 3 months.

This table indicates that our measurements have been performed over a period with slightly lower wind speeds than the 20 year average.

Measurement Site	Reference Site	r	$\overline{V}_{\text{Measured}}$ [m/s]	$\overline{V}_{\text{Long-term}}$ [m/s]	z [m]
Aarschot	Maastricht	0.7894	2.8	3.8	30
Beitem	Westdorpe	0.8623	3.8	4.0	10
Deurne	Westdorpe	0.8386	3.6	3.8	10
Diepenbeek	Eindhoven	0.8281	2.9	3.1	10
Dilbeek	Eindhoven	0.7724	2.6	2.8	15
Haacht	Eindhoven	0.8878	3.0	3.0	15
Kl-Brogel	Eindhoven	0.8650	3.1	3.2	10
Koksijde	Wilhelminadorp	0.8318	4.7	4.9	10
Melle	Westdorpe	0.8655	3.4	3.6	10
Middelkerke	Wilhelminadorp	0.8413	4.9	5.0	10
Ranst	Woensdrecht	0.7921	2.8	2.9	15
Retie	Eindhoven	0.8555	2.7	2.8	10
Semmerzake	Westdorpe	0.8574	3.3	3.4	10
St-Kt-Waver	Eindhoven	0.8521	3.2	3.3	10
Wachtebeke	Westdorpe	0.8012	2.6	2.6	15
Zaventem	Westdorpe	0.8223	3.7	3.9	10
Zeebrugge	Vlissingen	0.8229	6.1	6.0	10
Zelzate	Westdorpe	0.8602	3.5	3.7	10

Table 5.3: Results of the VR MCP method for the measurement sites in Flanders.

5.1.3   Wind Map of Flanders

We now use these wind data to produce two wind maps for Flanders: one at 15 m (the restricted hub height of small wind turbines in Flanders) and one at 30 m (a typical hub height for medium wind turbines). As these wind data are collected at different heights, we use the log law (Section 1.3) to extrapolate the wind data (or downscale the wind data for Aarschot). We note that for the extrapolation to 30 m, we deviate from our own recommendations made in Chapter 3 and violate the 2/3 rule. However, by extrapolating to 30 m, we can have at least have a rough idea about the wind situation for medium-sized wind turbines.

In Figures 5.3 and 5.4, these wind maps are shown. On each site the local average wind speed is indicated. What is clear from the wind map is that the largest wind speeds are found in the western part of Flanders, although in specific regions in the middle of Flanders there seems to be a potential for small- and medium-scale wind.
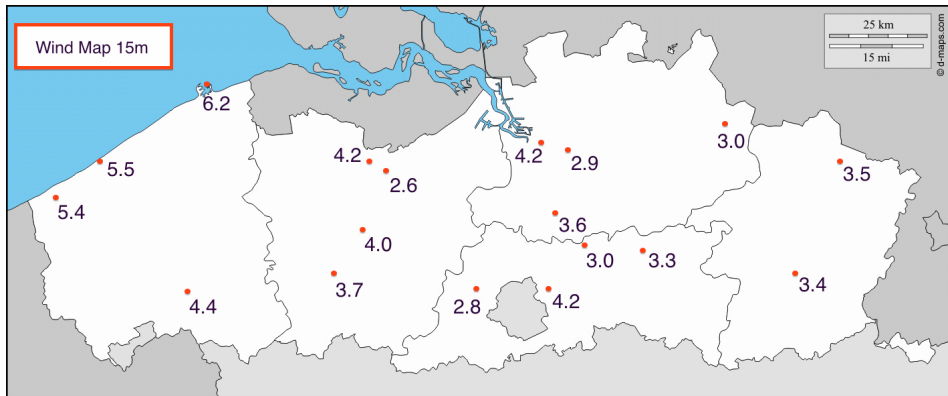
Figure 5.3: Wind map of Flanders at 15 m height.

Although such a wind map of Flanders is already present in the literature (Cabooter, Dewilde, and Langie, 2000), the presented wind maps are unique in that they indicate the very local long-term wind speeds at low heights. As this wind map represents measured data at low height, the wind map can be used to extrapolate the wind data (in combination with the roughness parameters in Table 5.2) to any desired hub height for small-scale wind energy. The wind map made by Cabooter, Dewilde, and
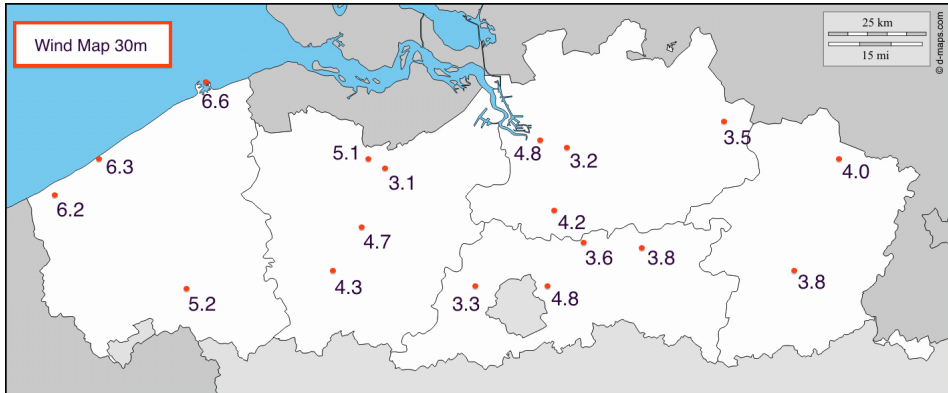
Figure 5.4: Wind map of Flanders at 30 m height.

Langie (2000) (Figure 5.2) only shows the regional wind speeds at 75 m and is therefore more directed to large-scale wind energy. When we compare these wind maps, the global trend of high wind speeds near the coastal region are indeed visible though the relatively high local wind speed in the centre of Flanders (such as Zaventem, Deurne and Zelzate) could not be identified from the map at higher altitudes.

5.2 Economic feasibility of SMWT in Flanders based on reliable AEP estimates

To study the economic feasibility of small and medium wind in Flanders, we selected the most appropriate turbines from our database, predicted the annual energy production (along the lines of Chapter 3), and then translated these AEP estimates into economic parameters. The conclusions of this study are specific for Flanders, as some determining factors (electricity price, financial incentives) are region-dependent.

Again it is important to note that, in order to provide a comprehensive and instructive conclusion, we have had to deviate from our own recommendations in Chapter 3. The long-term wind measurement data were obtained at 10 or 15 m height; which is too low for some of the appropriate turbines in our assessment. (For some turbines, the blades would hit the ground if the hub would be mounted at 10 m.) Therefore, we always used the hub height recommended by the manufacturer, and thus extrapolated from
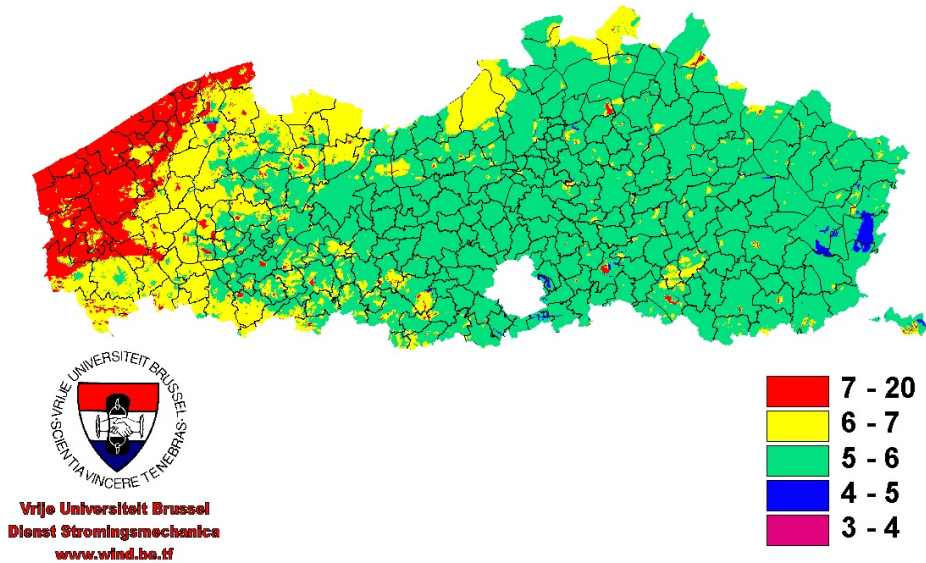
Figure 5.5: Wind map of Flanders at 75 m height (Cabooter, Dewilde, and Langie, 2000).

the measurement height to this height, even if we violated the 2/3 rule. We acknowledge that the so-obtained conclusions do have a large uncertainty bound[1]; yet we believe that in doing so we can provide a reasonable overview of the economic feasibility of both small and medium-sized wind turbines in Flanders.

5.2.1 Selection of the sample wind turbines

We restricted our list of viable turbines to those with a power curve measured by an independent test facility, and for which the investment cost is known. In Table 5.4, the database used for this feasibility study is presented. For each turbine, the rotor diameter, rated power (according to the BWEA standards (RenewableUK, 2014)) and hub height are listed.

As a next step in the selection process, the measured wind speeds are extrapolated to the corresponding hub height for each wind turbine. Us-

---

[1]Using the procedure presented in Section 3.5.1, we estimated the uncertainty on the AEP at 65.1 %. For this prediction, we assumed that the accuracy of the roughness parameters is 30 % and the measurement error on the wind speed is 0.1 m/s

Turbine	Rated Power [kW]	Rotor-diameter [m]	Hub height [m]
1	2.2	3.7	12
2	3.2	4.1	15
3	3.2	4.4	12
4	4.7	5.5	18
5	5.6	5.5	15
6	5.7	6.3	14
7	9.1	7.2	25
8	9.2	6.4	18
9	9.7	9	18
10	9.8	8	18
11	10.1	13.2	18
12	15.7	10.2	24
13	40.4	15	30.5
14	56.8	19.2	36

Table 5.4: Database of tested small and medium wind turbines wherefore the investment cost is known. The rated power is determined according to the BWEA standards.

ing these data, the annual energy production is estimated. Rather than determining the payback period and internal rate of return, the LCOE is determined for each case as it is a simple measure to compare the on-site performance of each turbine. We then averaged the LCOEs over all the measurement sites, to obtain the mean performance of the turbines in Flanders (as we use the wind data of Flanders). This is shown in Figure 5.6. From this comparison, eventually four wind turbines are selected. Each number on the abscissa represents the turbine in Table 5.4. As the turbines are ranked according to their rated power, each trough in the figure then represents the best turbine within a particular power range. The four selected turbines are the numbers 3, 7, 11 and 14 in the figure which have rated powers between 3 kW and 60 kW.

5.2.2 Long-term annual energy production

As stated before, we used the long-term wind data and extrapolated these to the hub heights of the four turbines: 12, 18, 25, and 36 m, using the log
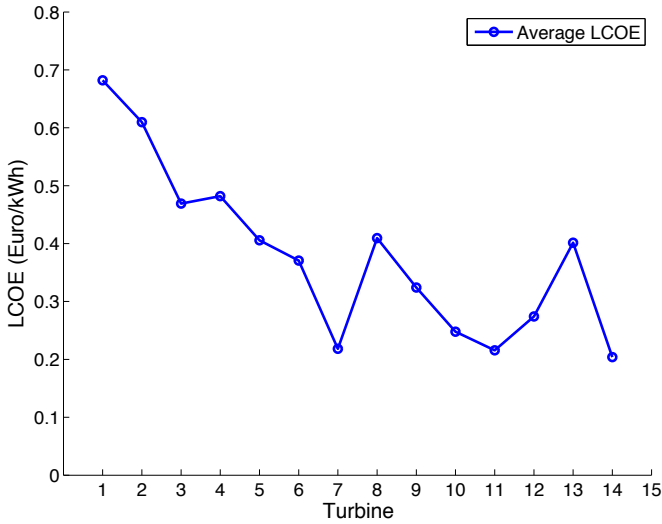
Figure 5.6: Average LCOE for each turbine in the database. The LCOEs are averaged over the measurement sites used to select four small wind turbines.

law (Eq. (1.4)):

$$V(z) = V_{\text{ref}} \frac{\ln\left(\frac{z}{z_0}\right)}{\ln\left(\frac{z_{\text{ref}}}{z_0}\right)} \tag{5.1}$$

where V_{ref} is the available wind speed measurement and z_{ref} the measurement height (listed in Table 5.2). The roughness lengths were derived based on the specifications of the terrain and roughness tables. In Table 5.6, the extrapolated average wind speed is shown for each of the hub heights used in this study. It is important to note that we excluded the sites of Haacht and Aarschot as the measurement period is too low to make a reliable prediction of the AEP.

Combining these extrapolated wind data and the power curves of the wind turbines, the annual energy production is estimated using the direct use of data approach (see Chapter 3). These results are presented in Table 5.6. As we either used 20 year data or applied MCP to normalise with these data, the results represent the AEP over the full expected lifetime of the wind turbine. A percentage of 5 % of the AEP is subtracted afterwards, to take into account the potential energy loss of the turbine (for maintenance or stand still due to errors). The AEPs are then used as an

	$\overline{V}_{\text{Long-term}}$	z_0	$\overline{V}_{12}$	$\overline{V}_{18}$	$\overline{V}_{25}$	$\overline{V}_{36}$
		Length				
	[m/s]	[m]	[m/s]	[m/s]	[m/s]	[m/s]
Beitem	4.0	0.25	4.2	4.6	5.0	5.3
Deurne	3.8	0.15	4.0	4.3	4.6	5.0
Diepenbeek	3.1	0.1	3.2	3.5	3.7	4.0
Dilbeek	2.8	0.25	2.6	2.9	3.1	3.4
Kl-Brogel	3.2	0.1	3.4	3.7	3.9	4.2
Koksijde	4.9	0.15	5.2	5.6	6.0	6.5
Melle	3.6	0.25	3.8	4.2	4.5	4.8
Middelkerke	5.0	0.15	5.2	5.7	6.1	6.6
Ranst	2.9	0.04	2.8	3.0	3.1	3.3
Retie	2.8	0.1	2.9	3.1	3.3	3.6
Semmerzake	3.4	0.15	3.5	3.8	4.1	4.4
St-Kt-Waver	3.3	0.15	3.5	3.8	4.0	4.3
Wachtebeke	2.6	0.39	2.4	2.7	3.0	3.2
Zaventem	3.9	0.1	4.0	4.4	4.6	4.9
Zeebrugge	6.0	0.0002	6.1	6.4	6.6	6.8
Zelzate	3.7	0.5	3.9	4.4	4.8	5.3

Table 5.5: 20-year averaged wind speed extrapolated to four different hub heights.

input for the economic analysis.

5.2.3 Discussion of the economic parameters

Investment cost The investment cost of each particular turbine is shown in Table 5.7. The purchase costs are based on quotations of the manufacturer. For the cost of the foundation and installation, an average cost is estimated based on the rated power of the turbine. The maintenance cost is estimated at 2 % of the purchase cost and the lifetime of the turbine is set at 20 years, as is customary.

Electricity Price The economic analysis is performed for private persons as well as SMEs. The energy consumption for private persons is set at 3 500 kWh/year while for SMEs an average energy consumption of 50 000 kWh/Year is used (VREG, 2014a). The average electricity price for private persons in Flanders is 18 c€/kWh according to the VREG (2014a). For

| Hub height | 12 m | 25 m | 18 m | 36 m |
| Turbine | T3 | T7 | T11 | T14 |
Site	[MWh/year]	[MWh/year]	[MWh/year]	[MWh/year]
Beitem	4.152	15.088	31.647	134.722
Deurne	3.795	13.061	28.623	117.060
Diepenbeek	2.314	7.798	19.490	73.163
Dilbeek	1.666	6.256	16.148	63.123
Kl-Brogel	3.062	10.124	22.649	90.011
Koksijde	6.915	22.649	40.613	180.787
Melle	3.392	12.303	26.775	112.097
Middelkerke	7.123	23.566	42.618	190.103
Ranst	1.498	5.322	14.930	54.775
Retie	1.501	5.118	14.501	51.780
Semmerzake	2.940	10.200	23.331	92.926
St-Kt-Waver	2.530	8.849	21.889	84.225
Wachtebeke	0.960	3.257	10.448	35.520
Zaventem	4.230	13.951	29.311	120.350
Zeebrugge	9.445	26.372	51.255	203.705
Zelzate	3.157	12.748	27.358	120.921

Table 5.6: 20-year annual energy production for the four wind turbines.

Turbine	T3	T7	T11	T14
Purchase	€15 000	€20 800	€53 000	€230 000
Installation and foundation	€4 000	€9 690	€15 858	€30 166
Maintenance cost	2 % of the purchase cost per year			

Table 5.7: Investment, maintenance and installation cost and lifetime of each wind turbine considered in the feasibility study.

SMEs, the average electricity price is 19 c€/kWh (VREG, 2014a). If more energy is produced by the wind turbine than consumed by the user, the electricity will be sold at a price of 4 c€/kWh (Mermuys, 2010).

Incentives In Flanders, the green certificates (GC) are used as incentive to support renewable energy technology. Before January 2013, a fixed amount of energy (1 MWh) had to be produced in order to receive such a certificate. Also a fixed minimum value was set dependent on the used

renewable technology.

Since January 2013, the minimum value was set at 97 € per GC independent on the type of technology. A bounding factor (bandingfactor) is then used to set up a distinction in the type of technology. This coefficient is recalculated each year for each particular technology. It determines the amount of energy that has to be produced to receive a GC. For wind energy, this coefficient is 0.796 (Vlaams Energie Agentschap, 2014), which means 97 € is granted for every 1 256 kWh. Compared to Brussels (see Chapter 6), this incentive can be used for 15 years instead of 10 years.

Additional incentives exist for SMEs. The 'ecologiepremie plus', 'VLIF' support or one-off investment deduction can be used for SME and they all have a similar effect on the economic results. In this feasibility study we assume a return of 25 % of the purchase cost of the turbine.

Other parameters The other economic parameters are set as follows:

- inflation of 2 %,

- increasing electricity price of 3.5 % each year and

- discount rate of 4 %.

These values are frequently used in feasibility studies (Mermuys, 2010).

5.2.4 Results

In Tables 5.8 to 5.10, the IRR, static and dynamic payback times are shown for each case. In the table, negative IRR are indicated with N/A as are payback times above 20 years with >20.

Using the economic parameters presented above, turbine 7 seems to be the best choice. In windy regions near the coast (Koksijde, Middelkerke and Zeebrugge), the dynamic payback time for SMEs is 4 to 5 years leading to an IRR of 25 to 30 %. Turbine 11 has similar results while for turbine 4 only the windiest regions can be exploited by an SME, at least for the current conditions in Flanders.

Although turbine 14 shows excellent figures in terms of LCOE (see Figure 5.6), with the applied economic parameters the investment is not profitable for most sites. The dynamic payback times are above 10 years (except for the coastal region). The main reason here is that most of the produced energy is not consumed but sold to the grid (at a lower electricity price).

For private users, only for a few combinations of wind turbines and sites, dynamic payback periods are below the lifetime of the turbine. The lack of a subsidy and the currently lower electricity price (as shown in Section 2 this price is expected to increase in the near future) are two of the causes. We emphasise that the values in the presented tables are strongly dependent on the applied economic parameters. Therefore, we perform a sensitivity analysis in the next section.

Site	SME [%]				Private [%]			
	T3	T7	T11	T14	T3	T7	T11	T14
Beitem	2.8	15.8	14.6	8.2	N/A	2.6	N/A	N/A
Deurne	1.6	13.1	12.8	6.8	N/A	1.2	N/A	N/A
Diepenbeek	N/A	5.1	6.6	3.1	N/A	1.2	N/A	N/A
Dilbeek	N/A	2.2	3.9	2.1	N/A	N/A	N/A	N/A
Kl-Brogel	N/A	9.0	8.9	4.6	N/A	N/A	N/A	N/A
Koksijde	10.5	24.9	19.7	11.6	1.9	7.1	2	2.3
Melle	0.10	12.1	11.6	6.4	N/A	0.7	N/A	N/A
Middelkerke	11.0	25.9	20.8	12.3	2.1	7.6	2.6	3.1
Ranst	N/A	N/A	2.8	1.3	N/A	N/A	N/A	N/A
Retie	N/A	N/A	2.4	1.0	N/A	N/A	N/A	N/A
Semmerzake	N/A	9.1	9.3	4.8	N/A	N/A	N/A	N/A
St-Kt-Waver	N/A	6.9	8.3	4.1	N/A	N/A	N/A	N/A
Wachtebeke	N/A	N/A	N/A	N/A	N/A	N/A	N/A	N/A
Zaventem	3.1	14.3	13.2	7.1	N/A	1.8	N/A	N/A
Zeebrugge	16.2	29.1	25.0	13.2	4.4	9.1	5.0	4.2
Zelzate	N/A	12.7	12.0	7.1	N/A	1.0	N/A	N/A

Table 5.8: Internal rate of return for each site and turbine. Not applicable (N/A) is used for values below 0.

Site	SME [Years]				Private [Years]			
	T3	T7	T11	T14	T3	T7	T11	T14
Beitem	>20	7	8	11	>20	20	>20	>20
Deurne	>20	9	9	13	>20	>20	>20	>20
Diepenbeek	>20	16	14	>20	>20	>20	>20	>20
Dilbeek	>20	19	>20	>20	>20	>20	>20	>20
Kl-Brogel	>20	12	12	16	>20	>20	>20	>20
Koksijde	10	5	6	9	>20	12	>20	17
Melle	>20	9	10	13	>20	>20	>20	>20
Middelkerke	10	5	6	9	>20	11	18	15
Ranst	>20	>20	>20	>20	>20	>20	>20	>20
Retie	>20	>20	>20	>20	>20	>20	>20	>20
Semmerzake	>20	11	11	15	>20	>20	>20	>20
St-Kt-Waver	>20	13	12	17	>20	>20	>20	>20
Wachtebeke	>20	>20	>20	>20	>20	>20	>20	>20
Zaventem	>20	8	9	12	>20	>20	>20	>20
Zeebrugge	7	4	5	8	15	10	13	14
Zelzate	>20	9	9	12	>20	>20	>20	>20

Table 5.9: Static payback time for each measurement site and turbine. When the payback time is above the lifetime of the turbine, it is replaced with >20.

Site	SME [Years]				Private [Years]			
	T3	T7	T11	T14	T3	T7	T11	T14
Beitem	>20	8	8	13	>20	>20	>20	>20
Deurne	>20	9	10	14	>20	>20	>20	>20
Diepenbeek	>20	18	15	>20	>20	>20	>20	>20
Dilbeek	>20	>20	>20	>20	>20	>20	>20	>20
Kl-Brogel	>20	12	13	19	>20	>20	>20	>20
Koksijde	11	5	6	9	>20	14	>20	>20
Melle	>20	10	10	15	>20	>20	>20	>20
Middelkerke	11	5	6	9	>20	13	>20	>20
Ranst	>20	>20	>20	>20	>20	>20	>20	>20
Retie	>20	>20	>20	>20	>20	>20	>20	>20
Semmerzake	>20	12	12	18	>20	>20	>20	>20
St-Kt-Waver	>20	15	13	20	>20	>20	>20	>20
Wachtebeke	>20	>20	>20	>20	>20	>20	>20	>20
Zaventem	>20	9	9	14	>20	>20	>20	>20
Zeebrugge	8	4	5	9	19	12	17	20
Zelzate	>20	10	10	14	>20	>20	>20	>20

Table 5.10: Dynamic payback time for each measurement site and turbine. When the payback time is above the lifetime of the turbine, it is replaced with >20.

5.2.5 Sensitivity analysis

In Section 5.2.4, we objectively presented the results of the economic analysis. Whether an investment is considered viable or non-viable depends on the SME. Each SME may use a different economic measure. While some SMEs use the internal rate of return to determine the viability of an investment, others use the payback time or the LCOE. A few examples of boundaries to determine the viability of a SMWT project then could be:

- IRR >12 %,

- Payback time <10 years, or

- LCOE <electricity price.

When such a fixed boundary is used, the viability decision may also depend on the economic parameters used in the economic analysis. One of the major difficulties is estimating these parameters. On the one hand they may have a large effect on the decision of the SMWT project, on the other hand they are all based on assumptions on how a certain value will vary over the lifetime of the turbine.

Therefore in this section, we will identify the key parameters that impact the economic analysis. First, we will use the economic parameters of our analysis and verify the impact if they would have been misjudged by 10 % (positively or negatively). Next, we repeat this analysis but use larger deviations from our values as a sort of worst case scenario and see whether our conclusions remain intact. Then we verify the impact of reducing the incentives, changing the energy consumption and adding the cost of a feasibility study to the total investment cost of the turbine.

Impact of misjudgement of 10 % In Figure 5.7, all economic parameters are varied with 10 % and the impact on the three economic measures is shown. To construct this figure:

- We only use turbine T11 (from Table 5.4), as this turbine has decent economic results and a low uncertainty on the estimation of the AEP (due to the limited height difference between hub and measurement height);

- For the discount rate (nominally 4 %), inflation (nominally 2 %) and the increase in electricity price (nominally 3.5 %) we impose an error term of 10 %. For example, for the discount rate we first apply a value of 3.6 % and repeat it for a discount rate of 4.4 %;

- For the AEP and the investment cost, we impose the 10 % error term on the value as such;

- For each measurement site, all three economic measures are determined. Then the median value of all measurement sites and each metric is determined and compared to the median value in the economic analysis of Section 5.2.4 (which will be used as a base in this section);

- In each figure, the left bar indicates a decrease of 10 % of the economic parameter, the right bar an increase of 10 % compared to the analysis of Section 5.2.4 ;

Figure 5.7 shows that varying the economic parameters with only 10 % has a rather small effect on the economic measures. Only varying the AEP or the investment cost lead to noticeable changes in the measures. An additional cost in the total investment cost (e.g. due to unforeseen costs) or an error in the estimation of the AEP (e.g. due to the extrapolation from measurement to hub height) may decrease/increase the dynamic payback times with approximately one year or the internal rate of return with approximately 2 %. Due to their definitions, varying the discount rate has no effect on the IRR and varying the inflation and electricity prices has no impact on the LCOE.
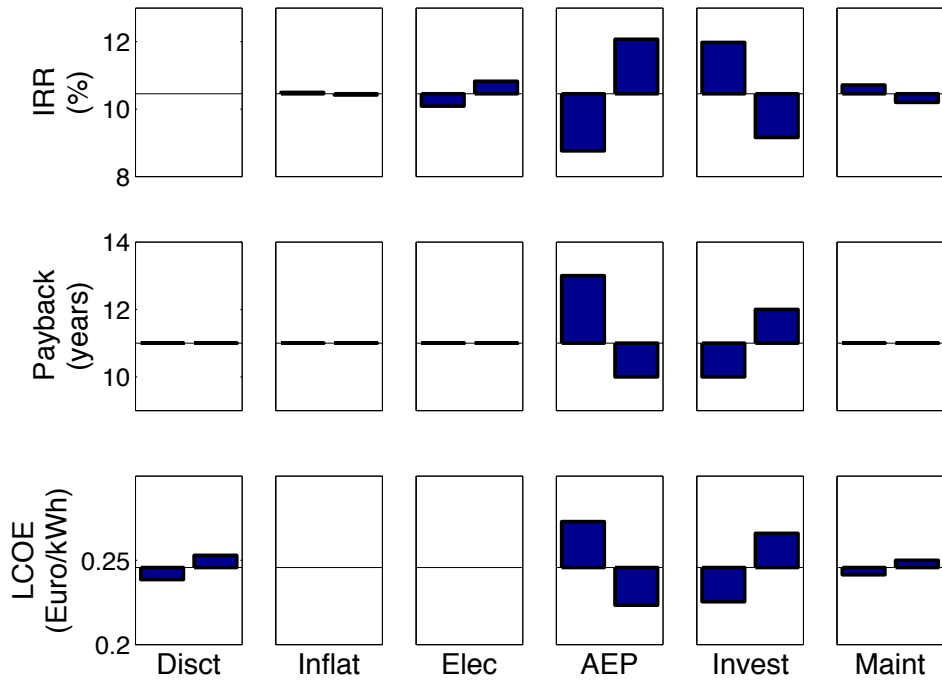
Figure 5.7: Impact of a decrease/increase of 10 % of the discount rate, inflation, electricity price, AEP, investment cost or maintenance costs on the economic viability. In each figure, the height of the left bar shows the results of a decrease of the economic parameters compared to the originally imposed parameters, the height of the right bar shows the results of an increase. The impact of varying each factor is shown for each economic metric for turbine 11 by determining the median value over all measurements sites and comparing this to the median value in the economic analysis of Section 5.2.4.

Worst Case scenario's Although our parameters are based on what is commonly used in literature, there are no standard values for each particular parameter. These parameters can be region dependent and also depend on the assumptions made about the future. We therefore apply a few other typical examples of economic parameters and verify if our conclusions remain intact. In this section, we vary:

- the discount rate: a value of 5 % (Drew et al., 2015) and a value of 1 % is used;

- the increase of electricity price: a stable electricity price and an increase of 5 % each year is applied;

- the maintenance cost: a maintenance-free turbine and a maintenance cost of 5 % each year is applied;

- the AEP: a wind turbine installed in a turbulent environment may experience a significant decrease in AEP due to yaw misalignment. Here we use 19 % (Hodkinson, Rowley, and Watson, 2013).

These scenarios are shown in figure 5.8, where the results are again compared to the results in Section 5.2.4. The impact of a stable electricity price, a maintenance cost of 5 % and a turbine installed on a turbulent site have a significant effect on the economic measures. In these worst case scenario's, the payback time may increase with 3 to 5 years or the value of the IRR may decrease with approximately 4 %.
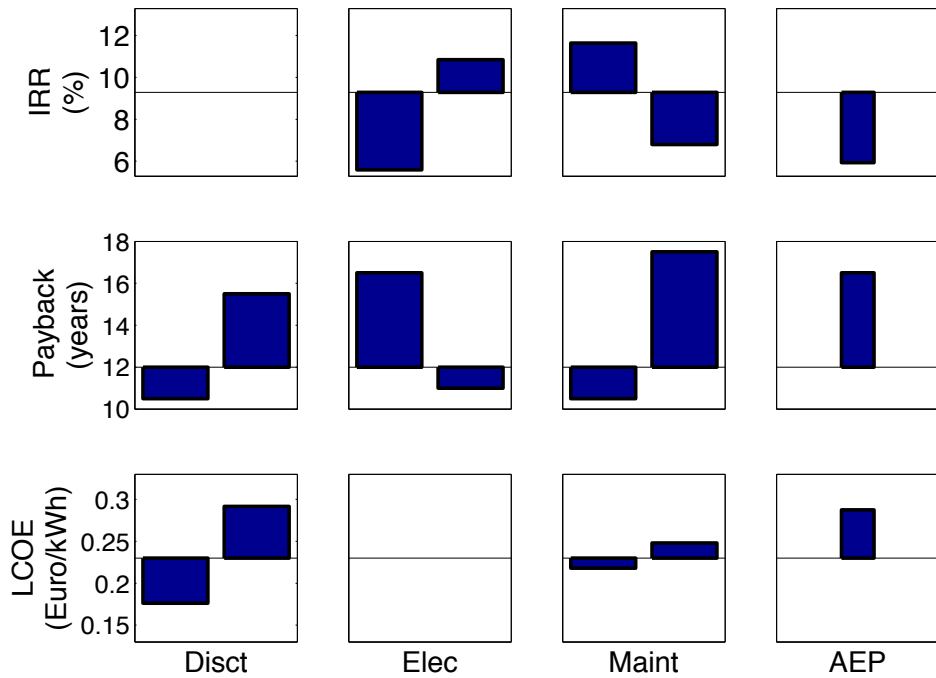
Figure 5.8: Impact of a decrease/increase of the discount rate (1 and 5 %), stable electricity price and increasing electricity price (5 % each year), maintenance cost (maintenance-free turbine and 5 % of the investment cost each year), overestimation of the AEP due to yaw misalignment (19 %) on the viability of turbine T11. The height of the bar represents the increase/decrease of the median value of the economic measure compared to the median value presented in Section 5.2.4. In each figure, the left bar represents a decrease of the economic parameter, the right bar an increase of the economic parameter.

One remark that should be made, is that Figure 5.8 only shows the decrease of the median value of the economic measure. A larger effect will be seen on the measurement sites where the financial benefits are already limited compared to good windy sites. On the windy sites, the impact will be much smaller. This is shown in Figure 5.9, where the same procedure is used though now the economic measures are shown for each measurement site. In each figure, the middle column shows the results presented in Section 5.2.4, the left column shows a decrease of the economic parameter and the right column an increase. For all measures, we propose a few boundaries to determine the viability of the SMWT project:

- IRR above 12 % (green solid) is considered a viable investment, below 8 % (red dotted line) is non-viable and between 8 to 12 % viable for some SMEs;

- Payback time below 9 years (green solid) is considered viable, above 12 years (red dotted line) is non-viable and between 9 to 12 years depends on the type of company;

- LCOE below the average electricity price (green solid) is considered viable.

If we concentrate on the sites above the green solid for the internal rate of return and below the green solid for the LCOE and payback times in Figure 5.9, we can see that our conclusions remain intact. On the windy sites, the installation of turbine T 11 remains viable as the varying economic parameters have negligible effect on the measures. For sites with a lower wind speed regime, these worst case scenario's have a significant impact. The more modest wind speed regimes turn out to be less affected be an increased discount rate or stable electricity price in comparison with an increased maintenance cost or reduction of the AEP.

Cost of feasibility study A typical cost for a feasibility study would be in the order of 5 k€ (roughly 4 k€ for a measurement campaign and 1 k€ for micro-siting). In this dissertation, we have shown that such a study is indeed imperative for SMWTs though it will lower the economic viability of the project. In Figure 5.10, the impact of adding the cost of a feasibility study to the total investment cost of the SMWT project is shown. The impact on each economic measure is determined by comparing the median value of the measurement sites to the median value of the base analysis (in

Section 5.2.4). We repeat this procedure for each of the selected turbines (see Section 5.2.1).

It stands to reason that the impact of such a study is larger for the cheaper turbines as the cost of the feasibility study is more or less independent of the cost of the turbine (for larger, more expensive wind turbines the measurement height may be higher). This can also be noticed from the results of turbine T7. This turbine has excellent economic results in the analysis in Section 5.2.4, though the impact of the additional cost of the feasibility study is larger than for turbine T11 which has similar results in the base analysis. This shows that turbine T7 has these excellent results rather through the low investment cost than through a high performance. If the cost of the feasibility study is added, the additional payback times is in the order of 2 to 3 years. Again the results presented in Figure 5.10 only show the median values. For the good and windy sites, the impact will be much lower and our conclusions made about the viability remain intact.

As the impact for the smaller (cheaper) turbines is larger, a few procedures to reduce the cost of the measurement campaign are proposed in this dissertation. A shorter measurement campaign (as shown in Chapter 3) and a simple approach to determine the most suitable location to install the turbine (which will be presented in Chapter 6) can significantly reduce the cost of the feasibility study and so reduce the impact on the economic viability.
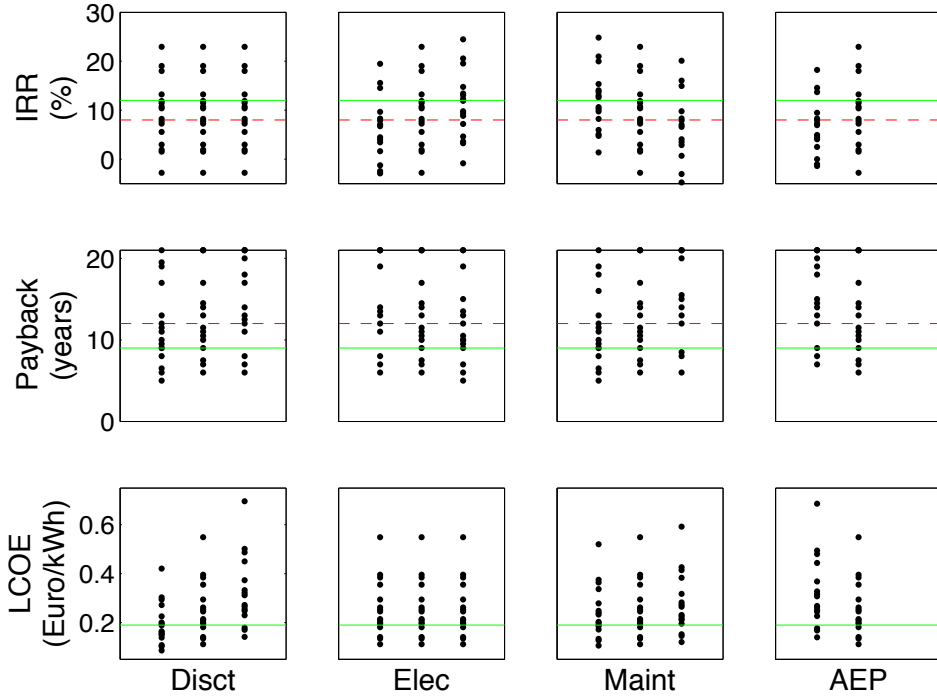
Figure 5.9: Impact of a decrease/increase of the discount rate (1 and 5 %), stable electricity price and increasing electricity price (5 % each year), maintenance cost (maintenance-free turbine and 5 % of the investment cost each year), overestimation of the AEP due to yaw misalignment (19 %) on the viability. In each figure, the middle column shows the results presented in Section 5.2.4, the left column a decrease of the economic parameter and the right column an increase. For each economic measure, boundaries to indicate the viability are set: Internal rate of return above 12 % is viable (green solid), below 8 % (red dotted line) is non-viable and between 8 to 12 % viable for some companies. Similar for the dynamic payback times: payback time below 9 years (green solid) is viable, above 12 years (red dotted line) is non-viable and between 9 to 12 years is viable for some SMEs. For the LCOE, we set the boundary at the average electricity price for SMEs (green solid).
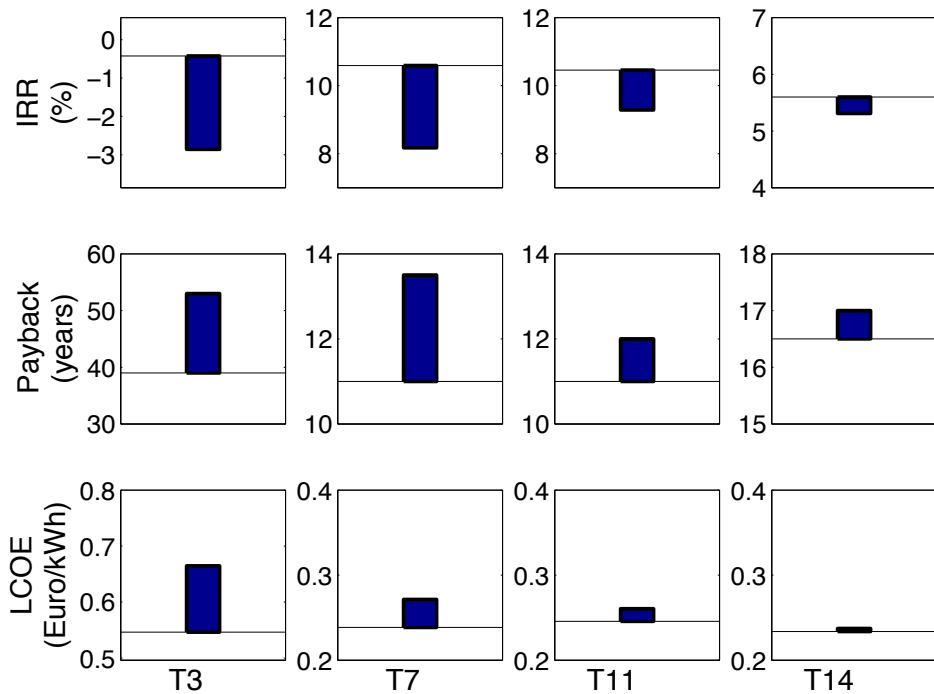
Figure 5.10: Impact of adding the cost of a feasibility study (5 k€) to the total investment cost of the turbine on the economic measures. For each measure, the median value of the measurement sites is compared to the median value of the base economic analysis. This procedure is repeated for each of the selected turbines (see Section 5.2.1). Due to the poor economic results of turbine T3, the median value of the internal rate of return is negative and the payback time is far above the lifetime of the turbine.

Incentives In Figure 5.11, the impact of reducing the incentives on the IRR and dynamic payback times is shown. The figure shows that the green certificates have the largest impact on the economic measures. The boundaries proposed in Figure 5.9 are again added to the figure. If these boundaries are used, only on the windiest site (average wind speeds above 5 m/s), turbine T11 can be viable without the incentives. Depending on which type of economic measure and boundary that is used, the threshold average wind speed is more than 1 m/s lower (below 4 m/s) when the incentives are added to the economic analysis. These incentives thus significantly increase the amount of sites that can be exploited by small-scale wind turbines.
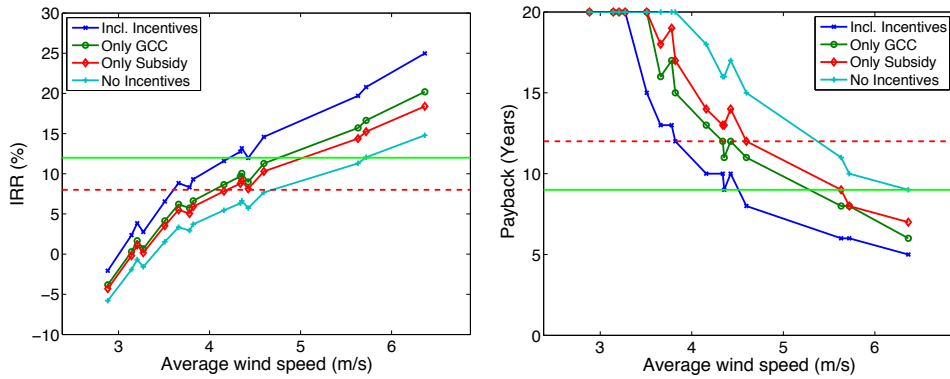

Figure 5.11: Impact of reducing the incentives on the internal rate of return (left) and the dynamic payback time (right) for turbine T11. For each economic measure, boundaries to indicate the viability are set: Internal rate of return above 12 % is viable (green solid), below 8 % (red solid) is non-viable and between 8 to 12 % viable for some companies. Similar for the dynamic payback times: payback time below 9 years (green solid) is viable, above 12 years (red solid) is non-viable and between 9 to 12 years is viable for some SMEs

Energy consumption Section 5.2.4 has shown that a parameter that has a large impact on the economic viability is the energy consumption. Although turbine T14 has shown excellent results in terms of LCOE, the payback times and IRR show a different picture. This is mainly caused by the fact that a large part of the energy has to be sold to the grid at a larger electricity price. A similar conclusion could be made for turbines T7, T11 and T14 for private users. To demonstrate this, we study the impact of a larger energy consumption by the user compared to the energy

consumption in the base analysis. This impact is shown in Figure 5.12.

In this figure, the red markers indicate the results for private users and turbine T7. The black markers show the results for SMEs and turbine T14. For private users the energy consumption is increased from 3 500 kWh/year (crosses) to 50 000 kWh/year (circles), for SMEs the energy consumption is increased from 50 000 kWh/year (crosses) to 100 000 kWh/year (circles). While for the lower energy consumption the payback periods are generally above the lifetime of the turbine, most of the payback periods are around 10 years when more energy is consumed. For turbine 14 and SMEs, a totally different conclusion can be made when the energy consumption is doubled. Less energy has to be sold to the grid leading to a payback period below 10 years for 50 % of the measurement sites. Payback periods can be as low as 4 years[2]. This figure shows that in order to increase the financial benefits of medium wind turbines, a right balance between the consumed and produced energy must be found.

Conclusions   This concise sensitivity analysis has indicated that the energy consumption, the estimation of the AEP and the incentives are the key parameters that determine the economic viability of a SMWT project. Other parameters such as the discount rate, electricity price and maintenance cost have a significant impact on the sites with lower wind speed regimes, though for the windiest sites their effect is more modest. From this analysis, we can conclude that our economic analysis has showed that small and medium wind turbines can indeed be a viable technology in Flanders. Varying the economic parameters may change the economic measures but will not change the viability of this technology.

---

[2]It should be noted that for these particular cases, the huge energy consumption will most likely lead to a significant decrease in the electricity price.
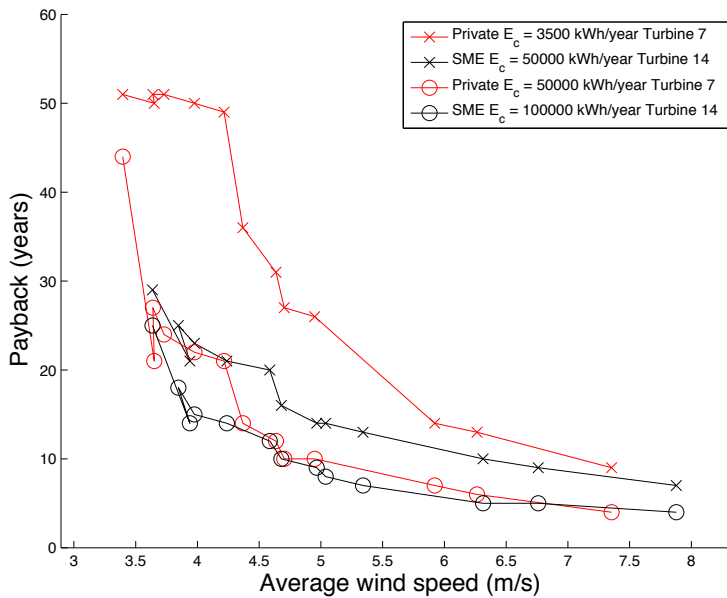
Figure 5.12: Dynamic payback period for each measurement site. The red markers show the results for private users and turbine 7, the black markers the SMEs and turbine 14. The cross marks represent the results as presented in Table 5.10. For the circles, the energy consumption of the users is set to $50\,000$ kWh/year (private users) and $100\,000$ kWh/year (SME user).

5.3   Legal framework in Flanders

In 2009, the Flemish government has set up a framework (Van Mechelen and Crevits, 2009) which describes the approval of permits of small and medium wind turbines. This framework distinguishes between small and medium wind turbines based on their hub height and rated power. In Flanders, small wind turbines are those with a hub height of 15 m or lower, measured from the base of the turbine. For ground-mounted turbines the hub height is thus measured from the ground; for building-mounted wind turbines the height is measured from the rooftop of the building. Medium wind turbines are wind turbines with a hub height higher than 15 m and a rated power lower than 300 kW. For both sizes a planning permission is needed, but the approval of the permission is done differently. Small wind turbines are approved on a community level, while medium wind turbines are approved on the provincial level. Only for large wind turbines (with rated power above 300 kW) an environmental permission is required.

For the approval or disapproval of the building permit, different judgement criteria are listed in the framework. These criteria do not only take into account the current situation, also future plans with the installation site are investigated. These criteria are:

- Shadow flicker: A rotating blade will generate light reflections and shadow flicker. Areas where these reflections occur should be avoided. These areas around the turbine are restricted for homes and businesses. Outside these areas, flicker is limited to 30 hours/year which is considered as acceptable. In Figure 5.13 the area to avoid is shown. Here R is two times the total height (hub height plus the rotor radius of the turbine) of the installation.

- Noise: A test certificate of the noise at a wind speed of 5 m/s should be included. Using these sound data, the sound pressure level L_p at a certain distance from the turbine can be determined with Figure 5.14. This figure allows to determine the maximum noise a turbine will produce at the closest building near the turbine. This value then has to be compared to the limit set by the regulations. A different limit is used for residential, industrial and rural areas. For example, for residential areas the maximum sound pressure level must not exceed 39 dB(A). Using Figure 5.14, this implies that for a distance of 60 m, the turbine is permitted to produce a sound power level L_w of 70
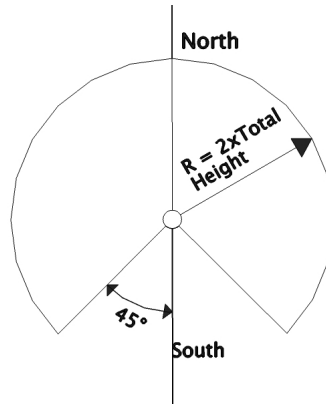
Figure 5.13: Area around the turbine that should be avoided according to the Flemish regulations to limit the shadow flicker. Reproduced from Van Mechelen and Crevits (2009).

dB(A).

- Safety: To ensure a safe operation, the turbine should be designed according to the IEC 61400-2 standards.

- Spatial implementation of the turbine: The spatial implementation of a wind turbines depends on the area:

  - Residential and urban areas: In these areas installing a wind turbine is often not desired. The negative effects and the impact of fast rotating object are large in these dense areas. Yet for specific cases, the planning permission can be approved if sufficient justification is provided.

  - Industrial, logistics, transport and recreational areas: In these areas, the decision to approve a medium wind turbine depends on the future plans for large wind turbines. For small wind turbines, the decision to approve a small wind turbine depends on the future plans for large and medium wind turbines for small wind turbines.

  - Rural areas: In this case a more restraint policy is maintained for the visual impact on the landscape and for the disturbance of the local wildlife.
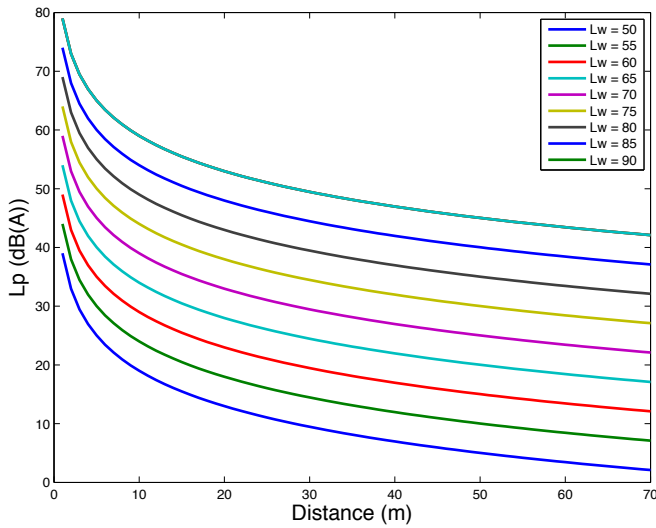
Figure 5.14: The sound pressure level as a function of the distance between a turbine and the closest building. Reproduced from Van Mechelen and Crevits (2009).

5.4 A market survey to study the socio-political acceptance

In order to assess the socio-political acceptance of small and medium wind turbines in Flanders, we conducted a market survey. An earlier study (Van Hamme and Loix, 2011) showed the public support for wind energy in Flanders: 63 % of the respondents expresses the importance of sustainable energy and 84 % is for the exploitation of wind turbines in Flanders. In this market survey, there was no specific distinction between small and large wind turbines, although the questionnaire was mainly focused on large wind turbines.

Our market survey, which was performed over the summer of 2012 in collaboration with GfK Significant, was mainly focused on the mentality regarding small and medium wind energy in Flanders. We interviewed SMEs, private persons as well as a representative part of the Flemish municipalities (as they are eventually responsible for permits of small wind turbines). A brief summary of the results of this survey is presented here, more details can be found in (Runacres, Vermeir, and De Troyer, 2012).

All Flemish municipalities believe energy should be generated in a clean

and sustainable way. They believe that governmental support is necessary for solar energy (66 %), wind energy (38 %), hydro energy (64 %), gas (38 %) and biomass plants (66 %). The support for nuclear power (18 %) and coal plants (15 %) is less important. Only 10 % of the questioned municipalities actually have wind turbines on their territory, while 77 % support the construction of wind turbines in general.

79 % of the Flemish municipalities are aware of the legal framework in Flanders and 38 % have already received one or more applications for the installation of a small wind turbine. In the period 2009-2012, on average 2.3 applications were received, 1.7 by private users and 0.7 by SMEs. Only for approximately one of the 2.3 applications, a building permit is granted. On average about 0.8 small wind turbines are installed per municipality (308 municipalities in Flanders). Remarkably, most communities are reluctant for future applications: only 18 % will grant a permit if the requirements are met, 25 % will reject future applications and 57 % doesn't know yet. Nevertheless, 97 % of the municipalities would use more wind energy as energy supply and 89 % believes wind energy in general will increase in the near future. The Flemish municipalities are rather anxious about the (visual) nuisance when more small wind turbines would be installed. Therefore, they will rather support the implementation of these wind turbines in industrial areas than for private areas.

Only 14 of the 200 contacted SMEs filled in the questionnaire. Although the results of the questionnaire are thus not representative for all SMEs, it was clear that those SMEs we interviewed have a rather positive attitude regarding wind energy in Flanders. Yet only a few of them are aware of the existence of small-scale wind energy. When they were informed about the technology, most of them underestimated the payback period and investment cost. Nevertheless, 50 % would be willing to invest in this technology when a (reasonable) investment cost pays itself back in a reasonable amount of years.

The Flemish households are generally in favour of wind energy: nearly 76 % is positive; regardless of whether they live in the countryside or in the city, and slightly more men (78.7 %) than women (72.1 %) are positive. Approximately 64 % are aware of the small-scale wind technology. 0.5 % of the respondents have one of their own and the most of them are located in West-Flanders (0.8 %) and Antwerp (0.8 %). Whether Flemish households asked whether they would install a wind turbine of their own, the opinion is rather divided: 32 % would consider it, 31 % would not and 37 % answered maybe. Flemish people in the countryside are more likely to consider a

small wind turbine compared to people in urban areas: 38.6 % against 36.8 %, and men (42.9 %) more than women (33.3 %).

5.5 Case-study: Ranst

We were contacted by a land owner, who owns a specific piece of land in a semi-rural area, and who wanted to exploit the possibility of installing a small wind turbine. In order to assess this possibility we performed a wind measurement campaign and a CFD-based micro-siting study for his site. We built a CFD model of the site and then used long-term wind data from a nearby measurement station as inlet condition, to find the suitable locations to install a wind turbine. Next, we validated our CFD simulations with a two-week measurement campaign with two anemometers at different locations on the site. Then, at the best location, we measured for about 15 months and normalised these data with the MCP-techniques to obtain a reliable estimate of the AEP, as described in Chapter 3.

5.5.1 CFD micro-siting

The complexity of the terrain is caused by the buildings and obstacles (e.g. the transmission towers, vegetation). Terrain topography such as hills can be treated in the same way. The buildings and obstacles are accurately modelled using a total station. The size of the domain and the amount of obstacles and buildings taken into account for the 3D model are based on rules of thumb. These rules describe the size of the recirculation zone and wake effects on a 2D obstacle. They describe the distance before the wind speed reaches the free stream velocity again and are available in the literature (Wegley et al., 1980; Tominaga and Stathopoulos, 2013). Data from the total station and terrain topography from Google Earth are combined into a 3D model of the site. This model is then introduced in the CFD code as a 3D surface. The 3D model of the terrain is shown in Figure 5.15.

To determine the inlet conditions for the numerical simulations, we used long-term data (12 years, 1-hour sampled data) from a nearby measurement station (Woensdrecht, Netherlands). Using these data, we identify the most dominant wind direction and derive the average wind speed per wind direction. This is shown in Figure 5.16. We used Eq. (1.11) as inlet condition for
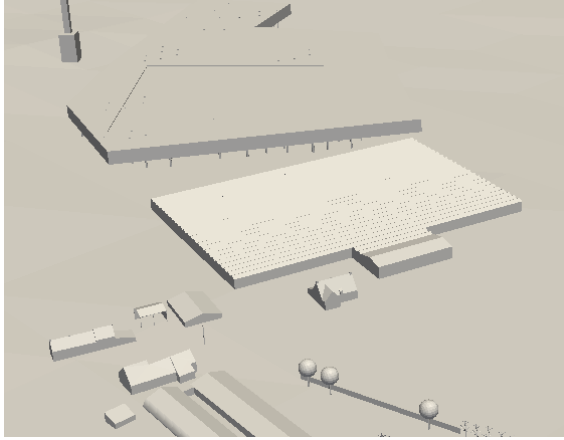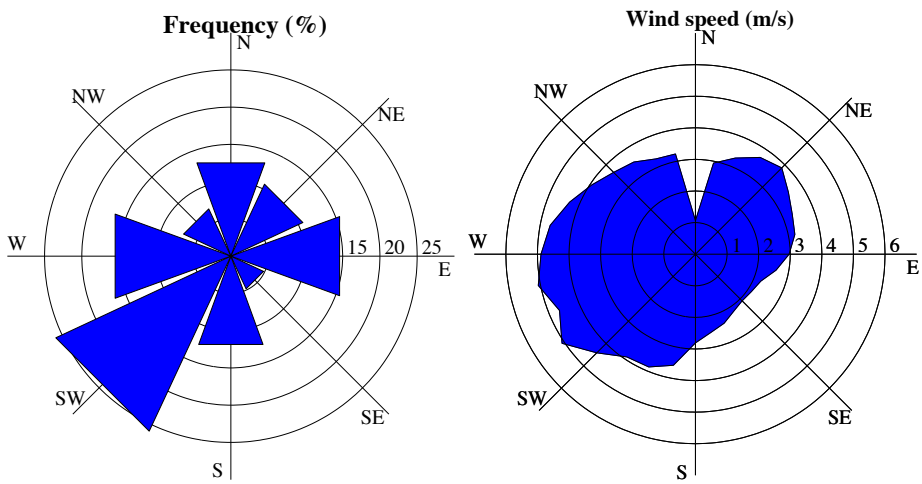
Figure 5.15: 3D model of the site

Figure 5.16: Wind rose with frequency of occurrence (left) and mean wind speed (right) per wind direction for nearby measurement station Woensdrecht (Netherlands).

the CFD simulations; z_0 was estimated using tables from Wieringa (1992), v^* followed from z_0 and the wind speed data.

Derivation of a suitable location   A siting study is performed to install a small-scale wind turbine on the terrain of the owner. The owner does not own all the terrain taken into account for the siting study, so only a small part of the terrain is available for the installation. As seen in Section 5.3, the maximum allowed hub height for small wind turbines in Flanders is 15 m and thus only this height is considered. As described in the section above, the boundary conditions are derived from measurement data from a nearby weather station. The analysis of the data showed the dominance of the southwest wind and a high mean wind speed for the west wind. These two wind direction are used in the simulations. The south wind direction is not simulated because no obstacles are located upstream of the terrain of the owner and therefore the unperturbed wind can be used. Due to the shape and complexity of the terrain and the relatively high mean wind speed in that direction, a simulation of the northeast wind direction is also required. The results of these 3 simulations are then combined to derive a good location to install a wind turbine (or in this case to put a measurement station to check the resources on site).

In Figure 5.17 (left), the wind flow distribution for the southwest wind direction is shown. The figure shows a slice plot at a height of 15 m. The area between the black lines shows a region where the wind speed is high on the terrain of the owner. This region is then used to determine a suitable area for a simulation of the northeast wind. This process is repeated for a simulation of the west wind. In Figure 5.17 (right) the results of the simulations for the northeast wind direction are shown. A large area in the area marked by the southwest wind direction has relatively low wind speeds, only a small surface has higher wind speeds.

In Figure 5.18 (left), the wind patterns for the west wind direction are shown. At first sight, there seem to be no regions with higher wind speed in the area between the black line. A closer look reveals (Figure 5.18 (right)) two areas where the wind flow is less disturbed. These areas are indicated with a circle and represent the most suitable location to install a wind turbine. For all wind directions, in the area within the circles, the flow is nearly undisturbed or even a small acceleration is noticed. On this location a wind measurement campaign can show whether the location is indeed suitable and the wind potential is high enough.

Figure 5.17: Wind speed distribution for the simulation of the southwest (left) and northeast (right) wind direction. The area between the black lines indicates a region where the wind speed is unperturbed on the terrain of the owner.

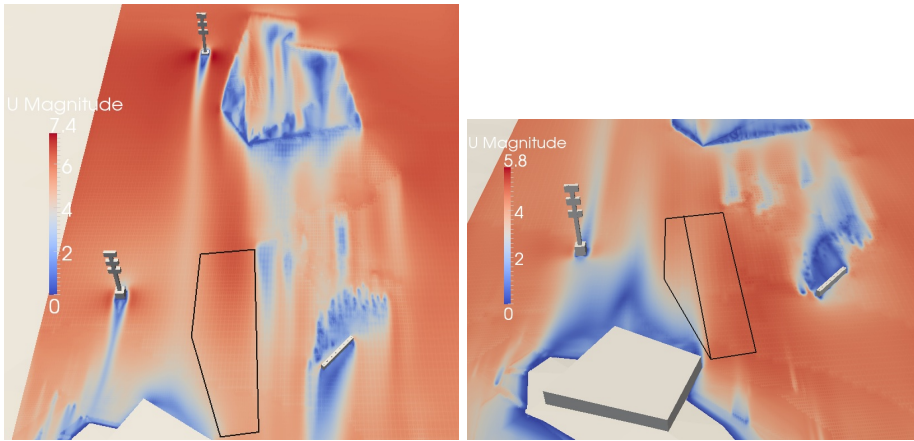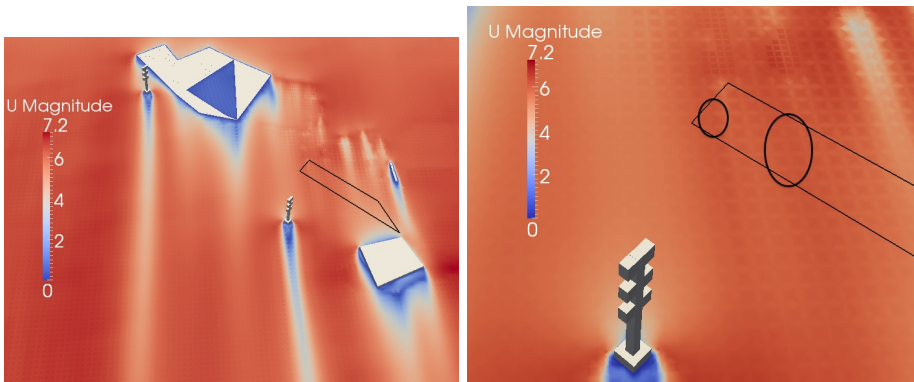
Figure 5.18: Wind speed distribution for the simulation of the west wind direction. The area between the black lines (left) indicates a region where the wind speed is unperturbed on the terrain of the owner. The circles (right) indicate suitable locations for the installation of (a) small wind turbine(s).

Another aspect in these kind of simulations is turbulence. The streamlines in the most suitable area can be plotted to give an idea of the turbulence. Zones where the turbulence is high, are not appropriate to install a wind turbine. These conditions will have a negative effect on the lifetime (due to fluctuating loads on the blades) of the turbine and the performance (due to the yawing required to adapt to the variable wind direction). The streamlines are investigated in these areas for each wind direction, and this showed a relatively low turbulence level. An example of such a plot is shown for the west wind in Figure 5.19.
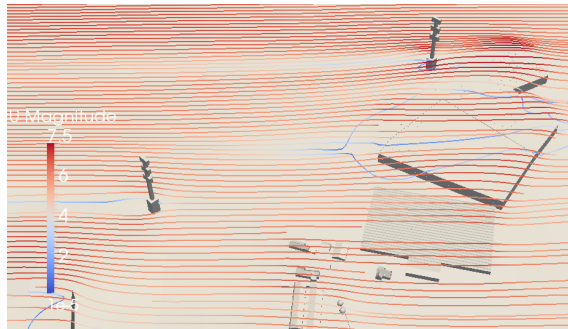
Figure 5.19: Streamlines at a height of 15 m in the areas defined as suitable locations.

With the results of the siting study and practical positioning on the terrain, a location on the terrain is identified as the most suitable location. To verify how the wind behaves on this position, we compare the wind speed at this position to the inlet wind speed at the same height (15 m). This comparison is shown in Table 5.11. This table shows that the wind speed is unperturbed for the northeast wind direction. For the west and southwest wind direction a local increase in wind speed is observed due to the characteristics of the terrain.

5.5.2 Validation of the selected location

To verify the accuracy of the predicted wind speed, the results of the simulations need to be validated. We therefore install two measurement masts on the site: a first mast to accurately measure the boundary conditions and a second mast to determine the wind speed at the most suitable location

Wind direction	Wind speed at the inlet [m/s]	Wind speed on suitable location [m/s]
NE	4.6	4.6
SW	5.3	5.8
W	5.6	5.7

Table 5.11: Comparison of the wind speed at the selected location and the inlet both on 15 m height.

(identified in the previous section).

For the validation, we perform a new simulation where the boundary conditions are not estimated from data of a nearby measurement station but measured. To measured these conditions, the first mast will be installed upstream from the site for the simulated wind direction (west). By measuring the wind speed at two heights (15 m and 10.5 m), we can derive the vertical wind profile (this procedure is presented in Section 5.5.2) and apply this profile in the simulation.

As a validation, we simulate the west wind direction using the measured inlet conditions, and compare the simulated wind speed with the measured wind speed at the second mast. This validation procedure is a well-known method for validating siting studies with field measurements at larger heights (Willemsen and Wisse, 2002) for large MW wind turbines. When comparing the field measurements with siting studies for these large wind turbines an averaging period of 10 minutes is used. For lower heights, methods are available in the literature explaining the validation of CFD simulations with wind tunnel experiments for the built environment (Wallbank, 2008). No validation of siting studies of CFD simulations by field measurements were found in the literature for lower heights. We therefore tested 1 minute as well as 10 minute averaging periods.

Field measurements for the validation The measurement period is set to 2 weeks. Due to the variability of the wind speed and direction at these low heights, a few hours would not suffice to make a good estimate. The inlet parameters can be calculated from the measurements using equation (1.11). It should be noted that we know use the linear log law instead of the log law, as this is the vertical wind profile used in the CFD code. As mentioned in Chapter 1, this law imposes a non-zero wind speed below the roughness length as this solves the problem of modelling the flow near the ground.

In Table 5.12 the results of the field measurements at mast 1 are shown. Using the wind speeds measured at both heights, the roughness length z_0 and the friction velocity v^* are estimated at respectively 1.38 m and 0.79 m/s.

	Top anemometer	Lower anemometer
Wind speed $\left[\frac{m}{s}\right]$	4.8	4.2
Turbulence Intensity [%]	17	18

Table 5.12: Results of the field measurements at mast 1. The turbulence intensity is the averaged value using 10-minute intervals.

A second measurement mast with 2 anemometers is placed on the most suitable location (based on the siting study) on the terrain (mast 2). The distance between both masts is measured using a total station. This distance is taken into account to make a time shift between the wind speed measured at mast 1 (i.e. inlet) and mast 2. As the wind speed is lower on the lower anemometer, different time shifts are used. The measurements from mast 2 are then compared to the numerical simulations. The averaging period to compare the field measurements with the simulations is first set to 10 minutes. Table 5.13 shows the results of the validation. The negative error indicates an overprediction of the wind speed by the CFD simulations.

	Top anemometer	Lower anemometer
Estimated wind speed $\left[\frac{m}{s}\right]$	5.5	4.6
Measured wind speed $\left[\frac{m}{s}\right]$	5.0	4.3
Estimated acceleration [%]	13.7	9.2
Measured acceleration [%]	4.9	3.2
Error [%]	-8.8	-5.6

Table 5.13: Results of the validation.

A comparison is also made by using a smaller averaging period from the field measurement. During a period of 10 minutes where the wind was predominantly west, a comparison was made between the 10 minute average and the average per minute of the same period. This implies a comparison of the validation of each minute in the given period, to the validation of the

10 minute average in the same period. This comparison was done because no recommendations were found in the literature describing the averaging period for the validation of CFD at lower heights. In Figure 5.20 the errors between the simulations and the measurements are plotted for the shorter averaging period. The red line indicates the mean value of the error which is comparable to the 10 minute averaging period.
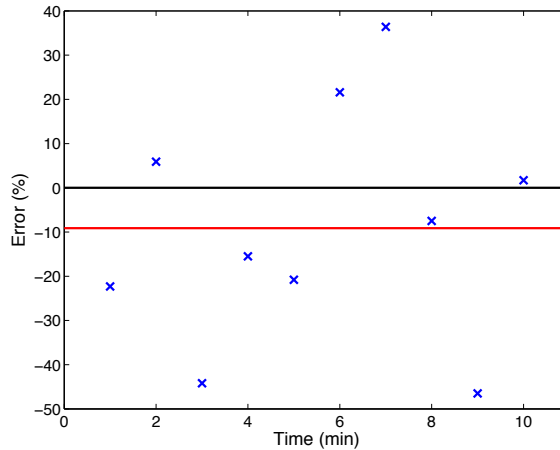
Figure 5.20: Validation of CFD using 1 minute averages. The blue cross markers represent the validation error for each wind speed averaged over 1 minute. The red line indicates the average validation error.

Discussion   An error of approximately 9 % is found from the validation. This error is comparable with validation studies in complex terrain for large wind turbines (Wallbank, 2008) and with validation of wind tunnel experiments in an urban environment (Willemsen and Wisse, 2002). The wind speed is systematically overpredicted by the simulations. This shouldn't be the case when using the RANS method, in most cases even an under prediction of wind flow is shown in the literature (Bechmann and Sorensen, 2010) (due to an overprediction of the seperation zone). The results for the averaging period of 10 minute are better than for the averaging period of 1 minute, as expected. There is much scatter in the results for the shorter averaging period.

Although the error on the predicted wind speed causes a significant error on the estimation of the AEP of a wind turbine, the CFD-study could

be used to derive the most suitable location. The simulations identified a region where the wind speed was locally increased. This increase in wind speed was confirmed by the field measurements.

5.5.3 On-site wind measurement campaign

The siting study has indicated a potentially good location to install a wind turbine. Although this location represents the location with the most wind resources on the site (for the simulated wind directions), only a wind measurement campaign can measure the true wind resources for this site. Therefore the wind measurements at mast 2, performed for the validation study, are continued for 15 months.

As described in Section 5.5.2, the wind speed is measured at two different heights, 15 and 10.5 m. The wind direction is measured at 13 m. An averaging interval of 1-minute and sample frequency of 1 Hz is used. In Figure 5.21, the monthly averaged wind speed is shown for each measurement height. The highest wind speeds are measured in the winter of 2012-2013 although the average wind speed in April 2012 is also relatively high. The wind speed averaged over the whole measurement period was 2.8 m/s at 15 m and 2.5 m/s at 10.5 m.
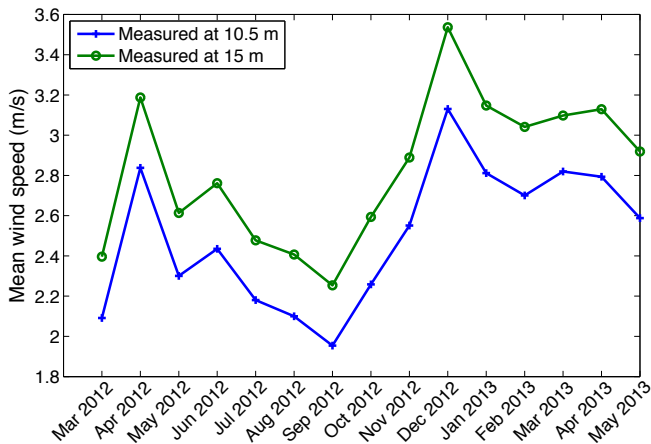

Figure 5.21: The monthly measured wind speed for the most suitable location derived by the siting study. The green line shows the wind speed at 15 m, the blue line the wind speed at 10.5 m.

To have an idea about the long-term wind potential, we apply a

measure-correlate-predict procedure (the variance approach) to the measurements. Data from a nearby meteorological station (Woensdrecht, KNMI) are used to perform this extrapolation. The long-term data consist of the wind speed measured at 10 m height over 20 years (May 1993 to may 2013). For the concurrent data a correlation factor of 0.7921 was found indicating a decent correlation between both data sets. After applying the MCP procedure, the long-term average wind speed was estimated at 2.9 m/s. This shows that although a suitable location is derived using the CFD, the on-site wind potential is too low for the exploitation of a small wind turbine. Therefore no economic feasibility study of this site performed.

5.5.4 Summary and conclusions

In this study, numerical experiments were carried out using the CFD code OpenFOAM. These experiments were used to derive the most suitable location to install a small wind turbine on a specific site in Flanders. To verify the accuracy of these simulations, the estimated wind speed at the selected location were validated by field measurements. To estimate the wind potential on this location, a wind measurement campaign was conducted.

For the siting study, we estimate the inlet conditions using long-term wind data from a nearby measurement station. The long-term data showed two most relevant wind directions to simulate in the siting study. An extra wind direction is required due to the complexity of the terrain. This siting study showed an interesting location on the terrain to install a small-scale wind turbine.

The results of the siting study are validated using two measurement stations. One measurement station is installed in front of the terrain (for the simulated wind direction) to estimate the inlet conditions for a simulation. The second measurement station is installed on the most suitable location identified by the siting study. The measured inlet conditions are then applied to a simulations and the estimated wind speed at the second measurement station is compared to the measured wind speed. This validation showed an error of less than 9 %. The simulations systematically overpredict the mean wind speed. Although the error could be significant when it used to estimate the energy yield of turbine, the siting study is capable to identify suitable locations to install a wind turbine. The simulations indicated an increase in wind speed on specific location and this increase was confirmed by the measurements.

To estimate the true wind potential on the selected location, the mea-

surements from the second measurement station were extended. The wind speed was measured at two different heights for 15 months. The wind speed averaged at 2.8 m/s at 15 m and 2.5 m/s at 10.5 m for the measurement period. The long-term average wind speed was estimated at 2.9 m/s at 15 m after applying a measure-correlate-predict procedure. This showed that even on the most suitable location, the wind conditions are insufficient to install a wind turbine.

5.6   Case-study: Puyenbroeck-Wachtebeke

In the context of a demonstration project, we bought, installed and tested a wind turbine with a rated power of 5 kW. The purpose of this project is to allow potential users/investors to become familiar with small wind turbine technology and allow participants (at first only installers and manufacturers were considered) to show and test their project. The performance of all turbines was monitored and compared throughout the project. At the end a ranking of the performance of each turbine was made, taking into account the investment cost and the energy production.

Specific requirements for the participating turbines were defined:

- Sound pressure level just below the hub height could not exceed 39 dB(A) at a wind speed of 5 m/s;

- The rated power could range between 0.5 to 10 kW;

- Power performance tests should be available;

- Hub height of maximum 15 m;

- Certified according to the IEC standards (IEC, 2013);

- Monopile tower (non-guyed tower).

Our objective to participate with this project was to identify a turbine which fits the above requirements, which was not available on the European market and for which no independent test results were available. This objective allows potential Flemish distributors (this work was performed under contract research IWT 090192 (Runacres, Vermeir, and De Troyer, 2012)) to extend their inventory with a good turbine. The turbine, installation cost and the measurement setup of the turbine were funded by an EFRO-project (EMOVO: multidisciplinair onderzoeks- en vormingscentrum rond energie- en milieutechnologiën, PO53).

Specifications and installation of the HY5kW wind turbine   Using our database, we identified the HY5kW from Huaying wind turbine as it nicely fits our objective and the requirements to participate to the project. This turbine has a rated power of 5 kW, a hub height of 15 m, a rotor diameter of 5.6 m and a monopile tower. The configuration of the rotor is downwind and the turbine uses an active system to pitch the blades and control the power (see Figure 5.22 (left)). Besides an electrical brake, an automatic mechanical brake is foreseen by pitching the blades over an angle of 90°.

One the factors that will have a major influence on the performance of the turbine is the appropriate siting of the turbine on the terrain. The site Puyenbroeck is a recreational domain with small woods and the open space is limited. Due to the high complexity of the site, we use a floor plan and basic rules of thumb (which will be presented in Chapter 6) to determine a suitable location for the turbine instead of using numerical simulations. In agreement with the project managers, we installed our turbine near the golf court. The turbine was installed before summer 2012 (see Figure 5.22 (centre and right)) and became operational just after summer 2012.

Figure 5.22: Rotor of the HY5kW wind turbine (left), lifting of the turbine for installation (middle) and low-tech procedure to level the turbine (right).

Wind speed and energy yield measurement setup   In order to obtain an independently tested power curve of this turbine, we simultaneously measure the wind speed and power of the turbine. These measurements are performed using the IEC 61400-12-1 standards (IEC, 2006). A measurement mast is installed at a distance of 13 m (or 2.3 times the rotor diameter) and the wind speed was measured at heights of 15 m and 10.5 m. The wind direction was measured at 13.5 m. The temperature and humidity were measured near the data logger at a height of 2-3 m. We

used a standard sample interval of 1-minute but also collected a limited set of 1-second data of the power and wind speed. The equipment used for the setup is listed below and shown in Figure 5.23:

- To measure the wind speed two Thies first class anemometers are used to measure the wind speed at 15 and 10.5 m and one Ultrasonic 3D R.M Young model 81000 to measure the wind speed at 15 m;

- To measure the wind direction, we use a Thies compact wind vane;

- To measure the air density, we combine the pressure and temperature measurements (Thies pressure and Thies Temperature/Humidity sensor);

- Data are collected with a data logger of Campbell scientific (CR 1000);

- The power is measured using a Sineax P530 (Class 0.5) power meter;

- The energy production is measured by the Finder 7E.153 energy meter.

Figure 5.23: Wind measurement mast (left) and power measurements (right) for the HY5kW wind turbine.

Discussion of the measurement results   In Figure 5.24 (left), the measured (normalised to sea-level) power curve is shown. This measured power curve is compared to the power curve supplied by the manufacturer. For lower wind speeds, a good agreement is found between the power curve of the manufacturer and our own measurements. For the higher wind speeds,

a significant deviation in power is observed between both power curves. Although more than one full year of useful data was collected, the test could not be completed. Due to the poor on-site wind conditions, the probability of wind speed above 12 m/s is too low to fulfill the requirements of the IEC standards. The wind histogram of the site is shown in Figure 5.24 (right).
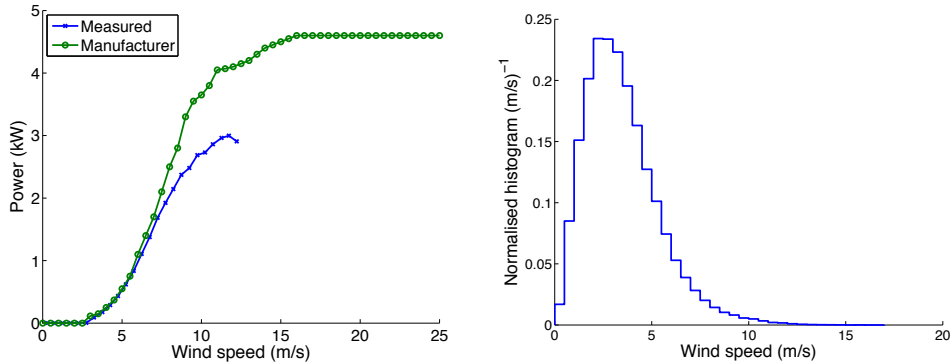
Figure 5.24: Measured power curve of the HY5kW wind turbine (left) and wind histogram of Puyenbroeck during the performance measurements (right). The measured power curve is compared to the power curve measured by the manufacturer (left).

The lack of a decent wind resource is of course the main limiting factor here; but still the turbine should have attained rated power now and then. We suspect that the reasons are mechanical. A few (small) issues with the turbine occurred within the first three years of its lifetime. Problems with the brake mechanism appeared (the cable which connects the actuator with the blade pitching mechanism came undone) and one of the bolts which connects the blades to the hub had to be fixed (the manufacturer states in the manual that each bolt should be fixed again after the first 2000 h of operation). In our view the costs for the repairs (rent of a steeplejack and man-hours) could be categorised as O&M costs and a long-term duration test is necessary to make solid statements about the reliability of the turbine.

Although our measurements have showed that the manufacturer exaggerated the performance of the turbine, it had the best investment cost/energy production ratio of all participants of the project (4 other candidates participated). This is most likely caused by two reasons:

- Our turbine is placed in a relatively open space compared to the other

turbines emphasising the importance of good micro-siting;

- Due to the poor wind conditions, the turbine is typically operating in the lower wind speed regions where the performance of the turbine is relatively good (in these regions the $C_{P_{el}}$ is comparable or even larger than similar tested wind turbines of our database).

5.7 Case-study: Strépy-Bracquegnies

In the context of contract research (Vermeir and Runacres, 2014), we were contacted by Electrabel to suggest viable medium wind turbines and to estimate the AEP for three sites. The rated power of the possible turbines was limited to 50 kW ($\pm$ 5kW) as they would be used for a specific call (Cahier spécial des charges 02.02.01-14C35) by the Walloon Region. For this study, the wind data were given; we used these data to select a suitable turbine and estimate the AEP. This case study is thus an example of the use of our database as a valorisation tool.

Presentation of the available wind data Wind data of three particular sites were supplied: Strépy, Peronnes and Ronquières. In Strépy and Peronnes, the wind speed was measured on 5 different locations along the highway. In Ronquières, four measurement stations were used. The measurement height was set to 30 m. In Table 5.14, the results of the measurements are shown. As the distance between the sites (and the measurement masts for each site) is limited, the average wind speeds and distributions (indicated with the Weibull parameters k and c) are very similar.

In Figure 5.25, the wind speed distribution of the three sites are shown. As no data were supplied about the roughness characteristics of the terrain, and since 30 m is a realistic hub height for 50 kW turbines, the wind speeds have not been extrapolated to other heights.

Estimation of the AEP Due to the specific demands of this study, the number of turbines considered is limited. As shown in Chapter 3, there are different definitions for the rated power of a wind turbine. Here, we used the IEC standards (IEC, 2006) that state that the rated power is assigned by the manufacturer. This has lead to a list of five wind turbines which

Site	$\overline{V}$ [m/s]	k	c	R^2
Strépy 1	4.8	2.109	5.407	0.9654
Strépy 2	4.8	2.099	5.439	0.9620
Strépy 3	5.0	2.102	5.596	0.9633
Strépy 4	5.2	2.080	5.830	0.9575
Strépy 5	5.0	2.117	5.636	0.9620
Peronnes 1	4.9	2.166	5.522	0.9728
Peronnes 2	5.0	2.170	5.694	0.9753
Peronnes 3	5.1	2.124	5.795	0.9633
Peronnes 4	5.0	2.118	5.689	0.9707
Peronnes 5	5.0	2.147	5.592	0.9717
Ronquières 1	5.2	2.116	5.841	0.9579
Ronquières 2	5.2	2.114	5.875	0.9620
Ronquières 3	5.2	2.103	5.886	0.9579
Ronquières 4	5.0	2.163	5.594	0.9652

Table 5.14: General results of the supplied wind data.
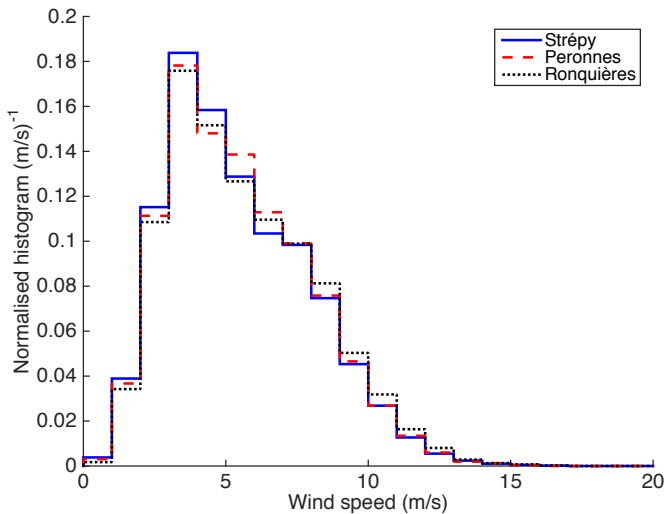
Figure 5.25: Wind speed histograms of the studied sites.
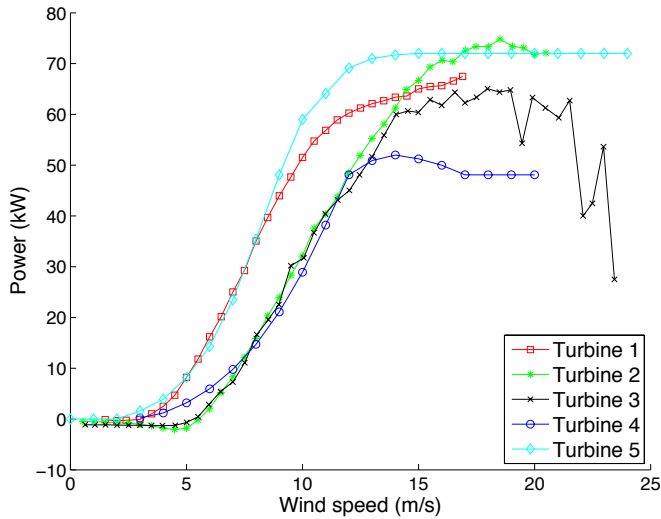
Figure 5.26: Power curves of the turbines with a rated power of 50 kW (according to the IEC standards (IEC, 2006)).

will be considered. In Figure 5.26, the power curves of these turbines are shown.

Except for turbine 4, these are all independently-measured power curves. It is noticed that only Turbine 4 fits the requirements for the call meaning that for the other turbines the maximum power should be restricted, i.e. the turbine should be *de-rated*. Such a restriction is a simple technical modification and is fairly common. Turbine 3 has an unconventional shape for the higher wind speed ranges ($\pm$ 20 to 24 m/s). This is due to two reasons: firstly, these high wind speeds occur less often and therefore these wind speed bins contain only few data points, secondly the turbine is stall-regulated and the discrepancy between the power measurements is larger in the wind speed ranges where stall occurs. Both lead to a larger uncertainty of each data point of the power curve. This is shown in Figure 5.27 where the standard uncertainty is shown for each datapoint for this particular power curve.

The properties of the wind turbines are shown in Table 5.15. Only one VAWT with a rated power of 50 kW is found in our database. Turbine 5 is a two-bladed HAWT. All the other turbines are classic three-bladed HAWTs.
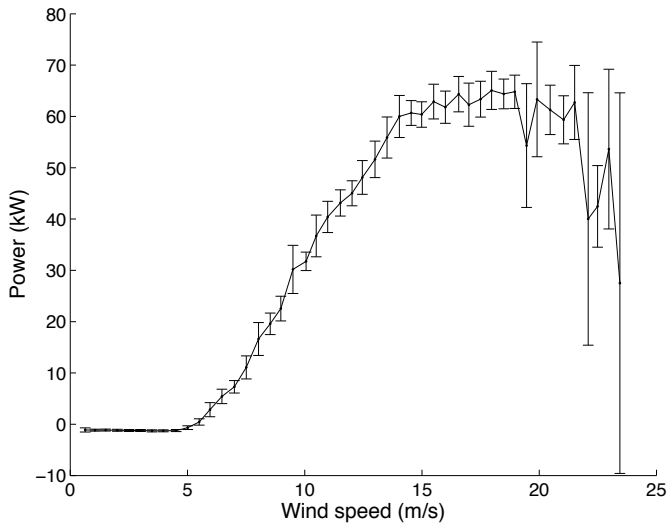
Figure 5.27: Power curve of turbine 3 with standard uncertainty interval for each datapoint.

Starting from the wind histograms, we predict the AEP with Eq. (3.9) in accordance with the IEC standards (IEC, 2006). In Table 5.15, the results are shown for each site. The AEP shown is an averaged value over the different measurement masts, so as to obtain one estimate per site.

Turbine	Type	# blades	Rotor diameter [m]	Strépy [MWh/ Year]	Peronnes [MWh/ Year]	Ronquières [MWh/ Year]
1	HAWT	3	19.2	113.021	116.010	123.468
2	HAWT	3	15	40.729	41.694	47.468
3	HAWT	3	15	40.380	41.443	47.042
4	VAWT	3	12	53.779	55.062	59.773
5	HAWT	2	20.3	122.378	125.188	133.545

Table 5.15: Properties and AEP of the wind turbines considered for this study.

Discussion of the results The predicted AEPs of turbine 1 and turbine 5 are significantly higher than the other turbines. These results shows the

direct impact of the immature SMWT market. All turbines are listed as 50 kW machines according to the manufacturer. If a non-expert user would randomly select on of these five wind turbines, the difference in predicted AEP could be enormous (the AEP of turbine 5 is more than 3 times the AEP of turbine 3).

One of the benefits of turbine 1 compared to turbine 5, is that it has a MCS (Microgeneration Certification Scheme) certification. Such a certification is an internationally recognised quality assurance scheme. In addition, this turbine also has a de-rated version of 35 kW. Therefore we can assume that limiting the maximum power to the specific demands of the call can be easily done by this manufacturer.

The energy loss of such a de-rated version of turbine 1 (shown in Figure 5.28) is less than 3 % compared to the original turbine. For a de-rated version of turbine 5, the energy loss is about 5 %. As a first estimate of the price[3] of one turbine shows a similar price ($\pm$ 220-240 k€, excluding installation, grid connection and foundation) for both turbines, the turbine is MCS certified and a de-rated version can be conducted by the manufacturer, we pinpointed turbine 1 as the most suitable turbine for the wind farm.

5.8 Conclusions

In this chapter, we have shown that the available wind resources in rural areas in Flanders and Wallonia at low height (10 m) vary from poor (about half the sites has a mean wind speed below 3.6 m/s) to favourable (up to 6 m/s). For the better half of the sites, and provided that a good small or medium-sized wind turbine is chosen, the dynamic payback time is as low as 5 to 8 year for SMEs (and even 4 year at Zeebrugge). For private persons, the payback times are invariably larger (10 year was the best result), mainly due to limited subsidies and the low electricity price. A wind map of Flanders serves to illustrate these findings.

To construct these conclusions, we performed wind measurements at five locations throughout Flanders. We also used long-term wind speed data from meteorological stations, either to normalise our own measurements using MCP or directly to estimate the AEP. The AEP prediction

---

[3]It was beyond the scope of this study to assess the economic viability of the turbines. As the purpose of this study is to install a complete wind farm, most likely the total cost of the wind farm will be agreed upon negotiation with the manufacturer/distributor of the turbines.
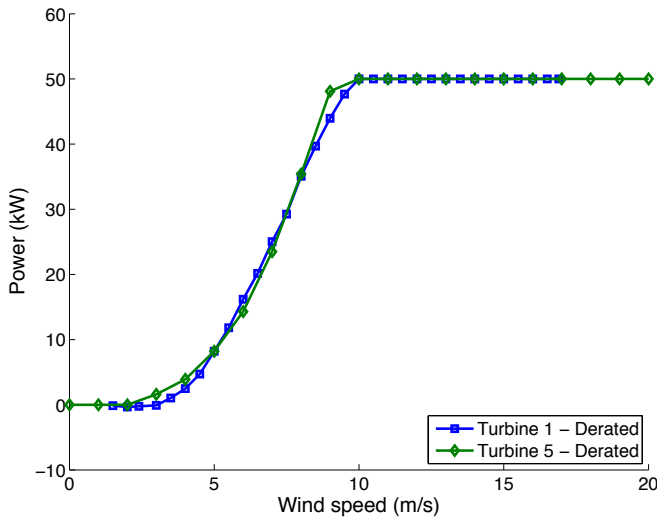
Figure 5.28: Power curves of the de-rated version of turbine 1 and 5.

was performed for a selected set of wind turbines from our database. We restricted ourselves to turbines with independently-tested power curves and for which the investment cost is known. We also performed a market survey to assess the socio-political acceptance of small and medium-sized wind turbines in Flanders.

Apart from the vertical extrapolation from measurement height to hub height, we applied our principles and recommendations from the previous chapters. We have showed how a micro-siting study can be executed using CFD simulations at a marginal cost, but to great advantage (avoidance of shadow zones, exploitation of local acceleration regions). We have demonstrated how AEP predictions can be translated into economic measures, and how sensitive these measures are to variations in electricity consumption. The difference in dynamic payback time between SMEs and private persons is enormous. We also show that de-rated turbines are a very useful option in moderate wind climates such as the rural areas in Flanders and Wallonia. These conclusions can make a future wind turbine project tip from economic nonsense to sense.

Chapter 6

Feasibility of small and medium-sized wind turbines in urban areas

Abstract—*We study the feasibility of small and medium-sized wind turbines in urban areas, with Brussels as the central case in this chapter. As in the previous chapter on rural areas, we demonstrate the wind potential in physical (AEP) and economic terms, illustrate how micro-siting can be done to advantage, and study the technical feasibility.*

The main novelty of this chapter lies in the combination of rooftop wind measurements, CFD analysis, and a study of technical aspects to formulate the economic viability of small and medium wind in Brussels (and similar cities worldwide). Also, the wind map of Brussels is an important contribution.

A major barrier for the deployment of wind turbines in urban areas is the difficulty in estimating the wind potential and the optimal placement for the wind turbines. Authors such as Islam, Saidur, and Rahim (2011) and Cabello and Orza (2010) assessed the wind energy resources in urban environments and measured them on one specific location. Millward-Hopkins et al. (2013b), Drew, Barlow, and Cockerill (2013) and Sunderland, Mills, and Conlon (2013) apply different methods to estimate the wind potential in a broader area. They apply different implementations of the so-called 'wind atlas methodology' (Landberg et al., 2003).

6.1 Wind map of Brussels

We created a map of the above-roof mean wind speed for the whole of Brussels based on an analytical method (as illustrated by the UK Met Office (Best et al., 2008; Landberg et al., 2003)). This methodology uses detailed geometrical data describing buildings, constructions and city topography to predict the aerodynamic characteristics of the urban environment. Next, an available measured wind speed (typically from meteorological stations, thus at low height and outside the urban environment) is scaled up to the geostrophic wind, where the height at which the frictional effect of the surface is negligible. This geostrophic wind speed is then scaled down again accounting for the effect of the surface roughness (determined in step 1) on the wind profile. This process is repeated for different locations in Brussels on a grid of 100 m by 100 m zones.

The roughness characteristics in urban terrain are typically quantified using the roughness length z_0 and the displacement height d; Eq. (1.10) governs the vertical wind profile. At meteorological stations, the roughness length is generally low (below 0.1 m) and thus the influence of the urban surface is assumed to be negligible there. The logarithmic profile with a reference value for open terrain (Wieringa, 1992) is used for the up-scaling procedure in step 1. The wind speed at the top of the urban boundary layer V_{UBL} is then defined as:

$$V_{\mathrm{UBL}} = V_{\mathrm{ref}} \frac{\ln(z_{\mathrm{UBL}}/z_{0\mathrm{ref}})}{\ln(z_{\mathrm{ref}}/z_{0\mathrm{ref}})} \tag{6.1}$$

where V_{ref}, z_{ref} and $z_{0\mathrm{ref}}$ are respectively the mean wind speed, the measurement height and the roughness length of the reference meteorological station. This boundary layer height z_{UBL} is dependent on the terrain, though it is usually set to a constant to value of 200-250 m (Landberg et al., 2003).

In step 2, the wind velocity at the top of the urban boundary layer is scaled down to the blending height z_{blending} on the regional scale (this area is chosen at ≈ 1 km^2 according to the literature (Bottema and Mestayer, 1998)). For each region, the aerodynamic parameters such as the roughness length (z_{0fetch}) and the displacement heights (d_{fetch}) are determined. The exact procedure we adopted to determine these roughness parameters is explained in the next paragraph. Next the down-scaling process is performed by:

$$V_{\text{blending}} = V_{\text{UBL}} \frac{\ln((z_{\text{blending}} - d_{\text{fetch}})/z_{\text{0fetch}})}{\ln((z_{\text{UBL}} - d_{\text{fetch}})/z_{\text{0fetch}})} \tag{6.2}$$

where the blending height is defined as 2 times the maximum building height in the specific region (Best et al., 2008).

Finally, the velocity at the blending height is scaled down again to the above-roof height, i.e. the expected hub height of rooftop-mounted turbines, z_{hub}, but now using roughness lengths and displacement heights (z_{0local} d_{local}) adapted to the local area in the surrounding 100 m by 100 m area. This local down-scaling process is given by:

$$V_{\text{hub}} = V_{\text{blending}} \frac{\ln((z_{\text{hub}} - d_{\text{local}})/z_{\text{0local}})}{\ln((z_{\text{blending}} - d_{\text{local}})/z_{\text{0local}})} \tag{6.3}$$

This means that, if we want to create a wind map of a greater area, it has to be divided into a grid (as shown by Drew, Barlow, and Cockerill (2013) and Bottema and Mestayer (1998)) first on a regional scale of ≈ 1 km^2 and after that on the local scale of 100 m by 100 m. This 'Wind Atlas Methodology' is summarized in a schematic diagram in Figure 6.1.
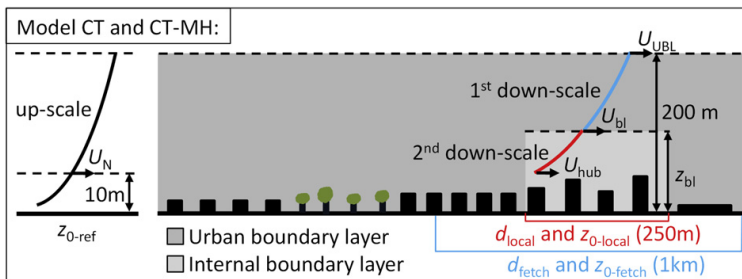

Figure 6.1: Schematic diagram of the wind atlas methodology (Millward-Hopkins et al., 2013a).

Determination of the aerodynamic parameters   Different methodologies to determine the aerodynamic parameters can be followed depending on the resolution and the level of detail of the available data. Here a classical method (Macdonald, Griffith, and Hall, 1998) is used that only requires a basic description of the buildings in the city. The method uses the average building height H and the building density λ_p. This building density is determined by:

$$\lambda_p = \frac{A_p}{A_d} \tag{6.4}$$

where A_p is the total area covered by the obstacles and A_d is the total considered area. Combining H and λ_p, the aerodynamic parameters can be determined using Figure 6.2 (λ_p is in this figure referred as Area density). The figures indicate that the d/H ratio increases with increasing building density. The z_0/H ratio on the other hand shows a peak around an intermediate level of the building density.
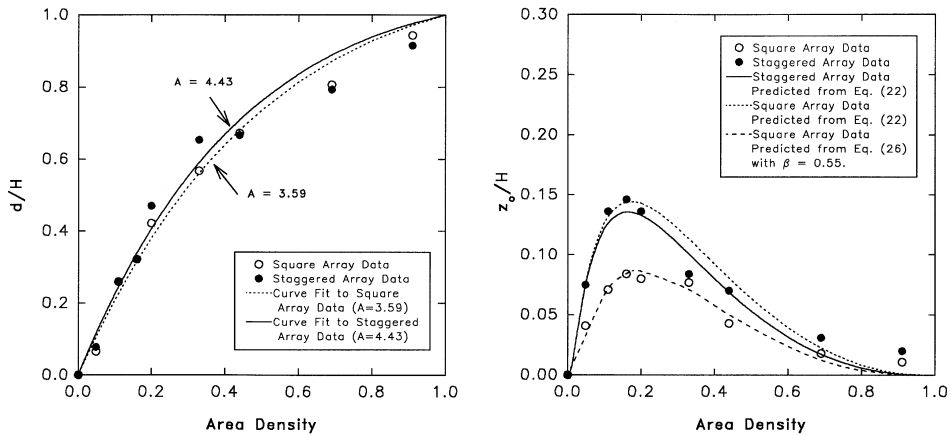
Figure 6.2: Determination of the aerodynamic parameters (Macdonald, Griffith, and Hall, 1998).

This behaviour has been linked to different flow regimes of the air around obstacles. These regimes are shown in Figure 6.3.

When the building density is low, the roughness elements are isolated, in the sense that each building is out of the wake of the building nearby. At intermediate densities there is wake interference, so that the wind does not have the space to fully recover to its undisturbed profile. At high densities
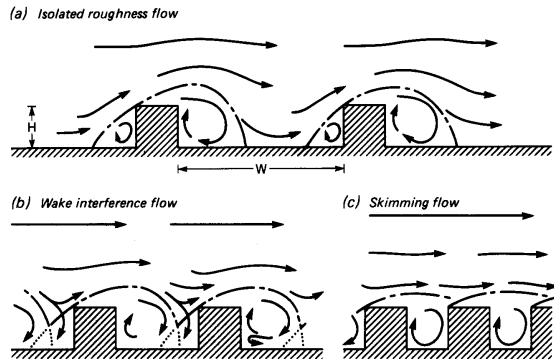
Figure 6.3: Isolated, wake and skimming flow (Oke, 1988).

skimming flow occurs, in which the roughness elements block the wind at the canopy level (or mean building height) and the origin is displaced upwards near the canopy height.

Thus for each scale (regional and local) the mean building height H and the building density λ_m within a certain cell is determined. Combining these parameters, Figure 6.2 can be used to derive the aerodynamic parameters $z_{0\text{fetch}}$ and d_{fetch} on a regional scale, $z_{0\text{local}}$ and d_{local} on the local scale.

Maps of the building height and density, roughness, and wind speed in Brussels We applied the 'wind atlas methodology' by converting geometrical data describing buildings and city topography from the NGI (Nationaal Geografisch Instituut Belgium) to a grid. First the map is used to determine the mean building height H for each 100 m by 100 m cell (local scale), as is shown in Figure 6.4 (left). The figure shows that the average building height in Brussels is higher in the city centre than near the borders. In this region the average building height is in the 30-50 m range, while an average building height of 10-20 m is typical for Brussels. With the maximum average building height we can derive the proper boundary layer height z_{UBL}. We set this at a constant value of 250 m which is about 3 times the maximum average building height. In the figure the blank regions indicate where the average building height is zero. In these regions, no buildings (such as parks, squares,...) are present and this areas could not be treated by the approach. Also the building ratio is determined for
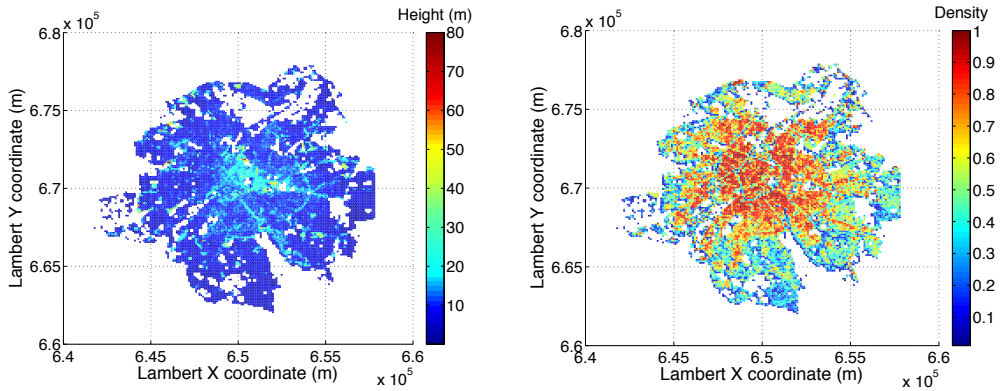
Figure 6.4: Average building height (Left) and building density (Right) of Brussels.

each cell (Figure 6.4, right panel).

Next, the average building height and building ratio are combined to determine the aerodynamic parameters (z_{0fetch} and d_{fetch}) on a regional scale (1 km by 1 km). These parameters are derived from Figure 6.2. With these parameters, the wind speed measured at the meteorological station is scaled up to the boundary layer height and scaled down again to the blending height. Now the aerodynamic parameters (d_{local} and z_{0local}) are calculated on a local scale. In Figures 6.5 these parameters are shown. The roughness in Brussels varies from 0.1 to 2.5 m with typical values below 1 m.
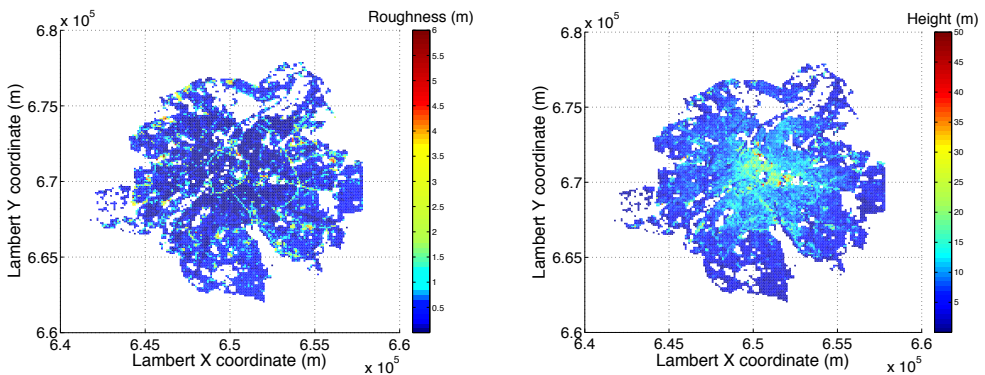
Figure 6.5: Roughness map (left) and displacement height (right) for Brussels.

Away from city the roughness length is zero, because no building data

were available for these regions. In the roughness map, some roads are visible as regions of high roughness. This is caused by the relatively lower building density in a region with a high mean building height, which leads to higher roughness values. In this region a wake flow regime occurs (see Figure 6.3). For the displacement height, obviously higher values are derived in the city centre. If the predicted roughness lengths are compared to typical values of urban environments (Wieringa, 1992), it seems that the method tends to underestimate the aerodynamic roughness. The approach provides good trends, but overall the values are too low. It is possible to find regions in the map with aerodynamic roughness below 0.15, which is impossible for urban areas. These errors are due to the simplicity of the method used for the calculation of the aerodynamic parameters, that only considers two input parameters: building-to-area ratio and average building height. This implies that for the calculation of the parameters the effect of vegetation and the shape of the urban features are not considered. As this wind map is used as a guideline to identify regions with a higher wind potential rather than using them for an accurate prediction of the mean wind speed, this approach suffices.

Using the local aerodynamic parameters, the wind speed is scaled down from the blending height to the average building height. In Figure 6.6 the wind speed is calculated at 10 m above the average building height for Brussels. (As before, the blank regions in the figure indicate where no wind speed could be calculated. As these open regions are located near buildings and the total height (10 m above the ground surface) is relatively low, these are less interesting locations to install small-scale wind energy systems.) In and near the city centre, the mean wind speed goes up to about 4.5-5 m/s, which is a wind speed generally measured at low heights close to the North Sea (which is considered to be a wind-rich region (Troen and Petersen, 1989)). It should be noted that the wind map as such should not be used separately from the average building height. For areas with a low average building height and for example one high-rise, the wind map will indicate a low value of the wind speed (lower on the vertical wind profile) although the average wind speed above the high-rise could be high.

Validation of the wind map   In order to validate the applied procedure, we have compared our wind map to measured wind speed data. These wind speed measurements are described in more detail in Section 6.2, but we use them here to validate the wind map.

We used the average wind speed measured at five sites to compare to
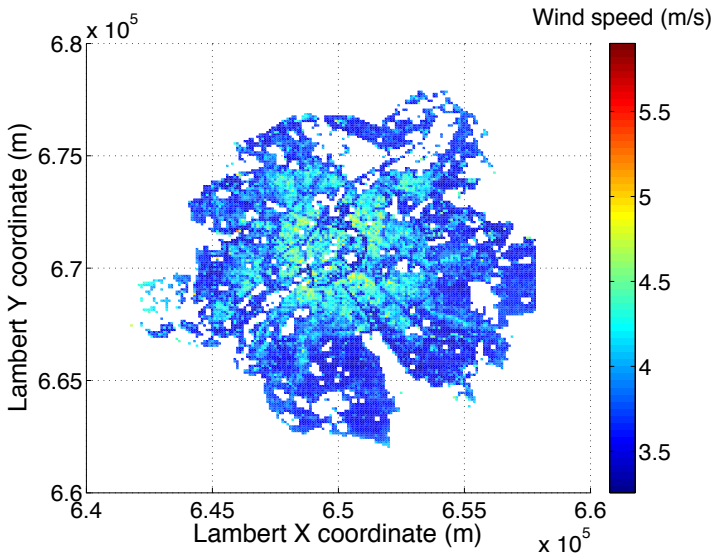
Figure 6.6: Wind map of Brussels

the wind speed estimated by the analytical methods. We emphasise that a different average wind speed is used for the upscaling procedure from the meteorological station to the geostrophic wind in the validation process. The average wind speed from the meteorological station is recalculated for the concurrent measurement period in order to ensure a proper validation of the procedure. For the downscaling process, we used the analytical procedure to derive the wind speed at the measurement height and not at 10 m above the mean building height (as is done for the wind map).

In Table 6.1, the regional and local aerodynamic parameters and measurement heights are shown. While the regional roughness lengths show values that normally can be expected in urban areas (Wieringa, 1992), the table shows relatively low values for the local roughness z_{0local}. For the Elia and ULB sites (see 6.2 for a description of the sites), extremely low values were found. As mentioned above, this is caused by the simplicity of the methodology. The Elia and ULB site are located nearby parks (with small forests) or industrial areas. In these areas, the mean building height is quite low as not all individual obstacles are modelled. For the Port of Brussels, the low roughness length could be explained by the presence of the canal, leading to a low building height. The values of The Hotel and the Manhattan tower are more in line with what is expected in city centres

(and for skimming flow patterns).

Location	Height	Aerodynamic parameters			
	[m]	$z_{0\text{fetch}}$ [m]	d_{fetch} [m]	$z_{0\text{local}}$ [m]	d_{local} [m]
Elia	59	0.19	1.26	0.001	0.02
Hotel	103	0.21	13.35	0.13	15
ULB	41	0.64	6.77	0.06	0.26
Manhattan	118.5	0.22	13.24	0.41	17.5
Port	12	0.21	9.85	0.08	9.6

Table 6.1: Aerodynamic parameters and measurement height above ground level for the five measurement locations.

In Figure 6.7 (left), the predicted and measured wind speeds are compared. Except for the Port of Brussels, the wind speed is overestimated. In right figure, the absolute error is shown. For the Elia-site and The Hotel, the absolute errors are below 5 %. For the other sites, the errors are much higher with a range of 20 to 25%.
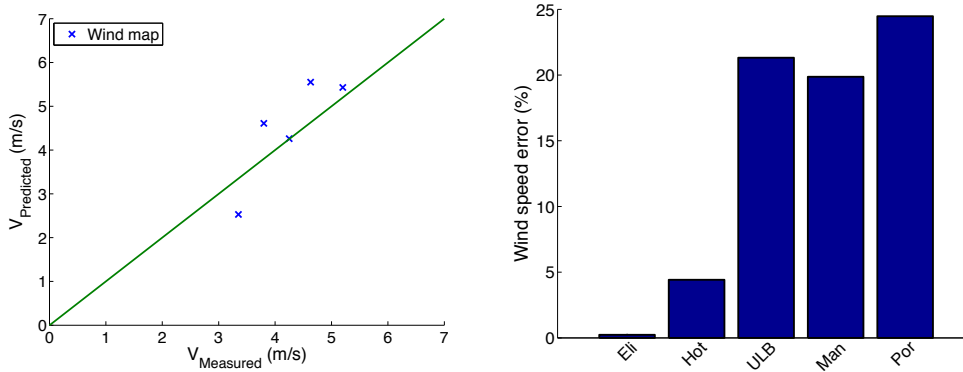
Figure 6.7: Validation of the wind map by comparing the predicted and measured wind speed for five measurement sites.

We conclude that a wind map is a good tool to provide a global overview of the wind situation. However, wind measurements are always necessary to ensure a reliable prediction of the AEP. The wind atlas approach tends to overestimate the wind speed, as a result of underestimated roughness lengths. For two sites of the five sites we validated, the error is below 5 %. For the other sites, the errors are in the order of 20 %.

6.2   Wind measurement campaigns in Brussels

To prepare an analysis of the economic viability of small and medium wind in the Brussels Capital Region, we performed wind measurements at multiple sites throughout the city. We first investigated a long-list of more than 100 possible measurement sites for the practical feasibility of installing measurement equipment. We considered open surface sites (for ground-based turbines) as well as tall buildings (for rooftop mounting). More than ten sites were visited to inspect for accessibility, presence of existing masts or structures, presence of obstacles. Eventually four measurement sites were selected: two on the rooftops of high-rises, one site near ground level (on a lighting pole of 12 m height) and a 72 m mast (which was suited for an extended campaign at multiple levels). In addition to these four sites where we performed the measurements, the company 3E provided us with access to wind measurements that they performed in the city centre (Guidon, 2011). These measurements were added to the data considered in the economic analysis. The five sites are geographically well distributed throughout Brussels:

- The Hotel, Waterloolaan 38, 1000 Brussel (50.837553°N, 4.357487°O)

- ULB Campus Solbosch, building D, Antoine Depagelaan 27, 1050 Elsene (50.811469°N, 4.383593°O)

- De Haven van Brussel, Redersplein 5, 1000 Brussel (50.864807°N, 4.352529°O)

- Elia, Vilvoordselaan 126, 1030 Schaarbeek (50.880601°N, 4.380237°O)

- Manhattan, Rogierplein 3, 1210 Sint-Joost-Ten-Node (50.856902°N, 4.358215°O)

In Figure 6.8 the locations of the measurement sites are shown on a map of Brussels.

More details on the measurement sites can be found in (Runacres, Vermeir, and De Troyer, 2014).

6.2.1   Data analysis and presentation

In Table 6.2 the measurement results for each site are given. In the table, the height represents the measurement height measured from the ground
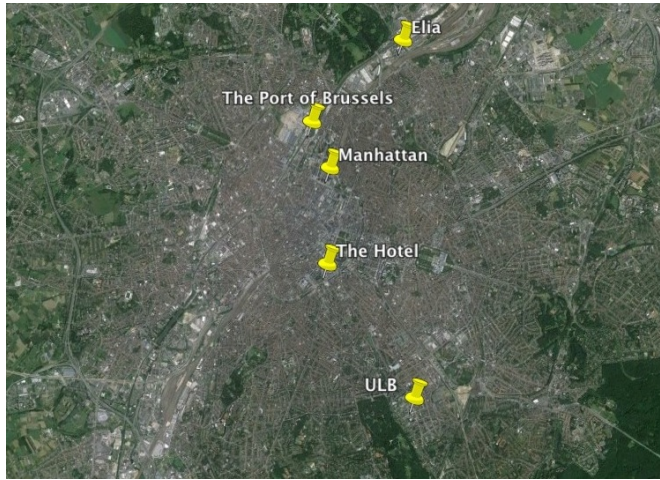
Figure 6.8: Location of the five measurement sites in the Brussels Capital Region.

level. For each site, a Weibull distribution is fitted to the data and the shape, k, and scale, c, parameters are shown in the table. Here, we used the Moment Method (see Chapter 3) to determine these parameters. The coefficient of determination or R^2 value then indicates how well the data fit the Weibull distribution.

Site	Height [m]	$\overline{V}$ [m/s]	Dominant wind direction	k	c	R^2	Meas. period [Months]
Hotel	103	5.8	W	2.187	6.580	0.987	13
ULB	41	4.3	WSW	2.371	4.803	0.973	10.5
Port	12	3.8	SW	2.034	4.290	0.963	7.4
	10	3.7	SW	2.120	4.171	0.956	7.4
Elia	59	5.2	S	1.958	5.826	0.988	6.5
	43	4.7	S	1.960	5.310	0.986	6.5
	24	3.8	S	1.793	4.270	0.980	6.5
Manh.	119	4.7	SW	1.899	5.206	0.984	13
	112	4.6	SW	1.806	5.121	0.985	13

Table 6.2: General results of the measurements performed in the Brussels Capital Region.

Only for The Hotel, the wind speed is measured for over 1 year. This

site shows the highest wind potential with a mean wind speed of 5.8 m/s. The wind speed at the Port of Brussels is 3.6 m/s, what is markedly higher than what normally can be expected at lower heights in urban areas. Due to the good (southwest to northeast) orientation of the Canal, the wind speed is locally increased by a concentrator effect. This hypothesis is confirmed by the wind rose, in which the orientation of the Canal is clearly visible (see Figure 6.9). For more than 80 % of the time, the wind direction is southwest or northeast. The hypothesis is also supported when comparing the wind speed at the Elia-site and the Port of Brussels (which are located quite close to each other and share the same topographical height). The average wind speed at 12 m for the Port of Brussels is equal to the one for the Elia-site at 24 m, for about the same measurement period.
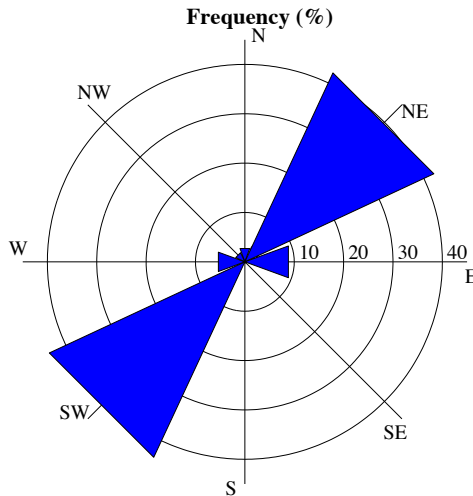
Figure 6.9: Wind rose of the frequency of occurrence for each wind direction for the Port of Brussels.

The Elia-site has the shortest measurement time. Our review of the MCP (Chapter 3) showed that if a measurement period of 6 months is used and these data are used to estimate the AEP, the mean error is approximately 5 %. In addition these data are collected in a favourable period (winter months) and so lowering this mean error. We can thus conclude that even for the Elia-site (with the shortest measurement time), an accurate estimate of the wind potential can be made.

In Figure 6.10, the average wind speed per measurement site and per

month is shown. If the wind speed was measured at different heights, only the highest measuring point is shown for that particular site. For all sites, the average wind speed in October 2013 and the period from December 2013 to February 2014 is significantly higher than other months. The lowest wind speeds are measured in July and August 2013. As the measurements at the Manhattan tower were performed during a different time period, the average wind speed per month is shown in a different figure (Figure 6.10, right panel). It is noticed that the monthly variation of the average wind speed is lower. To verify if this could be explained by the seasonal variation in the year 2010-2011 rather than a terrain effect (for example a building upstream blocking a dominant wind direction), we used data from three nearby measurement stations. We compared this particular period to the same period for other years (1999-2010) and averaged the wind speed over the measurement stations for each month. This comparison is shown in Figure 6.11. This figure indeed confirms that the wind speeds were lower in the winter of 2010-2011, leading to a weaker seasonal variation.
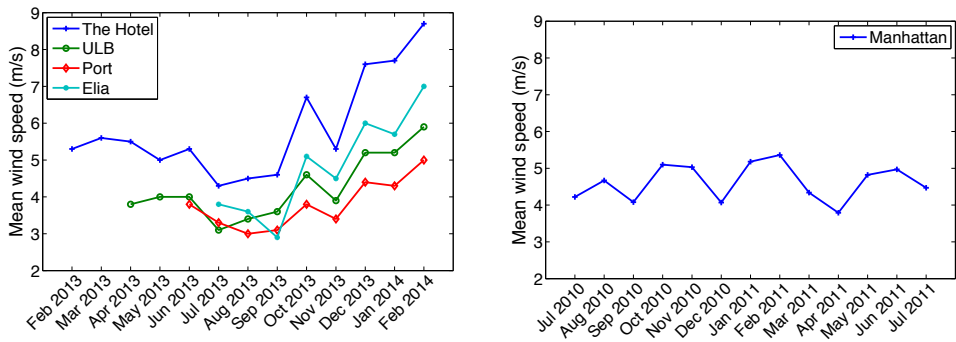
Figure 6.10: Monthly average wind speed for The Hotel, ULB, Port and Elia (left) and the Manhattan tower (right). Only the highest measurement height is shown on the figure (if measured at multiple heights).

Derivation of the roughness length and turbulence intensity from the measurements At the Elia-site and the Port of Brussels, the wind speed is measured at different heights and thus the vertical wind profile can be estimated. We use the same equation to estimate the roughness
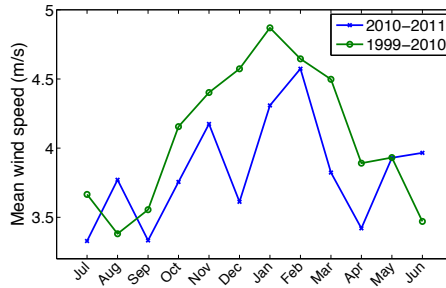
Figure 6.11: Monthly average wind speed of three meteorological station for the measurement period on the Manhattan Tower (2010-2011) and the same period for other years (1999-2010) . The data are averaged over the three measurement stations.

parameters as presented in Chapter 5 (and derived in Chapter 1):

$$z_0 = \frac{z_1^{\frac{V_2}{V_2 - V_1}}}{z_2^{\frac{V_1}{V_2 - V_1}}} \qquad (6.5)$$

The wind profile at the Port of Brussels is defined by a roughness length z_0 of 0.02 m and a friction velocity v^* of 0.24 m/s. On the Elia-site, the top and lowest anemometers are used to derive the roughness parameters. The parameters are estimated at 2.1 m for z_0 and 0.64 m/s for v^*. The roughness length for the Elia-site is thus significantly larger than for the Port of Brussels. This could be explained by the fact that the Port of Brussels is located near the Canal, where roughness tablesindicate a lower value for z_0. For the Elia-site, many urban obstacles such as antennas, a bridge, cranes and low buildings with a relatively large interspacing are present. Here, an isolated roughness flow will occur (see Figure 6.3) explaining the large value for z_0.

The average turbulence intensity is determined for each site using the standard procedure (IEC, 2006) and the standard time interval of 10 minutes. In Table 6.3 these results are presented. The level of turbulence is similar for all sites, except for the Elia-site and Manhattan tower where the turbulence intensity is slightly lower. For all sites, the values are relatively high. For the Port of Brussels, the wind speed is measured close to the ground in an urban area and thus such a high value is expected. The turbulence level at the ULB-site and The Hotel should normally be lower because they are measured at larger heights. The higher turbulence

is caused by the small distance between the rooftop and the anemometer. The micro-siting CFD study (see Section 6.4) will show that for The Hotel, the recirculation region at the centre of the roof is 12.3 m, while the measurement height is just 7 m. The anemometer is thus measuring the wind speed in the wake of the building. This causes the high turbulence level. The turbulence intensity of The Hotel and Elia-site are shown in Figure 6.12.

Site	Height [m]	Turbulence intensity [%]
Hotel	103	25.7
ULB	41	25.2
Port	12	26.9
	10	28.4
Elia	59	22.0
	43	24.1
	24	28.5
Manh.	119	20.0
	112	22.1

Table 6.3: Turbulence intensity for each measurement site using a time interval of 10 minutes.

6.2.2 Brussels' long-term wind potential

The long-term wind potential is assessed by applying the VR MCP method (see Section 3.6) using four MERRA (Modern-era retrospective analysis for research and applications, 2014) data sets. These MERRA data are generated by combining measurements and meteorological models, and represent the long-term wind climate with meteorological parameters such as wind speed, wind direction, temperature, etc. for different longitudes and latitudes. For this particular study, four points in the model are located close to Brussels and these are used for the extrapolation. The locations are shown in Figure 6.13.

The measurement period of these MERRA data is 31 January 1994 to 31 January 2014. Using these data, an estimate can be made of the wind speed and annual energy production of a wind turbine for a period of 20 years (what is generally assumed as the lifetime of small or medium wind
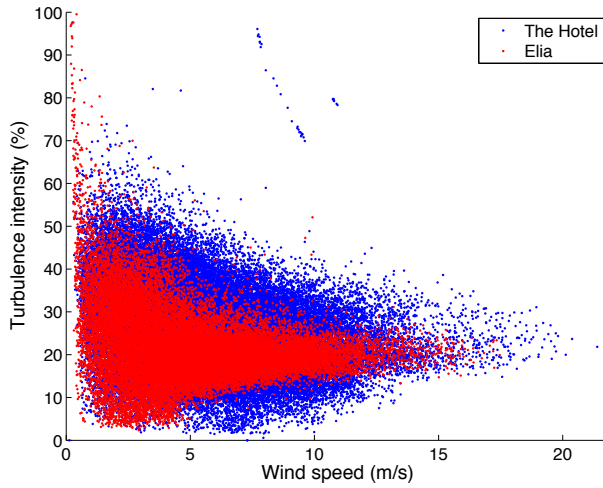
Figure 6.12: Turbulence intensity (interval of 10 minutes) as a function of wind speed for The Hotel and Elia-site.

turbine). Before applying the MCP procedure, the correlation coefficient R between the measured and concurrent data sets has to be determined. The data set with the highest correlation coefficient will be used for the extrapolation.

In Table 6.4 the results of the MCP method are shown. The table indicates the MERRA data set with best correlation for the concurrent measurement period. The results show that all the measurements are performed in windy periods as the wind speed decreases when they are extrapolated to the 20-year dataset. Particularly for the Elia-site, where 4 of the 6 months are windy months, a significant decrease in the average wind speed is determined. The correlation coefficient for the Port of Brussels and Elia is slightly lower, although it is still considered as a strong correlation coefficient for MCP purposes (Weekes and Tomlin, 2014a; Rogers, Rogers, and Manwell, 2005).

6.3   Economic feasibility of SMWT in Brussels

In this section we use our measurements from Section 6.2 to assess the economic feasibility of small and medium wind turbine projects in Brussels. We therefore select three small wind turbines based on several criteria. To
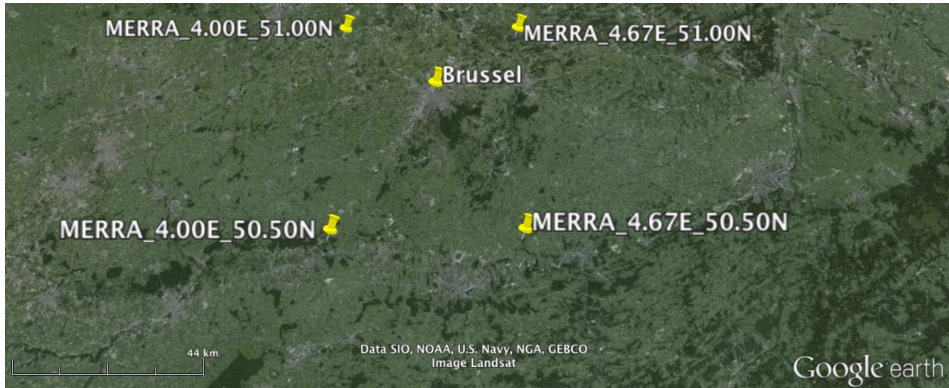
Figure 6.13: Location of the long-term data sets.

Site	MERRA data set	R	$\overline{V}_{\text{Measured}}$ [m/s]	$\overline{V}_{\text{Long-term}}$ [m/s]
Hotel	4.67E 50.5N	0.8790	5.8	5.6
ULB	4.67E 51N	0.8463	4.3	4.1
Port	4.67E 51N	0.7248	3.8	3.6
Elia	4.0E 50.5N	0.7889	5.2	4.4
Manhattan	4.67E 51N	0.8236	4.7	5.0

Table 6.4: Results of the MCP method for the measurement sites in Brussels.

also have an idea about the economic viability of medium wind in Brussels, one medium wind turbine is added to the analysis. By combining the power curve with the long-term wind speed data set, the annual energy production is estimated over the expected lifetime for each turbine and measurement site. This energy yield is then used as an input for the economic analysis. The profitability of a small or medium wind turbine project is then described by the payback period and internal rate of return. Both economic measures are determined for private persons as well as for small and medium enterprises (SMEs).

6.3.1 Selection of the sample turbines

As in Chapter 5, we first make a long-list of turbines with independently-tested power curves and for which price information was known. In Table 6.5 these turbines are listed and numbered for further analysis. Then we calculate the AEP and the LCOE according to the recommendations

of Chapter 3. In Figure 6.14, the average LCOEs (averaged over the measurement sites) are shown.

	Rated Power [kW]	Rotor-diameter [m]	Hub height [m]
1	0.9	2	13.7
2	1	1.2	6.1
3	2.2	3.7	12
4	2.5	4	18
5	3.2	4.4	12
6	3.2	4.1	15
7	4.7	5.5	18
8	5.2	5.6	9
9	5.4	6.4	28
10	5.5	6.2	18
11	5.7	6.3	14
12	7.6	8.5	25
13	9.1	7.2	25
14	9.8	8	18
15	10.1	13.2	18

Table 6.5: Database of small wind turbines used in this feasibility study. All wind turbines are horizontal axis wind turbines except number 2, which has a vertical axis.

In a next step, the database was further reduced by rotor diameter. We restricted the rotor diameter to 6.5 m. After this analysis, three wind turbines are selected to use further in the feasibility study. They are chosen because of their different properties:

- one vertical axis wind turbine to reduce the visual impact,

- one turbine with the lowest LCOE and

- one turbine with a decent LCOE but with a smaller size to simplify a possible implementation on the roof of a building.

As currently there is only one wind turbine on the market with a vertical axis combined with a certified power curve, this turbine is selected even though the efficiency of the turbine is low. Turbine 11 on Figure 6.14 has
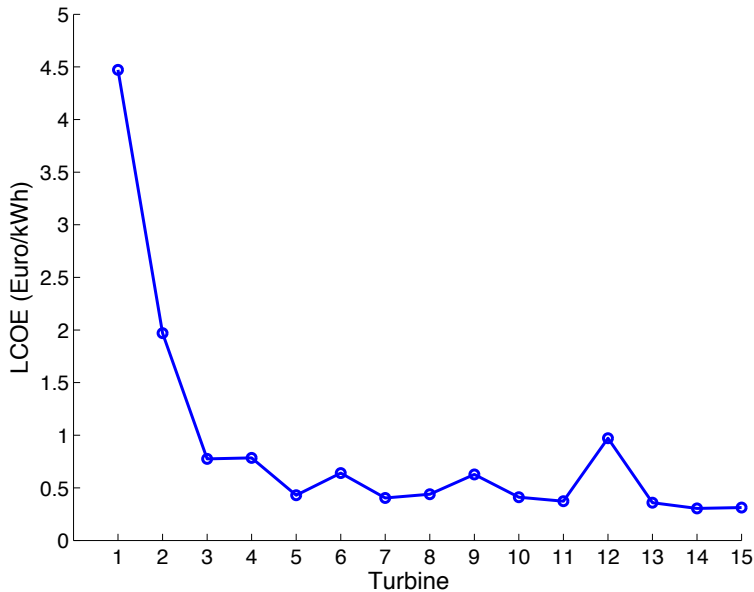
Figure 6.14: Average LCOE for each turbine in the database. The LCOEs are averaged over all measurement sites and used to select three small wind turbines.

the lowest LCOE for rotor diameters smaller than 6.5 m. This figure also shows a decent LCOE for turbine 5 taken the lower rotor size into account. The three small wind turbines selected for this analysis are the numbers 2, 5, and 11. As mentioned above, to analyse the economic viability of medium wind turbines, one medium wind turbine is added (number 16 in our analysis). This turbine has a rotor diameter of 23 m and a rated power of 100 kW. Due to the size of the turbine, it cannot be installed on the roof of a building. This turbine does not have a certified power curve.

6.3.2 Long-term annual energy production

In Table 6.6, the predictions of the AEP are shown for each of the selected wind turbines. To avoid to extrapolate the wind speed before estimating the AEP, only measured wind speeds are used. Therefore it is not possible to determine the AEP for each individual wind turbine and site. We make the following remarks:

- For The Hotel, the ULB-site and the Manhattan tower, installing a medium wind turbine on the roof is not technically feasible without

changing the structure of the building. Therefore the AEP of the turbine 16 is not estimated.

- For the Port of Brussels, the AEP was only determined for the small wind turbines using a hub height of 12 m. The extrapolation to 40 m (the hub height) of the medium wind turbine is not 'bankable' and could impose a significant error on the predicted AEP (Chapter 3).

- For the Elia-site, the AEP for the small wind turbines is predicted at 24 and 59 m. Installing a small wind turbine with a hub height of 59 m has no economic sense, though here the wind data is used as if the turbine would be installed on a hypothetical rooftop. As the hub height of turbine 16 is normally 40 m, the AEP is only estimated at 43 m for this turbine.

Site	Height [m]	T2 [kWh/year]	T5 [kWh/year]	T11 [kWh/year]	T16 [kWh/year]
Hotel	103	1776	8173	14201	\
ULB	41	459	3041	5202	\
Port	12	353	2582	4247	77695
Elia	24	302	1956	3322	\
Elia	43	\	\	\	111160
Elia	59	941	4804	8280	\
Manhattan	119	1384	6526	11255	\

Table 6.6: Annual energy production for the four selected wind turbines.

6.3.3 Discussion of the economic parameters

Investment cost

The total investment cost of a wind turbine depends on many factors including the site of installation. The foundation of a turbine for example is dependent of the type of the terrain, accessibility and the soil. As in this stage it is difficult to determine these costs for each individual turbine and site, we give a generic estimate for each turbine in Table 6.7. A distinction is made between turbines installed on ground level, on a rooftop with a crane and without a crane. The installation cost for a ground mounted turbine is the same as when it is installed without a crane. In this case, the turbine has no need for a concrete foundation but it is anchored to the

roof. We estimate that the cost for anchoring the turbine would be equal to using a concrete foundation. The turbine can be transported to the roof with the building elevator (with a modular mast in smaller sections) or with other lifting mechanisms (such as the steeplejack to clean the building's windows). The installation cost when using a crane is larger and will have a significant impact on the payback period and IRR. The lifetime and maintenance cost are given by the manufacturer.

Turbine	T2	T5	T11	T16
Purchase	€7500	€15000	€30350	€290000
Installation ground level	€3000	€5500	€6500	€36000
Installation rooftop w/o crane	€3000	€5500	€6500	\
Installation rooftop w/ crane	€8000	€10500	€11500	\
Maintenance cost	1% Purchase per year	2% Purchase per year	€200 per year	€5200 per year
Lifetime	15 years	20 years	20 years	20 years

Table 6.7: Investment, maintenance and installation cost and lifetime of each wind turbine considered in the feasibility study.

Electricity price

The payback period and IRR are determined for private persons as well as SMEs. The electricity price and the energy consumption for both categories is different and has therefore an impact on the analysis. For private persons, the energy consumption is set to 3500 kWh/year. The electricity price in the Brussels Capital Region, as calculated by CREG (CREG, 2014), in February 2014 is 20.93 c€/kWh on average. For SMEs, the energy consumption and electricity price is set to 50000 kWh/year and 16.28 c€/kWh. When the annual energy production is larger than the energy consumption of the user, the electricity will be sold to the grid. A price of 4 c€/kWh is used as selling price.

Incentives

In Belgium and The Netherlands, a green certificate (GC) system is used as initiative to support renewable energy. This system is similar to countries as the UK where feed-in tariffes are used as a support mechanism. Each GC has a guaranteed minimum value and is granted for a fixed amount of produced energy. Both parameters are region-depended. In the Brussels Capital Region 1.81 GC is given for an electricity production of 1 MWh (Brugel, 2013). This support mechanism is limited to 10 years.

For private persons an additional incentive is present in the Brussels Capital Region. The 'Energiepremie' can be granted and returns 25% of the purchase cost of the turbine. A similar incentive is present for SMEs, where a grant of 30% of the purchase cost is available. In addition, a fiscal exemption on taxes of 14.5% of the purchase cost can be used for these SME. A limitation to these incentives is €80000 per year and per SME.

Other parameters

Finally, other economic parameters are taken into account, such as:

- An inflation of 2% is used;

- Increase in electricity price per year is set to 3.5%;

- The discount rate is set to 4%.

These values are frequently used in feasibility studies (e.g. Mermuys (2010)).

6.3.4 Results and conclusions

In Tables 6.10 and 6.8 the static and dynamic payback periods and the IRR are shown for each site and each case. Negative values for the IRR and payback periods above the lifetime of the turbine are indicated with resp. N/A and >20 years in the table.

In general, The Hotel and the Manhattan tower are the best sites to install a small wind turbine. For none of the studied measurement sites and cases, the dynamic payback period of turbine 2 is below its lifetime. This turbine is therefore not suitable. Turbine 5 and 11 are both good and profitable turbines for SMEs and private persons when they are installed on a windy site. For turbine 11, the payback period can be as low as 7 years when it is installed without a crane.

The need for a crane has a significant impact on the profitability of the investment. The installation cost can then take import fractions of the total investment cost. When it is needed, the possibility of installing multiple turbines should be considered. This lowers the total installation cost and will consequently decrease the payback period and will enlarge the IRR.

At first sight, installing a medium wind turbine on one of the selected locations doesn't seem to make economic sense. However if an SME installs turbine 16 on the Elia-site and consumes all the produced electricity, the dynamic payback period decreases from 18 years to just 9 years. Increasing the energy consumption increases the profitability, as the price for selling the overproduced electricity is too low. Therefore, investing in these types of wind turbines is more interesting for SMEs despite the significantly lower electricity price.

Site	z [m]	Crane	SME [%]				Private [%]			
			T2	T5	T11	T16	T2	T5	T11	T16
Hot.	103	Yes	N/A	10.4	14.7	\	N/A	4.0	6.0	\
		No	2.1	15.1	17.2	\	3.5	8.3	7.9	\
ULB	41	Yes	N/A	N/A	0.3	\	N/A	N/A	N/A	\
		No	N/A	N/A	1.6	\	N/A	N/A	N/A	\
Por.	12	No	N/A	N/A	0.2	1.8	N/A	N/A	N/A	N/A
Eli.	59	Yes	N/A	0.3	5.8	\	N/A	N/A	1.1	\
		No	N/A	4.3	7.5	\	N/A	2.5	3.0	\
Eli.	43	No	\	\	\	4.9	\	\	\	N/A
Eli.	24	No	N/A	N/A	N/A	\	N/A	N/A	N/A	\
Man.	119	Yes	N/A	5.9	10.5	\	N/A	1.7	3.8	\
		No	N/A	10.2	12.6	\	0.1	5.3	5.7	\

Table 6.8: Internal rate of return including the incentives such as GCC and the 'Energiepremie'. Negative values for the IRR is indicated with N/A. Not for all sites and turbines an economic analysis is performed. Sites where this is not done are indicated with \.

Site	z [m]	Crane	SME [Years]				Private [Years]			
			T2	T5	T11	T16	T2	T5	T11	T16
Hot.	103	Yes	>20	9	7	\	>20	12	10	\
		No	16	7	6	\	15	9	9	\
ULB	41	Yes	>20	>20	19	\	>20	>20	>20	\
		No	>20	>20	17	\	>20	>20	>20	\
Por.	12	No	>20	>20	19	14	>20	>20	>20	>20
Eli.	59	Yes	>20	17	12	\	>20	17	14	\
		No	>20	13	11	\	>20	14	12	\
Eli.	43	No	\	\	\	11	\	\	\	15
Eli.	24	No	>20	>20	>20	19	>20	>20	>20	>20
Man.	119	Yes	>20	11	9	\	>20	15	13	\
		No	>20	9	8	\	20	11	11	\

Table 6.9: Static payback period including the incentives such as GCC and the 'Energiepremie'. Payback periods above the lifetime are indicated with >20. Not for all sites and turbines an economic analysis is performed. Sites where this is not done are indicated with \.

Site	z [m]	Crane	SME [Years]				Private [Years]			
			T2	T5	T11	T16	T2	T5	T11	T16
Hot.	103	Yes	>20	10	8	\	>20	20	15	\
		No	>20	7	7	\	>20	11	11	\
ULB	41	Yes	>20	>20	>20	>20	>20	>20	>20	>20
		No	>20	>20	>20	>20	>20	>20	>20	>20
Por.	12	No	>20	>20	>20	>20	>20	>20	>20	>20
Eli.	59	Yes	>20	>20	16	\	>20	>20	20	\
		No	>20	20	13	\	>20	17	16	\
Eli.	43	No	\	\	\	18	\	\	\	20
Eli.	24	No	>20	>20	>20	>20	>20	>20	>20	>20
Man.	119	Yes	>20	16	10	\	>20	>20	>20	\
		No	>20	10	9	\	>20	18	17	\

Table 6.10: Dynamic payback period including the incentives such as GCC and the 'Energiepremie'. Payback periods above the lifetime are indicated with >20. Not for all sites and turbines an economic analysis is performed. Sites where this is not done are indicated with \.

6.4 Micro-siting in an urban context

The wind patterns in and around a group of buildings (a *building block*) are generally complex and positioning a wind turbine in such an environment is not straightforward. In the section we show how we used CFD to derive suitable locations for some of the tested sites in Brussels. Often, this concerns the avoidance of the (low-speed and turbulent) wake behind buildings and building. CFD also gives insight in the wind patterns on site, possibly revealing concentrator effects where the wind speed is locally increased. As in rural areas (see Chapter 5), the careful placement of a turbine based on CFD analysis of the envisaged site can determine the economic viability.

Before discussing our CFD results, we briefly introduce some rules of thumb that are often used to derive suitable locations around (or on top of) building blocks. These rules either indicate the optimal placement of a (set of) wind turbine(s) on a rooftop or describe the dimensions of the wake in front, behind and on top of the buildings. In the Wineur project (Caca, 2007) a set of rules of thumb are presented for urban wind turbines. They indicate the optimal placement of a (set of) wind turbine(s) on a rooftop in the urban environment. The rules of thumb are:

- The mast or building should be approximately 50 % taller than the surrounding objects;

- The turbine should be positioned near the centre of the roof;

- The turbine should be positioned on the side of the most common wind direction;

- The lowest position of the rotor has to be above the roof by at least 30 % of the building height;

- If possible, choose a building which front facade is oriented towards the dominant wind direction at the site.

These rules are determined based on measurements, simulations and best practices.

Wegley et al. (1980) determined the size of the wake behind a single building. When the size of the wake is known, a location can be derived to install the wind turbine to avoid most of the adverse effect of the wake. In the literature, general rules determined by Wegley et al. (1980) are frequently used. They advise to site a small wind turbine:

- upwind, at a distance of more than two times the height of the building;

- downwind, at a minimum distance of ten (but preferably 20) times the building height; or

- downwind, but with a height of at least twice the building heigh;

Figure 6.15 illustrates this rule with a cross-sectional view of the wake of a small building. The above rules of thumb are not perfect because the size of the wake also depends upon the building geometry, shape and orientation to the wind. Therefore, different rules of thumb were presented for different types of geometries of the building. Lower buildings allow to install wind turbines closer than ten times the building height. For taller buildings, the minimum distance should be increased to 20 times the building height.
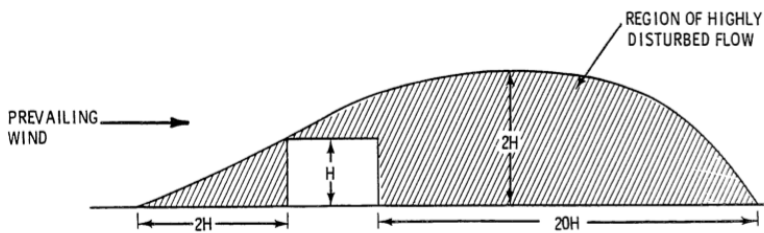

Figure 6.15: Zone of disturbed flow over a small building (Wegley et al., 1980).

6.4.1   Micro-siting of single buildings

Two specific sites in Brussels (identified by the wind map as potentially good locations) and one typical site in Brussels are studied. In this section, we simplify the sites and only simulate the highest building in the area. Each building has a different shape:

- Case 1 is The Hotel (shown in figure 6.16 top left). The Hotel is a building with a height of 94 m, a depth of 17 m and a width of 52 m[1];

---

[1]The wind map estimated the wind speed at 4.2 m/s at 28 m height (average building height 18 m) in the region where this site is located

- Case 2 is one of the SISP buildings in Anderlecht (shown in figure 6.16 top right). The height of the building is 66 m^2.;

- Case 3 is a typical building in Brussels with a height of 20 m (the average building height in Brussels). The width and depth of the building is respectively 30 m and 10 m (shown in figure 6.16 bottom);
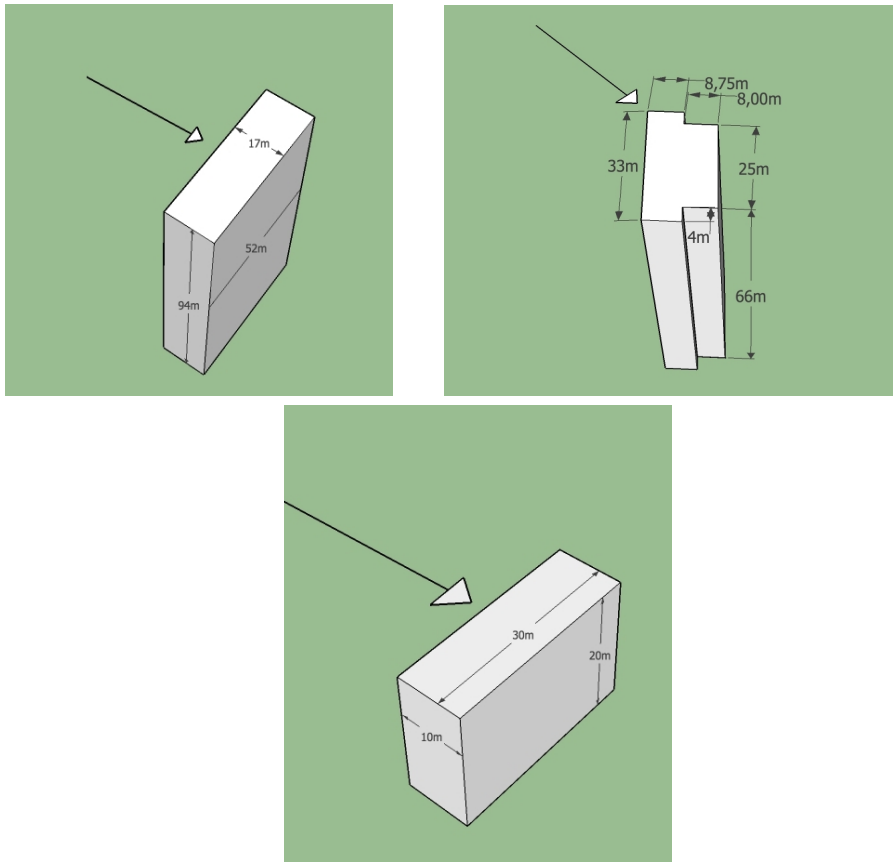

Figure 6.16: Shape of the building and wind direction of the incoming flow for each of the simulated cases (Top right: case 1, top left: case 2 and bottom: case 3).

---

[2]The wind map estimated the wind speed at 3.7 m/s at 14 m height (average building height 4 m) in the region where this site is located

In this study a realistic wind profile and terrain roughness for an urban environment is applied. As shown in Chapter 2 and 5, the CFD software OpenFOAM uses the linear log law, derived by:

$$V(z) = \frac{v^*}{\kappa} \ln \left(\frac{z + z_0}{z_0} \right) \tag{6.6}$$

A wind profile with a roughness length of 0.6 m (a typical value for urban terrain according to roughness tables (Wieringa, 1992)) and a friction velocity of 0.64 m/s is applied. For the first two cases, the incoming wind direction is southwest as this is the dominant wind direction in Brussels. The southwest wind direction is indicated on Figure 6.16 for the SISP building. For The Hotel, a southwest wind direction imposes a flow perpendicular to the front facade. Also for case three, the wind is perpendicular to the front facade. For this case, the simulations for the validation process of the CFD model were repeated, though a different inlet wind profile was applied.

A first step to derive suitable locations for these sites is to identify the dimensions of the wake. Any turbine installed on these sites should obviously be placed outside the wake of the building. On the roof of the building and in front of the building (as the southwest wind direction is simulated) are two obvious choices to install a turbine. We therefore determine the size of the recirculation regions on top and in front of the building.

In Figure 6.17, the vertical wind profile of The Hotel is shown. In this figure, the recirculation regions are clearly visible. In front and behind the building, a back flow is present and the wind speed is low. Using this figure, the wake dimensions can be derived for each individual case. In Table 6.11, these results are shown. In this table, these results are also compared to the rules of thumb proposed by Wegley et al. (1980). This comparison shows that for tall, slender buildings these rules are too conservative. The upwind wake and downwind wake is lower than indicated by Wegley et al. (1980). The flow behind the building also reattaches sooner and the height of the wake is smaller. For a wide and lower building such as in case 3, the agreement with the rules of thumb is much better. It is difficult to derive the exact length of the downwind wake, but the length of the wake for this building is 15 to 20 times the height of building.

If a turbine would be installed on the rooftop, it should either by positioned on the side of the most common wind direction or at the centre of the roof (if there is no single (very) dominant wind direction). A short mast could be used if the turbine would be installed at the side of the most
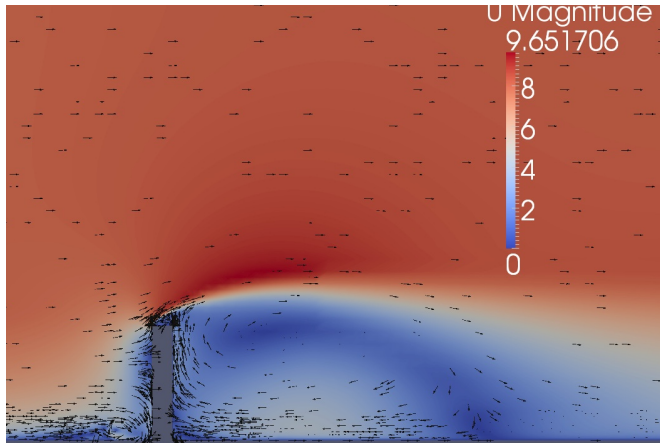
Figure 6.17: Vertical wind profile through the centreline of The Hotel.

Wake	Case 1 The Hotel	Case 2 SISP	Case 3 Reference	Rule of thumb
Upwind	1 H	1 H	2 H	2 H
Downwind	4-5 H	4-5 H	15-20 H	20 H
Height	1.4 H	1.2 H	2 H	2 H

Table 6.11: Dimensions of the wake around the building where H is the building height.

common wind direction. For the centre of the roof, the mast height should be chosen according the height of the recirculation zone. Therefore, the simulations are used to derive the point where the free stream velocity is recovered. This point can be found by comparing the vertical wind profile at the centre of the roof with the inlet wind profile. Figure 6.18 shows this comparison for The Hotel, where both wind profiles are shown as a function of the height above the roof H_r (divided by the building height H). At about 13 % (or 12 m) above the roof, the wind speed is fully recovered. This point is derived for each simulation and shown in Table 6.12. For case 2, the height of the mast at the centre of the roof can be as low as 5 % of the building height or 4 m. This is mainly caused by the fact that a different flow pattern is developed due to the non-perpendicular flow to the front facade. At the centre of the roof the recalculation region is a lot lower. In Table 6.12, these results are also compared to the rules of thumb proposed by Caca (2007). For the simulated cases, these rules are too conservative

as they advise that the mast height and the lowest tip of the blade should be respectively 50 % and 30 % of the building height. For tall buildings such as The Hotel, this would impose extremely large hub heights.
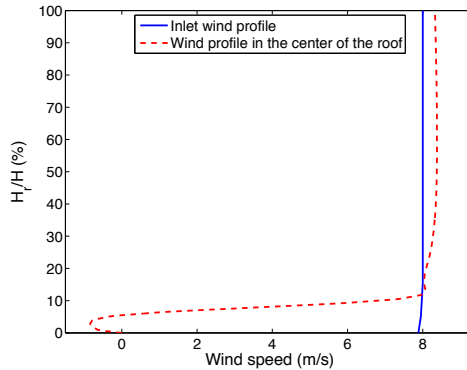

Figure 6.18: Comparison wind profile at the centre of the roof (dashed line) and inlet wind profile (solid line).

	Case 1 The Hotel	Case 2 SISP	Case 3 Reference	Rule of thumb
Height	12.3 % H	5.1% H	13.5% H	30 % H

Table 6.12: Height above the roof where the wind speed is fully recovered for the studied single buildings.

6.4.2 Micro-siting of building blocks

The CFD study performed in Section 6.4.1 is repeated, though now the surrounding buildings are added to the model. These simulations are used to study the effect of other buildings in the vicinity of the studied building on the flow patterns and rules of thumb. Possible concentrator effects due to the building configuration are identified. The studied building blocks are:

- Case 1 is The Hotel. As The Hotel site is complex (city centre) and it is difficult to accurately model all the buildings in the vicinity of The Hotel, we use a simplified model of the surrounding buildings.

The model is shown in Figure 6.19 (Top left). For this case we added 10 buildings around The Hotel with a height of 20 m, a depth of 20 m and width of 20 m. Four buildings were placed in front and four buildings in the back of The Hotel. Two buildings were located at the sides. The distance between the buildings was 10 m;

- For case 2, the site is less complex. An accurate model of the surrounding buildings is added to the SISP building. In Figure 6.19 (top right), this model is shown. The SISP building is the last T-shaped building on the figure and is the highest building in the neighbourhood. Eight different building are placed upstream of the building and the heights of the surrounding buildings vary from 20 m to 55 m;

- Case 3 is not a specific site. The purpose of this simulation is to gain insight in flow patterns on and open spaces in a city. This model is shown in Figure 6.19 (bottom). The same configuration as case 1 is used with The Hotel building removed from the model.

The wind direction and vertical wind profile applied in the simulations is equal to the simulations in the previous section. In Figure 6.20, the simulation for case 2 is shown. This figure shows a vertical slice of the flow pattern through the centreline of the SISP building. The wind direction vectors of the flow are added to show the back flow in front and behind the building. Similar to Section 6.4.1, such a figure is used to derive the wake dimensions for the highest building (the single building in the previous section). This table can then be used to derive suitable locations to install a wind turbine on ground level (to avoid installing them in the wake of (a) building(s)). In Table 6.13, these results are shown. For case 1 and 2, a comparison can be made with the results for a single building (SB) or a building block (BB). Adding the lower buildings to The Hotel has negligible effect on the dimensions of the wake. For case 2, the surrounding buildings do have a significant effect on the dimensions of the wake. The upwind wake is much higher caused by wake interference with the other buildings. A better agreement with the rules of thumbs are found. For case 3, the rules of thumb give a good prediction of the dimensions of the wake.

Similar to Section 6.4.1, the minimum height where the lowest tip of the rotor is 'wake free' is derived from the simulations. In Table 6.14, these results are shown. For case 1, the lower buildings in the vicinity of The
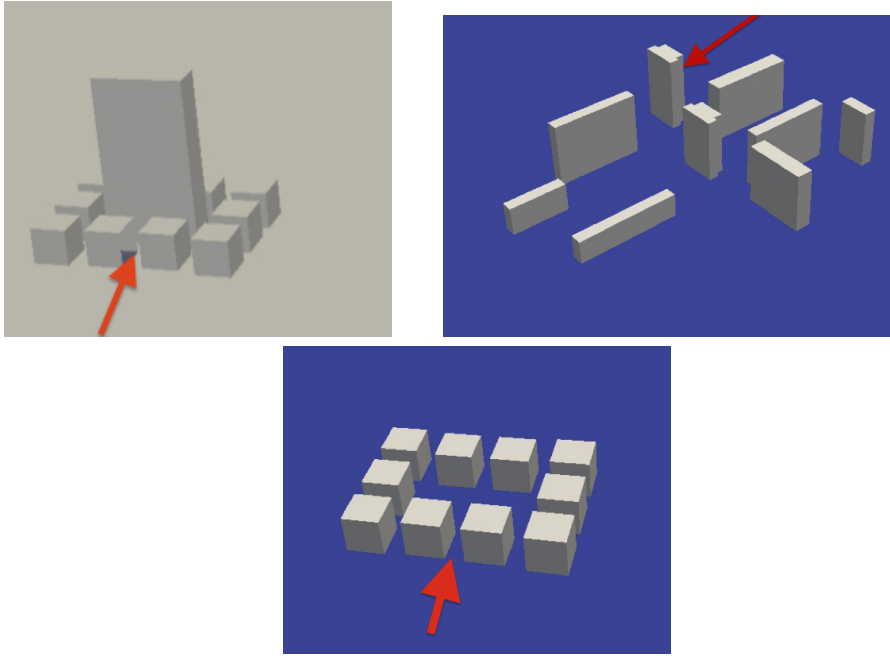
Figure 6.19: Configuration of building blocks and wind direction of the incoming flow for each of the simulated cases (Top right: case 1, top left: case 2 and bottom: case 3).

Wake	Case 1 SB	Case 1 BB	Case 2 SB	Case 2 BB	Case 3 BB	Rule of thumb
Upwind	1 H	1.15	1 H	3.6 H	2 H	2 H
Downwind	4-5 H	5-6 H	4-5 H	10 H	16-17 H	20 H
Height	1.4 H	1.4 H	1.2 H	2.1 H	2 H	2 H

Table 6.13: Dimensions of the wake where H is the building height. For case 1 and 2, the results of the single buildings (SB) are compared to the building blocks (BB).

Hotel have no impact on the minimum height. A significant increase in the height where the wind speed is fully recovered is noticed for case 2. The increase in the wake height is caused by the close distance and similar height of surrounding buildings to the SISP building. The restricted height now agrees well with the rule of thumb, the lowest tip of the blade should be at 17 m above the building. For case 3, the most obvious rooftop to
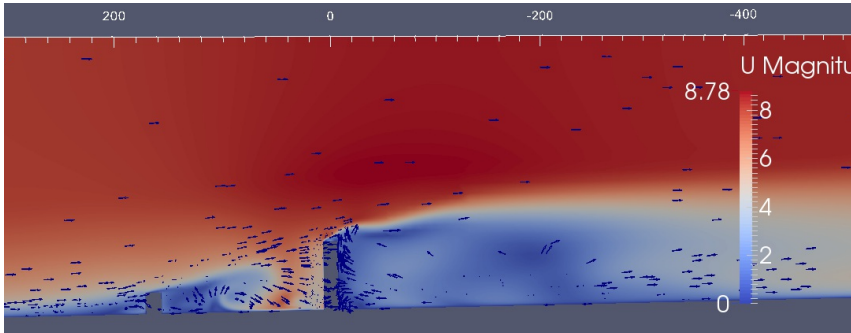
Figure 6.20: Wind velocity with vector plot in the centre of the SISP building.

install a wind turbine is on the buildings on the side of the most common wind direction (also indicated by the rules of thumb (Caca, 2007)). In Table 6.14, the minimum height for this first row of buildings is shown. In Figure 6.21, the wind profile at the centre of the roof for each row of buildings is compared to the inlet wind profile. This figure shows that the wind speed is recovered at 30.5, 46.1 and 86.2% of the building height for respectively the first, second and third row. Rules of thumb are thus too moderate for building blocks with a homogeneous building height.

Wake	Case 1 SB	Case 1 BB	Case 2 SB	Case 2 BB	Case 3 BB	Rule of thumb
Height	12.3% H	12.3% H	5.1% H	25.3% H	30.5% H	30 % H

Table 6.14: Height above the roof where the wind speed is fully recovered for the studied single buildings (SB) and building blocks (BB).

When buildings are positioned close to each other, concentrator effects can appear. If a wind turbine is positioned in a region where the wind speed is locally increased, the energy yield is positively affected. This turbine would be ground based and installed along these buildings. To investigate the effect on the wind speed, the horizontal wind speed at 15 m above the ground is examined for each case. In Figure 6.22 (left), the results are shown for The Hotel. The most prominent increase is present at the second row of buildings, just beside The Hotel. When the wind speed in this region is compared to the inlet wind speed at 15 m, an increase of 26% is measured. At this point the wind speed is comparable with the
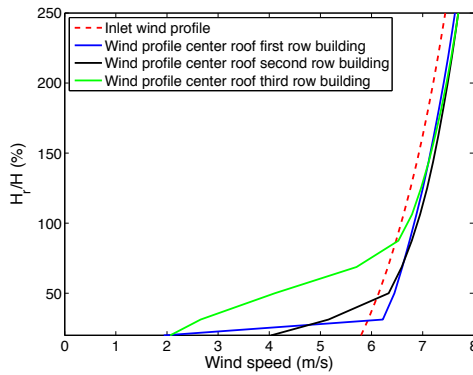
Figure 6.21: Comparison wind profiles at the inlet and at the center of the roof for each row of buildings.

free stream wind speed at 37.5 m. In Figure 6.22 (right), the horizontal wind speed is shown for case 2. Different concentrator effects are observed. The wind speed is locally increased, at the square just in front of the SISP building. To emphasise the concentrator effects, the wind speed along two different distances upstream of the SISP building are shown in Figure 6.23. Distance A is indicated with a white line and distance B with a black line. The maximum acceleration factor (ratio of the wind speed in a point and the free stream wind speed) was determined along distance A, where an acceleration factor of 1.35 is observed. This position is just between the wakes of two buildings northeast of the SISP building. At this point the wind velocity at 15 m was similar to the free stream wind velocity at 55 m. The horizontal wind speed distribution for case 3 is shown in Figure 6.24 (left). The open square itself is not a suitable location to install a wind turbine. If a wind turbine would be installed, it should be positioned between the buildings in the first row. At the most optimal position the acceleration factor is 1.17.

This increase in wind speed imposes a higher turbulence level due to the abrupt changes in wind direction and a sooner detachment of the flow. This effect can be seen in the right Figure 6.24 where the streamlines that pass the acceleration zone are shown. The turbulence just behind the buildings is significant.
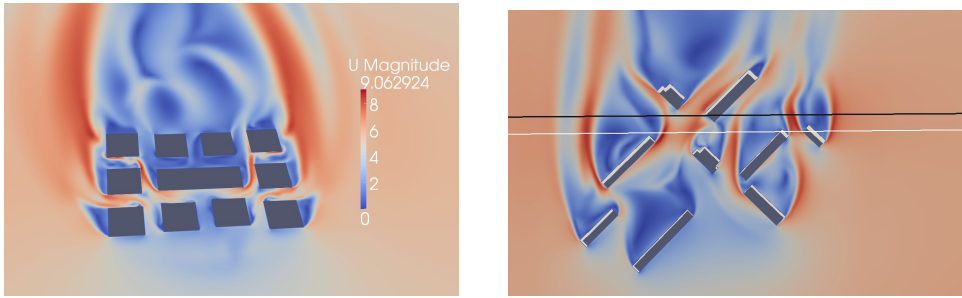
Figure 6.22: Horizontal wind speed distribution at 15 m above the ground for case 1 (left) and horizontal wind speed distribution at 15 m above the ground for case 2 (right). The acceleration factors along the white (distance A) and black (distance B) are shown in Figure 6.23
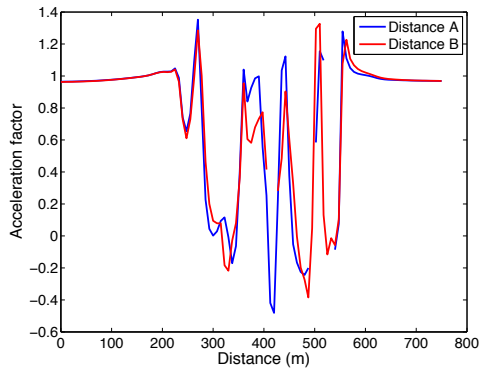
Figure 6.23: Acceleration factor at different distance upstream of the SISP building at a height of 15 m.

6.4.3 Discussion

In this section, CFD simulations are conducted for two specific and one idealised case in Brussels. These specific sites were selected where the wind map of Brussels (presented in Section 6.1) indicated a higher wind potential. The simulations are used to derive suitable locations to install a wind turbine. In order to generalise the simulations, we verified if rules of thumb, present in the current literature, could indeed be used to pinpoint these suitable locations. To avoid installing a turbine in the wake of the building, a turbine should be placed 1-2 times H in front, 1-2 times H above and 4 to 20 times H behind a building (where H is the building

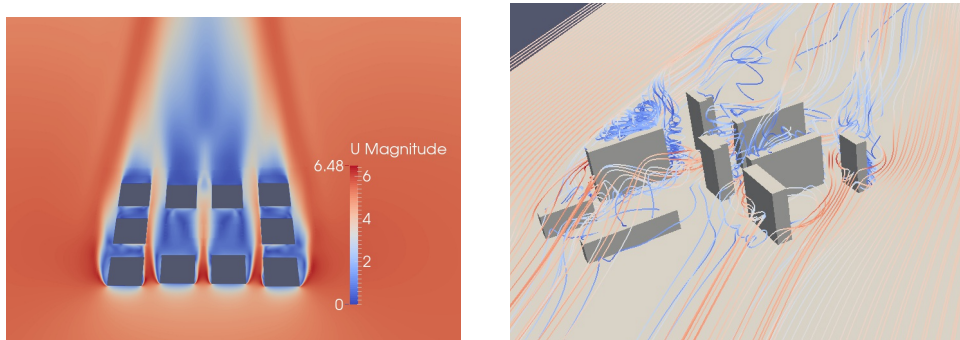Figure 6.24: Horizontal slice of the wind velocity at 15 m above the ground for case 3 (left) and plot of the streamlines along distance A and B upstream of the SISP building (right).

height). This showed that the rules of thumb describing the dimensions of the wake (Wegley et al., 1980) could be applied on wide buildings but for slender buildings they are too conservative. For slender buildings, the wake is smaller than indicated by the rules of thumb and thus a turbine can be located at a closer distance.

If a wind turbine would be placed on top of the roof, obviously it should be placed on the side or building of the most common wind direction. If there is not one very dominant wind direction, the centre of the roof can be a suitable location as well. The minimum height of the tower of a wind turbine is then strongly dependent on the size and shape of the building and the height of the surrounding buildings. Our CFD study shows that the rules of thumb to determine the mast height on the rooftop of a building (Caca, 2007) are generally too strict. We found that the wind speed is already recovered at 5-14 % of the building height above the rooftop for tall, slender buildings. For wide buildings or buildings influenced by the wake of upstream buildings, the rules of thumb could be used as they agree with the results of our simulations.

When buildings are positioned in certain configurations, concentrator effects can appear at lower heights. In these regions, the wind speed is locally increased. For the three types of configurations simulated in this study, acceleration factors up to 1.35 were measured (an increase in wind speed of 35% leads to an increase in power output of 146%). Although these locations seem potentially interesting, they are extremely wind direction dependent. If a wind turbine would be installed at a low height in the vicinity of buildings, a detailed CFD study must be performed and the

rules of thumb are too general to determine the most suitable location. Besides the impact of the changing wind direction, it is important to study the turbulence level in these zones as they will impact the lifetime and performance of the turbine (as shown in Chapter 4).

6.5 Technical feasibility of SMWT in Brussels

Besides the economic viability, the successful technical implementation of a wind turbine in an urban area is crucial for the feasibility of such a project. When a wind turbine is installed in a densely populated area such as Brussels, the possible nuisance to the surrounding community must be studied. This nuisance should be kept as low as possible. In this technical feasibility study, we discuss the following aspects specifically for Brussels:

- legal framework,

- noise,

- shadow flicker,

- biodiversity,

- visual impact and

- impact on the flight routes.

When one of these aspects is studied in more detail, the technical feasibility is assessed for two specific sites, The Hotel and Port of Brussels (see Section 6.2 and 6.3), and two specific wind turbines, turbine 2 and 6 (see Section 6.3).

6.5.1 Legal framework

In Brussels, there is currently no legal framework for wind energy. As a first step to develop such a framework, the Brussels Capital Region (Leefmilieu Brussel) has set up a call for a feasibility study 'E11-359: Identificatie sites, opzetten van windmetingscampagnes en uitvoering van haalbaarheidsstudies in het Brussels Hoofdstedelijk gewest'. We have coordinated and partly executed this study. The results of this study are partly presented in this chapter. As a next phase, the authors of this dissertation are preparing pilot projects in the context of a follow up on the 'Brussels Retrofit XL' project supported by Innoviris. During this preparation, we will perform

a detailed technical feasibility study for possible candidate sites and users where also the structural impact of a small wind turbine on a rooftop will be investigated. The purpose of this project is to guide users in the application for a building permit by the end of 2015. The feasibility study presented in this chapter and these pilot projects will serve as a base to develop a legal framework for Brussels.

6.5.2   Noise

Methodology   As mentioned in Chapter 2, planning permissions are often contested because of the expected noise nuisance. We therefore assess this nuisance on two locations: just below the turbine and at the closest building in the vicinity of the turbine (taking the dominant wind direction into account). This is assessed by:

- determining the day-evening-night sound pressure level, L_{den}, according to the European regulations (European Commission, 2012). This is an indicator of the overall noise level which is used to describe the annoyance caused by exposure to noise;

- comparing the sound pressure level to the limits introduced by the Flemish regulations (as there is no legal framework in Brussels);

We repeat this assessment for two sites, The Hotel and Port of Brussels, and two turbines, turbine 2 and 11. The sound data from the turbine, either supplied by the manufacturer or by an independent test facility, are used to predict the sound pressure levels according to the IEC standards (IEC, 2012). As for turbine 2 only the sound pressure level at one specific wind speed is available, we use the trend (sound data as a function of wind speed) of turbine 11.

For The Hotel, the dominant wind direction is west and the closest building upstream is 95 m. The second location to derive the nuisance is just below the turbine. As for this particular case the turbine would be installed on the roof, this point is on the top floor of the building. The distance is only 15 m however for this site we take the average acoustic insulation of a roof into account (35 dB). For the port of Brussels, the dominant wind direction is southwest, the closest building upstream is already at a distance of 380 m. On this location, the noise nuisance will be negligible, we therefore determine the sound pressure levels on two specific locations: the street below the turbine (distance is 20 m) and the closest building (distance 40 m).

Day-evening-night sound pressure level The day-evening-night sound pressure value L_{den} is the average equivalent sound level over a 24 hour period, with a penalty added for noise during the nighttime (22:00-06:00) and evening hours (18:00 to 22:00). During the nighttime period 10 dB and during evening hours 5 dB is added to reflect the impact of the noise. It is expressed as (European Commission, 2012):

$$L_{\text{den}} = 10 \log \left[\left(\frac{12}{24} \right) 10^{\frac{L_{\text{day}}}{10}} + \left(\frac{4}{24} \right) 10^{\frac{L_{\text{evening}}+5}{10}} + \left(\frac{8}{24} \right) 10^{\frac{L_{\text{night}}+10}{10}} \right] \quad (6.7)$$

where L_{day}, L_{evening} and L_{night} are the average day, evening and night equivalent sound pressure levels. These sound pressure values are derived in two steps. First, for each wind speed measured in the concurring time of the day, the source sound from the turbine is derived and converted into a sound pressure level at a certain distance from the turbine by:

$$L_p = L_w + 10 \log \left(\frac{S_0}{4 \pi r^2} \right) \quad (6.8)$$

with L_p the sound pressure level, L_w the sound power level, S_0 the reference area of 1 m^2 and r the distance from the turbine. Second, the average or equivalent sound pressure level L_{eq} for day, night and evening are derived by:

$$L_{eq} = 10 \log \left[\frac{1}{T} \left(10^{\frac{L_{p1}}{10}} + 10^{\frac{L_{p2}}{10}} + ... + 10^{\frac{L_{pn}}{10}} \right) \right] \quad (6.9)$$

with L_{pn} the sound pressure level at wind speed n. In Table 6.15, the L_{den} values are shown for each turbine, site and distance to the turbine.

Site	Turbine 2		Turbine 11	
	Closest building [dB(A)]	Below turbine [dB(A)]	Closest building [dB(A)]	Below turbine [dB(A)]
Hotel	43.7	24.8	38.6	19.6
Port	47.5	53.5	42.4	48.4

Table 6.15: The day-evening-night sound pressure level for each turbine, each site below the turbine and at the closest building. Below the turbine at the Hotel, the average acoustic insulation is included in the calculations.

To verify the impact of the turbine on the total noise level, we use measured sound data from a typical urban site (near the rue Dansaert) in

Brussels as background noise (as we have no sound data from each specific site). The L_{den} value for the background noise at this particular site is 58.3 dB(A). This background noise can be added to the noise of the turbine and we can repeat this for each site and distance from the turbine. These L_{den} values are shown in Table 6.16. From this table we can conclude that on these specific sites, the turbines will have negligible effect on the total sound pressure level.

It should be noted that for the acoustic assessment on The Hotel, we have neglected the fact that vibrations of the turbine may be transmitted to structural elements and may also generate noise. Such a vibration study is (at least in the context of this dissertation) not included in the feasibility study for Brussels.

Site	Turbine 2		Turbine 11	
	Closest building [dB(A)]	Below turbine [dB(A)]	Closest building [dB(A)]	Below turbine [dB(A)]
Hotel	58.5	27.1	58.4	24.9
Port	58.6	59.6	58.4	58.7

Table 6.16: The day-evening-night sound pressure level for each turbine, each site below the turbine and at the closest building. In this table, the background noise is included. Below the turbine at the Hotel, the average acoustic insulation is taken into account.

Limits Flemish framework   The legal framework in Flanders has been discussed briefly in Chapter 1 and more in detail in Chapter 5. A planning permit will be granted if certain criteria are met.

According to the framework, the so-called source sound (sound power level) should be derived at a wind speed of 5 m/s and converted into a sound-pressure level at the distance from the observer of the source. For The Hotel, which is a residential area, this sound pressure level is limited to 39 dB(A). The Port of Brussels is located in an industrial area where the sound pressure levels are limited to 49 dB(A). The sound power level at a wind speed of 5 m/s is 85 dB(A) for turbine 2 and 80 dB(A) for the turbine 11.

Using the source sound and the distance to the closest observer, the sound pressure levels can be derived using Figure 6.25 (or via Eq. (6.8)). For turbine 2 the black line should be used, for turbine 11 the blue line.

At the Port of Brussels the distance to the street is 20 m and the distance to the closest building is 40 m. The observed sound pressure level for turbine 2 and the street is just below 49 dB(A) and within the limits of the regulations. At The Hotel, the closest building is at 96 m. This distance is not shown on the figure, however the sound pressure levels is for both wind turbines below 39 dB(A). The regulations concerning noise nuisance thus allow to install both wind turbines on both sites.
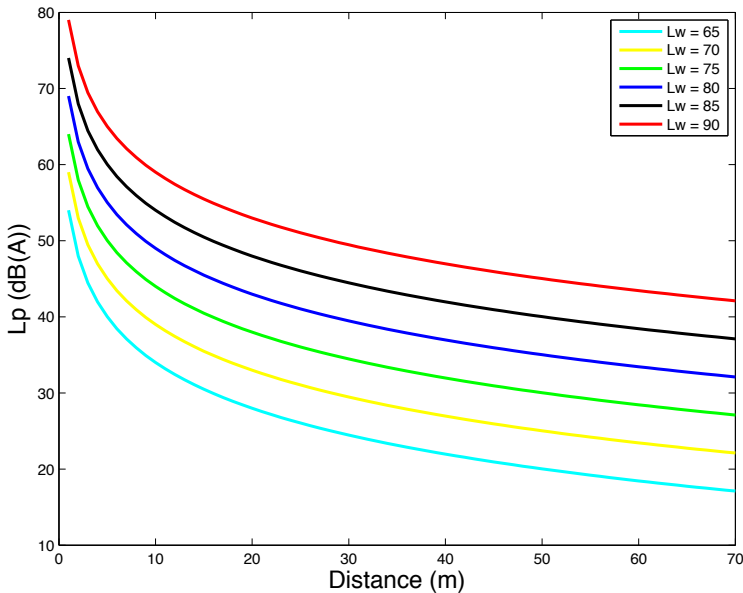

Figure 6.25: Flemish regulations describing the relationship between the distance and the observed sound pressure levels for different source sound pressure levels (Van Mechelen and Crevits, 2009).

6.5.3 Shadow flicker

Shadow flicker depends on the topographics location of the terrain. A shadow which extends over the roof of a building will create less nuisance than a shadow reflected to the walls of a building. In addition, the distance between the building and the observer plays is important. As the distance increases, diffuse light creates a weakening of the shadow effects.

As there are no regulations in Brussels, the criteria of the Flemish framework are used. In this framework, an area around the turbine equal to twice

the total height of the wind turbine is set as the area where shadow flicker can occur. This area is discussed for the two studied sites:

The Hotel

If a wind turbine with a hub height of 15 m and a rotor diameter of 5 m is installed on top of The Hotel, a large area around the turbine is affected by shadow flicker. As the wind turbine is installed on the rooftop, the building height should be added to the total height of the turbine. A radius of 227 m around the turbine defines the restricted area prescribed by the regulations (in Flanders). As the turbine is located into a densely builded area, many buildings are within this area. For this site, a detailed analysis of the shadow flicker is necessary. For each neighbouring window, the time that shadow flicker occurs should be verified and checked with the regulations. A brief analysis is presented here.

In Figures 6.26 and 6.27, the reflected shadow on the surrounding area of The Hotel is shown for two particular moments. On the rooftop of The Hotel, turbine 2 and 11 are installed. A simplified model of the surrounding environment is constructed. By comparing two snapshots (Figure 6.26 and 6.27) within a time frame of just 15 minutes, it can be observed that the shadow reflecting on the building is shifted from the left of the building to the right. Therefore the shadow is sufficiently shifted and the shadow nuisance will be far below the limit of 30 minutes per day. Note that these two snapshots only represent an approximation and the position and the movement of the shadow will depend on the time of the year.

Port of Brussels

When a small wind turbine with a hub height of 15 m and a rotor diameter is installed at the port of Brussels, the restricted area around the turbine is only 35 m. As the distance to the closest building is 40 m, there are no restrictions concerning the shadow nuisance on the installation of a small wind turbine. Even when installing a medium wind turbine on this site, could not be prohibited as it is an open area and the only buildings are located south of the turbine (where the nuisance is significantly less).
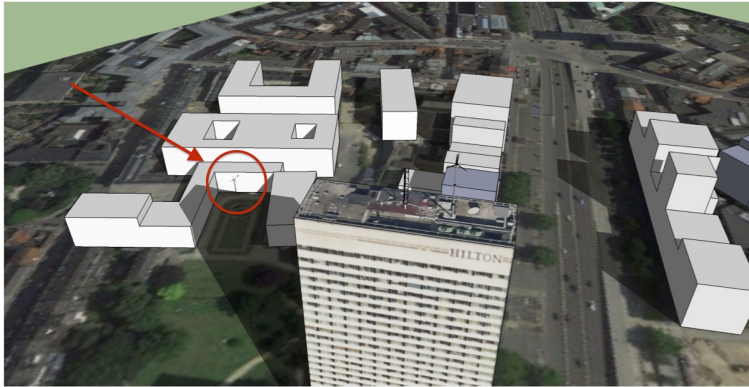
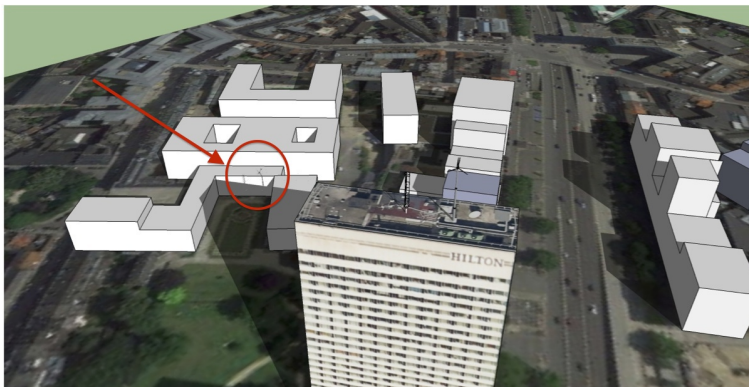Figure 6.26: Shadow nuisance on the first of March at 13h40.

Figure 6.27: Shadow nuisance on the first of March at 13h55.

6.5.4   Biodiversity

A brief analysis of the biodiversity was performed by a subcontractor under the contract research (Hendrick, 2014). He concluded that the impact of a small wind turbine on the biodiversity at the two selected sites is expected to be small. This is due to the small rotor size (potential risk for birds) and the low pressure variation (potential risk for bats) of the turbine. However, for the Port of Brussels a more detailed analysis is necessary as such a narrow corridor could be used as passages by especially migratory birds or hunting areas for bats and birds.

6.5.5   Visual impact

The visual impact of a wind turbine on the landscape can be studied using digital mockups. These mockups take into account the type of turbine, hub height and include important landscape elements.

Mockups of the two selected turbines (turbine 2 and turbine 11) are made for The Hotel and the Port of Brussels. These are shown in Figure 6.28 to 6.31. The visual impact on the landscape is small for both sites:

- The Port of Brussels is located in an industrial area;

- On the rooftop of the Hotel obstacles such as masts and telecommunication equipment are already present. The additional mast and rotor would not harm the integrity or character of the building.

6.5.6   Analysis of flight routes

The city centre of Brussels and a large part of the Brussels Capital Region are located in 'local traffic area', just under the airspace controlled by the control tower of the Brussels airport (Figure 6.32). For every new obstacle placed in the area, it is necessary to determine if it is an obstruction to air traffic. The Directorate General Aviation (DGA) is authorised to give advice concerning building permits for these possible obstructions. These advises cover only solid structures which are placed on top of other objects or obstacles. Therefore the DGA is authorised to give advise for wind

Figure 6.28: Mockup of the turbine 2 at the Port of Brussels.

turbines placed on existing masts, structures or buildings but not for ground mounted wind turbines.

If an application for advice is submitted to the DGA, three possible outcomes are possible:

- Implicit positive advice: When there is absolutely no danger whatsoever on the air traffic;

- Provisional positive advice: If the obstruction imposes possible danger to air traffic, but the risk can be brought down to an acceptable level. This can be done by applying colour or light marking on the obstacle or parts of the obstacles;

- Negative advice: When constructing the obstacle leads to an unsafe air traffic and it can not be brought down to an acceptable level.

Both measurement sites are outside the area where the height of the obstacles in the vicinity of the airstrip are limited. For each of the measurement sites, the following conclusions can be made:

- The Hotel is indicated as an obstacle on the visual approach chart. In the vicinity of this site, other buildings are above the height of The Hotel. A small wind turbine with a total height equal or just

Figure 6.29: Mockup of the turbine 11 at the Port of Brussels.

above the height of the highest antenna will not impose any danger on the air traffic. Therefore it is likely that a positive advice would be received.

• The canal zone is also under a critical routes for departing flights, though a wind turbine would be installed on ground level and therefore imposes no danger on the departing flights. Buildings with heights over 100 m are present in the direct vicinity of this site.

6.5.7 Discussion of the technical feasibility

In this analysis, the technical feasibility of installing a wind turbine in Brussels was analysed. As there is no framework in Brussels, the regulations of Flanders concerning noise and shadow flicker were used. For the two measurement sites and two wind turbines used in this analysis, the noise nuisance is below the limits of the Flemish regulations. The day-night-evening sound pressures values of the wind turbines are within a lower sound class and have negligible effect on the overall sound level when the background noise is included.

At the Port of Brussels, there will be no shadow nuisance for the surrounding buildings for none of the proposed wind turbines. The closest
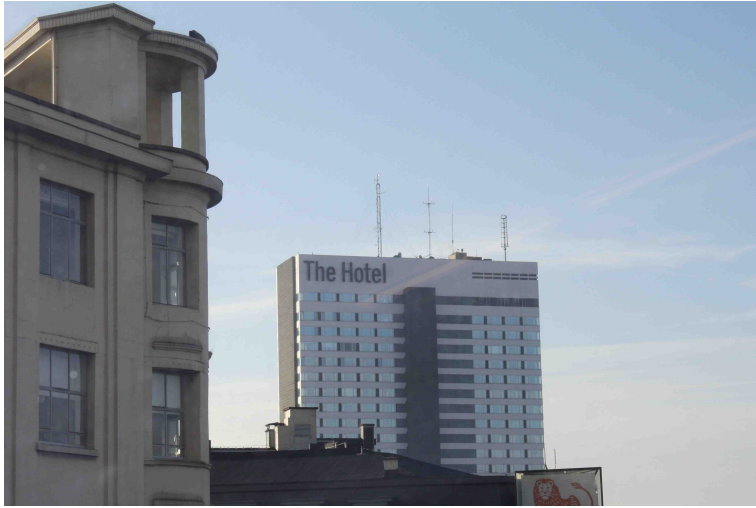
Figure 6.30: Mockup of the turbine 2 at The Hotel.

building is located south of the wind turbine and therefore shadow flicker will not be of concern even if a medium wind turbine were to installed. If a wind turbine would be installed on a rooftop of The Hotel, the area where shadow effects can occur is large. A first analysis was performed for a 'worst case' scenario and this showed that the shadow moves fast from one window to another in just a small timeframe. A detailed analysis is necessary to ensure that no surrounding windows are affected for more than 30 hours/year or 30 minutes/day.

The impact of these types of turbines on the biodiversity in Brussels seems to be small. Only the role of the canal zone as a possible migration route for birds and bats should be analysed more closely. For none of the measurement sites, installing a wind turbine would cause any danger for air traffic.

Both the Port of Brussels and The Hotel seem to be favourable locations for the implementation of a wind turbine. The Port of Brussels is located in an industrial area and the equipment and masts on the rooftop of The Hotel have similar heights to a small wind turbine. Therefore their visual impact will be low.
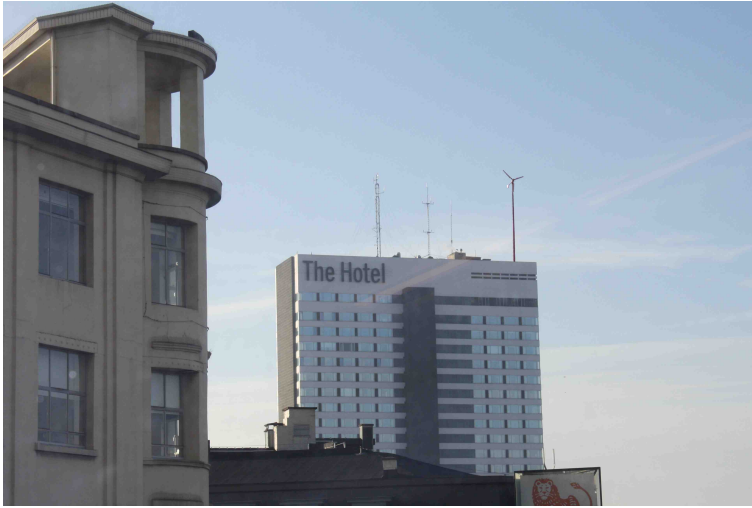
Figure 6.31: Mockup of the turbine 11 at The Hotel.

6.6   SMWT potential in Brussels

This chapter has demonstrated the economic and technical feasibility for rooftopmounted small-scale wind turbine. Based on first principles we can roughly estimate the potential market size for a city like Brussels.

MacKay (2009) have showed that a typical HAWT wind farm yields about 2 W per square meter ground surface (power density). A first rough estimate, taking into account the practical limitations, is that in Brussels 50 sufficiently large and high buildings can be used to install wind turbines, each with an average area of about 800 m^2 (approximately the area of The Hotel). If we use the power density per square meter proposed by MacKay (2009), this would yield to about 80 kW total installed capacity. As this value for the power density takes into account the load factor of the turbine (a compensation for the fact that the turbines are not always operating at rated power), this would result into an installed capacity of 320 kW. Assuming that at every site, a turbine with a rated power of 5 kW is installed (similar to turbine 11 from our economic analysis), this would translate into nearly 65 individual roof top mounted installation in Brussels. This is approximately 35 % market size in Flanders and would therefore imply a significant market growth in Belgium.

6.7 Conclusions

In this chapter, a feasibility study is performed for the Brussels Capital region. As a first step the wind resources in Brussels are assessed. In and near the city centre, the wind speed can easily go up to 5 m/s at a mean building height of 40-70 m. We have validated the accuracy of the wind map by comparing specific sites in the map with field measurements. For two sites, the errors are below 5 %. For the three other sites, the errors are in the order of 20 %. Although this indicates that a measurement campaign is still necessary to ensure a reliable prediction of the AEP, the wind map was able to pinpoint windy areas.

To assess the (very) local wind potential, we measured the wind speed at four sites in Brussels. A fifth site of a previous measurement campaign (Guidon, 2011) was added to this study. On four of the five sites, the average wind speed was above 4 m/s, emphasising the wind potential throughout Brussels. We applied a measure-correlate predict procedure to correlate the measured wind data to the long-term. These long-term data were then used to assess the AEP for three small wind turbines and one medium wind turbine. Using these predictions, an economic analysis is performed for both SMEs and private persons.

For one of the sites, The Hotel, a dynamic payback period of just 7 years was found, far below the normal expectation for a small wind turbine in an urban environment. For this particular case, the internal rate of return was above 17 %. For SMEs, installing a medium wind turbine on the Elia-site or the Port of Brussels is economically feasible if all the generated electricity is consumed. Balancing the produced and consumed energy is important for SMEs to select the appropriate turbine for a specific site. As this analysis shows the potential of small and medium wind in Brussels, we also assessed the technical feasibility. Our analysis showed that there were no significant problems to be expected for the implementation of a small wind turbine in such areas.

As the wind patterns at low heights in an urban area are generally complex, installing a wind turbine on a suitable location requires care. We used CFD simulations to derive suitable locations on specific sites in Brussels. In order to generalise these simulations, we verified if rules of thumb could be applied to identify these locations. One of these rules, proposed by Wegley et al. (1980), describes the dimensions of the wake behind a single building. We found that these rules of thumb are too conservative for slender buildings but can indeed be applied on wide buildings. If a wind turbine would be installed on the rooftop of a building the rules of thumb

(proposed by Caca (2007)) to avoid the recirculation region are generally too strict. The mast height can thus be lower as prescribed by the rules of thumb. In addition, the benefits of the CFD simulations is that possible concentrator effects can be also identified. For the building blocks (specific sites in Brussels) we simulated, local increases in wind speed up to 35 % were found at the typical hub height of a small wind turbine.
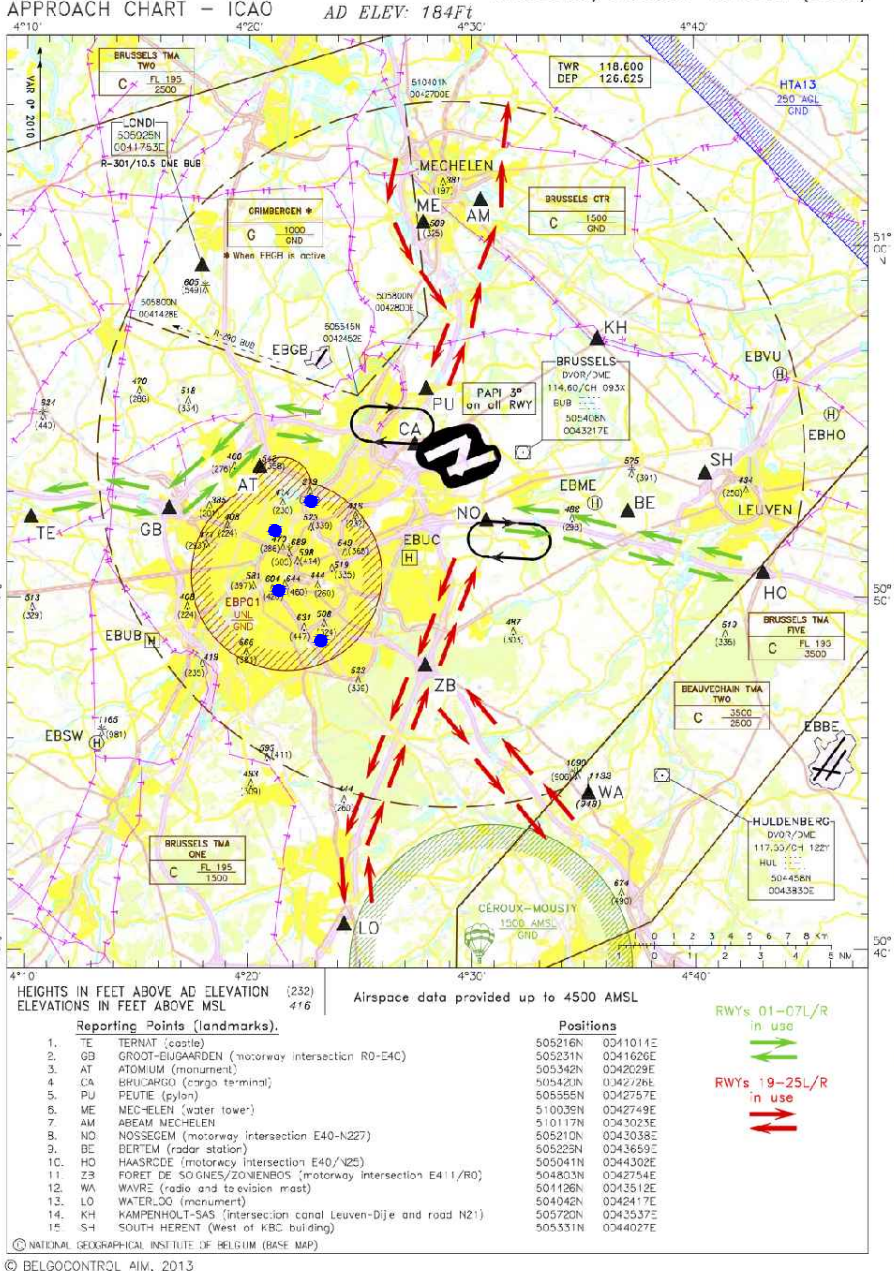
Figure 6.32: Indication of the measurement sites (blue dots) on a flight chart of Brussels. The local airspace area is indicated with a dotted line (circular shape).

Chapter 7

Conclusions and recommendations

7.1 Conclusions and main results

This dissertation offers a more reliable and accurate prediction of the annual energy production for small and medium size wind turbines. The methods presented have found an immediate practical application in a number of feasibility studies in urban and rural areas.

In Chapter 2, we pinpoint the main factors holding back the further development of the small and medium wind turbine market. An immature market, improper assessment of on-site wind conditions and improper on-site positioning of the turbine are shown to be the three basic causes of failed wind turbine projects. Such failed projects have created a negative perception about small-scale wind in general, hampering the further development of a potentially valuable market. A further increase in the number of independently-tested power curves, the development of low-cost resource assessment tools, increased standardisation and certification, and the realisation of successful pilot projects (as a direct follow up of this dissertation) are developments that would certainly contribute to changing this negative perception and establishing a more mature market.

In Chapter 3, we provide an in-depth discussion of four techniques to reliably predict the annual energy production of small and medium wind turbines. When and how to best apply these techniques depends on the available information on the site. This information could include the mean wind speed, actual wind data or an approximate statistical distribution, wind data below hub height or wind data measured over a limited mea-

surement period. We analyse these methods by comparing the AEP of 29 wind turbines on 23 measurement sites. We find that the rated power, although often used, is not satisfactory to predict the AEP as it doesn't take into account the typical operating conditions of small and medium wind turbines. The AEPs available in the test reports, based on the Rayleigh distribution, provide a valid alternative as it was possible to predict the AEP with an accuracy of 10 % for most of the sites. If wind measurements are available, our recommendation is to use them directly (or through a histogram of wind speeds) rather than by fitting a statistical distribution to the data. Even when the Weibull distribution appears to accurately fit the wind speeds, the error on the AEP can be as high as 20 %. The behaviour of methods based on the maximum-entropy principle is too unpredictable (in particular due to the arbitrary choice of the pre-exponential term) to provide an improvement over other methods.

To cover the interannual variations of the wind speed, wind data should be correlated with long-term reference data to predict the long-term wind conditions. This so-called measure-correlate-predict technique can be applied using several procedures. We compare three of them and conclude that the variance-ratio procedure provides the most accurate results and ease of use. We also verify if limiting the time of measurements may present an opportunity to lower the cost of resource assessment studies. We here corroborate the recommendation available in the literature that 9 months provides decent accuracy and for shorter measurement periods it is better to start the measurements in the winter months as it reduces the error on the AEP. Finally, we compare three methods to extrapolate the wind speed from measurement height to hub height. We conclude that the 2/3 rule, often used, is too mild and can impose a significant error on the prediction of the AEP.

In Chapter 4, we discuss the importance of averaging times for reliable estimates of the AEP. We analyse the importance of the effect for the prediction of the AEP and we present a theoretical framework to study this effect. By treating the increased variance within every wind speed sample, the same way as we would do with an increase turbulence intensity, we correct the power curve. This correction will partially compensate the loss in apparent power. We applied our technique to two very different sets of wind speed measurements and one 5 kW power curve. Without correcting for the mismatch in averaging times, we found that the error on the AEP could be as high as 20 %. We therefore suggest to always correct for the turbulence intensity, and this at the correct averaging time.

The methods of Chapters 3 and 4 can be summarised in a set of recommendations for stakeholders (see below) that greatly reduce the uncertainty of a SMWT project, and should contribute to an increase of the number of installed turbines.

As stated above, the market of small and medium wind turbines is immature. Simply stated, this means that a large fraction of the SMWT market does not meet the quality standards that one may expect in a more mature market. In particular, the majority of SMWT have a high LCOE (or, equivalently, long pay-back times) even in windy conditions. One of of the main conclusions of our work is that no SMWT project should be undertaken without a thorough knowledge of the market. To that end, we have assembled a database of more than 750 wind turbines with a rated power of 100 kW or less. We have chosen not to make this database publicly available, as it is an important lever for consultancy activities undertaken by the research team where this work was conducted.

In Chapter 5 we investigate the viability of small and medium wind turbines in rural areas in Flanders. We have created wind maps indicating the mean wind speed at the typical hub height of 15 m of a small wind turbine in Flanders. The wind maps are based on actual wind data from meteorological measurement stations as well as our own measurements. Using our database of SMWT and the wind map, we have investigated the economic viability of SMWT. If we use a dynamic payback time of 10 years as the upper boundary of what is economically viable, we find that SMWT are economically viable for SMEs on 50 % of the studied sites. We cannot recommend, at this stage, SMWT for private use. It is important to note that an increase of production volumes of SMWT is bound to lead to a reduction in the investment cost, with a positive effect on LCOE and payback times. Regions with good wind conditions abound near the Belgian coast, as expected, but can also be found in the centre of the country.

The lowest pay-back time we find is 4 years, with an internal rate of return of 29 %. Such values are only possible when the correct balance is found between the locally produced and consumed energy, the payback period of such a wind turbine can be below 4-5 years. In these feasibility studies we showed how a micro-siting study can be executed using CFD simulations at a marginal cost, but to great advantage (avoidance of shadow zones, exploitation of local acceleration regions). We also identified the sense of using de-rated turbines in moderate wind climates such as the rural areas in Flanders and Wallonia. In these wind climates, a de-rated turbine will only produce marginally less than a non de-rated turbine. This

technique represents an opportunity for SMWT manufacturers as a reduction in generator size will not only reduce the cost but will also increase the efficiency of the generator in lower more frequent wind speeds.

In Chapter 6 we show that wind energy is economically viable on the tallest buildings of the Brussels Capital Region. Also in this case, a micrositing study can be executed using CFD simulations at a marginal cost. The availability of 3D building models in tools such as Google Earth is largely responsible for the affordability of CFD simulations (where perhaps surprisingly the largest cost is the CAD rather than the CFD). For the cases we studied, we found, after verifying with a Total Station, that the dimensions of the building models in Google Earth are accurate to 5% or better. We also compared these results to low-tech procedures (rules of thumb) to derive suitable locations and concluded that they can only be used for simple cases (where there is less interactions between different buildings). Any project involving SMWT in an urban setting should therefore include a CFD micrositing study. We also show that the impact of a small wind turbine mounted on top of a high-rise is expected to be limited. As with the rural applications, knowledge of the market is again crucial, as the good economic viability only holds for the best turbines on the market.

7.2 Recommendations to stakeholders

A major contribution of this dissertation is the formulation of a number of concrete recommendations and guidelines to industrial partners, authorities, and end users. Below we summarise the main recommendations.

Always use independently-tested power curves The market of small and medium-sized wind turbines is immature. More than half of the commercially available turbines can be discarded as not suitable even on windy sites. Power curves as provided by the manufacturer invariably lead to overestimated annual energy yields. Our advice here is simple: never trust the power curve provided by the manufacturer; it is a marketing tool. The only way to obtain a reliable prediction of the annual energy production is through the use of power curves determined by independent test institutions. The good news is that more and more of these data are becoming available to the public. In our database we currently have 42 turbines with independently-tested curves.

Use the IEC test reports to predict the AEP when only the mean wind speed is known   Even though the published rated power of a turbine is often representative of the maximum power, it is rarely a good predictor of the annual energy production. When only the (hub height) wind speed is known, we recommend to estimate the AEP for that site and a given turbine by interpolating the predictions of the IEC test report. These IEC predictions are done for a Rayleigh-distributed wind of 4, 5, 6, 7, 8, 9, 10 and 11 m/s. We found errors smaller than 10 % in AEP for the sites we tested in Belgium and the Netherlands (provided that the standard deviation did not differ more than 10 % from the value assumed in the Rayleigh distribution).

Directly use wind data to predict the AEP when data are available   When on-site wind speed data are available, these should be used directly to calculate the AEP, rather than first fitting an approximate statistical distribution (as is often done with a Weibull distribution). Though the Weibull distribution often yields a good fit of the data, it is only an approximation. We found that using a Weibull distribution introduced an error of a few per cent in AEP for most our test sites, though higher errors cannot be excluded.

Correlate measurement data with long-term wind conditions   As a complement to our previous recommendation, on-site measurements should always be adjusted against long term (climatological) data. The variance-ratio measure-correlate-predict procedure provides a simple and adequate tool to improve the prediction of (long-term) annual energy production.

Be careful with the vertical extrapolation of wind speed   All extrapolation should be done with care, and this is not different with wind speed. We have shown that the typical laws used to describe the evolution of wind speed with height are very sensitive to variations in the wind speed values used to fit the law. Thus, small errors in the wind speed can lead to significant errors in the extrapolated wind speed and thus the prediction of the AEP. Even sticking to the often-used two-thirds rule (do not extrapolate more than 50 % above the highest measurement position) does not guarantee a reliable extrapolation of the wind speed in all cases.

Use CFD for micro-siting Computational fluid dynamics simulations can be used to study the local wind patterns on complex sites. We showed how CFD can predict low-speed highly-turbulent recirculation zones behind obstacles (to be avoided) as well as locally accelerated flow in between obstacles. Given that computer simulations have become much cheaper and that terrain information is often freely available, the potential gains are high at low cost. Certainly for complex sites (which is almost always the case for small and medium wind turbines given the low hub heights) and in urban sites, micro-siting with CFD simulations is a must.

Correct the power curve for the averaging time and turbulence intensity of the wind measurements It is well known that turbulence affects the power of a turbine. We have shown that different averaging times (used to sample the wind speed measurements) lead to different values of the turbulence intensity of the site, and thus require a different compensation of the power curve. We therefore suggest to always correct the power curve for the turbulence intensity measured at the installation site, taking into account the effect of the averaging time.

Install small and medium wind turbines in Flanders and Brussels Our last (but certainly not least) recommendation is to go out and install small and medium wind turbines in Belgium. We have shown that the wind climate is decent: near the coast (in Flanders), on top of high rises (in Brussels), as well as for some specific sites throughout Belgium and the Netherlands. For SMEs we found payback times as low as 4 years, taking into account all costs and benefits. When all of the above recommendations are followed, small and medium wind surely is a sound investment in Flanders and Brussels.

7.3 Valorisation of our SMWT database

An important contribution of this dissertation has been the assembly of a database of small and medium-sized wind turbines, with rated powers below 100 kW. As far as we know from discussions at international conferences, this is the largest database to date. Our database has not been made publicly available, as it is an important lever for our research group to obtain contracted research projects for industry. In this section we briefly explain how this database has been used in the context of this dissertation, and what our valorisation strategy is for the future.

The database gathers relevant information (geometry, power output, price, etc.) of the turbines, as was described in Section 2.1. We have aimed for comprehensiveness and thus included turbines with power curves from independent test facilities as well as those provided by the manufacturer. Given that small wind turbines display a huge, and sometimes bewildering, variation of quality over different manufacturers, having a clear distinction between independently-measured and manufacturer-provided power curves is a first important benefit of our database. It has allowed us to select dependable data for our studies of the wind potential in Flanders and Brussels. It has also initiated privileged contacts with manufacturers, who shared their unpublished (but independent) test results to be included in our database.

But also, and more importantly, this knowledge of the market has been crucial for economic success. Our group has been selected by a number of public and private partners for wind resource assessment and feasibility studies for small and medium wind turbines. In all projects, we were able to suggest suitable turbines with an accurate (and dependable) estimate of the annual energy production. (We always restricted ourselves to independently-tested power curves; in the one exception where we could not avoid using the manufacturer's data, we explicitly mentioned it.)

In the business model of our research group, the database is an important lever to obtain new projects and a strong pillar of the service that we provide to the customer. We plan to further develop our expertise into a streamlined set of services that we can offer. These services consist of wind resource assessment (wind speed prediction based on roughness maps, meteorological data, mesoscale models, CFD simulations, and on-site wind speed measurements, on the ground as well as on rooftops), micro-siting (using CFD simulations), feasibility studies (choice of the most suited turbine, energy yield prediction, economic analysis, impact assessment), and guidance with the preparation of permit demands. Our research group has already concluded a number of such projects. Further development of these activities shall be either in-house (by hiring personnel specifically for these services) or through the creation of a spin-off company, possibly within the 'Launch - Brussels spin-off' programme of Innoviris.

7.4   Future research

The main objective of this dissertation has been to improve the reliability of the prediction of the annual energy production specifically for small and

medium wind turbines, and to investigate whether SMWT can contribute meaningfully to the production of sustainable energy.

Estimates of annual energy production invariably use a statistical distribution to fit wind data. The Weibull distribution is the most commonly used and is part and parcel of commercial codes such as WAsP and WIND-PRO. It is a simple distribution which is able to describe the wind data in just two parameters. Our analysis has shown that in some cases using the Weibull distribution can lead to a significant error. The more advanced distribution, maximum entropy principle (MEP), uses more parameters and if the correct pre-exponential term were to be determined a priori, it could provide a better alternative for Weibull. Although several authors have tried to predict the behaviour of this method (particularly the influence of the pre-exponential term), assessing the performance over numerous sites (ensuring a larger variety of the wind conditions) might lead to a better understanding of this approach and an objective way to determine the optimal pre-exponential term.

The practical application of MCP will generally lead to a loss in the apparent power available in the wind. In wind measurement campaigns for wind energy purposes, the averaging times with which wind speeds are sampled is usually 1 or 10 minutes. As these collected wind data are used to predict the AEP over the lifetime of the turbine, MCP is used to correlate these data to long-term reference data. Often these long-term data are collected for meteorological purposes using longer averaging times of 1 hour. Therefore the collected short-term wind data are then averaged to 1 hour samples and correlated with the long-term data to predict the long term wind potential. As we have shown in Chapter 4, this would lead to an underprediction of the AEP. It should be tested and verified to what extent our presented procedure can increase the accuracy of the prediction of the long-term AEP. If these tests indeed confirm our recommendations, this procedure should be included in the standards and short-term, representative data (with a sufficiently-high sample frequency) of these meteorological stations should be made publicly available (and measured if these data are not present).

In Chapter 6, we have presented and validated a wind map for Brussels. Our validation showed a relatively good agreement between the measured and predicted wind speed. However, we present here a few recommendations that may improve the accuracy of this wind map. In the current methodology, the approach neglects the ambient regional roughness and predicts the wind speed only for each particular region. In Millward-

Hopkins et al. (2013a), a procedure to incorporate the influence of the wind direction and the upstream roughness in the down-scaling of the wind speed is presented. We tested this approach and found no improvement in the accuracy of the predictions. A more advanced approach has been suggested in the same paper. As the areas where we validated our approach showed rather low roughness values (compared to what normally can be expected in urban terrain), it could be worthwhile to verify if this approach would improve the accuracy. Another more structural improvement of the 'wind atlas methodology', particularly when producing detailed wind maps of larger areas (such as Flanders), is to incorporate changes in the topographical height and potential concentrator effects. In a small area with modest height differences in the topography such as Brussels, these topographical effects will most likely be rather small.

A direct follow-up of our feasibility studies for Flanders and Brussels are pilot projects. Successful pilot projects are vital to convince local authorities, stakeholders, end-users and investors of the benefits of SMWT. If our recommendations are followed and one of the better sites of our feasibility study is used, the chance of success will be large. However, specifically in an urban context, a few additional assessments are imperative. The structural impact of installing a wind turbine on the rooftop should be analysed before installation and shadow flicker on neighbouring building must be investigated. During these first pilot projects, the turbine should be closely monitored for performance and safety. As mentioned in Chapter 5 and 6, in the coming year(s) such pilot projects will be launched. In West-Vlaanderen, five sites will be identified where the feasibility will be assessed. For Brussels, our research team has been granted an additional project year for the 'Brussels Retrofit XL' project supported by Innoviris. The purpose of this project is to guide users for the application for a building permit by the end of 2015. Our feasibility study and these pilot projects are presently being used as a base to develop a legal framework for Brussels.

Bibliography

Akpinar, S. and Kavak Akpinar, E. (2007). "Wind energy analysis based on maximum entropy principle (MEP)-type distribution function". *Energy Conversion and Management* 48, pp. 1140–1149.

Asmus, P. et al. (2003). *Permitting small wind turbines: A handbook*. American Wind Energy Association.

AWEA (2009). *9.1-2009: Small Wind Turbine Performance and Safety Standard*. 9.1.

AWS Scientific Inc., N. (1997). *Wind resource assessment handbook*.

Bechmann, A. and Sorensen, N. (2010). "Hybrid RANS/LES method for wind flow over complex terrain." *Wind Energy* 13.36-50.

Bendat, J. S. and Piersol, A. G. (1971). *Random Data: Analysis and Measurement Procedures*. John Wiley & Sons.

Bernd, M. (2005). "Changing wind-power landscapes: regional assessment of visual impact on landuse and population in Northern Jutland, Denmark." *Applied Energy* 83, pp. 477–494.

Best, M. et al. (2008). *Small scale wind energy*. Tech. rep. Met Office.

Betz, A. (1926). *Windenergie und Ihre Ausnutzung durch Windmüllen*. Vandenhoeck and Ruprecht.

Blocken, B., Stathopoulos, T., and Carmeliet, J. (2007). "CFD simulation of the atmospheric boundary layer: wall function problems". *Atmospheric Environment* 41, pp. 238–252.

Borg, N. v.d et al. (1986). *Accuracy of power curve measurements*. Tech. rep. Risø-M-2632. Risø National Laboratory.

Bottema, M. and Mestayer, P. G. (1998). "Urban roughness mapping - validation techniques and some first results". *Journal of Wind Engineering and Industrial Aerodynamics* 74, pp. 163–173.

Brothers, C., Arthur, H., and Keller, J. G. (1985). *Effects of wind speed sampling and averaging intervals on accuracy of wind energy estimations*. National Research Council Canada.

Brugel (2013). *Observatorium van de gas- en elektriciteitsprijzen in het Brussels hoofdstedelijk gewest*. Tech. rep. Brusselse regulator voor Energie.

Burton, T. et al. (2001). *Wind energy handbook*. John Wiley & Sons.

Cabello, M. and Orza (2010). "Wind speed analysis in the province of Alicante, Spain. Potential for small-scale wind turbines". *Renewable and Sustainable Energy Reviews* 14.3185-3191.

Cabooter, Y., Dewilde, L., and Langie, M. (2000). *Een windplan voor Vlaanderen: Een onderzoek naar mogelijke locaties voor windturbines*. Tech. rep. Vrije Universiteit Brussel and ODE Vlaanderen.

Caca, J. (2007). *Guidelines for small wind turbines in the built environment*. Tech. rep. Intelligent Energy Europe.

Cace, J. (2013). *Praktische toepassing van mini-windturbines*. Tech. rep. Agentschap energie en klimaat.

Carta, J. A. and Mentado, D. (2007). "A continuous bivariate model for wind power density and wind turbine energy output estimations". *Energy Conversion and Management* 48, pp. 420–432.

Carta, J. A., Ramírez, P., and Velázquez, S. (2009). "A review of wind speed probability distributions used in wind energy analysis: Case studies in the Canary Islands". *Renewable and Sustainable Energy Reviews* 13, pp. 933–955.

Celik, A. N. (2003). "Energy output estimation for small-scale wind power generators using Weibull-representative wind data". *Journal of Wind Engineering and Industrial Aerodynamics* 91, pp. 693–707.

Chang, T. (2011). "Estimation of wind energy potential using different probability density functions". *Applied Energy* 88, pp. 1848–1856.

Chellali, F. et al. (2012). "A comparison between wind speed distributions derived from the maximum entropy principle and Weibull distribution. Case of study; six regions of Algeria". *Renewable and Sustainable Energy Reviews* 16, pp. 379–385.

Control Alt Energy LLC (2014). *Wind Myths*. `http : / / www . controlaltenergy.com/Wind_Myths.htm`.

CREG (2014). *Maandelijkse boordtabel elektriciteit en aardgas februari 2014*. Tech. rep.

Derrick, A. (1992). "Development of the measure–correlate–predict strategy for site assessment". In: *proceedings of the British Wind Energy Association Conference*.

Drew, D., Barlow, J., and Cockerill, T. (2013). "Estimating the potential yield of small wind turbines in urban areas: A case study for greater

London". *Journal of Wind Engineering and Industrial Aerodynamics* 115, pp. 104–111.

Drew, D. et al. (2015). "The importance of accurate wind resource assessment for evaluating the economic viability of small wind turbines". *Renewable Energy* 77, pp. 493–500.

Elkinton, M., Rogers, A. L., and McGowan, J. G. (2006). "An investigation of wind-shear models and experimental data trends for different terrains." *Wind engineering* 30, pp. 341–350.

Elliot, D. and Infield, D. (2014). "An assessment of the impact of reduced averaging time on small wind turbine power curves, energy capture predictions and turbulence intensity measurements". *Wind Energy* 17.DOI: 10.1002/we.1579, pp. 337–342.

Ellison, S. L. R., Barwick, V. J., and Farrant, T. J. D. (2009). *Practical statistics for the analytical scientist, a bench guide.* RSC Publishing.

Encraft (2009). *Warwick wind trials: Final report.* `http://tinyurl.com/WarwickWindTrials`.

Engstrom, S. and Pershagen, B (1980). *Aesthetic Factors and Visual Effects of Large-Scale WECs.* National Swedish Board for Energy Source Development.

Erlass des Innenministerium (2010). *Bauplanungsrechtliche Zulässigkeit von Kleinwindkraftanlagen.* Tech. rep.

Eurobats (2006). *Eoliennes et chiroptères – Recommandations pour la planification des projets et les études d'impact.* Tech. rep. Eurobats.

— (2012). "Report of the IWG on wind turbines and bat populations". In: *17th Meeting of the Advisory Committee.*

European Commission (2012). *2002/49/EC: The Environmental Noise Directive.* IEC 61400-12-1.

European commission (2014). *SWD(2014)20 final/2: Energy prices and costs in Europe.*

European Commission Eurostat (2014). *Electricity and natural gas price statistics 2014.* `http : / / ec . europa . eu / eurostat / statistics - explained / index . php / Electricity _ and _ natural _ gas _ price _ statistics`.

Firtin, E., Guler, O., and Akdag, S. A. (2011). "Investigation of wind shear coefficients and their effect on electrical energy generation". *Applied Energy* 88, pp. 4097–4105.

Fox, N. I. (2011). "A tall tower study of Missouri winds". *Renewable Energy* 36, pp. 330–7.

Gsanger, S. (2014). *Small wind world report 2014*. World Wind Energy Association.

Gualtieri, G. and Secci, S. (2014). "Extrapolating wind speed time series vs. Weibull distribution to assess wind resource to the turbine hub height: A case study on coastal location in Southern Italy". *Renewable Energy* 62, pp. 164–176.

Guidon, N. (2011). *Etude de gisement éolien : Tour Manhattan*. Tech. rep. Leefmilieu Brussel.

Hau, E. (2006). *Wind Turbines: Fundamentals, Technologies, Application, Economics*. Springer-Verlag.

Hedevang, E. (2014). "Wind turbine power curves incorporating turbulence intensity". *Wind Energy* 17, pp. 173–195.

Hendrick, P. (2014). *Etude d'impact sur la biodiversité*. Tech. rep. ULB.

Hodkinson, T., Rowley, P., and Watson, S. (2013). "Analysing the Performance of a Building-Mounted Battery Charging Wind Turbine with Particular Emphasis on the Effect of Yaw Misalignment". In: *In prepints of the European Wind Energy Association Conference*.

Huang, S., Li, Q. S., and Xu, Q. (2007). "Numerical evaluation of wind effect on a tall steel building by CFD". *Journal of constructional steel research* 63, pp. 612–627.

Huppop, O. et al. (2006). "Bird migration studies and potential collision risk with offshore wind turbines". *Ibis* 148, pp. 90–109.

IEC (2006). *61400-12-1:2006: Wind turbines - Part 12-1: Power Performance measurements of electricity producing wind turbines*. IEC 61400-12-1.

— (2012). *61400-11:2012: Wind Turbines - Part 11: Acoustic Noise Measurement Techniques*. IEC 61400-11.

— (2013). *61400-2:2013: Design requirements for small wind turbines*. IEC 61400-2.

Islam, M. R., Saidur, R., and Rahim, N. A. (2011). "Assessment of wind energy potentially at Kudat and Labuan, Malaysia using Weibull distribution function". *Energy* 36.985-992.

Jamieson, P. (2011). *Innovation in wind turbine design*. Wiley.

Jowder, A. L. (2009). "Wind power analysis and site matching of wind turbine generators in Kingdom of Bahrain". *Applied Energy* 86, pp. 538–545.

Justus, G. et al. (1977). "Methods for estimating wind speed frequency distributions". *Journal of applied meteorology* 17, pp. 350–353.

Katsaprakakis, D. A. (2012). "A review of the environmental and human impacts from wind parks. A case study for the Prefecture of Lasithi, Crete". *Renewable and Sustainable Energy Reviews* 16, pp. 2850–2863.

Kikuchi, R. (2008). "Adverse impacts of wind power generation on collision behaviour of birds and anti-predator behaviour of squirrels." *Journal for Nature Conservation* 16, pp. 44–55.

Kubik, M. L. et al. (2013). "A study into the accuracy of using meteorological wind data to estimate turbine generation output". *Renewable Energy* 51, pp. 153–158.

Lackner, M. A., Rogers, A. L., and Manwell, J. F. (2008). "The round robin site assessment method: A new approach to wind energy site assessment". *Renewable Energy* 33, pp. 2019–2026.

Landberg, L. et al. (2003). "Wind resource estimation - an overview". *Wind energy* 6, pp. 261–271.

Li, M. and Li, X. (2005). "MEP-type distribution function: A better alternative to Weibull function for wind speed distributions". *Renewable Energy* 30, pp. 1221–1240.

Ligue pour la Protection des oiseaux (2014). *Eolien et biodiversité – Eoliennes et oiseaux*. Tech. rep. Ligue pour la Protection des oiseaux.

Lubitz, W. D. (2014). "Impact of ambient turbulence on performance of a small wind turbine". *Renewable Energy* 61, pp. 69–73.

Macdonald, R. W., Griffith, R. F., and Hall, D. J. (1998). "An improved method for the estimation of surface roughness of obstacle arrays". *Atmospheric Environment* 32.11, pp. 1857–1864.

MacKay, D. J. C. (2009). *Sustainable Energy—Without the hot air*. UIT Cambridge Ltd.

Makkawi, A., Celik, A., and Muneer, T. (2009). "Evaluation of micro-wind turbine aerodynamics, wind speed sampling interval and its spatial variation". *Building services engineering research and technology* 30, pp. 7–14.

Manwell, F. J., McGowan, J. G., and Rogers, A. L. (2009). *Wind Energy Explained*. John Wiley & Sons.

Measnet (2009). *Procedure: Evaluation of site-specific wind conditions*.

Mermuys, K. (2010). *Windmakers*. Tech. rep. Provinciaal onderzoeks- en voorlichtingscentrum voor land- en tuinbouw.

Mertens, S. (2009). *Eerste evaluatie meetresultaten testveld kleine windturbines Zeeland*. Tech. Rep. 0904000.R01. Ingreenious.

Met Office and Entec (2008). *Small-scale wind energy: Policy insights and practical guidance*. Tech. rep.

Microgeneration certification scheme (2011). *MCS 020: Standard for permitted development of wind turbines and air source heat pumps on domestic premises.* Tech. rep. Department of Energy and Climat change.

Millward-Hopkins T., J. et al. (2013a). "Mapping the wind resource over UK cities". *Renewable Energy* 55, pp. 202–211.

Millward-Hopkins, J. T. et al. (2013b). "Assessing the potential of urban wind energy in a major UK city using an analytical model". *Renewable Energy* 60, pp. 701–710.

Modern-era retrospective analysis for research and applications (2014). *Long-term wind speed data.* `http://gmao.gsfc.nasa.gov/merra/`.

Mostafaeipour, A. (2013). "Economic evaluation of small wind turbine utilization in Kerman, Iran". *Energy Conversion and Management* 73, pp. 214–225.

National Renewable Energy Laboratory (2014). *Small wind turbine independent testing.* `http://www.nrel.gov/wind/smallwind/independent_testing.html`.

Nollet, J.-M. and Di Antonio, C. (2013). *Cadre de Référence pour l'implantation d'éoliennes en région Wallone.* Tech. rep. Gouvernement Wallon.

Oke, T. R. (1988). "Street design and urban canopy layer climate". *Energy build* 11, pp. 103–113.

Okulov, V. and Kuik, G. van (2012). "The Betz–Joukowsky limit: on the contribution to rotor aerodynamics by the British, German and Russian scientific schools". *Wind Energy* 15.2, pp. 335–344.

OpenEI (2014). *Small wind guidebook.* `http://en.openei.org/wiki/Small_Wind_Guidebook`.

Papoulis, A. (1991). *Probability, Random Variables and Stochastic Processes.* 3rd ed. McGraw-Hill.

Peacock, A. et al. (2008). "Microwindturbines in the UK domestic sector". *Energy and Buildings* 40, pp. 1324–1333.

Plate, E. J. (1995). "Urban climates and urban climate modelling: An introduction". *Wind climate in Cities* J. E. Pp. 22–29.

Ragwitz, M. et al. (2012). *Recent developments of feed-in systems in the EU.* Ministry for the Environment, Nature Conservation and Nuclear Safety.

Ramírez, P. and Carta, J. A. (2006). "The use of wind probability distributions derived from the maximum entropy principle in the analysis of wind energy. A case study". *Energy Conversion and Management* 47, pp. 2564 –2577.

Ray, M., Rogers, A., and McGowan, J. (2006). "Analysis of wind shear models and trends in different terrains". *AWEA conference proceedings.*

Renewable Energy Research Lab (2002). *Wind Fact Sheets: Wind power: Performance and economics.* Tech. rep. University of Massachusetts.

RenewableUK (2011). *Small wind: Plannning guidance.* Tech. rep. RenewableUK.

— (2014). *Small Wind Turbine Standard.*

Rideout, K., Copes, R., and Constance, B. (2010). *Wind turbines and health.* Tech. rep. National Collaborating Centre for Environmental health.

Rogers, A. L., Rogers, J. W., and Manwell, J. F. (2005). "Comparison of the performance of four measure-correlate". *Journal of Wind Engineering and Industrial Aerodynamics* 93, pp. 243–264.

Romo Perea, A., Amezcua, J., and Probst, O. (2011). "Validation of three new measure-correlate-predict models for the long-term prospection of the wind resource". *Journal of Renewable and Sustainable Energy* 3, pp. 23105–23105.

Royal Meteorological Institute (2014). *Belgian Synoptical Network.* http://www.meteo.be/meteo/view/nl/124570-Waarnemingsnetwerk.html.

Rumeau, M. et al. (2006). *Impacts sanitaires du bruit généré par les éoliennes.* Tech. rep. Afsset.

Runacres, M. C., Vermeir, J. J., and De Troyer, T. (2012). *IWT 090192 Final Report—On the use of small wind turbines for sustainable energy production for SME's and individuals.* Erasmushogeschool Brussel.

— (2014). *BIM E11-359 Final Report—Identificatie Identificatie sites, opzetten windmetingscampagnes en uitvoering van haalbaarheidsstudies in het Brussels Hoofdstedelijk Gewest.* Leefmilieu Brussel.

Sagrillo, M. (2002). "The monthly newsletter of the American Wind Energy Association–Small turbine column: Wind system operation and maintenance costs".

Salvatore, J. (2013). *World Energy Perspective – Cost of Energy Technologies.* World Energy Council.

Schallenberg-Rodriguez, J. (2013). "A methodological review to estimate techno-economical wind energy production". *Renewable and Sustainable Energy Reviews* 21, pp. 272–287.

Siemens (2009). *ERWP-SP-30: Shadow control description.*

Sunderland, K. M., Mills, G., and Conlon, M. (2013). "Estimating the wind resource in an urban area: A case study of micro-wind generation po-

tential in Dublin, Ireland". *Journal of Wind Engineering and Industrial Aerodynamics* 118, pp. 44–53.

Takle, E. S. and Brown, J. M. (1977). "Note on the Use of Weibull Statistics to Characterize Wind-Speed Data". *Iowa Agriculture and Home Economics Experiment Station* 8941, pp. 556–559.

Taylor, J. et al. (2013). "Noise levels and noise perception from small and micro wind turbines". *Renewable Energy* 55, pp. 120–127.

Taylor, M. et al. (2004). "An analysis of wind resource uncertainty in energy production estimates". In: *proceedings of the European Wind Energy Association Conference*.

Tominaga, Y. and Stathopoulos, T. (2013). "CFD simulation of near-field pollutant dispersion in the urban environment: A review of current modeling techniques". *Atmospheric Environment* 79, pp. 716–730.

Tominaga, Y. et al. (2008). "AIJ guidelines for practical applications of CFD to pedestrian wind environment around buildings". *Journal of Wind Engineering and Industrial Aerodynamics* 96, pp. 1749–1761.

Troen, I. and Petersen, E. L. (1989). *European Wind Atlas*. Risø National Laboratory.

USA Energy Information Administration (2014). *Electricity Prices for Households for Selected Countries*. `http://www.eia.gov/countries/prices/electricity_households.cfm`.

Van Hamme, E. and Loix, E. (2011). *VEA—draagvlak windenergie 2011*. `http://www.energiesparen.be/node/880`. Vlaams Energieagenschap en GfK Significant.

Van Mechelen, D. and Crevits, H. (2009). *Beoordelingskader voor de inplanting van kleine en middelgrote windturbines*. Omzendbrief LNE/2009/01—RO/2009/01. Vlaamse Regering.

Vermeir, J. J. and Runacres, M. C. (2014). *WDGO 1165—Keuze windturbine en schatting jaaropbrengst*. Electrabel.

— (2015). *WDGO 1072—Rooftop wind resource assessment in Mannheim*. Wattwerk Energiekonzepte.

Vermeir, J. J., Runacres, M. C., and De Troyer, T. (2012). "CFD modelling and measurements of the atmospheric boundary layer for micrositing of small wind turbines." In: *proceedings of the European Wind Energy Association Conference*. EWEA.

Vlaams Energie Agentschap (2014). *Technologieën met projectspecifieke steun*. `http://www.energiesparen.be/monitoring-en-evaluatie/technologieen-met-projectspecifieke-steun`.

VREG (2012). *De prijs per kWh elektriciteit voor particulieren en kmo's.* `http://www.vreg.be/hoeveel-kost-1-kwh-elektriciteit-en-aardgas`. Vlaamse Reguleringsinstantie voor de Elektriciteits- en Gasmarkt.

— (2014a). *Maandelijkse boordtabel elektriciteit en aardgas november 2014.* Tech. rep.

— (2014b). *Mededeling van de Vlaamse Regulator van de elektriciteits- en gasmarkt.* `http://www.vreg.be/hoeveel-kost-1-kwh-elektriciteit-en-aardgas`. Vlaamse Reguleringsinstantie voor de Elektriciteits- en Gasmarkt.

Wallbank, T. (2008). *WindSim validation study: CFD validaiton in complex terrain.* Windsim.

Wang, F. et al. (2008). "Development of small domestic wind turbine with scoop and prediction of its annual power output". *Renewable Energy* 33, pp. 1637–1651.

Weekes, S. and Tomlin, A. S. (2013). "Evaluation of a semi-empirical model for predicting the wind energy resource relevant to small-scale wind turbines". *Renewable Energy* 50, pp. 280–288.

Weekes, S. M. and Tomlin, A. S. (2014a). "Data efficient measure-correlate-predict approaches to wind resource assessment for small-scale wind energy". *Renewable Energy* 63, pp. 162–171.

Weekes, S. M. and Tomlin, A. S. (2014b). "Low-cost wind resource assessment for small-scale turbine installations using site pre-screening and short-term wind measurements". *Renewable Power Generation, IET* 8.4, pp. 349–358.

Wegley, H. L. et al. (1980). *A siting handbook for small wind energy conversion systems.* Batelle Memorial institute.

Whale, J., McHenry, M., and Malla, A. (2013). "Scheduling and conducting power performance testing of a small wind turbine". *Renewable Energy* 55, pp. 55–61.

Wieringa, J. (1992). "Updating the Davenport roughness classification". *Journal of Wind Engineering and Industrial Aerodynamics* 41-44, pp. 357–368.

Willemsen, E. and Wisse, J. (2002). "Accuracy of assessment of wind speed in the built environment". *Journal of Wind Engineering and industrial Aerodynamics* 90.1183-1190.

Windtest Grevenbroich GmbH (2014). *Power curve measurements.* `http://www.windtest-nrw.de`.

Yoshie, R. et al. (2007). "Cooperative project for CFD prediction of pedestrian wind environment in the Architectural Institute of Japan". *Journal of Wind Engineering and Industrial Aerodynamics* 95, pp. 1551–1578.

Zhang, P. (2012). *Small wind world report.* World Wind Energy Association.

Zhou, J. et al. (2010). "Comprehensive evaluation of wind speed distribution models: A case study for North Dakota sites". *Energy Conversion and Management* 51, pp. 1449–1458.